

2013-12-09

In-Situ Upgrading and Recovery Enhancement of Athabasca Bitumen by Ultra-Dispersed Nanocatalysts

Hashemi, Rohallah

Hashemi, R. (2013). In-Situ Upgrading and Recovery Enhancement of Athabasca Bitumen by Ultra-Dispersed Nanocatalysts (Doctoral thesis, University of Calgary, Calgary, Canada).

Retrieved from <https://prism.ucalgary.ca>. doi:10.11575/PRISM/26558

<http://hdl.handle.net/11023/1189>

Downloaded from PRISM Repository, University of Calgary

UNIVERSITY OF CALGARY

In-Situ Upgrading and Recovery Enhancement of Athabasca Bitumen by Ultra-Dispersed
Nanocatalysts

by

Rohallah Hashemi

A THESIS

SUBMITTED TO THE FACULTY OF GRADUATE STUDIES

IN PARTIAL FULFILMENT OF THE REQUIREMENTS FOR THE

DEGREE OF DOCTOR OF PHILOSOPHY

DEPARTEMENT OF CHEMICAL AND PETROLEUM ENGINEERING

CALGARY, ALBERTA

December, 2013

© Rohallah Hashemi 2013

Abstract

Thermal methods are extensively used to extract heavy oil and bitumen with reasonable recovery percentages to compensate for the light oil production decline in recent years. In addition, new technologies are tested to increase the value of the produced liquids. Nanoparticles technology is emerging as a new alternate technology for enhancing the upgrading and recovery processes of heavy oil. Ultra-dispersed nanocatalysts can be injected into the reservoir along with hydrogen to enhance both the upgrading and recovery of heavy oil. Nanocatalysts can be introduced into the reservoir at a typical SAGD configuration (in the area between injector and producer) with the desired residence time to produce higher quality products with enhanced heavy oil recovery. However, before applying these nanocatalysts in the field and testing their performance, their transport behavior inside the porous media and catalytic activity towards heavy oil upgrading and subsequently recovery enhancement has to be determined.

In this study, a pilot plant unit was built in-house to investigate the performance of multi-metallic nanoparticles in an oil sand packed bed column at high pressure and temperature conditions. Results showed that nanoparticles could be controllably delivered inside the medium with a meager influence on the medium permeability. In addition, deposition of the nanoparticles mainly occurs at the entrance of injection zone and rapidly decreases across the reaction zone.

Moreover, effect of different hot fluid injection scenarios on recovery enhancement has been evaluated in presence and absence of tri-metallic nanocatalysts. Comparing the

recovery curves show effectiveness of nanocatalysts on recovery enhancement. In addition, presence of nanocatalysts inside the porous media along with hydrogen enhanced the quality of produced liquids by reducing the hydrocarbon residue and micro carbon content. Furthermore, significant enhancement of liquid viscosity and API gravity was achieved. In the other side, using the nanocatalysts enhanced the hydrocracking reactions by reducing coke formation as well as reduction of carbon dioxide emission, which reduces the environmental impact of nanocatalysts on the in-situ upgrading processes.

Acknowledgments

Throughout the completion of this study, many people have helped and support me. I would like to take this opportunity to thank them all.

First, I would like to express my sincere gratitude to my supervisor Dr. Pedro Pereira Almao for giving me the opportunity to be a member of his great team. My special thanks and appreciation is expressed to Dr. Pereira for his endless support during hard times and his beneficial advises to continue the research work. I have not only benefited from his incredible talent and outstanding knowledge but also have learned numerous moral lessons from him. He also gave the whole research steering wheel to me that boosted my confidence and independency.

I would like to express my sincere thanks to Dr. Nashaat Nassar for his co-supervision, guidance, encouragement, support, timely advices and cooperation. I wish to thank the members of my advisory committee, Dr. Jalal Abedi and Dr. Brij Maini as well as my examining committee, Dr. Larry Lines, Dr. Gordon R. Moore and Dr. Ashok Singhal for their time and comments.

Special thanks go to my good friends in the pilot plant team Redescal Gomez, Gustavo Trujillo and Clementina Sosa; for their help during the construction and operation of the unit and Redescal and Andrew Carss for their help with the feed preparation. Also, to the analytical team specially Lante Carbognani and Francisco Lopez for their help in the sample analysis; Linda Roa for her support during the sample

analysis in the lab and Dr. Carlos Scott for his valuable advices. We have accomplished some incredible jobs collaboratively on the topic of in-situ upgrading which always remind me of those sweet days of working together.

I would also like to thank all my friends and fellow graduate students, in particular: Morteza Dejam, Seyed Javad Payetakhti, Mehdi Bahonar, Amir Ghaderi and Moslem Hosseininejad, for their continuous friendship and support from my undergraduate to Ph.D. studies. The friendships with them are one of the most important treasures of my life.

I gratefully acknowledge the University of Calgary specially the Schulich School of Engineering, the Catalysis for Bitumen Upgrading Group (CBUG) and the Alberta Ingenuity Centre for In Situ Energy (AICISE) and its sponsors for their financial support.

Finally, and the most importantly, I would like to express gratitude to my parent (Abootaleb Hashemi and Mahin Mohammad Sharifi), my sisters (Maryam and Fatemeh Hashemi), and my brothers (Mohsen and Mahmood Hashemi) for the love, support, and encouragement they have given me throughout my Ph.D. study, without which this work would not have been accomplished.

Humbly Dedicated to
Imam Hussein
And
His Loyal Companions
That Their Supreme Sacrifice Will Not Be Forgotten

Table of Contents

Abstract	ii
Acknowledgments.....	iv
Dedication	vi
Table of Contents	vii
List of Tables	x
List of Figures	xi
Chapter 1 Introduction.....	1
1.1 Background	1
1.2 Motivation	4
1.3 Objectives.....	5
1.4 Organization of the thesis	6
Chapter 2 Transport Behavior of Multimetallic Ultra-Dispersed Nanoparticles in an Oil Sands-Packed Bed Column at High Temperature and Pressure. 10	
2.1 Abstract	10
2.2 Introduction	11
2.3 Materials and methods	13
2.3.1 Chemicals	13
2.3.2 Porous media	14
2.3.3 Preparation of nanoparticles suspension	15
2.3.4 Experimental set-up.....	16
2.3.5 Experimental procedure.....	18
2.3.6 Analytical methods	20
2.4 Results and discussions	21
2.4.1 Estimating size of colloidal nanoparticles and their concentration in the feed	21
2.4.2 Transport of colloidal nanoparticles in oil sands packed bed column....	22
2.4.2.1 First test	23
2.4.2.2 Second test.....	29
2.4.2.3 Third test.....	35
2.4.2.4 Fourth test.....	41
2.5 Conclusions	46
Chapter 3 Enhanced Heavy Oil Recovery by In-Situ Prepared Ultra-Dispersed Multi-metallic Nanoparticles: A Study of Hot Fluid Flooding for Athabasca Bitumen Recovery.....	48
3.1 Abstract	48
3.2 Introduction	49

3.3	Materials and methods	54
3.3.1	Fluids and chemicals	54
3.3.2	Preparation of nanocatalysts suspension	55
3.3.3	Experimental set-up.....	57
3.3.4	Experimental procedure.....	59
3.3.5	Analytical methods	61
3.4	Results and discussion.....	63
3.4.1	Flood of saturated porous media by steam	64
3.4.2	Hot fluid flood study	65
3.4.2.1	Hot VGO injection	66
3.4.2.2	Effect of light pentane injection	67
3.4.2.3	Effect of nanocatalysts	69
3.5	Conclusions	74
Chapter 4 In situ Upgrading of Athabasca Bitumen Using Multimetallic Ultra-Dispersed Nanocatalysts in a in an Oil-Sands-Packed Bed Column: Part 1, Produced Liquid Quality Enhancement.....		75
4.1	Abstract	75
4.2	Introduction	76
4.3	Materials and methods	83
4.3.1	Chemicals	83
4.3.2	Preparation of nanoparticles suspension	84
4.3.3	Experimental set-up.....	85
4.3.4	Experimental procedure.....	86
4.3.5	Analytical methods	88
4.4	Results and discussions	90
4.4.1	Recovery enhancement and overall mass balance analysis.....	91
4.4.2	Enhancement of API gravity and viscosity	93
4.4.3	Residue conversion.....	96
4.4.4	Micro carbon residue (MCR) content.....	101
4.4.5	The homogeneity of the produced liquid.....	103
4.4.6	Sulfur content	105
4.4.7	Nitrogen content	106
4.4.8	Average quality enhancement	108
4.5	Conclusions	109
Chapter 5 In situ Upgrading of Athabasca Bitumen Using Multimetallic Ultra-Dispersed Nanocatalysts in an Oil-Sands-Packed Bed Column: Part 2, Solid Analysis and Gaseous Product Distribution.....		111
5.1	Abstract	111
5.2	Introduction	112
5.3	Materials and methods	115
5.3.1	Chemicals	115
5.3.2	Preparation of nanoparticles suspension	116

5.3.3	Experimental procedure.....	116
5.4	Results and discussions	119
5.4.1	Solids characterization and morphology	119
5.4.1.1	Coke content.....	120
5.4.1.2	Characterization and morphology of packed bed solids after reaction	124
5.4.2	Characterization of produced gases during bitumen upgrading	129
5.4.2.1	Blank experiments, without tri-metallic nanocatalysts	131
5.4.2.2	Effect of tri-metallic nanocatalysts.....	132
5.4.2.2.1	Carbon dioxide and monoxide	133
5.4.2.2.2	Hydrocarbon gases	134
5.4.2.2.3	Hydrogen sulfide (H ₂ S)	137
5.4.2.2.4	Ethylene and propylene.....	138
5.5	Overall product distributions.....	140
5.6	Conclusions	141
Chapter 6 Nanotechnology for heavy oil upgrading and recovery: Opportunities and challenges		143
6.1	Abstract	143
6.2	Introduction	144
6.3	In-situ prepared ultradispersed nanoparticles.....	147
6.4	Synthesis of nanocatalysts.....	150
6.5	Required facilities for nanocatalysts application in heavy oil upgrading and recovery.....	155
6.6	Nanocatalysts transport behavior inside the porous media	157
6.7	Modeling of reaction kinetics.....	161
6.8	Bitumen recovery enhancement	165
6.9	Quality Enhancement	166
6.10	Sulfur removal.....	174
6.11	Coke formation mitigation	175
6.12	Gas emission reduction	178
6.13	Nanocatalysts recycling.....	179
6.14	Hydrogen consumption	181
6.15	Environmental effect of nanocatalysts	182
6.16	Conclusions	184
Chapter 7 Conclusions and Recommendations.....		185
7.1	Conclusions	185
7.2	Recommendations for Future Work.....	187
References.....		189

List of Tables

Table 2-1: Properties of Athabasca bitumen and Nexen VGO considered in this study..	14
Table 2-2: Concentration of multimetallic colloidal nanoparticles in the feed	22
Table 2-3: Specifications of the experimental tests considered in this study	23
Table 2-4: Mass balance for the first test.....	26
Table 2-5: Mass balance for the second test	31
Table 2-6: Mass balance for the third test.....	37
Table 2-7: Mass balance for the fourth test	43
Table 3-1: Properties of Athabasca bitumen and Nexen VGO used for experiments	55
Table 3-2: Concentration of colloidal tri-metallic nanocatalysts in the feed.....	57
Table 3-3: Specifications of the experimental tests considered in this study	64
Table 4-1: Properties of Athabasca bitumen and Nexen VGO considered in this study..	84
Table 4-2: Specifications of the experimental tests considered in this study	90
Table 5-1: Compositional analysis (wt %, atomic %) of zone indicated in Figure 5.4 ..	124
Table 5-2: Compositional analysis (wt %, atomic %) of zones indicated in Figure 5.5.	127
Table 5-3: Compositional analysis (wt %, atomic %) of zone indicated in Figure 5.7 ..	129

List of Figures

Fig 1.1: World Oil Reserve in 2008 (Erdoğan 2013).....	2
Fig 2.1: Schematic of the experimental setup.....	18
Fig 2.2: DLS characterization of multimetallic colloidal nanoparticles size distribution in VGO matrix at 25 °C.....	22
Fig 2.3: Breakthrough curves for experiments conducted with different nanoparticles of 34 ± 0.5 nm diameters suspended in VGO matrices in an oil sands packed bed column with clean silica sand of 12-20 mesh size saturated with Athabasca bitumen. Other experimental conditions include residence time: 36 h, porosity: 33.1%, pressure: 3.5 MPa, and temperature: 300 °C	24
Fig 2.4: Calculated distribution of specific deposit of different nanoparticles at different bed depth (across the reaction zone) for time period of 36 h.....	26
Fig 2.5: Pressure drop across the oil sands packed bed column during the run of the first test	28
Fig 2.6: DLS characterization of colloidal nanoparticles size distribution in heavy oil matrix for original feed sample and samples obtained during the run of the first test at different values of PV	28
Fig 2.7: ESEM microphotographs of Ni-Mo-W-nanoparticles deposited onto high permeability oil sands porous media at (a) Top of the reactor column (b) Bottom of the reactor column. Experimental conditions include; residence time: 36 h, porosity: 32.9%, pressure: 3.5 MPa, and temperature: 300 °C....	29
Fig 2.8: Breakthrough curves for experiments conducted with different nanoparticles of 34 ± 0.5 nm diameters suspended in VGO matrices in an oil sands packed bed column with clean silica sand of 12-20 mesh size saturated with Athabasca bitumen. Other experimental conditions include; residence time: 36 h, porosity: 32.9%, pressure: 3.5 MPa, and temperature: 320 °C	31
Fig 2.9: Calculated distribution of specific deposit of different nanoparticles at different bed depth (across the reaction zone) for time period of 36 h.....	33
Fig 2.10: DLS characterization of colloidal nanoparticles size distribution in heavy oil matrix for original feed sample and samples obtained during the run of the second test at different values of PV	33
Fig 2.11: Microphotographs of Ni-Mo-W-nanoparticles deposited onto high permeability oil sands porous media at (a) top of the reactor column (b) bottom of the reactor column. Experimental conditions include; residence time: 36 h, porosity: 32.9%, pressure: 3.5 MPa, and temperature: 320 °C.....	34

Fig 2.12: Pressure drop across the oil sands packed bed column during the run of the second test	35
Fig 2.13: Breakthrough curves for experiments conducted with different nanoparticles of 34 ± 0.5 nm diameters suspended in VGO matrices in an oil sands packed bed column with clean silica sand of 100-140 mesh size saturated with Athabasca bitumen. Other experimental conditions include; residence time: 36 h, porosity: 33.2%, pressure: 3.5 MPa, and temperature: 300 °C	37
Fig 2.14: Calculated distribution of specific deposit of different nanoparticles at different bed depth (across the reaction zone) for time period of 36 h.....	38
Fig 2.15: Pressure drop across the oil sands packed bed column during run of the third test	40
Fig 2.16: DLS characterization of colloidal nanoparticles size distribution in heavy oil matrix for original feed sample and samples obtained during the run of the third test at different values of PV	40
Fig 2.17: ESEM microphotographs of Ni-Mo-W-nanoparticles deposited onto low permability oil sands porous media at (a) top of the reactor column (b) bottom of the reactor column. Experimental conditions include; residence time: 36 h, porosity: 33.2%, pressure: 3.5 MPa, and temperature: 300 °C	41
Fig 2.18: Breakthrough curves for experiments conducted with different nanoparticles of 34 ± 0.5 nm diameters suspended in VGO matrices in an oil sands packed bed column with clean silica sand of 100-140 mesh size saturated with Athabasca bitumen. Other experimental conditions include; residence time: 36 h, porosity: 33.7%, pressure: 3.5 MPa, and temperature: 320 °C	42
Fig 2.19: Calculated distribution of specific deposit of different nanoparticles at different bed depth (across the reaction zone) for time period of 36 h.....	44
Fig 2.20: Pressure drop across the oil sands packed bed column during run of the fourth test	45
Fig 2.21: DLS characterization of colloidal nanoparticles size distribution in heavy oil matrix for original feed sample and samples obtained during the run of the fourth test at different values of PV	45
Fig 2.22: ESEM microphotographs of Ni-Mo-W-nanoparticles nanoparticles deposited onto low permability oil sands porous media at (a) top of the reactor column (b) bottom of the reactor column. Experimental conditions include; residence time: 36 h, porosity: 33.7%, pressure: 3.5 MPa, and temperature: 320 °C....	46
Fig 3.1: Schematic representation of colloidal tri-metallic nanocatalysts preparation algorithm	56
Fig 3.2: Schematic representation of the experimental setup	58

Fig 3.3: Schematic representation of the Dean-Stark distillation unit setup (Dean and Stark 1920).....	62
Fig 3.4: Recovery performance and SOR of steam injection into the high permeability sand packed bed at pressure of 3.5 MPa, steam injection rate of 1 cm ³ /min, and temperatures of 243.5 °C	65
Fig 3.5: Performance of VGO injection into the high permeability sand packed bed at different times in the absence of tri-metallic UD nanocatalysts at pressure of 3.5 MPa, VGO injection rate of 0.01 cm ³ /min, hydrogen flow rate of 1 cm ³ /min, and temperatures of 320 and 340 °C.....	67
Fig 3.6: Recovery performance of mixed VGO and pentane (0 wt%, 5 wt%, 10 wt% and 15 wt%) injection into the high permeability sand packed bed at different times in the absence of tri-metallic UD nanocatalysts at pressure of 3.5 MPa, hot fluid injection rate of 0.01 cm ³ /min, hydrogen flow rate of 1 cm ³ /min, and temperatures of 340 °C	69
Fig 3.7: Recovery performance of hot VGO injection into the high permeability sand packed bed at different times in the presence of tri-metallic UD nanocatalysts at pressure of 3.5 MPa, hot fluid injection rate of 0.01 cm ³ /min, hydrogen flow rate of 1 cm ³ /min, and temperatures of 320 and 340 °C	71
Fig 3.8: Material balance for the hot VGO injection into the high permeability sand packed bed at different times in the presence of tri-metallic UD nanocatalysts at pressure of 3.5 MPa, hot fluid injection rate of 0.01 cm ³ /min, hydrogen flow rate of 1 cm ³ /min, and temperatures of 320 and 340 °C	72
Fig 3.9: Total volume of produced gases at standard condition (T=25°C , P=0.1 MPa) for the hot VGO injection into the high permeability sand packed bed in the presence and absence of tri-metallic UD nanocatalysts at pressure of 3.5 MPa, hot fluid injection rate of 0.01 cm ³ /min, hydrogen flow rate of 1 cm ³ /min, and temperatures of 320 and 340 °C.....	73
Fig 4.1: Schematic representation of the experimental setup	86
Fig 4.2: Material balance for the hot VGO injection into the an oil sand packed bed at different conditions: (a) in the absence of UD nanocatalysts and temperature of 320 °C, (b) in the absence of UD nanocatalysts and temperature of 340 °C, (c) in the presence of UD nanocatalysts and temperature of 320 °C, (d) in the presence of UD nanocatalysts and temperature of 340 °C. System pressure was 3.5 MPa, hot fluid injection rate of 0.01 cm ³ /min, and hydrogen flow rate of 1 cm ³ /min	92
Fig 4.3: Simulated distillation analysis of produced liquid samples obtained from an oil sand packed bed at different conditions: (a) in the absence of UD nanocatalysts and temperature of 320 °C, (b) in the absence of UD nanocatalysts and temperature of 340 °C, (c) in the presence of UD nanocatalysts and	

temperature of 320 °C, (d) in the presence of UD nanocatalysts and temperature of 340 °C. System pressure was 3.5 MPa, hot fluid injection rate of 0.01 cm ³ /min, and hydrogen flow rate of 1 cm ³ /min	93
Fig 4.4: API gravity of produced liquid samples from porous media at different times in the absence and presence of tri-metallic UD nanocatalysts at pressure of 3.5 MPa, hydrogen flow rate of 1 cm ³ /min, and temperatures of 320 and 340 °C	95
Fig 4.5: Viscosity of produced liquid samples from porous media at 40 °C. Sample was produced at different times in the absence and presence of tri-metallic UD nanocatalysts at pressure of 3.5 MPa, hydrogen flow rate of 1 cm ³ /min, and temperatures of 320 and 340 °C.....	96
Fig 4.6: Boiling point simulated distillation curves for different produced liquid samples obtained at different temperatures in presence and absence of nanocatalysts for reaction time of 45 h, hydrogen flow rate of 1 cm ³ /min, and total pressure of 3.5 MPa. The horizontal dashed line is the cut points between distillates and residual components.....	98
Fig 4.7: Residue contents of produced liquid samples from porous media as a function of time in the presence and absence of tri-metallic nanocatalysts at pressure of 3.5 MPa, hydrogen flow rate of 1 cm ³ /min, and temperatures of 320 and 340 °C	99
Fig 4.8: Percentage of residue content reduction of produced liquid samples from porous media in the presence of nanocatalysts with respect to control experiments (without nanocatalysts) as a function of time at pressure of 3.5 MPa, hydrogen flow rate of 1 cm ³ /min, and temperatures of 320 and 340 °C.....	100
Fig 4.9: MCR content of produced liquid samples from porous media as a function of reaction time in the absence and presence of tri-metallic UD nanocatalysts at pressure of 3.5 MPa, hydrogen flow rate of 1 cm ³ /min, and temperatures of 320 and 340 °C.....	101
Fig 4.10: Percentage of MCR content reduction of produced liquid samples from porous media at different times in the absence and presence of tri-metallic UD nanocatalysts at pressure of 3.5 MPa, hydrogen flow rate of 1 cm ³ /min, and temperatures of 320 and 340 °C.....	102
Fig 4.11: Optical micrographs (40×) of a liquid drop for samples obtained at different conditions: (a) virgin Athabasca bitumen, (b) virgin Nexen VGO, (c) VGO emulsion containing tri-metallic nanocatalysts, (d) produced from porous media in presence of nanocatalysts at 320 °C, (e) produced from porous media in presence of nanocatalysts at 340 °C, (f) produced from porous media in the absence of nanocatalysts at 340 °C	104
Fig 4.12: Sulfur content of produced liquid samples from porous media at different times in the absence and presence of tri-metallic UD nanocatalysts at pressure of 3.5 MPa, hydrogen flow rate of 1 cm ³ /min, and temperatures of 320 and 340 °C	106

Fig 4.13: Nitrogen content of produced liquid samples from porous media at different times in the absence and presence of tri-metallic UD nanocatalysts at pressure of 3.5 MPa, hydrogen flow rate of 1 cm ³ /min, and temperatures of 320 and 340 °C	107
Fig 4.14: Average quality enhancement of produced liquid from porous media during the whole life of process at different temperatures in the presence of tri-metallic UD nanocatalysts at pressure of 3.5 MPa, hydrogen flow rate of 1 cm ³ /min, and temperatures of 320 and 340 °C	109
Fig 5.1: Schematic representation of the gaseous emissions experimental set-up	117
Fig 5.2: Images for different filter papers after filtering different produced liquid samples obtained from porous media at pressure of 3.5 MPa and temperatures of 340 °C. (a) sample produced in absence of nanocatalysts, (b) sample produced in presence of tri-metallic nanocatalysts	121
Fig 5.3: Coke content of produced samples from porous media as function of reaction time in the absence and presence of tri-metallic UD nanocatalysts at pressure of 3.5 MPa, hydrogen flow rate of 1 cm ³ /min, and temperatures of 320 and 340 °C	122
Fig 5.4: ESEM micrographs of filter paper after the filtration process for selected produced liquid sample obtained at 340 °C in the presence of nanocatalysts. Red area shown indicates the zone where EDAX analysis was performed...	123
Fig 5.5: ESEM microphotographs of an oil sand sample containing tri-metallic nanocatalysts obtained from the top of the reactor column. Experimental conditions include; residence time: 36 h, porosity: 32.9%, pressure: 3.5 MPa, and temperature: 320 °C	124
Fig 5.6: ESEM microphotographs of an oil sand sample containing tri-metallic nanocatalysts obtained from the top of the reactor column for selected zones a, b, c and d in Figure 5.5. Experimental conditions include; residence time: 36 h, porosity: 32.9%, pressure: 3.5 MPa, and temperature: 320 °C	126
Fig 5.7: ESEM microphotographs of an oil sand sample containing tri-metallic nanocatalysts obtained from the bottom of the reactor column. Experimental conditions include; residence time: 36 h, porosity: 32.9%, pressure: 3.5 MPa, and temperature: 320 °C	128
Fig 5.8: Produced gas mass balance of hot VGO injection into the high permeability sand packed bed at different times in the presence of tri-metallic UD nanocatalysts at pressure of 3.5 MPa, hot fluid injection rate of 0.01 cm ³ /min, hydrogen flow rate of 1 cm ³ /min, and temperatures of 320 and 340 °C	130
Fig 5.9: Accumulative volume of carbon dioxide produced from oil sand porous media at different times, in the absence of tri-metallic nanocatalysts and test pressure of pressure of 3.5 MPa and temperatures of 320 and 340 °C	132

Fig 5.10: Accumulative volume of carbon dioxide and monoxide production from porous media in presence of tri-metallic nanocatalysts as function of time at pressure of 3.5 MPa and temperatures of 320 and 340 °C	134
Fig 5.11: Accumulative volume of methane, ethane propane and butane production from porous media in the presence of tri-metallic nanocatalysts as function of time at a pressure of 3.5 MPa. (a) temperatures of 340 °C, (b) temperatures of 320 °C	135
Fig 5.12: Accumulative volume of pentane production from porous media in presence of tri-metallic nanocatalysts as function of time at pressure of 3.5 MPa and temperatures of 320 and 340 °C.....	136
Fig 5.13: Accumulative volume of H ₂ S production from porous media in the presence of tri-metallic nanocatalysts as a function of time at pressure of 3.5 MPa and temperatures of 320 and 340 °C.....	138
Fig 5.14: Accumulative volumes of ethylene and propylene production (measured at standard condition) from porous media in the presence of tri-metallic nanocatalysts for pressure of 3.5 MPa and temperatures of 320 and 340 °C	140
Fig 5.15: Overall gas and solid distribution from HCK of Athabasca bitumen in the presence and absence of UD tri-metallic at oil sand packed bed column at a pressure of 3.5 MPa, residence time of 36 h, and hydrogen flow rate of 1 cm ³ /min	141
Fig 6.1: Cartoon representation of in-situ heavy oil upgrading and recovery coupling ultradispersed nanocatalysts and the SAGD process, whereupon light oil is produced at the surface and heavy molecules, solids and minerals stay sub-surface. Obtained from (Nassar, Husein et al. 2011) with permission.	150
Fig 6.2: Schematic representation illustrating the top-down and bottom-up approaches for nanocatalysts preparation. Obtained from (Nassar 2012) with permission. ..	151
Fig 6.3: Schematic representation of water-in-oil microemulsions. The water pools solubilise the precursors and accommodate the resultant nanoparticles. The size of the water pool can be manipulated by controlling the ratio of mole water/mole surfactant. Obtained from (Nassar, Husein, and Pereira-Almao 2011b) with permission.....	153
Fig 6.4: Schematic representation of the experimental setup for in- situ upgrading and recovery enhancement of Athabasca bitumen. Obtained from (Hashemi et al. 2013) with permission.....	157
Fig 6.5: Proposed scheme for lumped-kinetic modeling of HCK reactions. Obtained from (Scherzer and Gruia 1996, Sánchez, Rodríguez, and Ancheyta 2005) with permission.	162
Fig 6.6: Proposed scheme for lumped-kinetic modeling of HCK reactions. Obtained from Sanchez, Rodriguez et al. 2005 with permission.	163

Fig 6.7: Proposed kinetic models (a) hydroprocessing of bitumen in presence of UD catalysts (Sánchez, Rodríguez, and Ancheyta 2005) with permission; (b) Modified model for the UD catalyst (Loria et al. 2011) with permission.....	164
Fig 6.8: Hydrogen to carbon ratio for the various petroleum cuts (Billon and Bigeard 2001) with permission.....	167
Fig 6.9: Hydrogen-to-carbon ratio (H/C) of Athabasca bitumen at different conversion of residue for reaction performed at 380 °C (Galarraga and Pereira-Almao 2010) with permission.	168
Fig 6.10: Viscosity of liquid products from reaction at constant pressure of 3.45 MPa, temperatures of 320, 350 and 380 °C at reaction times from 3 up to 70 hours (Galarraga March 2011) with permission.	169
Fig 6.11: Viscosity of produced liquid samples from oil sand porous media measured at 40 °C. Sample was produced at different times in the absence and presence of tri-metallic UD nanocatalysts at pressure of 3.5 MPa, hydrogen flow rate of 1 cm ³ /min, and temperatures of 320 and 340 °C. Obtained from reference (Hashemi et al., 2013) with permission.	170
Fig 6.12: API gravity of liquid products as a function of conversion for dry emulsion of UD nanocatalysts in batch reactor. Obtained from (Galarraga et al., 2011) with permission.	171
Fig 6.13: API gravity of produced liquid samples from porous media at different times in the absence and presence of tri-metallic UD nanocatalysts at pressure of 3.5 MPa, hydrogen flow rate of 1 cm ³ /min, and temperatures of 320 and 340 °C. Obtained from (Hashemi et al., 2013) with permission.	172
Fig 6.14: MCR content of produced liquid samples from porous media as a function of reaction time in the absence and presence of tri-metallic UD nanocatalysts at pressure of 3.5 MPa, hydrogen flow rate of 1 cm ³ /min, and temperatures of 320 and 340 °C. Obtained from (Hashemi et al., 2013) with permission.....	173
Fig 6.15: Hydrodesulfurization of Athabasca bitumen as a function of reaction time evaluated at 3.45 MPa of hydrogen pressure and at temperatures of 320, 350, 380 °C using UD NiWMo catalysts. Obtained from (Galarraga et al., 2011) with permission.	174
Fig 6.16: Sulfur content of produced liquid samples from porous media at different times in the absence and presence of tri-metallic UD nanocatalysts at pressure of 3.5 MPa, hydrogen flow rate of 1 cm ³ /min, and temperatures of 320 and 340 °C (Hashemi et al., 2013) with permission.	175
Fig 6.17: Coke content of produced samples from porous media as a function of reaction time in the absence and presence of tri-metallic UD nanocatalysts at pressure of 3.5 MPa, hydrogen flow rate of 1 cm ³ /min, and temperatures of 320 and 340 °C (Hashemi et al., 2013) with permission.	177

Fig 6.18: Schematic representation of in-situ upgrading (ISU) process for non-conventional oil in the presence of UD catalysts. Obtained from (Peluso 2011) with permission. 180

Chapter 1 Introduction

Heavy oil and bitumen are playing increasingly important role in the world's energy market with the decline of conventional oil production. High viscosity oil is produced by thermal recovery mechanisms to allow for flowing to the surface and then diluent is used to transport heavy oils for further upgrading processes. There exist extensive efforts to improve the thermal methods with both recovery and quality enhancement simultaneously. In this context, a promising application that incorporates ultra-dispersed nanocatalysts and heat in the reservoir was conducted to fulfill the idea of underground upgrading with the benefit of less environmental footprints.

1.1 Background

Canada's oil sands and heavy oils are important hydrocarbon resources that play an increasingly important role in the Canadian economy. With more than 170 billion barrels of estimated oil sands, Canada has the third largest oil reserve in the world. Figure 1-1 shows the Canada rank in terms of proven global crude oil reserve (Erdoğan 2013). 80 percent of these reserves are deep underground and cannot be accessed by surface mining (Bergerson and Keith 2006, Patel 2007, St-Denis 2007). Many in-situ methods have been developed to extract heavy oil and bitumen from deep reservoirs (Paitakhti Oskouei et al. 2010, Sharpe, Richardson, and Lolley 1995, Chu 1977, Weissman et al. 1996, Greaves, Xia, and Ayasse 2005, Liu et al. 2004, Butler and Mokrys 1991, Moore, Mehta, and Ursenbach 2002). Once produced, bitumen is transferred to upgrading units converting

low quality oil to synthetic crude oil (Martínez-Palou et al. 2011a). Transportation of bitumen to a location for upgrading is a challenging aspect for heavy oil industry. In addition to processing costs, the level of contaminants in bitumen, such as sulphur, metal and nitrogen requires special equipment, and also has environmental repercussions.

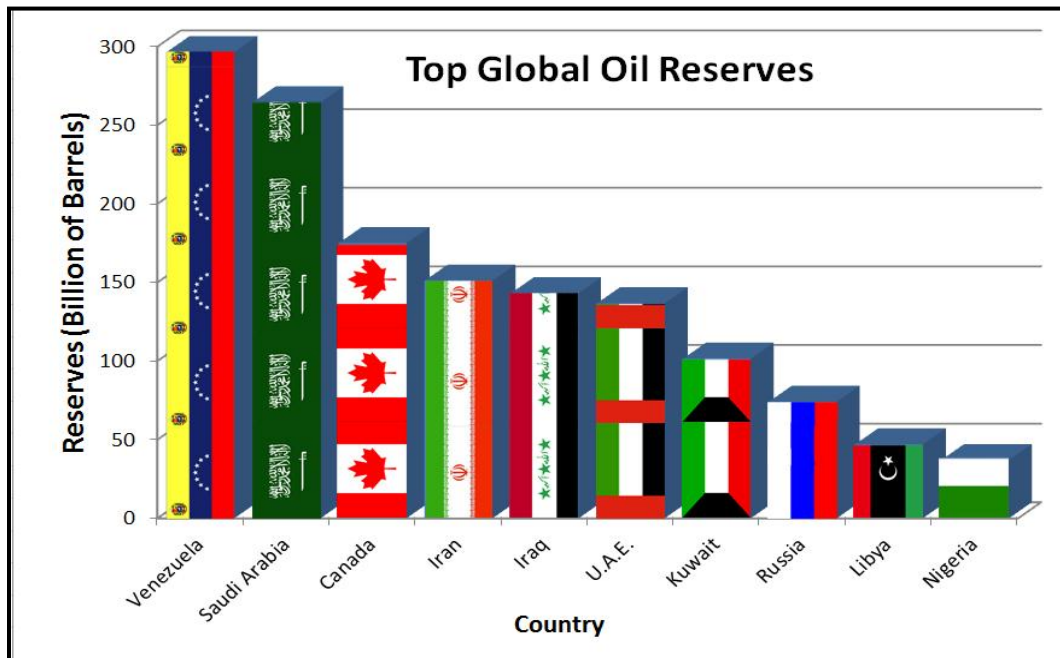


Fig 1.1: World Oil Reserve in 2008 (Erdoğan 2013)

Many recovery techniques have been developed to assist heavy oil and bitumen production. Steam drive, cyclic steam stimulation, steam assisted gravity drainage and in situ combustion are so far the field implemented thermal techniques beyond piloting. These thermal methods can be divided into two main categories based on the change into the oil properties. First and most common category includes those methods that use heat as a source of energy to reduce the viscosity and to increase the mobility. In these processes (i.e., hot water injection, steam flooding, Steam Assisted Gravity Drainage

(SAGD), etc.) bitumen composition remains unchanged and the only change occurs in the physical properties. The second category includes those processes that produce energy from the oil resources to oxidize and eventually or partially crack the heavy oil and bitumen molecules into some lighter components reducing viscosity, but also pushing the bitumen out of the reservoir, like in-situ combustion technique.

The “Underground Refinery” using nano-size ultra-dispersed (UD) catalyst is one of the alternatives to surface upgrading that may become the “next generation” of oil sands industry improvement. Coupling it with SAGD a dispersion of nano-size particles could be injected into a reservoir to enhance upgrading and recovery of heavy oil. Nanocatalysts can pass through the micro porous medium and create a series of chemical reactions which produce high value energy product with extremely low to zero environmental footprints.

Converting bitumen to high value crude oil using UD catalyst requires certain conditions of pressure and temperature, which can be limited by the type of reservoir and SAGD process. The ultimate goal of underground refineries is to achieve this pressure and temperature conditions at which nano-size catalysts react and upgrade heavy oil and bitumen in-situ. Employing nanocatalysts performing at least part of the refinery work is economically beneficial because of capital cost reduction in surface equipment and minimizing of environmental impact. Existing studies have shown that using catalysts can have a visible result on in-situ processes but it requires a lot of energy input with the possibility of catalyst deactivation as well as coke deposition and plugging (Shah et al. 2011).

There exist numerous challenges to be addressed before commercializing the UD nanocatalysts injection process and some of the challenges were investigated in this study.

1.2 Motivation

Successful results have been observed recently on the transport of suspended ultra-dispersed catalysts in heavy oil matrix at low temperature through oil sands media and in the absence of any chemical reaction (Zamani and Maini 2009, Zamani, Maini, and Pereira-Almao 2010, 2011). Results demonstrated that it is feasible to propagate UD nanoparticles in oil sands media without major permeability reduction and significant pressure drop. In addition, published results show that tri-metallic nanocatalysts (NiMoW) enhanced the quality of heavy feedstocks at mild temperatures and long residence times in the batch reactor experiments (Frauwallner 2009, Galarraga and Pereira-Almao 2010). Furthermore, in continuous mode experiments (Rendon, 2011) reported that bitumen viscosity was reduced from 9,545 to 258 cP (at 40 °C), and that API gravity was improved from 9.85 to 14.3 which clearly proves the effectiveness of tri-metallic nanocatalysts (Rendon 2011).

Special intrinsic properties of nanocatalysts help the propagation of these particles inside the porous media with the lower risk of plugging (Hamed Shokrlu and Babadagli 2010). In addition to the propagation of nanocatalysts at high pressure and temperature testing, it is very beneficial to investigate the effect of nanocatalysts on the recovery performance of Athabasca bitumen since these particles are injected at the same

conditions of in-situ bitumen recovery. Furthermore, there exists lack of published results on gaseous products in the area of Athabasca bitumen upgrading with the UD nanocatalysts. To fulfill the recovery performance enhancement as well as detailed gas distribution analysis, this study was conducted.

1.3 Objectives

The main objective of this study is to investigate the extent of in-situ upgrading and recovery enhancement as well as propagation quality via injection of tri-metallic (NiMoW) UD nanocatalysts inside the porous medium of oil sand packed bed column.

The specific objectives are:

1. Investigate the transport behavior of ultradispersed multimetallic nanoparticles inside an oil sands packed bed column at high temperature and pressure.
2. Evaluate the effect of different hot fluid injection scenarios on Athabasca bitumen recovery performance inside a continuous oil sands packed bed column.
3. Determine the extent of liquid quality enhancement at different reaction times and temperatures, on the basis of its viscosity, API gravity and content of sulfur, nitrogen, and MCR.
4. Evaluate the effectiveness of the ultradispersed tri-metallic nanocatalysts in reducing coke formation and CO₂ emission during bitumen upgrading as well

as quality of produced gas via hydroprocessing reaction inside the medium.

5. Investigate the advantages of nanocatalysts employment for in-situ catalytic upgrading and recovery of heavy oil. For further application and studies, limitations and challenges facing this new technology were discussed and current situation of this process was presented.

1.4 Organization of the thesis

This thesis consists of seven chapters and is a collection of five articles, which two of them already published and others are in progress. In Chapter 1, background, motivation, objective and organization of thesis are presented. A brief introduction has been included in this chapter since each chapter has a detailed introduction related to the subject of the paper.

Chapter 2 describes the transport behavior of in-situ prepared multimetallic nanoparticles in an oil sand packed bed column at reservoir conditions. This chapter was included in a paper entitled “*Transport Behavior of Multimetallic Ultra-Dispersed Nanoparticles in an Oil Sands-Packed Bed Column at High Temperature and Pressure*” (Hashemi, Nassar, and Pereira-Almao 2012). The transport behavior of multi-metallic nanoparticles (W, Ni and Mo) of potential catalytic value suspended in vacuum gas oil using different packed bed column experiments at different pressures and temperatures was investigated. In this study, the quality of produced particles, the percentages of deposition inside the medium, the deposition trend and the effect of in-situ deposition on

the pressure drop curve as well as formation properties were demonstrated.

Chapter 3 describes the recovery enhancement via injection of nanocatalysts inside the packed bed medium. This chapter was part of an article entitled “*Enhanced Heavy Oil Recovery by In-Situ Prepared Ultra-Dispersed Multi-metallic Nanoparticles: A Study of Hot Fluid Flooding for Athabasca Bitumen Recovery*” (Hashemi, Nassar, and Pereira Almaso 2013c). Hence delivery of UD nanoparticles inside the porous media is controllable with a meager influence on the medium permeability, it is expected that the presence of these particles enhances the recovery via viscosity reduction mechanism. Different hot fluid injection scenarios were tested and the results were demonstrated to prove the effectiveness of UD nanocatalysts on recovery enhancement of Athabasca bitumen in a sand packed bed column. All results were compared with the base case to observe the incremental enhancement of recovery in each scenario.

The produced liquid and gas quality enhancement as well as coke reduction are discussed in Chapters 4 and 5. Chapter 4 is part of an article entitled “*In situ Upgrading of Athabasca Bitumen Using Multimetallic Ultra-Dispersed Nanocatalysts in a in an Oil-Sands-Packed Bed Column: Part 1, Produced Liquid Quality Enhancement*” (Hashemi, Nassar, and Pereira Almaso 2013a). This chapter covers the produced liquid analysis results. Produced liquid samples from porous media after chemical reaction were analyzed by standard techniques to determine the extent of enhancement via hydrocracking. Liquid properties such as residue conversion, micro carbon residue (MCR) content, sulfur and nitrogen contents, API gravity and viscosity were evaluated and compared with the base case. Experiments were repeated in some pressure and

temperature conditions to ensure the reproducibility of the results.

Chapter 5 of this work presents the solid and gas analysis results. This chapter is part of an article entitled “*In situ Upgrading of Athabasca Bitumen Using Multimetallic Ultra-Dispersed Nanocatalysts in an Oil-Sands-Packed Bed Column: Part 2, Solid Analysis and Gaseous Product Distribution*” (Hashemi, Nassar, and Pereira Almao 2013b). The chapter evaluates the extent of upgrading in the solid and gas components. Particularly, second part of the analysis explores the effectiveness of the ultradispersed tri-metallic nanocatalysts in reducing coke formation as well as CO₂ emission during bitumen upgrading. Accordingly, this chapter presents the compositional analysis of emitted gases during in-situ catalytic upgrading of Athabasca bitumen in oil sands packed bed reactor. On the solid analysis section, the characterization of the nanocatalysts after the reaction, specifically in the liquid filtrate and packed bed solids were reported.

Based on the successful results obtained in this study, Chapter 6 was considered to address the opportunity and challenges facing the employment of nanoparticle technology in heavy oil industry. This chapter is to be considered as an article entitled “*Nanotechnology for heavy oil upgrading and recovery: Opportunities and challenges*”. During this study, many challenges were identified that should be considered in future research studies and industrial implementations. To the best of our knowledge, potential areas briefly were explained about nanoparticles and their behavior as adsorbent/catalysts for heavy oil upgrading and recovery as well as possible challenges for future implementations.

Finally, Chapter 7 concludes the important aspects of this research and provides recommendations for future studies. It should be noted that the present thesis is in part based on refereed papers that have already been published or are in the last stages of final publication. Unavoidably, there will be some repetitions between the chapters particularly in the introduction part or in the sections dealing with the experimental set-up and analytical sections.

Chapter 2 Transport Behavior of Multimetallic Ultra-Dispersed Nanoparticles in an Oil Sands-Packed Bed Column at High Temperature and Pressure¹

2.1 Abstract

Water-in-vacuum gas oil microemulsion containing ultradispersed multimetallic colloidal nanoparticles can facilitate in-situ delivery of nanoparticles into heavy oil reservoir. This study investigated the transport of multi-metallic nanoparticles (W, Ni and Mo) of potential catalytic value suspended in vacuum gas oil using different oil sands packed bed column breakthrough experiments at typical pressure and temperature of steam assisted gravity drainage (SAGD) recovery process. The nanoparticles (34 ± 0.5 nm) were transported into two different permeability oil sands. Experiments were performed at a pressure of 3.5 MPa, residence time of 36 h, and temperatures from 300 to 320 °C in both low and high permeability oil sands packed bed. At full breakthrough, a constant normalized concentration plateau was achieved, ranging from 0.50 for low permeability to 0.60 for high permeability oil sands. Deposition and transport of nanoparticles were strongly dependent on their metallic type, temperature and porosity of oil sands. Despite aggregation of nanoparticles at high temperature, neither major permeability reduction

¹ Hashemi, Rohallah, Nashaat N. Nassar, and Pedro Pereira-Almao. Transport Behavior of Multimetallic Ultradispersed Nanoparticles in an Oil-Sands-Packed Bed Column at a High Temperature and Pressure. *Energy & Fuels* 26.3 (2012): 1645-1655.

nor pore plugging were observed. Therefore, propagation of multimetallic ultradispersed nanoparticles in oil sands media seems feasible under typical pressure and temperature of SAGD process.

2.2 Introduction

The worldwide global demand for oil has recently grown to 80 million barrels per day, and is estimated to grow by 50% in next 20 years while conventional resources are declining (U.S. National Commission on Energy Policy 2004). Alternative energy resources will ultimately be required to sustain industrial activities, but immediate needs require a greater recovery of the unconventional resources. Heavy oil and bitumen have been considered as long term replacement for conventional resources (Assessment June 2006). However, the current technologies for upgrading heavy oil/bitumen are more complex than the ones used for conventional crude oil. Actually, the current heavy oil recovery and upgrading processes faces a number of environmental challenges (Gosselin 2010). These challenges stem from the large amounts of energy and water required for production and upgrading processes, and the large amounts of solid waste, wastewater, and gaseous emissions that are generated (Nassar, Husein, and Pereira-Almao 2011b). Nonetheless, several research projects have been conducted to reduce the environmental footprint of oil sands industry and to improve the quality of produced oil with cost-effective and environmentally friendly techniques (Galarraga and Pereira-Almao 2010, Zamani, Maini, and Pereira-Almao 2011, Thompson et al. 2008, Nassar, Husein, and Pereira-Almao 2011b, Hashemi, Nassar, and Pereira-Almao 2012).

In-situ upgrading of heavy oil and bitumen using ultra-dispersed (UD) nanoparticles is a promising technology aiming at improving the quality of produced liquids with less environmental impact. In this process, hydrogen and nanoparticles suspension could be injected into the reservoir during the steam assisted gravity drainage (SAGD) or thermal recovery process. Presence of nanoparticles combined with SAGD process will upgrade the heavy oil within the reservoir, whereupon light oil comes to the surface and waste hydrocarbons, solids and minerals stay subsurface (Nassar, Husein, and Pereira-Almao 2011b).

One important step in this proposed *in-situ* upgrading process is the placement of the nanoparticles deep underground to provide reaction between co-reactants without major formation damage or pore plugging. In fact, *in-situ* catalytic upgrading using nanoparticles is a relatively new field of interest and consequently there is very little research published on the issue of nanoparticles propagation inside the oil sands medium at recovery or upgrading conditions. Most of the studies pertaining to the transport behavior of the nanoparticles in porous media are mainly focused on deep bed filtration for wastewater treatment, and the obtained results could not be applied for reaction conditions in oil-based matrix (Herzig, Leclerc, and Goff 1970, Rege and Fogler 1988, Tien and Payatakes 1979). Nonetheless, our research group has reported recently on the transport of suspended ultra-dispersed catalysts in heavy oil matrix at low temperature through oil sands media and in the absence of any chemical reaction (Zamani and Maini 2009, Zamani, Maini, and Pereira-Almao 2010, 2011). Results demonstrated that it is feasible to propagate UD nanoparticles in oil sands media without major permeability

reduction and significant pressure drop. It was found that the sand media, mainly at the bed entrance, retained 14 to 18 percent of injected UD nanoparticles.

This study is actually a continuation on our previous work aiming at experimentally investigating the transport behavior of nanoparticles in an oil sands porous media at high pressure and temperature of SAGD conditions. The specific objectives are to test: (i) the transport, deposition and retention of multimetallic nanoparticles through 1-D column experiments with two models of different permeabilities; (ii) test the effects of temperature on the transport behavior of nanoparticles. This work will give an insight into the transport behavior of nanoparticles in the presence of reaction in an oil sands matrix and help in finding the best way of placing these nanoparticles in oil reservoirs for the petroleum industry. The selected metal nanoparticles are commonly used as catalysts in the petroleum industry. To the best of our knowledge, a study on the transport of multimetallic nanoparticles in an oil sands packed bed column at high temperature and pressure is conducted for the first time. It should be noted that a later study would consider the employment of the transported nanoparticles for catalytic heavy oil upgrading in an oil sands packed bed.

2.3 Materials and methods

2.3.1 Chemicals

Sand packed beds preparation was performed by using silica sand as porous media (99% of SiO₂, AGSCO, NJ, USA). Athabasca bitumen (JACOS, Alberta, Canada) was used as a source of heavy oil to saturate the porous media. Vacuum gas oil, VGO (Nexen,

Alberta, Canada) was used as oil medium for nanoparticle suspension and carrier for the stabilized nanoparticles. Table 2.1 shows the properties of Athabasca bitumen and Nexen VGO. The following metal precursors were used to prepare the corresponding metal oxide nanoparticles in the VGO matrix; namely: nickel acetate tetrahydrate (99%, Sigma-Aldrich), ammonium metatungstate (99%, Sigma-Aldrich), and ammonium molybdate tetrahydrate (99%, Sigma-Aldrich). Nitric acid (70%, Sigma-Aldrich) and phosphoric acid (85%, Sigma-Aldrich) were used as digesting agents for oil sands containing metal oxide nanoparticles for metal analysis.

Table 2-1: Properties of Athabasca bitumen and Nexen VGO considered in this study

Property	Bitumen	VGO	
Viscosity at 40 °C, (cP)	7550	122.314	
API gravity, (°API)	9.5	19.1	
Microcarbon Residue, (wt%)	12	NA	
H/C (atomic ratio)	1.52 ± 0.001	NA	
Sulfur, (wt%)	4.25	2.73	
Distillation Cuts, (wt %)		Distillation Cuts, (wt%)	
Naphtha: IBP- 213 °C	2.76± 0.29	IBP- 235 °C	10.92
Distillates: 213 - 343 °C	14.89 ± 0.81	235 - 280 °C	7.97
VGO: 343 - 545 °C	34.68 ± 1.81	280 - 343 °C	16.60
Residue: >545+ °C	47.95 ± 1.57	Residue: >343+ °C	64.51

*NA: not available

2.3.2 Porous media

Two model porous media were selected for column breakthrough experiments, including clean unconsolidated silica sands (US Sieves 12-20 and 100-140 mesh). The absolute permeability of the porous media for 12-20 mesh size was about 250 Darcy and about 10 Darcy for 100-140 mesh size. The sands were purchased from AGSCO Corporation. Before any use, the sand was washed with deionized water to remove any kind of dust or

surface impurities and then was placed in vacuum oven at 60 °C for 24 h to evaporate any remaining water. Then the sand was transferred to a stainless steel column for packing.

Absolute permeability of the porous media was measured by injecting water after sand packing. Water was injected inside the porous media at different rates and two pressure transducers were used to record pressure at injection and production points. Accordingly, the porous media permeability was estimated following Darcy's law.

2.3.3 Preparation of nanoparticles suspension

The suspension of nanoparticles in an oil matrix can be achieved by using a variety of methods (Camacho-Bragado et al. 2005, Afanasiev and Bezverkhy 2002, Afanasiev et al. 1999, Eriksson et al. 2004). In this work, a water-in-oil (w/o) microemulsion technique was employed for *in-situ* nanoparticles preparation as this system represents heavy oil matrices under SAGD conditions to a good extent (Nassar and Husein 2010, Husein et al. 2010). Also, w/o microemulsion is an attractive media for nanoparticles preparation due to their ability to form and stabilize a wide variety of nanoparticles with controlled sizes (Eriksson et al. 2004, Nassar 2010, Husein and Nassar 2008, Nassar and Husein 2007a, b).

The *in-situ* preparation of colloidal tri-metallic nanoparticles in VGO matrices followed a similar procedure developed in our previous studies (Zekel' et al. 2007, Thompson et al. 2008, Vasquez 2009). In brief, an organic component was prepared by mixing 99.57 wt% VGO and 0.43 wt% surfactant at 700 rpm and 60 °C. The mixture was stirred for about 30 min to reach stability. The surfactant was formulated in house to give a hydrophilic-lipophilic balance (HLB) = 8 by combining two commercial surfactants,

namely, SPAN 80 and TWEEN-80 from Sigma-Aldrich at a ratio (0.65:0.35, wt/wt). An aqueous solution of the corresponding metal salt was added to the mixture, and agitated for a period of time. Total water content of the emulsions was 2.11 wt%. After that the mixture was heated to a high temperature that was sufficient to evaporate the water and subsequently initiate nucleation and growth of metal oxide nanoparticles, which remain stable in suspension (Zekel' et al. 2007, Thompson et al. 2008, Vasquez 2009). The total metallic concentration of the as prepared nanoparticles was approximately 720 ppmw. The atomic metallic ratios (metal/total metal) were as follows: Mo = 0.6267, Ni = 0.1808 and W = 0.1924.

2.3.4 Experimental set-up

The transport behavior of nanoparticles through the oil sands porous media was investigated through a series of fixed-bed column experiments. The experimental setup is shown in Figure 2.1. The setup consists mainly of a VGO tank containing suspended nanoparticles under nitrogen atmosphere, bitumen tank under nitrogen atmosphere; Isco pumps (Teledyne Isco, NE, US), fraction collectors and stainless steel column reactor.

Three Tee-shape Swagelok unions are installed at injection points, top and bottom of the column reactor. The hot fluid generator is connected into the top section of oil pool (lower part of the sand packed bed column, between the injection and production points) and hot suspension (VGO containing nanoparticles) was injected from this point into the porous media. It should be noted here that the injecting fluids (VGO containing nanoparticles) were heated to the test temperature before being injected to the porous media. One 10-point thermocouple was placed in the middle of the sand packed column

all along the column reactor to record temperature inside the porous media. Recorded temperatures were used to obtain temperature profile distribution inside the reactor.

Reactor pressure of 3.5 MPa was maintained by a pressure regulator connected to the production line at the end of the column. The produced fluid from the porous media was collected inside a hot separator of 500 cm³ volume installed downstream of the production line and subsequently transferred to sampling container for further analysis. VGO containing nanoparticles mixtures were injected into the porous media from the injection point by positive displacement pump. The column has 2.16 cm inside diameter and 90 cm height. In a certain time interval, produced sample is collected and analyzed to measure concentration and size of nanoparticles. Two pressure transducers were used to record the pressures of injection and production lines to calculate pressure drop across the reaction zone.

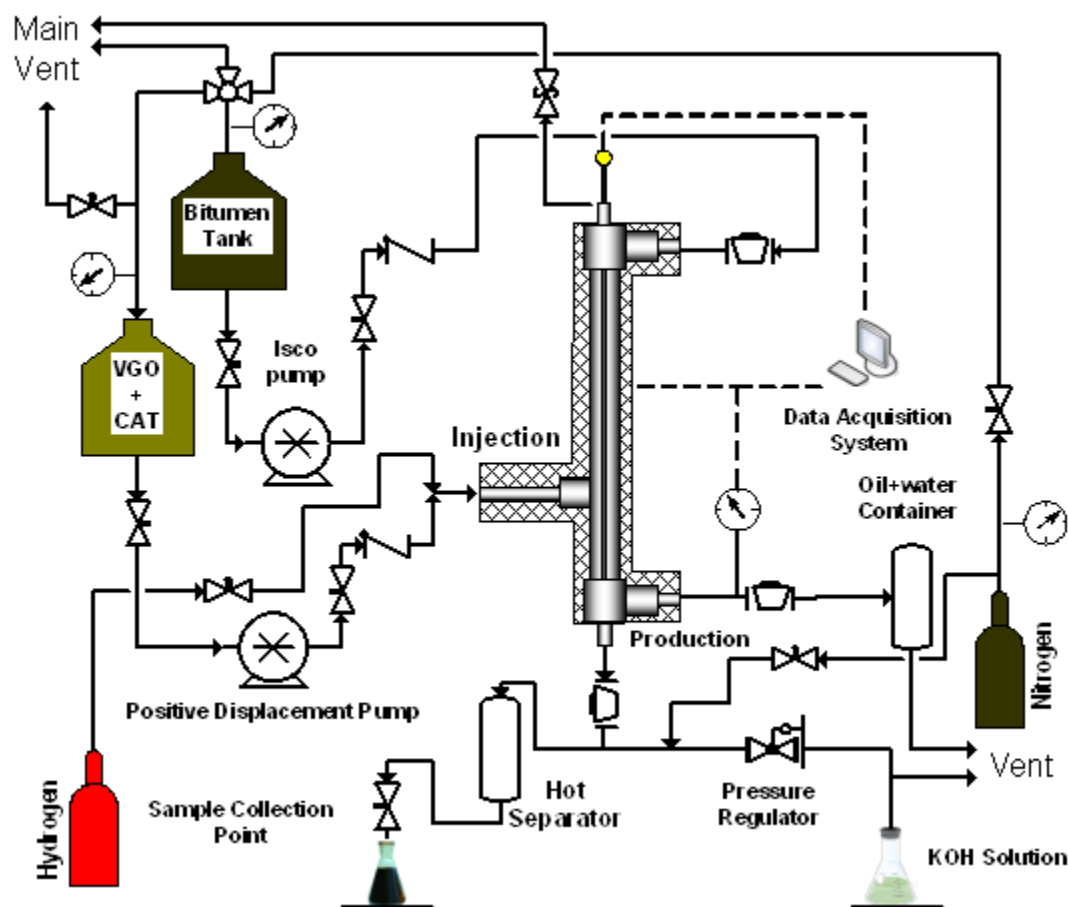


Fig 2.1: Schematic of the experimental setup

2.3.5 Experimental procedure

Experimental procedure was started with installing the packed bed reactor column in its pre-designed place in the pilot plant. In all tests, approximately 452 g silica sand was packed in the column. Mesh rings were placed at the ends of the column to prevent sand escaping. To ensure a uniform sand packing and to avoid air entrapment, the column was first filled with water and the sand media was introduced into the column from the top while the column was constantly patted with a metal rod until it was fully packed.

To maintain test temperature, the outside body of the reactor column was covered with heating tapes and the column was insulated by fiber glass casing. A leak test was performed by pressurizing the packed bed reactor with pure nitrogen up to 5.5 MPa. A 1% change in pressure per hour was considered as the maximum allowable pressure reduction during the leak test. A 3.5 MPa pressure was maintained after the termination of the leak test. Nitrogen was also used for purging the system until oxygen disappeared completely, as confirmed by the gas chromatograph. Following purging, the packed bed column was heated to the desired temperature.

When the reactor column working pressure and temperature were attained, approximately 5 pore volumes of bitumen were first pumped through the column in the down-flow mode to displace the water and saturated the bed with bitumen to mimic the oil sands conditions. Bitumen and irreducible water saturation were calculated by mass balance. The actual experiment started by switching of the inlet gas from pure nitrogen to a hydrogen feed and introducing the injecting fluid (VGO containing nanoparticles). At this point, the zero time for nanoparticles breakthrough was considered.

The run was conducted until approximately 100 cm³ of VGO containing nanoparticles was injected into the porous media. Once the breakthrough experiment was complete, the reactor column was cooled to room temperature. After that, the oil sands sample was carefully discharged from the reactor column for analysis, and the column and assembly were washed with toluene so the apparatus could be ready for another cycle of experiments.

2.3.6 Analytical methods

The size and concentration of the nanoparticles in the VGO matrices were measured before and after injection inside the reactor by an inductively coupled plasma-atomic emission spectroscopy, ICP-AES (IRIS Intrepid II XDL, Thermo-Instruments Canada Inc., Ontario, Canada) and dynamic light scattering, DLS (Malvern Instruments Ltd., Worcestershire, UK) instruments, respectively.

Before particle size measurement, about 2 drops of the produced heavy oil liquid sample containing nanoparticles were diluted with 5 mL of toluene, mixed for 1 min and then introduced to DLS instrument for measurement. It should be noted that a control sample (bitumen diluted in toluene) was introduced into the DLS for comparison and no significant peak was observed, indicating that the sample has no nanoparticles. Before the metal elemental analysis, the oil samples containing nanoparticles was burned at 600 °C to remove the hydrocarbons, and the residue was digested with acidic solution consisting of 70% HNO₃ and 85% H₃PO₄ at a volume ratio (HNO₃/H₃PO₄) of 0.14. After that the mixture was left shaking in a temperature incubator for 24 h at 70 °C, which was sufficient to completely dissolve the nanoparticles.

To estimate the amount of nanoparticles deposited in the sand surface, the oil sands column was divided to five regions and one sample was taken from each region for metal digestion followed by ICP-AES analysis. Selected samples of deposited nanoparticles in different permeability oil sands media (obtained from top and bottom sections of the sand packed bed column) were analyzed by environmental scanning electron microscopy, (ESEM Philips model XL-30, Reston, Virginia, USA).

2.4 Results and discussions

2.4.1 Estimating size of colloidal nanoparticles and their concentration in the feed

Figure 2.2 shows DLS results for sample of VGO containing multimetallic colloidal nanoparticles of 720 ppmw at 22 °C. The average particle size diameter was about 34 ± 0.5 nm. The concentration of the colloidal nanoparticles was measured by ICP-AES and results are tabulated in Table 2.2. As seen in Table 2.2, no significant difference is observed between nominal and experimental values of metal concentrations.

It should be noted that heavy oil/bitumen contains different types of metals, such as sodium, potassium, lithium, calcium, copper, iron, nickel, vanadium, manganese, etc.; with nickel and vanadium being the most common metals present in the heavy oil matrix (Ovalles et al. 1996). Actually, during our ICP-AES metal analysis appreciable amount of vanadium and nickel in the virgin bitumen matrix were observed and quantified. This explains the early breakthrough of nickel in all the breakthrough experiments. However, transportation behavior of injected tri-metallic nanoparticles (Ni, Mo, W) and their retention inside the porous media was the main target of this work because of their unique catalytic properties. Thus, vanadium and other detected metals were excluded from final analysis.

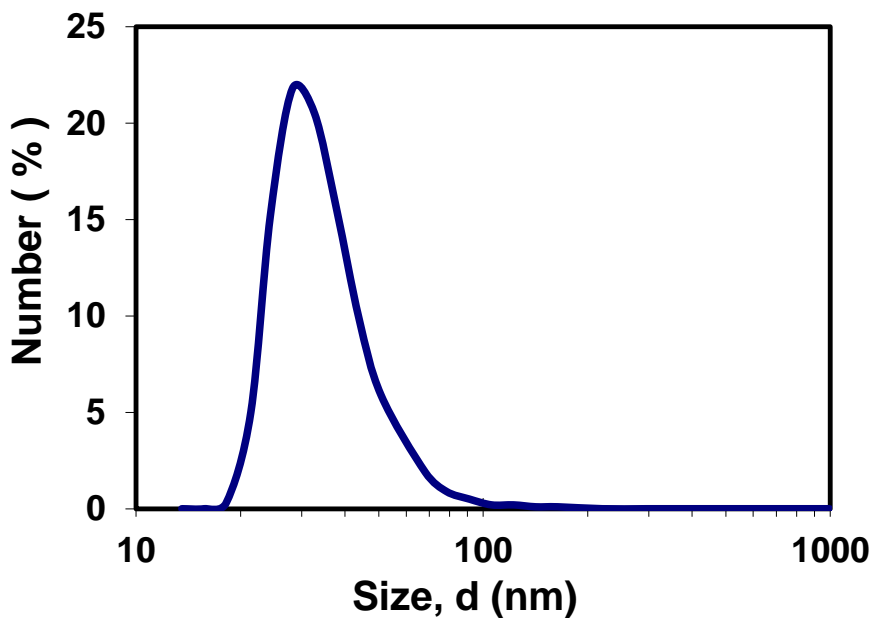


Fig 2.2: DLS characterization of multimetallic colloidal nanoparticles size distribution in VGO matrix at 25 °C

Table 2-2: Concentration of multimetallic colloidal nanoparticles in the feed

Metal content of injecting fluid		
Nominal values		Experimental values
Component	ppm	ppm
Ni	72	81
MO	240	230
W	408	396
Additives		
Component	Percentage (with respect to oil)	
Water (wt%)	2.11	
Surfactant (HLB-8)	0.43	

2.4.2 Transport of colloidal nanoparticles in oil sands packed bed column

As the main goal of this study was to investigate the transport behavior of the colloidal nanoparticles in oil sands packed bed column, the experimental plan was designed to

investigate the effect of temperature and permeability on the transport behavior of nanoparticles in oil sands matrix. Table 2.3 shows the specifications of four breakthrough tests considered in this study. It should be noted that residence time, reactor pressure, particle concentration and injection rates were kept fixed for all the four tests.

Table 2-3: Specifications of the experimental tests considered in this study

Properties	First Test	Second Test	Third Test	Fourth Test
Temperature (°C)	300	320	300	320
Pressure (MPa)	3.5	3.5	3.5	3.5
Porosity (%)	33.1	32.9	33.2	33.7
Absolute permeability (Darcy)	246.8	244	9.6	8.9
Nominal particle concentration (ppm)	720	720	720	720
Residence time (h)	36	36	36	36
Suspension injection rate (cm³/min)	0.01	0.01	0.01	0.01

2.4.2.1 First test

Figure 2.3 shows the breakthrough curves of different nanoparticles through high permeability oil sands porous media at the experimental conditions presented in Table 2-3. The breakthrough curve represents the fraction of nanoparticles concentration in the effluent fluid (C_e) from the reactor column over that in the feed (C_o) as a function of injected fluid oil pool pore volume (reaction zone only). In all cases, the effluent concentration of nanoparticles increased dramatically and rapidly reached a plateau at approximately 1.0 PV, although the levels of the plateau differed among the types of nanoparticles. This suggests that the transport and deposition behavior of the

nanoparticles are affected by the type of nanoparticles, but their deposition mechanism could be similar.

Mass balance calculation showed that about 11 wt% of Ni, 17.8 wt% of Mo, and 30 wt% of W inlet concentration remained inside the oil sands porous media. This would make around 21 wt% of the total (Ni+Mo+W) nanoparticles. Nanoparticles remained inside the oil sands porous media were either deposited on the sand grains or still were suspended in the fluid that remained inside the porous media. Total amount of retained suspended and deposited nanoparticles was obtained from the post mortem analysis.

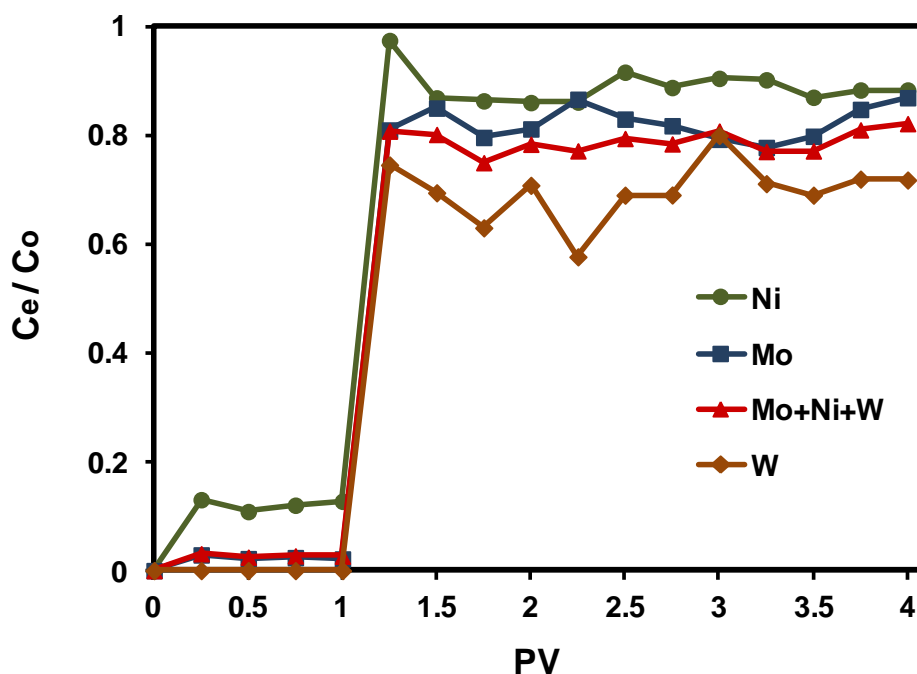


Fig 2.3: Breakthrough curves for experiments conducted with different nanoparticles of 34 ± 0.5 nm diameters suspended in VGO matrices in an oil sands packed bed column with clean silica sand of 12-20 mesh size saturated with Athabasca bitumen. Other experimental conditions include residence time: 36 h, porosity: 33.1%, pressure: 3.5 MPa, and temperature: 300 °C

Table 2.4 shows the summary of mass balance for metal concentration inside the oil sands porous media. Total mass of the injected nanoparticles was calculated on the basis of the total volume of injected fluid containing nanoparticles. Total mass of produced nanoparticles (i.e., nanoparticles at the effluent of the reactor column) was estimated experimentally by ICP-AES analysis. Accordingly, the deposited and retained masses of nanoparticles in oil sands porous media were calculated from the difference between the injected and produced nanoparticles.

Total mass of nanoparticles that remained suspended in the fluid (retained in the porous media) was calculated on the basis of the volume of the remaining fluid inside the porous zone. It should be noted that the concentration of nanoparticles in this fluid was estimated as average concentration of nanoparticles in injected and produced fluids.

The obtained results are tabulated in Table 2.4. As seen, 30.46 wt% of injected nanoparticles concentration remained inside the oil sands column (reaction zone), among which 16.59 wt% was deposited onto the sand grains. Individual and collective specific deposit trends along the reactor column of the selected nanoparticles are shown in Figure 2.4. This figure depicts the amount of nanoparticles (g) deposited per unit bed volume (L) of sand against the length of reactor column (reaction zone). As seen, for all types of nanoparticles, higher concentration was obtained at the entrance of the column, close to the injection point; although the concentration values differed among the types of nanoparticles with Mo being the highest followed by W and then Ni. This again, supports that the transport behavior of nanoparticles is strongly affected by the type of the metal. Nonetheless, the deposition trends of the three types of nanoparticles along the reactor

column were identical as all showed that retention tendency is exponentially decreased from injection to production points within the selected reaction time.

Table 2-4: Mass balance for the first test

Parameters	Values
Total injected nanoparticles (g)	0.0714
Total produced nanoparticles (g)	0.0497
Total (deposited + retained) nanoparticles (g)	0.0217
Total retained nanoparticles (g)	0.0099
Total deposited nanoparticles (g)	0.0119
(Retained+ deposited nanoparticles)/injected (wt%)	30.46
(Deposited nanoparticles/injected) (wt%)	16.59

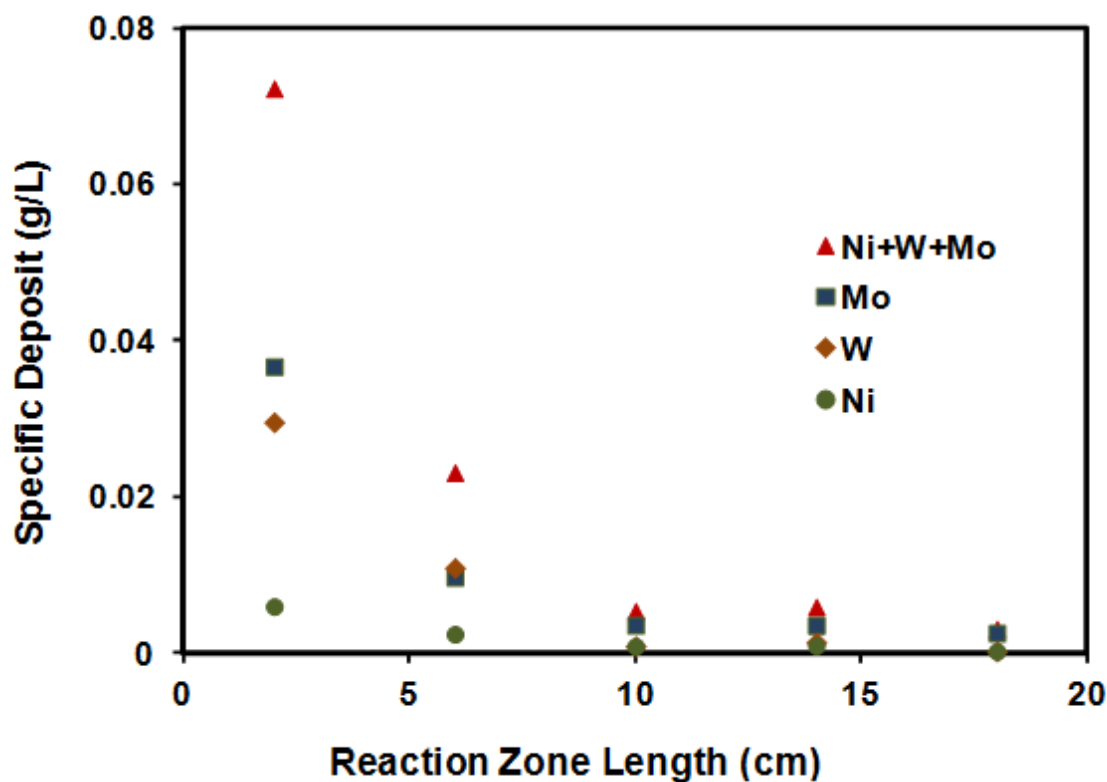


Fig 2.4: Calculated distribution of specific deposit of different nanoparticles at different bed depth (across the reaction zone) for time period of 36 h

The pressure drop across the column was also measured to study the impact of nanoparticles deposition on the sand permeability. Figure 2.5 shows the pressure drop across the reaction zone against the pore volume injected (PV). As seen in the figure, pressure drop across the zone remained constant during the experiment. This suggests that stable experimental conditions were maintained during the test run and there was no plugging occurred across the reaction zone. Accordingly, one can anticipate that the effect of nanoparticles injection on sand permeability reduction is meager as insignificant damage occurred on the sand packed bed during the test.

To support this conclusion measurement of the size of nanoparticles at different PVs were deemed necessary. Figure 2.6 shows DLS measurements of particle size distribution for different PVs during this test. Clearly, no significant effect was observed on the particle size after 1.5 PV, which again supports the no plugging effect that was found by the pressure drop measurement.

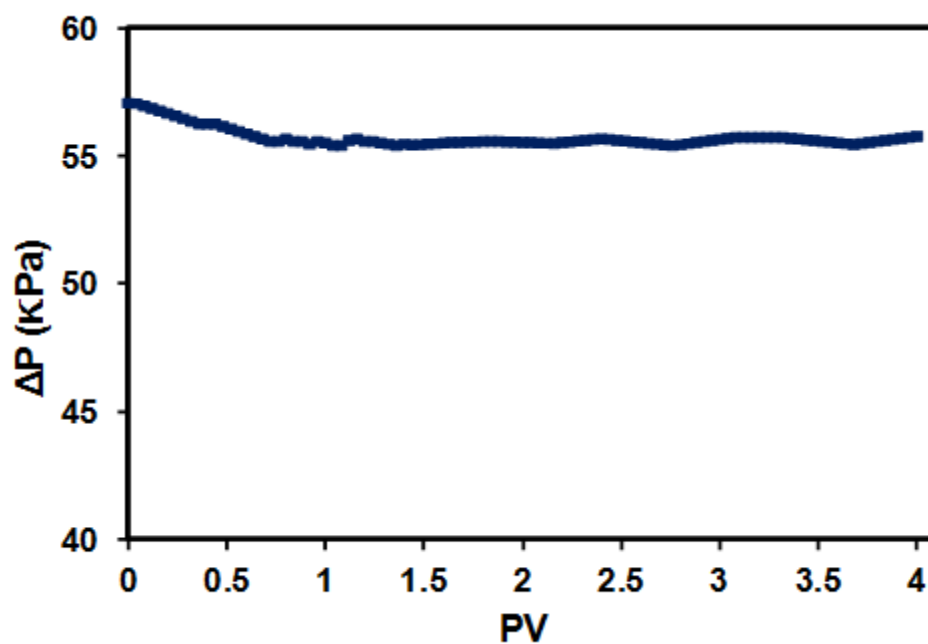


Fig 2.5: Pressure drop across the oil sands packed bed column during the run of the first test

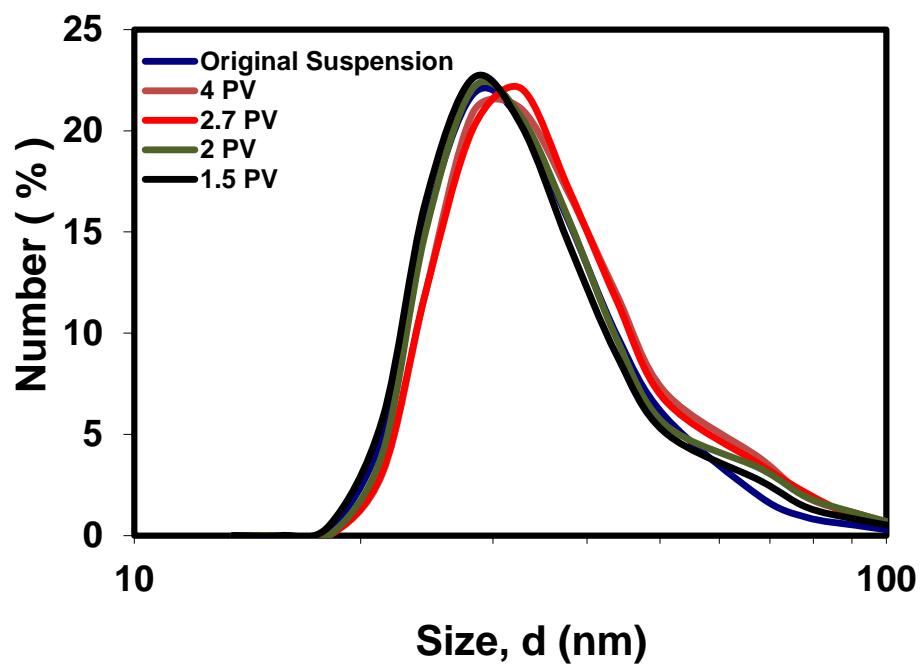


Fig 2.6: DLS characterization of colloidal nanoparticles size distribution in heavy oil matrix for original feed sample and samples obtained during the run of the first test at different values of PV

Figure 2.7 shows ESEM microphotographs of two selected samples from top and bottom of the reaction zone. Clearly, higher population of deposited particles appeared at the top of reaction zone compared to bottom zone. These images support the findings obtained by the ICP-AES analysis on the trend of specific deposit. Further, despite the aggregation of particles at the entrance of the reaction zone nanoparticles can still propagate through the sand packed bed column as smaller particles were observed at the production point (bottom of the column), in agreement with the DLS measurements.

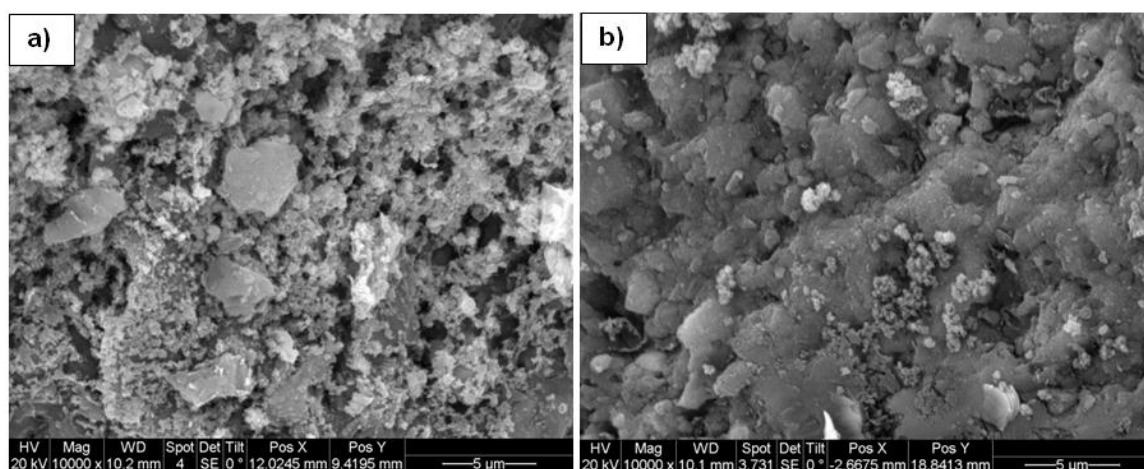


Fig 2.7: ESEM microphotographs of Ni-Mo-W-nanoparticles deposited onto high permeability oil sands porous media at (a) Top of the reactor column (b) Bottom of the reactor column. Experimental conditions include; residence time: 36 h, porosity: 32.9%, pressure: 3.5 MPa, and temperature: 300 °C

2.4.2.2 Second test

The second test was conducted at higher temperature to investigate the effect of temperature on the transport behavior of nanoparticles in high permeability sand packed bed. Therefore, the experimental conditions of this test were similar to the first test,

except the temperature was fixed at 320 °C. Detailed experimental conditions are shown in Table 2.3.

Figure 2.8 presents the normalized breakthrough curves of produced nanoparticles against PV. Again, for all cases, the effluent concentration of nanoparticles increased rapidly and reached a plateau at 1.0 PV, and the levels of the plateau differed among the types of nanoparticles. It is obvious that, in all cases, the level of the plateau in this test is less than the one observed in the first test. Therefore, the total amount of remained nanoparticles inside the porous media has increased during this test.

Mass balance calculations showed that about 51.7 wt% of W, 25 wt% of Ni, and 25 wt% of Mo remained inside the medium either as deposited on the sand grains or retained suspended inside the fluid in the porous media. The total metal concentration remained inside the medium was 33.7 wt%, which is approximately 1.7 times higher than the amount obtained in the first test. This increase in the particle retention can be due to the increase in particle size due to particle aggregation which, in turn, caused pore plugging and subsequently reduced the particle transportation.

Particle aggregation occurred due to the increase in temperature which favored particle collision due to heavy oil viscosity reduction and subsequently higher aggregation rate (Nassar and Husein 2010). This supports that temperature plays a role on nanoparticles deposition inside the porous media. Table 2.5 shows the nanoparticles concentration mass balance for this test.

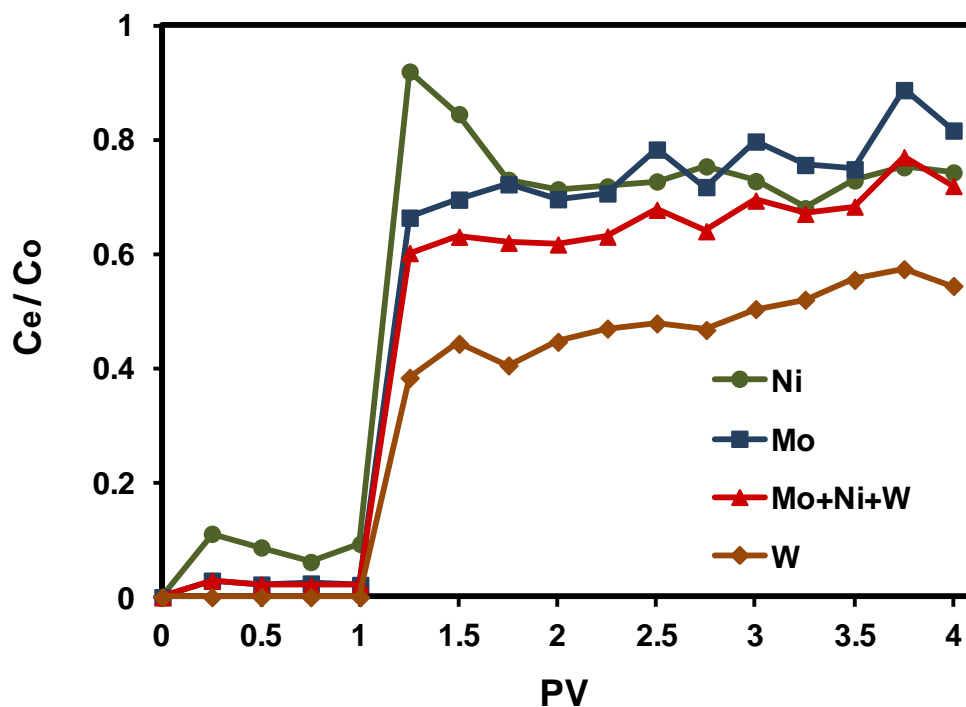


Fig 2.8: Breakthrough curves for experiments conducted with different nanoparticles of 34 ± 0.5 nm diameters suspended in VGO matrices in an oil sands packed bed column with clean silica sand of 12-20 mesh size saturated with Athabasca bitumen. Other experimental conditions include; residence time: 36 h, porosity: 32.9%, pressure: 3.5 MPa, and temperature: 320 °C

Table 2-5: Mass balance for the second test

Parameters	Values
Total injected nanoparticles (g)	0.0714
Total produced nanoparticles (g)	0.0489
Total (deposited + retained) nanoparticles (g)	0.0225
Total retained nanoparticles (g)	0.0031
Total deposited nanoparticles (g)	0.0194
(Retained+ deposited nanoparticles)/injected (wt%)	31.51
(Deposited nanoparticles/injected) (wt%)	27.11

Qualitative behavior of nanoparticles specific deposit into the sand grains is depicted in Figure 2.9. Clearly, concentration of nanoparticles decreased exponentially along the

reaction zone in agreement with the trend reported for the first test within the selected reaction time. However, the retention of nanoparticles at the entrance of the reactor column is much higher than the one observed in the first test. This again supports that the pore plugging has occurred due to particle aggregation. Further, the deposition of nanoparticles followed the order $Mo > W > Ni$, which is similar to the order observed in the first test.

Figure 2.10 shows the particle size distribution of nanoparticles samples taken at different PVs. Clearly, the average particle size in the produced samples is greater than the one in the feed. Further, no significant increase in the particle size can be observed at different values of PV, which suggests that particle aggregation had no effect on sand permeability during the residence time of this test.

It should be noted that, compared to the first test, the size of the deposited nanoparticles in the oil sands media for this test was larger as confirmed by ESEM measurements presented in Figure 2.11. This caused a slightly increase in the pressure drop as can be seen in Figure 2.12. Again, as seen in Figure 2.11, high population of deposited aggregated nanoparticles is appeared at the top of reaction zone and low population as well as smaller aggregates appeared at the bottom zone; in agreement with the ICP-AES and DLS measurements.

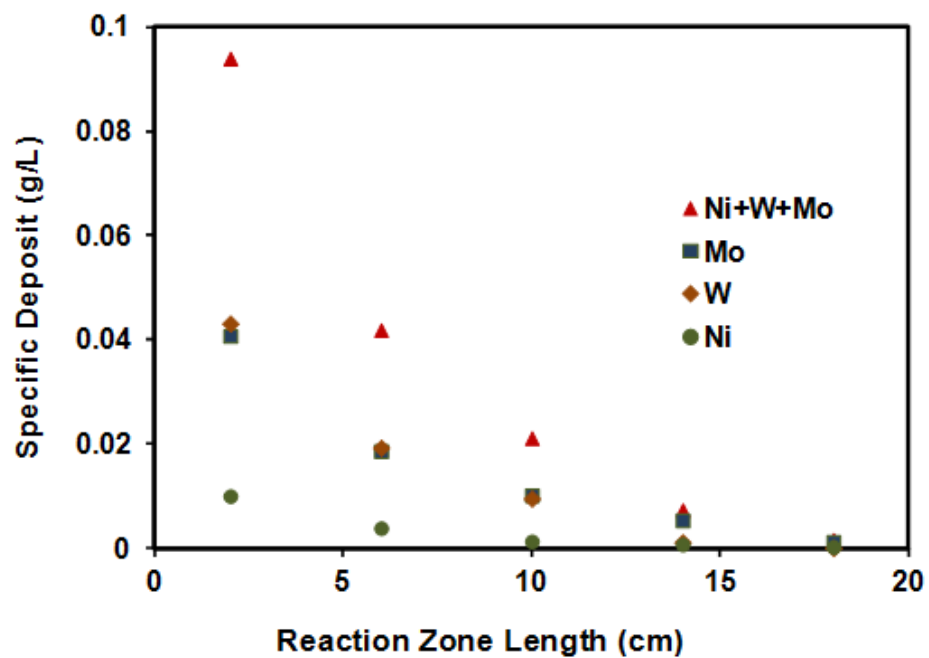


Fig 2.9: Calculated distribution of specific deposit of different nanoparticles at different bed depth (across the reaction zone) for time period of 36 h

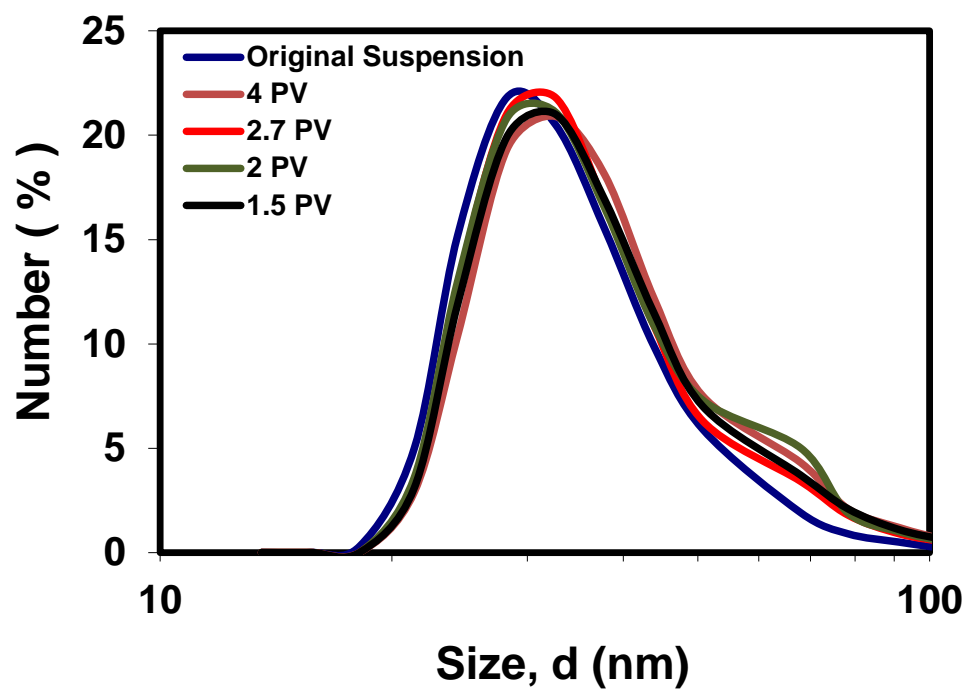


Fig 2.10: DLS characterization of colloidal nanoparticles size distribution in heavy oil matrix for original feed sample and samples obtained during the run of the second test at different values of PV

Figure 2.12 shows the pressure drop across the reaction zone against the PV. Despite a slightly higher pressure drop compared to Test 1, pressure drop profile across the reaction zone remained constant throughout the experiment, which again supports that the presence of nanoparticles inside the oil sands bed has no significant damage effect to the porous media.

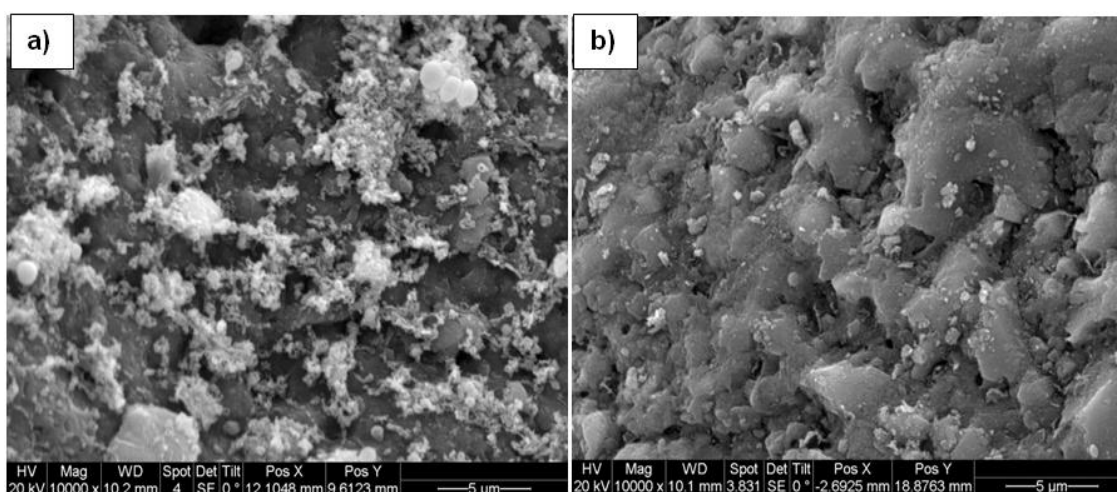


Fig 2.11: Microphotographs of Ni-Mo-W-nanoparticles deposited onto high permeability oil sands porous media at (a) top of the reactor column (b) bottom of the reactor column. Experimental conditions include; residence time: 36 h, porosity: 32.9%, pressure: 3.5 MPa, and temperature: 320 °C

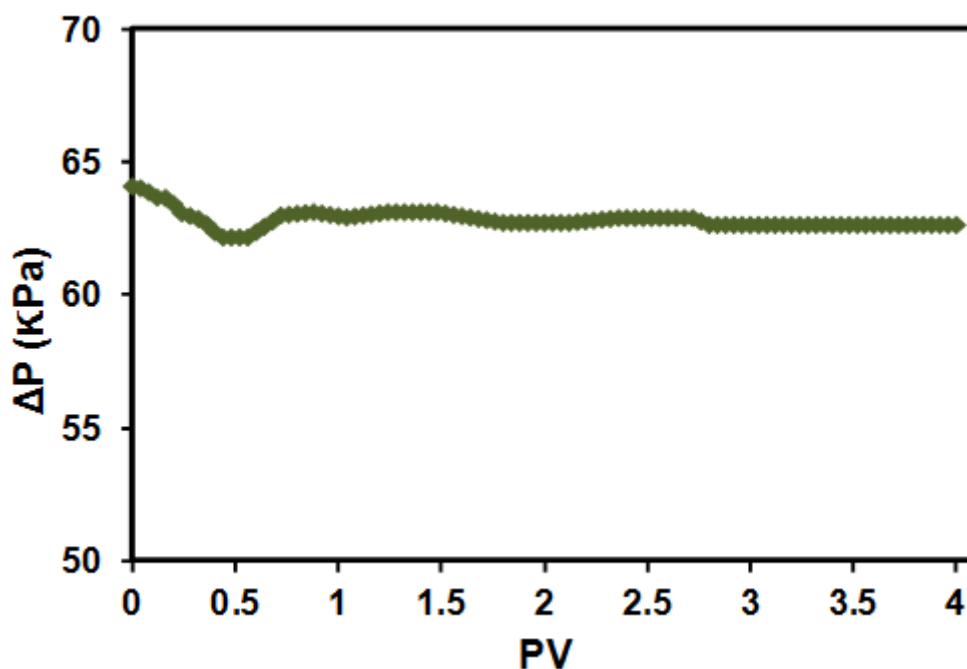


Fig 2.12: Pressure drop across the oil sands packed bed column during the run of the second test

2.4.2.3 Third test

First and second tests were performed in high permeability oil sands packed bed (~245 Darcy). However, permeability of a typical Athabasca bitumen reservoir is much smaller (Akin and Bagci 2001). To simulate the lower permeability conditions and study the effect of permeability on the transport behavior of nanoparticles, the conditions of this test run were kept similar to the one adopted in the first test, except the permeability was fixed at 9.6 Darcy (approximately 25 less than the one in the first test). Detailed experimental conditions can be seen in Table 2.3.

Figure 2.13 presents the normalized breakthrough curves of produced nanoparticles against PV in a low permeability oil sands packed bed. As seen, similar to the high

permeability oil sands, after 1.0 PV of injection, metal concentrations dramatically increased and rapidly reached a plateau, but it never reached to its feed concentration. Further, in all cases, the level of the plateau in the low permeability oil sands is lower than the one found in the high permeability oil sands (Figure 2.3), suggesting higher amount of remained nanoparticles inside the porous media occurred at lower permeability.

Calculated values for metal concentrations showed that about 51.7 wt% of W, 25 wt% of Ni and 25 wt% of Mo of inlet metal concentration remained inside the medium either as deposited or retained suspended inside the fluid in the porous media. The total amount of metal that remained in the medium was 49.35 wt%, which is much higher than the one reported at high permeability sand (first test). Also the amount of nanoparticles deposited on sand grains was approximately two times higher than the one for high permeability oil sands. Detailed mass balance calculations for this test are shown in Table 2.6.

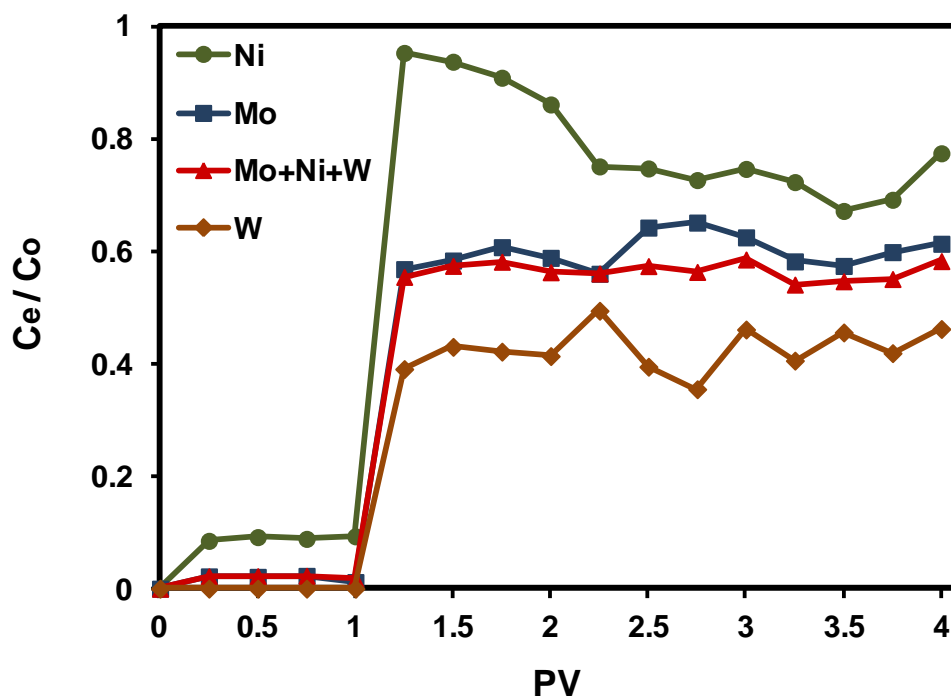


Fig 2.13: Breakthrough curves for experiments conducted with different nanoparticles of 34 ± 0.5 nm diameters suspended in VGO matrices in an oil sands packed bed column with clean silica sand of 100-140 mesh size saturated with Athabasca bitumen. Other experimental conditions include; residence time: 36 h, porosity: 33.2%, pressure: 3.5 MPa, and temperature: 300 °C

Table 2-6: Mass balance for the third test

Parameters	Values
Total injected nanoparticles (g)	0.0714
Total produced nanoparticles (g)	0.0362
Total (deposited + retained) nanoparticles (g)	0.0352
Total retained nanoparticles (g)	0.0111
Total deposited nanoparticles (g)	0.0241
(Retained+ deposited nanoparticles)/injected (wt%)	49.35
(Deposited nanoparticles/injected) (wt%)	33.82

Specific deposit behavior of nanoparticles into the sand surface is presented in Figure 2.14. As expected, high percentage of deposited nanoparticles were located at the

entrance of the reaction zone (i.e., near the injection zone). The deposition profiles for all metal nanoparticles followed the same trend of the previous tests, decreasing exponentially within the selected reaction time. However, specific deposit value was much higher than in the high permeable oil sands (the first test). For instance, the specific deposit at the entrance of the reaction zone in low permeability oil sands is approximately two times higher than the one of the high permeability oil sands.

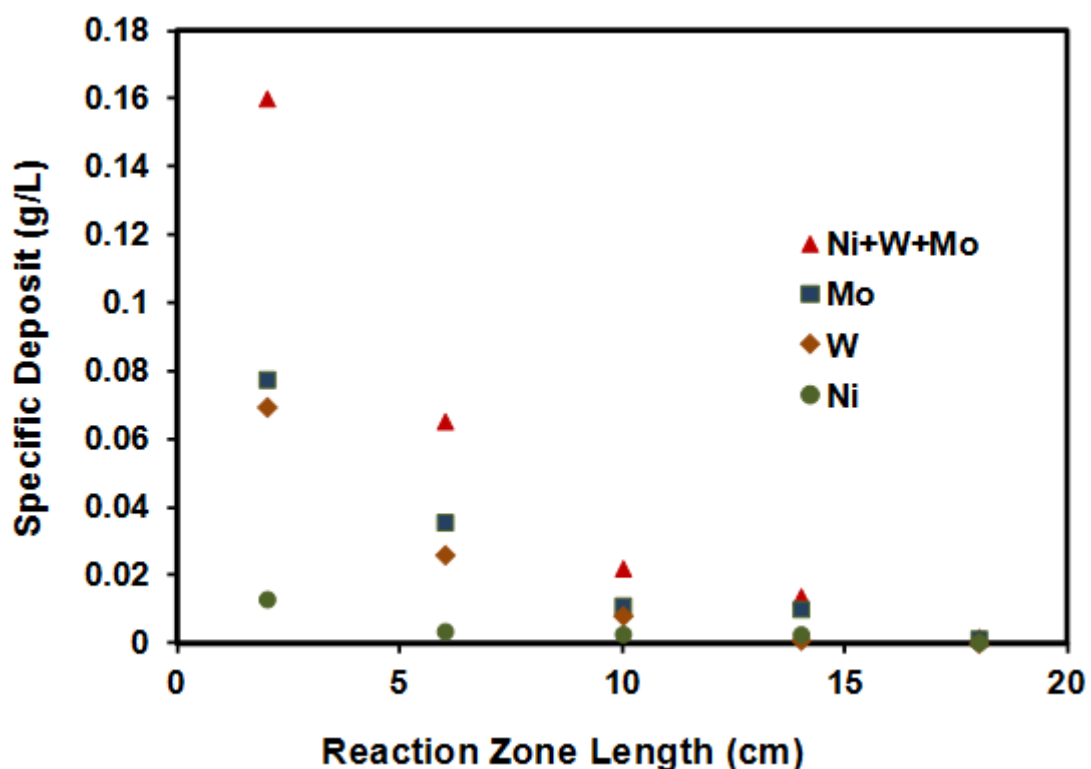


Fig 2.14: Calculated distribution of specific deposit of different nanoparticles at different bed depth (across the reaction zone) for time period of 36 h

It should be noted that, despite the high deposition rate of nanoparticles on sand media, no significant impact of nanoparticles on oil sands permeability could be observed. Figure 2.15 shows the pressure drop across the reaction zone against PV.

Except the very early time of test run, pressure drop across the zone remained constant during the experiment. This suggests a stable condition was maintained during the test run and there was no pore plugging or sand pack damage across the reaction zone. This again was supported by the DLS measurements shown in Figure 2.16, which represents the particle size distribution for different PVs during this test. Similar to the other tests, the average particle size in the effluent samples was greater than the one in the feed.

However, clearly no significant increase in the particle size can be observed for the samples taken at different values of PV, which again suggests that particle aggregation had no effect on the oil sands permeability during the residence time of this test. It is worth mentioning that the aggregation of nanoparticles deposited onto oil sand porous media in this test was greater than the one found at the same temperature in the first test as can be seen in Figure 2.17. This again supports that low permeability sand has higher deposition rate of nanoparticles than high permeability sand due to particle aggregation. Again, despite the high aggregation of nanoparticles at the top of reaction zone, nanoparticles could propagate through the sand packed bed column as smaller nanoparticles were observed at the production point, in agreement with the DLS measurements.

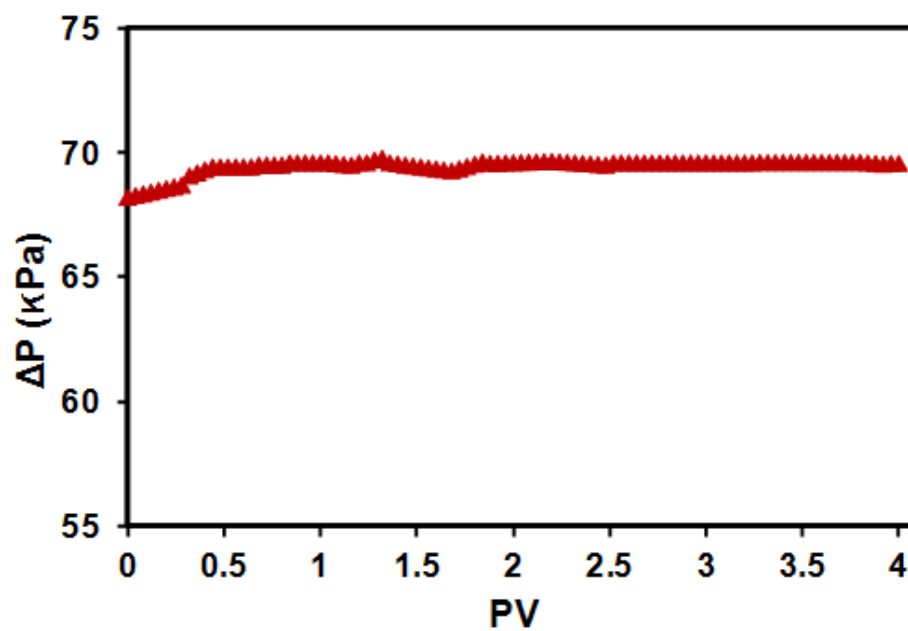


Fig 2.15: Pressure drop across the oil sands packed bed column during run of the third test

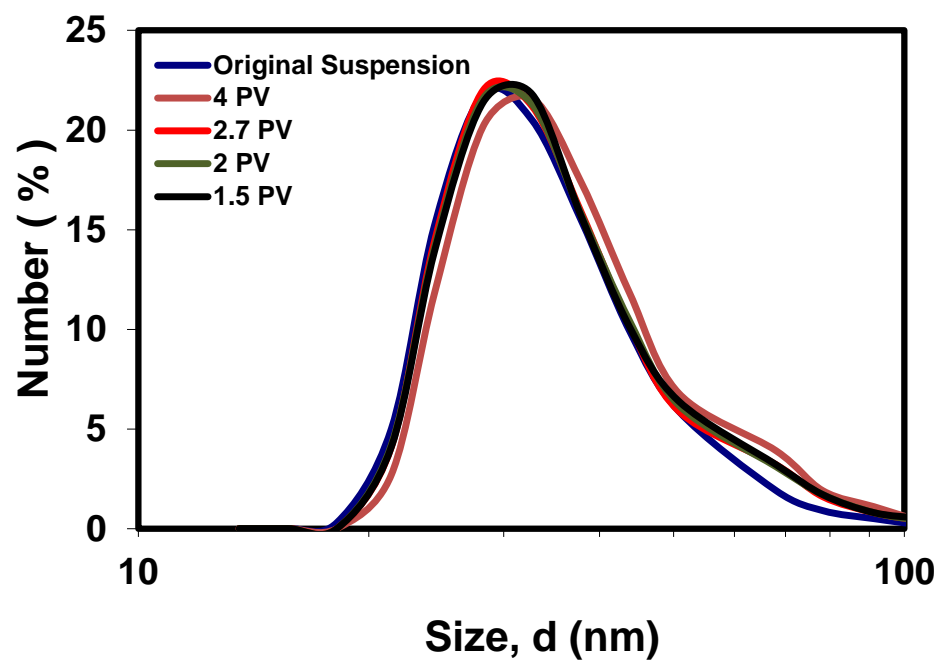


Fig 2.16: DLS characterization of colloidal nanoparticles size distribution in heavy oil matrix for original feed sample and samples obtained during the run of the third test at different values of PV

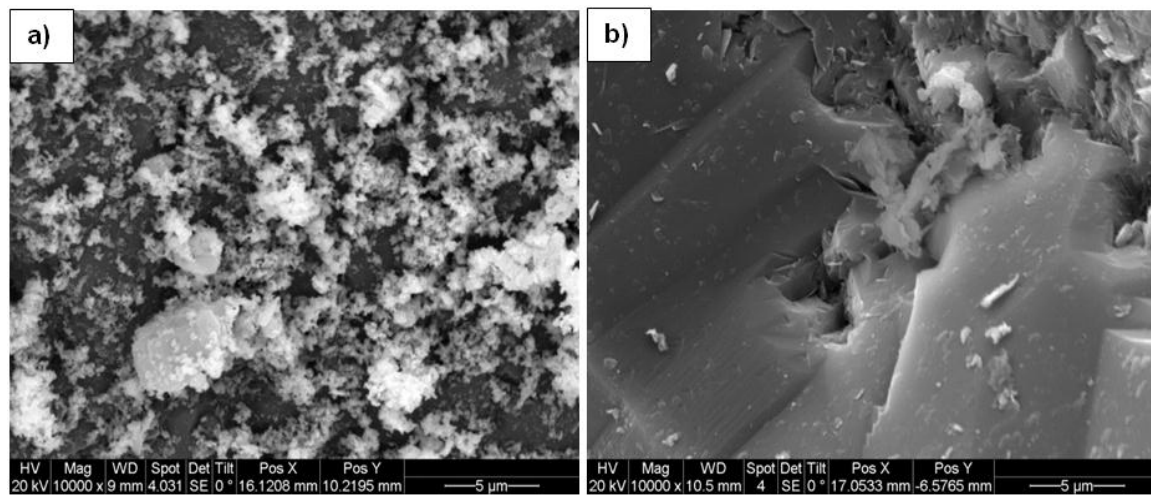


Fig 2.17: ESEM microphotographs of Ni-Mo-W-nanoparticles deposited onto low permeability oil sands porous media at (a) top of the reactor column (b) bottom of the reactor column. Experimental conditions include; residence time: 36 h, porosity: 33.2%, pressure: 3.5 MPa, and temperature: 300 °C

2.4.2.4 Fourth test

This test was mainly performed to investigate the effect of temperature on transport behavior of nanoparticles in low permeability oil sands packed bed column. Accordingly, the experimental conditions for this test were similar to the ones reported for the third test except that the temperature was fixed at 320 °C. Detailed experimental conditions can be found in Table 2.3.

Figure 2.18 shows the normalized breakthrough curves for different nanoparticles in low permeability oil sands packed bed. As expected, the effluent metal concentrations increased rapidly and reached a plateau after 1.0 PV of injection. Again, the levels of the plateau did not reach the original concentration and differed among the types of nanoparticles. Further, in all cases, the level of the plateau in this test is less than the one observed in the third test, indicating that the total amount of remained nanoparticles

inside the porous media has been increased during this test. Results of metal concentration analysis showed that 60wt% of W, 23 wt% of Ni and 44.3 wt% of Mo remained inside the oil sands packed bed column either as deposited or remained inside the fluid in the porous media.

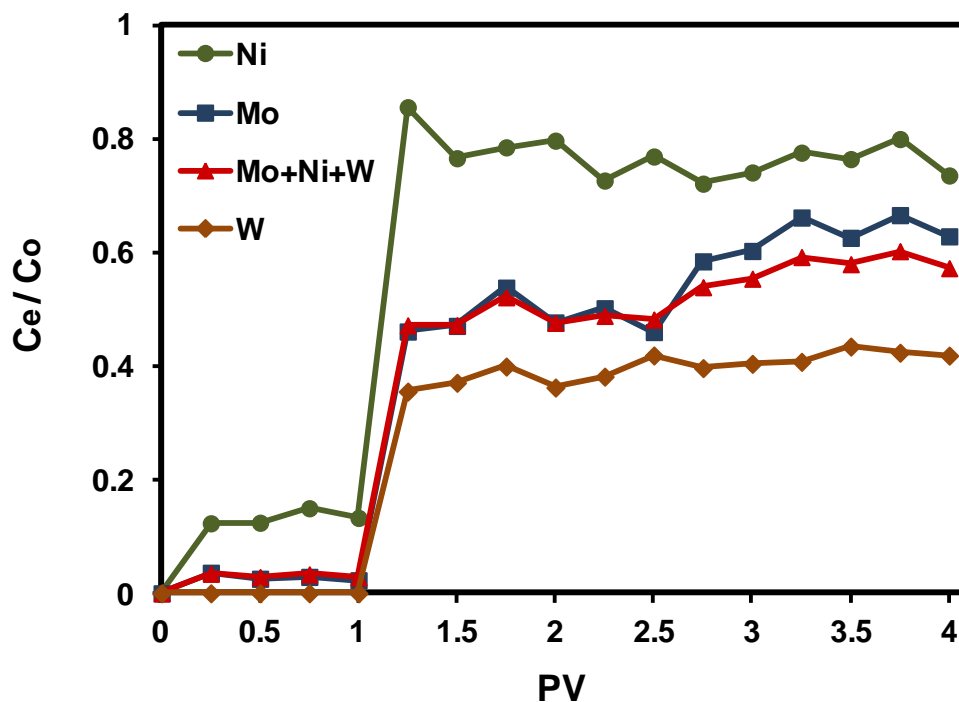


Fig 2.18: Breakthrough curves for experiments conducted with different nanoparticles of 34 ± 0.5 nm diameters suspended in VGO matrices in an oil sands packed bed column with clean silica sand of 100-140 mesh size saturated with Athabasca bitumen. Other experimental conditions include; residence time: 36 h, porosity: 33.7%, pressure: 3.5 MPa, and temperature: 320 °C

Table 2.7 shows the nanoparticles concentration mass balance in more details. Calculation results showed that 45.13 wt% of the total injected nanoparticles concentration remained inside the medium, among which 36.11 wt% of the total concentration was deposited onto the sand grains, which is slightly higher than the one

found in the third test. This again could be attributed to particle collision and aggregation due to the decrease in heavy oil viscosity in response to the temperature increase.

Table 2-7: Mass balance for the fourth test

Parameters	Values
Total injected nanoparticles (g)	0.0714
Total produced nanoparticles (g)	0.0392
Total (deposited + retained) nanoparticles (g)	0.0322
Total retained nanoparticles (g)	0.0064
Total deposited nanoparticles (g)	0.0258
(Retained+ deposited nanoparticles)/injected (wt%)	45.13
(Deposited nanoparticles/injected) (wt%)	36.11

Deposition behavior of nanoparticles in this test is portrayed in Figure 2.19. Similarly, in all cases, exponential deposition profiles were obtained within the selected reaction time. Again, the retention of nanoparticles was much higher at the entrance of the reaction zone and declined rapidly throughout the zone length. Deposition values in this test also confirmed that the slight reduction of sand pack permeability in comparison to the third test caused higher amount of particle retention inside the porous media.

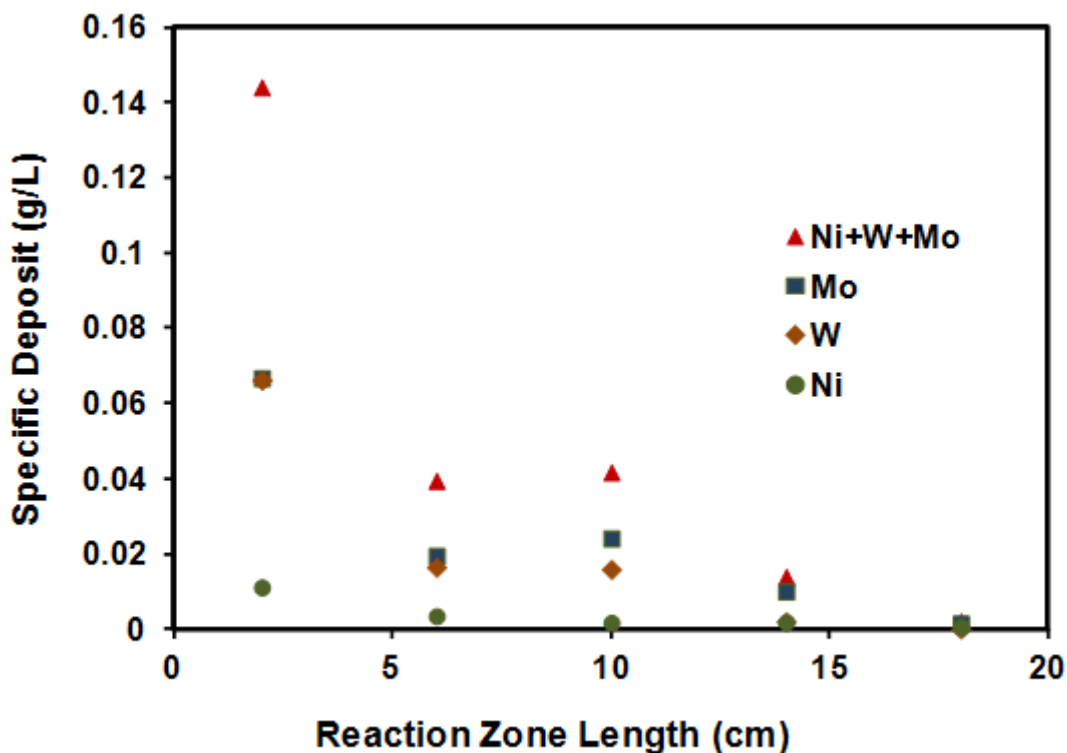


Fig 2.19: Calculated distribution of specific deposit of different nanoparticles at different bed depth (across the reaction zone) for time period of 36 h

Figure 2.20 shows the pressure drop profile across the reaction zone for this test. As seen, pressure drop across the reaction zone during the test run was almost steady and constant, which suggests no major permeability reduction or plugging during the test run occurred. As a support to this claim, DLS measurements for particle size distribution at different PVs were performed and presented in Figure 2.21. Clearly, no significant change in the average particle size was observed at different values of PV. However, the average particle size of samples obtained in this test was higher than the one obtained in the third test; suggesting the presence of high temperature inside the porous media

avored particle aggregation as explained earlier. This is further supported by the ESEM images shown in Figure 2.22.

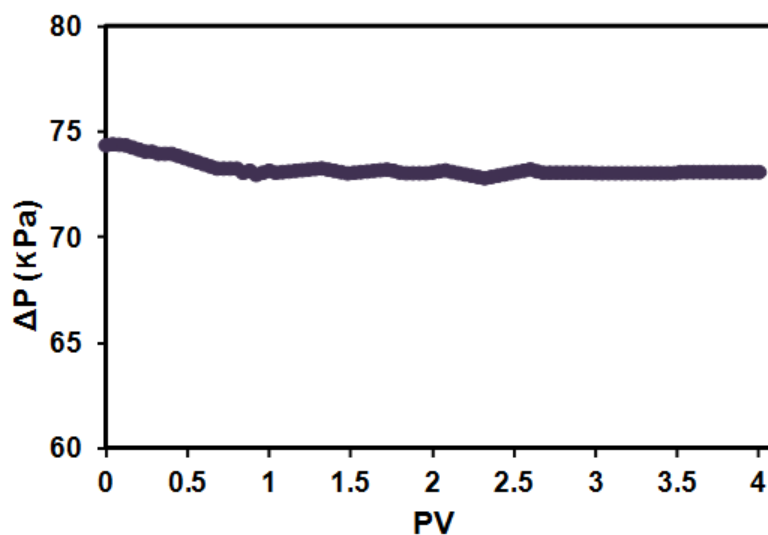


Fig 2.20: Pressure drop across the oil sands packed bed column during run of the fourth test

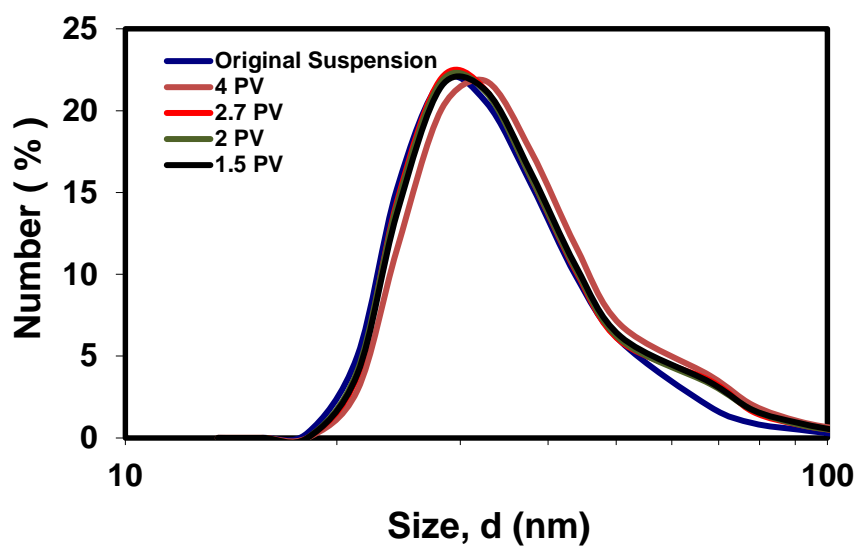


Fig 2.21: DLS characterization of colloidal nanoparticles size distribution in heavy oil matrix for original feed sample and samples obtained during the run of the fourth test at different values of PV

Figure 2.22 shows that there is a high population of aggregated nanoparticles in top of the reaction zone, while smaller aggregation appeared at the bottom of the reaction zone.

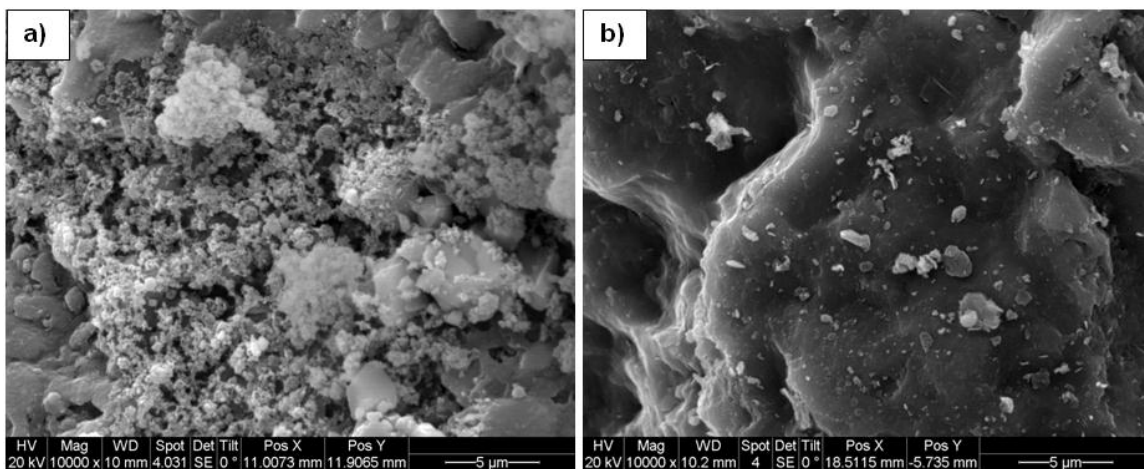


Fig 2.22: ESEM microphotographs of Ni-Mo-W-nanoparticles nanoparticles deposited onto low permeability oil sands porous media at (a) top of the reactor column (b) bottom of the reactor column. Experimental conditions include; residence time: 36 h, porosity: 33.7%, pressure: 3.5 MPa, and temperature: 320 °C

2.5 Conclusions

In this study, the transport behavior of ultradispersed multimetallic nanoparticles inside an oil sands packed bed column at high temperature and pressure has been investigated. The stabilization of the multimetallic nanoparticles in heavy oil matrices consisting of vacuum gas oil, VGO, and in house prepared surfactants was evaluated. Column experiments were mainly conducted in this study to evaluate the transport of ultradispersed multimetallic colloidal nanoparticles in two model bitumen saturated porous media. Particularly, different models of oil sands were employed to mimic the transport of nanoparticles in an oil reservoir during heavy oil recovery and upgrading for field application.

The effect of temperature and permeability on nanoparticles mobility in oil sands media was also evaluated. In all column experiments, aggregation of nanoparticles was observed. This was attributed to the increase in temperature, which favored particle collision due to heavy oil viscosity reduction and subsequently higher aggregation rate. Results showed that high permeability oil sands packed bed has lower amount of deposited particles compared to low permeability medium. Deposition of nanoparticles mainly occurred at the entrance of injection zone and rapidly decreased across the reaction zone. It appeared that the deposition tendency for nanoparticles is strongly affected by the type of metal, temperature, and sand permeability. Deposition of nanoparticles inside the porous media has a meager influence on medium permeability. Nonetheless, pressure drop analysis showed no major permeability damage across the reaction zone. Also, it should be noted that total mass of used nanocatalysts is very small number compared to total oil saturated the medium.

This study showed that ultradispersed multimetallic nanoparticles could be controllably delivered through oil sands porous media into a targeted heavy oil reservoir, where they could work as catalysts for heavy oil upgrading. The targeted transport depth can be achieved by manipulating a number of factors, such as injection temperature, pressure and flow rate.

Chapter 3 Enhanced Heavy Oil Recovery by In-Situ Prepared Ultra-Dispersed Multi-metallic Nanoparticles: A Study of Hot Fluid Flooding for Athabasca Bitumen Recovery²

3.1 Abstract

Many in situ recovery methods have been developed to extract heavy oil and bitumen from deep reservoirs. The approach of “Underground Refinery” by using nano-size ultra-dispersed (UD) catalyst is one of the alternatives to surface upgrading that may become the “next generation” of oil sands industry improvement. Water-in-vacuum gas oil microemulsion containing tri-metallic (W, Ni and Mo) ultradispersed colloidal nanoparticles could penetrate inside the porous medium and react with the bitumen. This study is aimed at developing a catalytic-enhanced oil recovery method for Athabasca bitumen recovery through the viscosity reduction mechanism with the aid of tri-metallic nanoparticles. In this study, series of experiments were conducted at a pressure of 3.5 MPa, residence time of 36 h, and temperatures from 320 to 340 °C in an oil sands packed bed column. Results of three consecutive categories of hot fluid injection (in the presence

² Hashemi, Rohallah, Nashaat N. Nassar, and Pedro Pereira-Almao. Enhanced Heavy Oil Recovery by In-Situ Prepared Ultra-Dispersed Multi-metallic Nanoparticles: A Study of Hot Fluid Flooding for Athabasca Bitumen Recovery. *Energy & Fuels* 27.4 (2013): 2194-2201.

or absence of tri-metallic nanoparticles) were presented. For the first category, the obtained experimental results showed that recovery curve for vacuum gas oil injection without nanocatalysts was at a plateau. In the second series of tests, observations proved that adding certain percentage of pentane enhanced the recovery performance of injection tests. The third phase of experiments was conducted in presence of tri-metallic nanocatalysts in emulsion with VGO. Results showed the effectiveness of nanocatalysts for enhancing the recovery performance compared with the cases where no nanoparticles were implemented.

3.2 Introduction

Heavy oil and bitumen are important hydrocarbon resources that play increasingly important role in the global economy (Alberta_Energy 1995). At the commercial scales, many in-situ thermal recovery methods have been proposed and developed to extract heavy oil and bitumen from deep reservoirs (Paitakhti Oskouei et al. 2010, Sharpe, Richardson, and Lolley 1995, Chu 1977, Weissman et al. 1996, Greaves, Xia, and Ayasse 2005, Liu et al. 2004, Butler and Mokrys 1991, Moore, Mehta, and Ursenbach 2002). These in-situ thermal recovery methods can be divided into two main categories, steam injection and in-situ combustion (Xu 2001).

In-situ thermal recovery methods resemble the recovery of conventional oil, whereby bitumen extraction is accomplished by drilling horizontal wells and consequently injecting steam or generating heat which reduces bitumen viscosity and allows it to flow to the surface. In steam injection process, known as steam-assisted gravity drainage

(SAGD), the steam is used as the heat carrier to reduce the viscosity of bitumen, and consequently reduce the flow resistance of bitumen through porous media which increase the cumulative recovery and production rate (Butler 1991a, Saskoil and Butler 1990).

For in-situ combustion, or “fire flood”, the heat is generated and propagated along the reservoir by igniting a part of the original heavy oil-in-place and subsequently reducing the viscosity of the unburnt bitumen, thereby improving its flow (Kok and Okandan 1995, Xu 2001). The high energy intensity and huge amount of water consumption, especially for SAGD process, as well as the low quality of produced bitumen through the in-situ thermal recovery processes pose challenges on the future deployment of the current technologies. Therefore, it is necessary to search for new ideas or alternatives in the field of in situ recovery to improve current technologies and make it environmentally sound and cost-effective.

In-situ upgrading of bitumen or heavy oil is an innovative environmentally friendly approach and recently is attracting considerable attention (Assessment June 2006, Almao 2012, Hashemi, Nassar, and Pereira Almao 2013c). This approach uses the reservoir as a high-temperature reactor and it is based on integrating the catalytic hydrogenation reaction with thermal recovery methods (Weissman 1997, Weissman and Kessler 1996, Weissman et al. 1996). The idea of underground refinery project is to use porous media as a chemical reactor with series of chemical reactions (i.e., hydrocracking, hydrotreating, etc) to improve the quality of produced heavy oil and bitumen (Weissman and Kessler 1996, Moore et al. 1999). This requires placement of the catalyst deep into the heavy oil plume by transporting a catalyst suspension through the sand medium.

In order to conduct a successful underground upgrading process several steps are considered to improve the quality of products (Weissman and Kessler 1996), namely: (1) presence of catalyst in formation or an appropriate zone near production well, (2) mobilization of reactants including heavy oil and co-reactants such as steam or hydrogen, and (3) creation of necessary processing conditions to achieve reasonable degree of upgrading (i.e., sufficient temperature and pressure). It should be noted here that several important underground heavy oil recovery and upgrading processes have been reported, which are implemented at the pilot plant and field scales. These include steam distillation and in situ upgrading processes (Sharpe, Richardson, and Lolley 1995), conventional fireflood field projects and dry combustion (Chu 1977), solvent-based in situ processes and propane deasphalting (Bohn 1988, Mokrys and Butler 1993, Duerkson and Eloyan 1995), thermal upgrading and visbreaking of heavy oil (Shu and Hartman 1986, Monin and Audibert 1988, Kasraie 1989), in situ hydrogenation and hydroprocessing (Dew and Martin 1965, Hamrick and Rose 1976, Stine 1984), Toe-to-Heel air injection (THAI) process (Greaves, Xia, and Ayasse 2005, Al-Honi, Greaves, and Zekri 2002), aquathermolysis (Jiang et al. 2005, Liu et al. 2004) and in situ combustion (ISC) (Belgrave, Nzekwu, and Chhina 2007, Moore, Mehta, and Ursenbach 2002, Paitakhti Oskouei et al. 2010).

The main mechanism of the in situ recovery and upgrading processes is to decrease bitumen viscosity and enhancing the liquid quality which subsequently improve productivity index of the producer well. In recent years, there has been extensive effort to create an economically efficient underground in-situ upgrading and recovery process for

unconventional oils such as heavy oil and bitumen. There are several advantages for underground upgrading processes such as: (1) capital cost reduction of lifting operation and transportation from downhole to refinery centre, (2) production of higher value energy by viscosity reduction, and (3) extremely low to zero environmental footprints due to reduction in contaminants level such as metals, sulphur content and waste hydrocarbons.

In situ upgrading using ultra-dispersed (UD) nanocatalysts is one of the promising options from both environmental and economical aspects, which may become the “next generation” of oil sands industry improvement (Hashemi, Nassar, and Pereira Almao 2013c). In this process, a suspension of ultra-dispersed nano-sized particles is injected into reservoir to upgrade heavy oil and bitumen. Nano-sized particles were chosen due to their unique properties, such as high surface area to volume ratio, high degree of dispersion in porous media, excellent adsorption affinity and high catalytic activity, etc (Nassar, Husein, and Pereira-Almao 2011b, Nassar, Hassan, and Pereira-Almao 2011b, c, Nassar, Hassan, and Pereira-Almao 2011a, Nassar, Hassan, and Pereira-Almao 2011d, Nassar et al. 2012). It should be noted here that the subject of down-hole upgrading by UD nanocatalysts is relatively new and consequently the available published literature data are limited.

UD nanocatalysts for hydroprocessing reactions were successfully developed in heavy oil matrix and subsequently tested in a batch reactor for Athabasca bitumen upgrading by our research group at the University of Calgary (Vasquez 2009, Nassar, Hassan, and Pereira-Almao 2011a). Experimental results showed that UD nanocatalysts

enhanced the upgrading of Athabasca bitumen by significantly increasing the hydrogen/carbon atomic ratio and reducing both viscosity and coke formation (Galarraga and Pereira-Almao 2010). In addition, a significant reduction of sulfur and micro carbon residue was observed. However, before any field test or industrial application of these in-situ prepared UD nanocatalysts it is deemed necessary to test their performance in a continuous flow mode. To better mimic the SAGD process conditions, a pilot plant setup is designed and constructed to simulate the major elements of SAGD reservoir, such as injection and production lines, oil pool (area between injector and producer in SAGD operation fields) and reservoir top.

The UD nanocatalysts were injected into the oil pool by hot fluid nanocatalysts carrier. The transport behavior of these multimetallic UD nanocatalysts in an oil sands-packed bed column at a typical SAGD temperature and pressure was investigated in our previous study (Hashemi, Nassar, and Pereira-Almao 2012). It was found that propagation of multimetallic UD nanocatalysts in oil sands media is feasible under a typical pressure and temperature of SAGD process, as neither major permeability reduction nor pore plugging were observed. This work is a continuation on our previous studies (Hashemi, Nassar, and Pereira-Almao 2012, Galarraga March 2011), and it aims at experimentally investigating the effect of UD nanocatalysts on the recovery enhancement of Athabasca bitumen in a one dimensional (1D) continuous flow oil sand packed bed column. The effect of nanocatalysts content in the porous media and temperature on extent of Athabasca bitumen upgrading and subsequent liquid quality

improvement shall be communicated in another study. The present work holds great promise for in-situ heavy oil recovery and upgrading.

3.3 Materials and methods

3.3.1 Fluids and chemicals

Silica sand was purchased from AGSCO (99% of SiO₂, AGSCO, NJ, USA) and used as a sand source for porous media fill up. Absolute permeability of about 250 Darcy was measured by using the sand size of 12-20 mesh (US Sieves) for packing the reactor. Porous medium was saturated with Athabasca bitumen (JACOS, Alberta, Canada). For pentane experiments, pentane (C₅H₁₂, 99%, Sigma Aldrich) was used as diluent and vaporizing component.

Vacuum Gas Oil (VGO) (Nexen, Alberta, Canada) which consists of heavy petroleum distillates cuts was used as nanocatalysts carrier into the porous media. Properties of the utilized Athabasca bitumen and VGO were reported in our previous study and are presented in Table 3.1 as a reference. The following precursors were used to prepare tri-metallic nanocatalysts, namely: nickel acetate tetrahydrate (99%, Sigma-Aldrich), ammonium metatungstate (99%, Sigma-Aldrich), and ammonium molybdate tetrahydrate (99%, Sigma-Aldrich). Carbon disulphide (99%, Sigma-Aldrich) was used to prepare the produced liquid samples for simulated distillation analysis. Utilized gases for experiments including nitrogen, helium, hydrogen, air and argon were provided by Praxair Specialty Gases & Equipment (Calgary, Alberta, Canada).

Table 3-1: Properties of Athabasca bitumen and Nexen VGO used for experiments

Property	Bitumen	VGO
Viscosity at 40 °C, (cP)	7550	122.314
API gravity, (°API)	9.5	19.1
Microcarbon Residue, (wt %)	12	NA
H/C (atomic ratio)	1.52 ± 0.001	NA
Sulfur, (wt %)	4.25	2.73
<i>Distillation Cuts, (wt %)</i>		<i>Distillation Cuts, (wt %)</i>
Naphtha: IBP- 213 °C	2.76 ± 0.29	IBP- 235 °C 10.92
Distillates: 213 - 343 °C	14.89 ± 0.81	235 - 280 °C 7.97
VGO: 343 - 545 °C	34.68 ± 1.81	280 - 343 °C 16.60
Residue: >545 ⁺ °C	47.95 ± 1.57	Residue: >343 ⁺ °C 64.51

3.3.2 Preparation of nanocatalysts suspension

Water-in-vacuum gas oil microemulsion method was employed for preparing nanocatalysts suspension (Nassar and Husein 2010, Husein et al. 2010) (Eriksson et al. 2004, Nassar 2010, Husein and Nassar 2008, Nassar and Husein 2007a, b). Details on the preparation procedure of colloidal tri-metallic nanocatalysts in VGO have been described in our previous studies (Zekel' et al. 2007, Thompson et al. 2008, Vasquez 2009). Figure 3.1 shows a schematic of nanocatalysts preparation algorithm. In brief, preparation of nanocatalysts suspension was started by mixing 99.57 wt % VGO and 0.43 wt % HLB-8 surfactant at 700 rpm and 60 °C, and then the mixture was stirred for about 30 min to reach stability.

Aqueous solutions of the corresponding metallic precursors were added to the mixture and then agitated for about 30 min at 60 °C. Mixture of metallic precursors, surfactant and VGO was kept for 8 h at a high temperature and under low stirring (200 rpm) to evaporate the water (down to at least 0.5 wt %) and subsequently initiate nucleation and growth of tri-metallic nanoparticles, which remained stable in suspension

(Zekel' et al. 2007, Thompson et al. 2008, Vasquez 2009). Table 3.2 shows the concentration of tri-metallic nanocatalysts used in this study as well as percentages of water and surfactant. The atomic metallic ratios (metal/total metal) were as follows: Mo = 0.6267, Ni = 0.1808 and W = 0.1924.

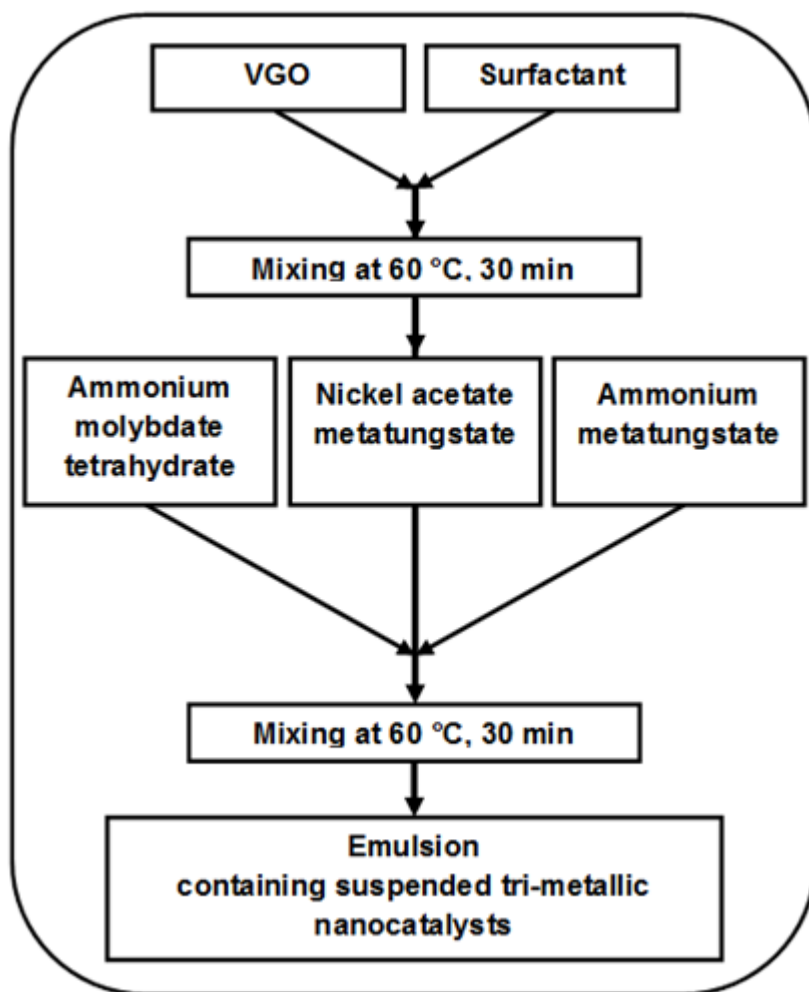


Fig 3.1: Schematic representation of colloidal tri-metallic nanocatalysts preparation algorithm

Table 3-2: Concentration of colloidal tri-metallic nanocatalysts in the feed

Metal content of nanocatalysts suspension			
Component	ppm	Additives	
Ni	72	Component	Percentage (with respect to oil)
Mo	240	Water (wt%)	2.11
W	408	Surfactant (HLB-8)	0.43

3.3.3 Experimental set-up

Schematic of the experimental setup can be seen in Figure 3.2, which mainly consists of the following elements: reserve tanks; vertical stainless steel reactor covered by insulators; Isco pumps (Teledyne Isco, NE, US) for injection of hot fluid into the medium as well as saturating the porous media with Athabasca bitumen; nitrogen and hydrogen gas cylinders for pressurizing and saturating the free radicals, gas analysis instruments and produced samples collectors.

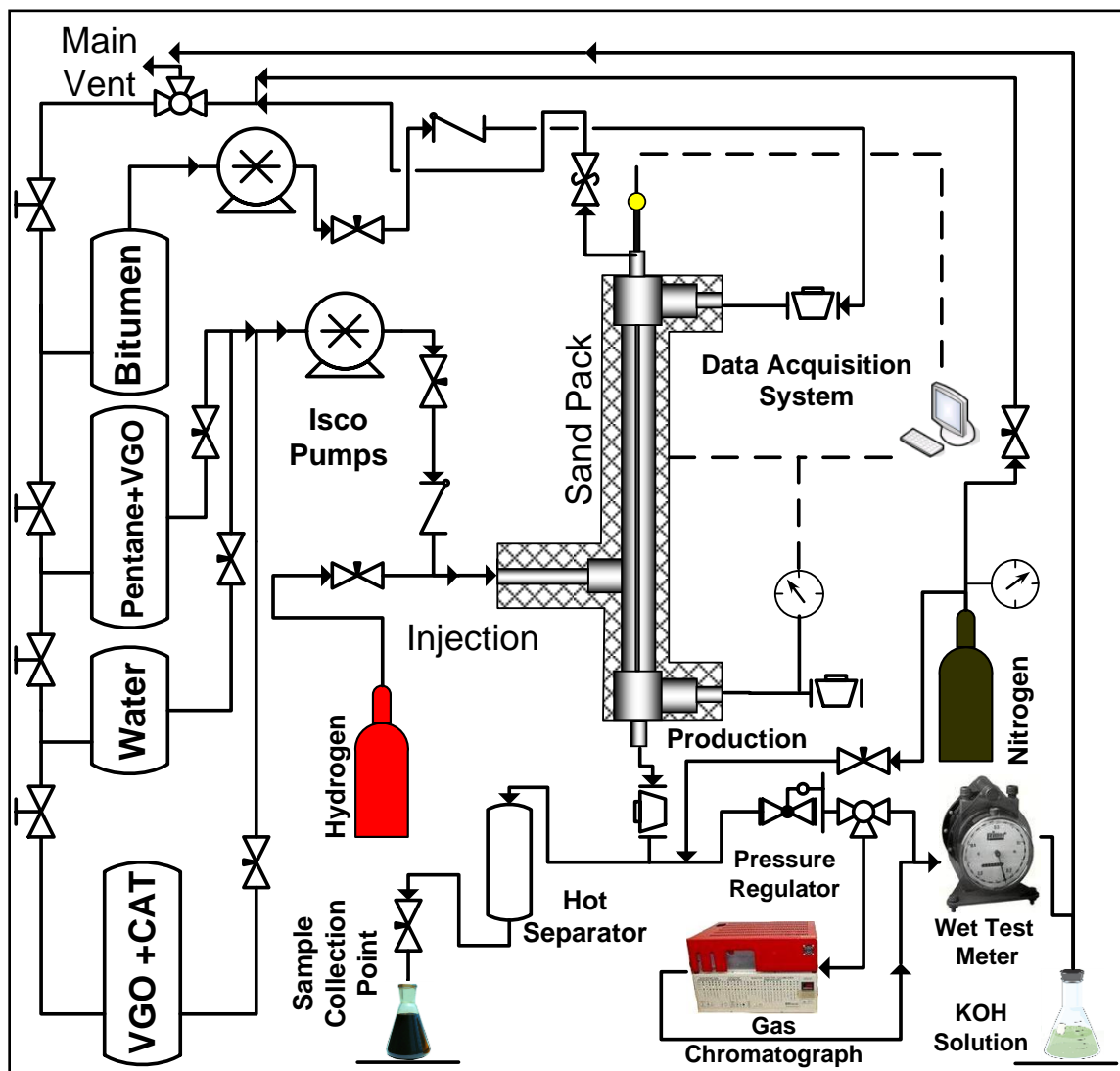


Fig 3.2: Schematic representation of the experimental setup

The reactor column is made of stainless steel and has 90 cm height and 2.16 cm inner diameter. Reserve tanks were used to contain all injecting fluids before injection inside the medium. To help filling the pumps, all liquids except water were maintained under low nitrogen pressure. Hot fluids (VGO containing nanocatalysts, steam, and mixed VGO) were injected individually inside the porous media via a hot fluid generator into the top section of oil pool (lower part of the sand pack column).

All fluids were heated to the test temperature by covering the hot fluid generator with heating tapes. Hot fluids were injected from injection point and after entering inside the medium affect the contained fluids of porous media and subsequently enhance the production of heavy liquids from the production point. To monitor the temperature inside the reactor, a special designed 10-point thermocouple was placed in the middle of packed bed reactor and fixed by two mesh rings at top and bottom of the reactor. Isco pumps were used to inject liquids with the desired rates inside the medium. Produced liquids from porous media were collected inside a hot separator (500 cm³) and at certain time intervals were transferred to sampling containers for post mortem analysis.

Hydrogen was used during the injection process to saturate the free radicals (coming from thermal cracking of heavy oil) and to reduce the possibility of coke formation as well as plugging of the reactor. Nitrogen as an inert gas was used to purge and pressurize the lines at the start of experiments. All produced gases from porous media were passed through the wet test meter and gas chromatography to measure rates and compositions.

3.3.4 Experimental procedure

Preparation of porous media for experiments was started with washing the silica sands by deionized water to remove dust, cement, tiny particles and any kind of impurities that may exist within the sands provided by vendor. Washed sands were kept inside a vacuum oven for 24 h at 60 °C to be dried. About 452 g of dried and cleaned sands were used to fill the stainless steel column reactor for each experiment.

To avoid sand production, three mesh rings were used in the top, bottom and entrance of injection point. Test temperature was provided by using special type of heating tapes installed at the outside body of the reactor. At the same time, the reactor body was covered by fiber glass casing to reduce the heat loss. Nitrogen was also used for purging the system until oxygen disappeared completely, as confirmed by the gas chromatograph (GC).

To ensure the integrity of the system for the experiments, leak test was performed by pressurizing the packed bed reactor with nitrogen up to 5.5 MPa. A 1% change in pressure per hour was considered as the maximum allowable pressure reduction during the leak test. After that, the reactor pressure was reduced to 3.5 MPa and then the column was heated to the desired temperature while maintaining the pressure at 3.5 MPa. When the reactor column working pressure and temperature were attained, approximately 5 pore volumes of Athabasca bitumen were first injected through the column in the down-flow mode to displace the water and saturate the bed with bitumen to simulate the oil sands conditions. Residual water saturation of the porous media was measured about 3-4%.

The actual experiment started by switching of the inlet gas from pure nitrogen to a hydrogen feed and introducing the injecting fluid (VGO containing nanocatalysts). At this point, the zero reaction time for recovery and upgrading experiment was considered. The run was conducted until approximately 100 cm³ of VGO containing nanocatalysts was injected into the porous media.

During the tests and at different time intervals, the produced liquid sample was taken for analysis and the produced gas was taken from the bottom of the reactor column to be

analyzed by the GC. At the end of the run, the reactor column was vented and cooled to room temperature, and the solid products (packed media) were carefully discharged from the reactor column for analysis. After that, the column and assembly were washed with toluene, soap and hot water; therefore, the apparatus could be ready for another cycle of experiments.

3.3.5 Analytical methods

To confirm the extent of recovery enhancement, different characterization techniques were implemented to analyze the produced liquid streams. In this part of study, the produced liquid samples were analyzed using standard characterization techniques as follows: (a) water content in produced liquid was measured by the Karl Fischer titration method using Mettler- Toledo model DL-32 (A. Daigger & Company, Illinois, USA); (b) residue content ($545\text{ }^{\circ}\text{C}^+$) was estimated following ASTM procedure (D7169-2005) by using high-temperature simulated distillation (HTSD) that was carried out in a Agilent GC (Mississauga, ON, Canada) following the method developed by Carbognani et al (Carbognani et al. 2007).

In case of steam injection test, water content of the produced stream was quantified using Dean-Stark distillation method (Dean and Stark 1920). Figure 3.3 shows a schematic representation of Dean-Stark distillation unit which is used for water-bitumen separation. In this method, produced liquid samples (water + bitumen) were mixed with excess toluene and then the mixture was transferred into a boiling flask. To avoid any bubble bumping, small amount of boiling chips were added into the mixture and then boiling flask was heated by an electrical mantel.

Vapors of water and toluene passed through the fractionating column and after cooling condensed on the condenser wall. All condensates dripped down into the graduated burette with a distinct phase level between organic and aqueous phases. Continuous heating of the flask was caused to fill the burette up and overflowing of the collected condensates. Since the top phase of the burette column was toluene, it was recycled into the flask and the cycle of extraction continued until no water could be seen inside the column.

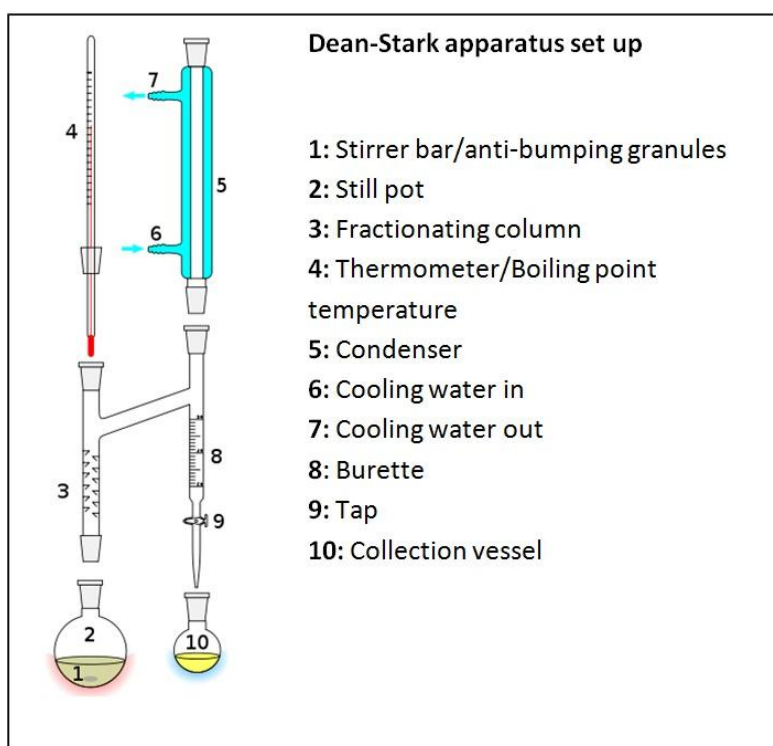


Fig 3.3: Schematic representation of the Dean-Stark distillation unit setup (Dean and Stark 1920)

3.4 Results and discussion

The main goal of this study was to investigate the effectiveness of ultra-dispersed nanocatalysts for enhancing the recovery of Athabasca bitumen in an oil sand packed bed column. The experiments were conducted in a consecutive order to apply a systematic approach for the study. Results of eight experiments are presented in this paper.

Table 3.3 shows the specifications of the tests considered in this study. It should be noted that reactor pressure, hydrogen flow rate, initial hot fluid injection rates and medium permeability were kept fixed for all tests. First test was conducted by steam injection into the porous media to ensure that the selected sands can represent a typical SAGD reservoir. Two next tests were considered as control tests, without tri-metallic nanocatalysts, to evaluate the recovery performance in absence of the tri-metallic nanocatalysts. After that, Tests 4, 5 and 6 were conducted to evaluate the presence of a light solvent at different mass fraction in VGO matrix as injecting fluid. Last two tests were performed at different temperatures in the presence of tri-metallic nanocatalysts to study the effect of temperature on the recovery enhancement.

The results of these tests are presented as recovery curves to evaluate the effectiveness of different type of hot fluid on recovery enhancement. It is worth noting that the steam injection test was performed in a lower permeability sand pack (Absolute permeability about 10 Darcy) as well. However, in low permeability media steam chamber growth was very weak and the presented recovery curve was not matched with a typical SAGD reservoir performance. This was the reason that high permeability sands were selected in the current study.

Table 3-3: Specifications of the experimental tests considered in this study

Test Number	1	2	3	4	5	6	7	8
Injecting liquid	Steam	VGO	VGO	Pentane (5 wt %)	Pentane (10 wt %)	Pentane (15 wt %)	VGO +CAT	VGO +CAT
Temperature (°C)	243.5	320	340.0	340.0	340.0	340.0	320.0	340.0
Pressure (MPa)	3.5	3.5	3.5	3.5	3.5	3.5	3.5	3.5
Porosity (%)	33.0	33.1	33.2	33.1	33	33.4	32.9	33.2
Absolute Permeability (Darcy)	243.9	246	245.3	240.7	242.5	244.5	244	244.7
Nominal Particle Concentration (ppm)	0.0	0.0	0.0	0.0	0.0	0.0	720	720.0
Residence Time (h)	NA	36.0	36.0	36.0	36.0	36.0	36.0	36.0
Hot Fluid Injection Rate (cm ³ /min)	NA	0.01	0.01	0.01	0.01	0.01	0.01	0.01
Hydrogen flow rate (cm ³ /min)	NA	1.0	1.0	1.0	1.0	1.0	1.0	1.0

3.4.1 Flood of saturated porous media by steam

To evaluate the porous media, steam injection test was carried out by using the same sand for the nanocatalysts experiments. Before steam injection, porous medium was saturated by Athabasca bitumen. The main reason was to ensure that this model has the same recovery performance as a typical SAGD process. Experimental temperature of 245 °C (steam quality of 100%) was used, as it corresponds to the steam saturation temperature at 3.5 MPa. Figure 3.4 shows steam oil ratio (SOR) and percentage of Athabasca bitumen recovery at different times. As seen, the SAGD performance is quite reasonable based on cumulative recovery (about 50% of IOIP) and steam oil ratio. Although SOR is higher than a typical SAGD process, which is expected because of compensation for high amount of heat loss occurring from the reactor wall

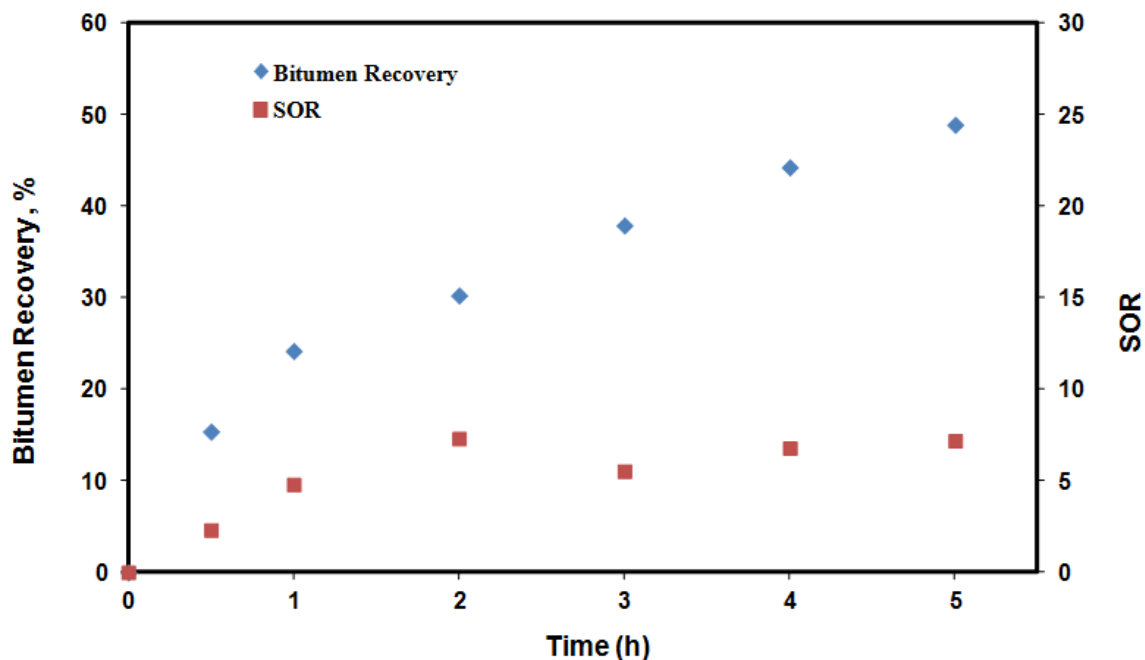


Fig 3.4: Recovery performance and SOR of steam injection into the high permeability sand packed bed at pressure of 3.5 MPa, steam injection rate of 1 cm³/min, and temperatures of 243.5 °C

The findings of this experiment show that by using the sand size of 12-20 mesh (US Sieves) and designed reactor height, a typical SAGD configuration was simulated. Higher permeability of the medium is a compensation for the lower height of the reactor compared with a real bitumen reservoir.

3.4.2 Hot fluid flood study

To evaluate the effectiveness of nanocatalysts on enhancement of the Athabasca bitumen recovery, series of experiments were conducted in the sand pack. With these tests, the incremental oil recovery of different injection scenarios was obtained, and in each test the effect of one parameter on the recovery curve was studied. First series of tests were conducted in the absence of nanocatalysts while the last two tests were performed in the

presence of nanocatalysts. Produced fluids were analyzed by standard techniques to determine the bitumen content and to demonstrate the recovery curves.

3.4.2.1 Hot VGO injection

As a blank or control experiment (i.e., in the absence of nanocatalysts), Nexen VGO was injected inside the medium saturated with Athabasca bitumen at 3.5 MPa, and different temperatures of 320 and 340 °C. Figure 3.5 shows the production percentage of IOIP against the injection time. As seen, cumulative bitumen production curve increased with time and leveled off after approximately 95 hours. Analysis of produced liquid showed no trace of bitumen in the sample collected after 95 hours. This indicates that, after depletion of oil pool region, all produced liquid was mainly VGO, and injection of hot steam was not effective on the recovery enhancement. Moreover, temperature shows slightly significant effect on the bitumen production from porous media.

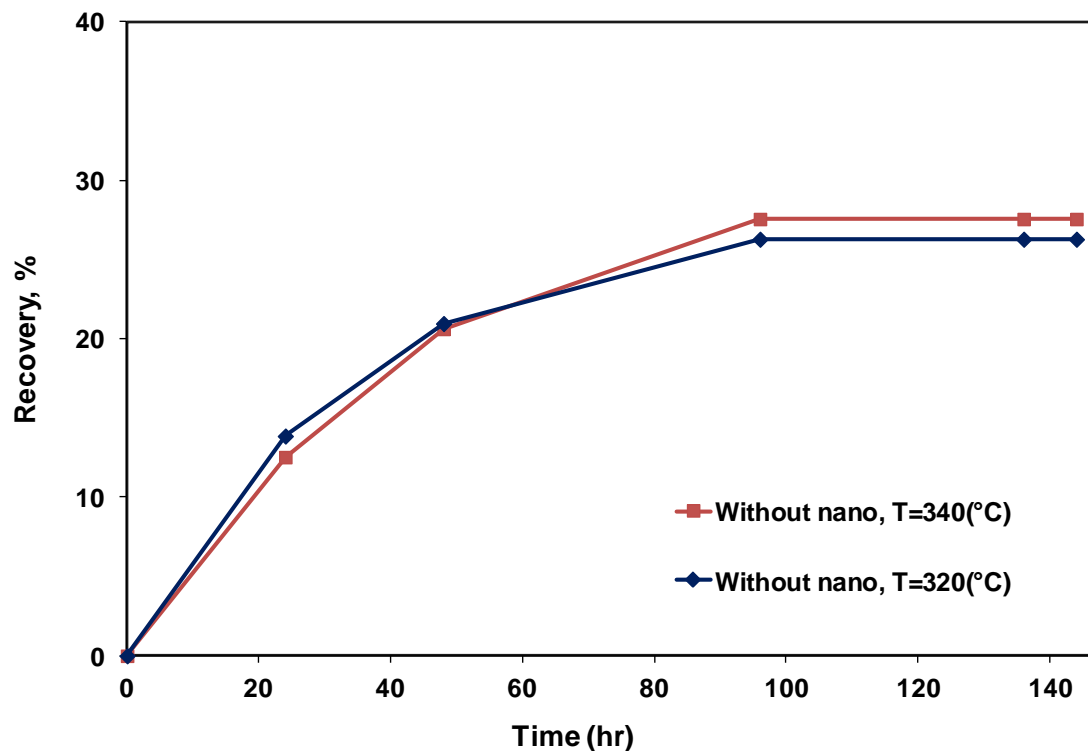


Fig 3.5: Performance of VGO injection into the high permeability sand packed bed at different times in the absence of tri-metallic UD nanocatalysts at pressure of 3.5 MPa, VGO injection rate of 0.01 cm³/min, hydrogen flow rate of 1 cm³/min, and temperatures of 320 and 340 °C

3.4.2.2 Effect of light pentane injection

Presence of light hydrocarbon in injection stream enhances the production of heavy hydrocarbon deposit. To evaluate the effect of light hydrocarbon component (light solvent) on recovery of bitumen, three sand pack flood tests were carried out at 3.5 MPa, temperature of 340 °C, and different mass percentage of pentane (5%, 10% and 15%). Figure 3.6 shows the recovery curves for this set of experiments. Clearly, oil recovery increased with increasing solvent concentration.

The lowest recovery was attained for the experiment conducted with 5 wt% pentane in the injection fluid and the highest recovery was attained for 15 wt% pentane test. This is expected as pentane acts as a diluent for bitumen as well as vaporizing component, so increasing pentane concentration will favor the reduction of bitumen viscosity and subsequently enhance its mobility, which in turn, results in higher recovery. More importantly, in comparison with the control experiments, Figure 3.6 shows that the recovery is increased and shifted up from the level plateau stage. Furthermore, with careful observations on the trend recovery curves, it was concluded that after depletion of oil pool, production of bitumen continues from the upper section of oil pool.

Mechanism of enhancement could be related to expansion of solvent and consequent viscosity reduction of Athabasca bitumen. Nevertheless, it should be noted here that the high cost of solvent-based process makes it challenging for future application, as solvent price is an important factor to select the percentages of mixture (Ananth Govind et al. 2008).

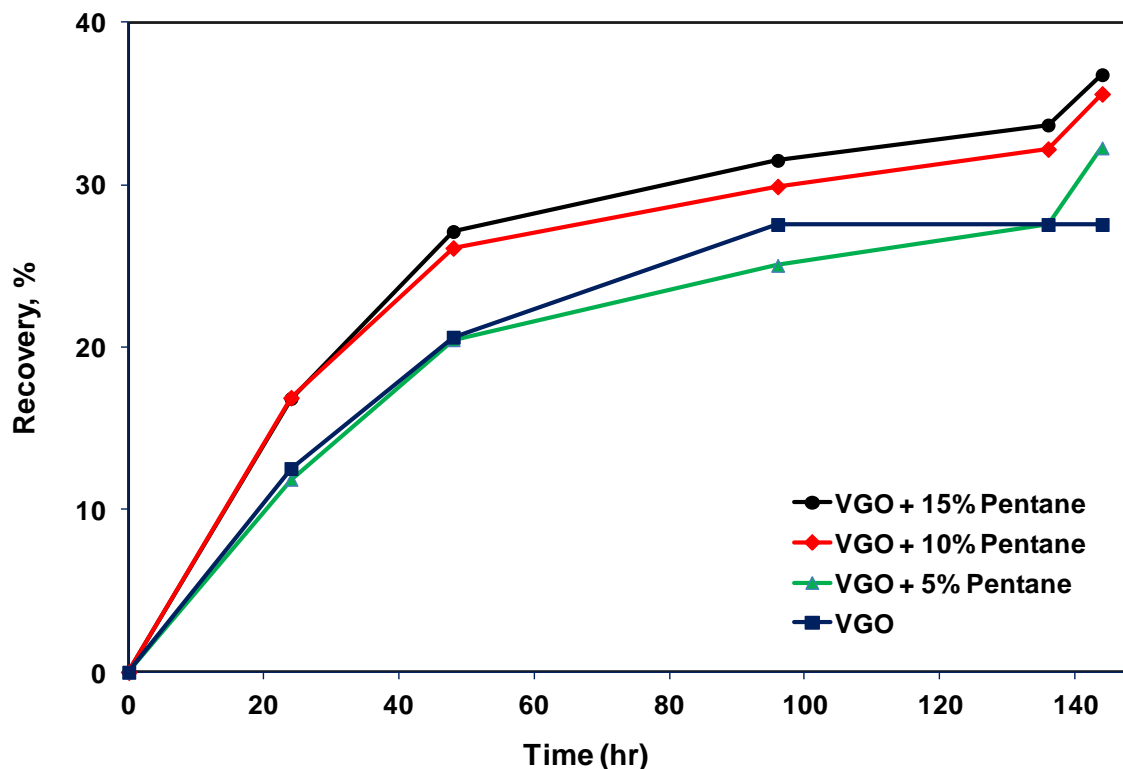


Fig 3.6: Recovery performance of mixed VGO and pentane (0 wt%, 5 wt%, 10 wt% and 15 wt%) injection into the high permeability sand packed bed at different times in the absence of tri-metallic UD nanocatalysts at pressure of 3.5 MPa, hot fluid injection rate of 0.01 cm³/min, hydrogen flow rate of 1 cm³/min, and temperatures of 340 °C

3.4.2.3 Effect of nanocatalysts

Since the bitumen recovery was enhanced by light hydrocarbon injection and our previous study for a batch experiment mode showed that UD nanocatalysts enhanced the upgrading of Athabasca bitumen by significantly increasing the hydrogen/carbon atomic ratio and reducing both viscosity and coke formation (Galarraga and Pereira-Almao 2010). This phenomenon was used to implement nanocatalysts injection concept inside the porous media, as it is anticipated that the produced light liquid as well as emitted gases during the upgrading will contribute to bitumen viscosity reduction and

subsequently enhance its recovery as well as upgrading from the oil pool. Therefore, to evaluate the effectiveness of nanocatalysts present inside the porous media, two sets of experiments were conducted at the same conditions of control experiments except certain concentration of nanocatalysts was added to the injecting fluid.

Details of nanocatalysts concentration was demonstrated in Table 3.2. Tests were performed at pressure of at 3.5 MPa and temperatures of 320 and 340 °C. Figure 3.7 shows the bitumen recovery as a function of the injection time. As seen, recovery of bitumen increased with time and continues until the end of the experiments. It should be noted that the observed trends were similar to the experiments conducted with pentane injection. It can be interpreted that the presence of nanocatalysts inside the medium caused the production of lighter components via catalytic hydrocracking which were confirmed with the analysis of produced gas from porous media. In addition, higher temperature experiments showed higher ultimate recovery.

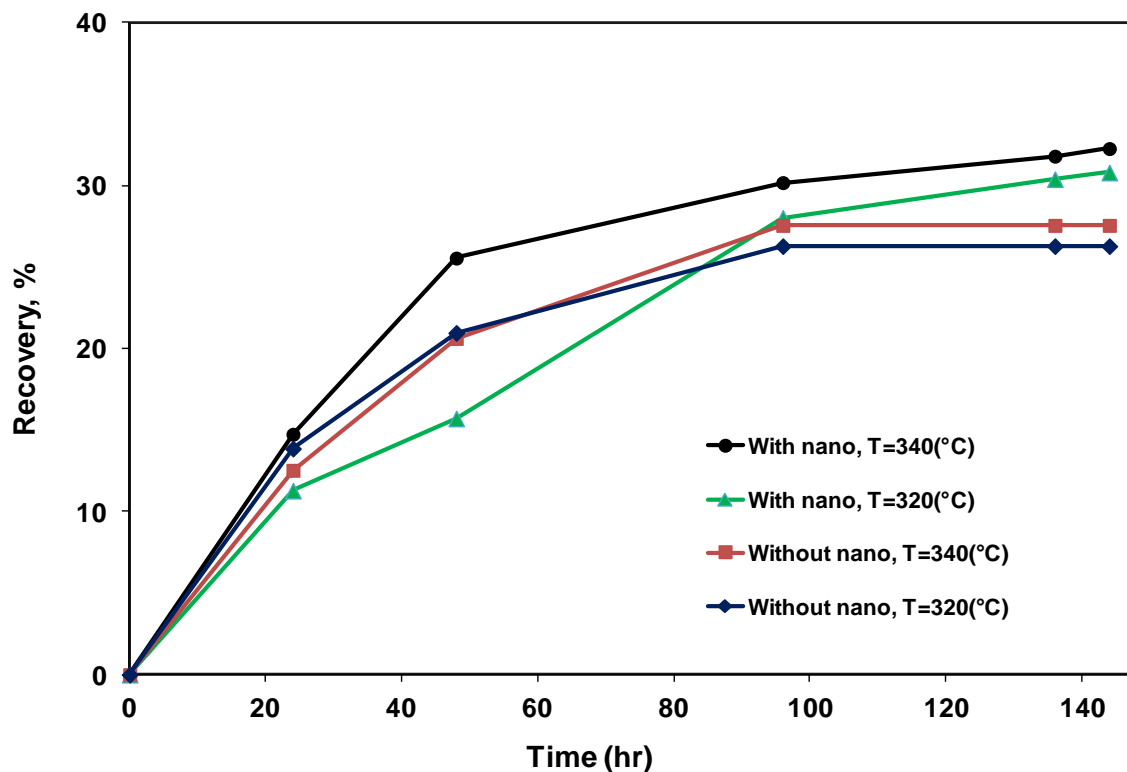


Fig 3.7: Recovery performance of hot VGO injection into the high permeability sand packed bed at different times in the presence of tri-metallic UD nanocatalysts at pressure of 3.5 MPa, hot fluid injection rate of 0.01 cm³/min, hydrogen flow rate of 1 cm³/min, and temperatures of 320 and 340 °C

Results of the recovery curves clearly show the significant effect of nanocatalysts presence inside the porous media. It should be noted that recovery enhancement was proved by closing the total material balance of the nanocatalysts tests. Figure 3.8 shows the graphs for total injected hot fluid and total produced liquid for the nanocatalysts experiments at the temperatures of 320 and 340 °C.

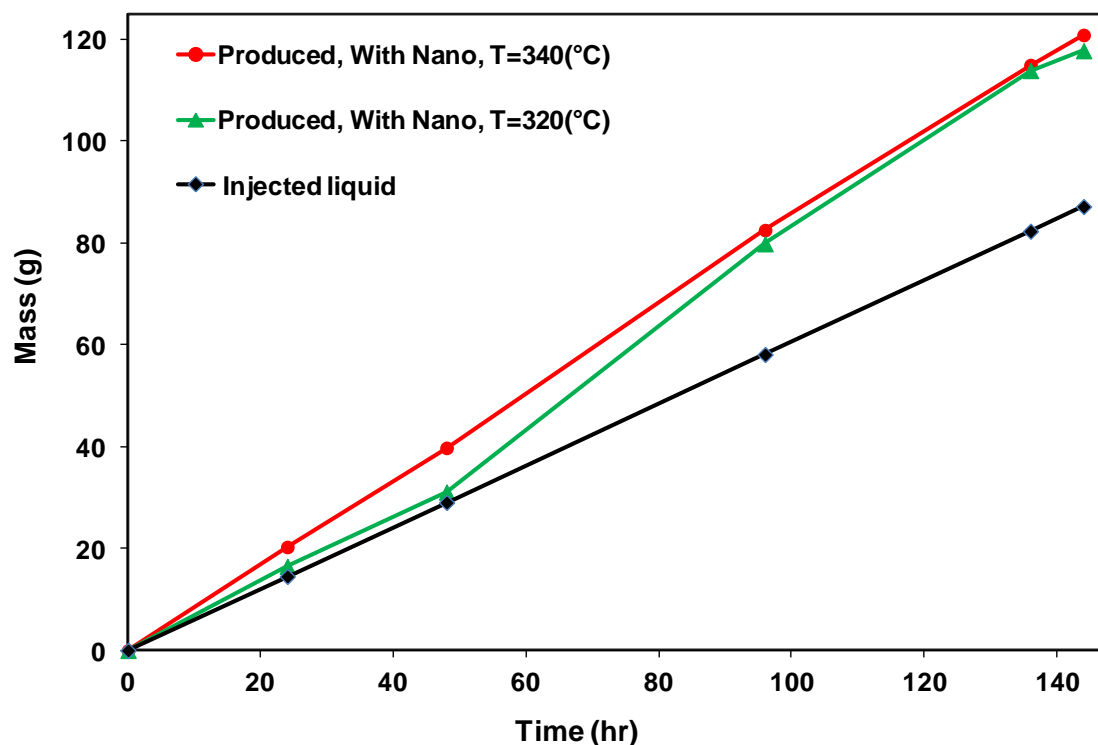


Fig 3.8: Material balance for the hot VGO injection into the high permeability sand packed bed at different times in the presence of tri-metallic UD nanocatalysts at pressure of 3.5 MPa, hot fluid injection rate of 0.01 cm³/min, hydrogen flow rate of 1 cm³/min, and temperatures of 320 and 340 °C

As seen, the differences between the injected and produced liquid interpreted as the total amount of produced bitumen. This graph clearly shows the enhancement of bitumen production via injection of the nanocatalysts. As mentioned, presence of nanocatalysts inside the medium enhanced the cracking of the heavy bitumen and produce lighter components and gaseous emission.

The penetration of the produced gases toward the top section of oil pool as vaporizing components was considered as the main reason for the increase in the recovery of bitumen. In this process, vaporized hydrocarbon mixture acts as solvent to diffuse and dissolve in bitumen to reduce the viscosity and makes it mobile. Figure 3.9 shows the

total volume of produced gases for the experiments conducted in presence and absence of nanocatalysts. It can be observed that total volume of gas produced in the experiments with nanocatalysts is at least twice the volume of gases produced from experiments without nanocatalysts. In addition, a considerable percentage of gases in the experiment without nanocatalysts was carbon dioxide (hydrogenation process has less efficiency) while in the experiments conducted in the presence nanocatalysts the volume of hydrocarbon gases were quite significant. It is worth noting that detailed analysis of the produced liquid and gases as well as quality enhancement of produced liquids shall be communicate in another study.

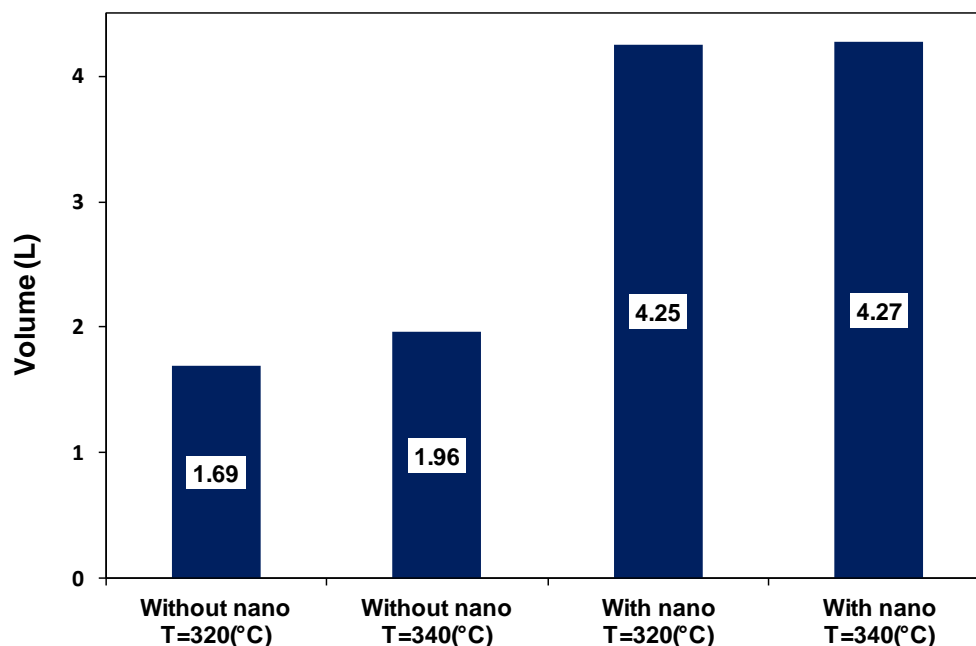


Fig 3.9: Total volume of produced gases at standard condition ($T=25^{\circ}\text{C}$, $P=0.1\text{ MPa}$) for the hot VGO injection into the high permeability sand packed bed in the presence and absence of tri-metallic UD nanocatalysts at pressure of 3.5 MPa, hot fluid injection rate of 0.01 cm³/min, hydrogen flow rate of 1 cm³/min, and temperatures of 320 and 340 °C

3.5 Conclusions

In this study, the effect of different hot fluid injection scenarios on Athabasca bitumen recovery performance inside a continuous packed bed reactor was investigated. The amount of produced bitumen was depicted by recovery curves, at different times and temperatures for each scenario. The recovery curve behavior for the VGO injection, without nanocatalysts, increased with time and leveled off after 95 hours.

Adding different mass percentage of pentane to the VGO enhanced the recovery of bitumen from the oil pool due to expansion of solvent and consequent viscosity reduction of Athabasca bitumen (pentane exists in vapor phase under experimental conditions). Presence of tri-metallic nanocatalysts in the injecting hot fluid (VGO matrix) enhanced the Athabasca bitumen recovery. This may be due to the presence of nanocatalysts inside the medium led to the production of lighter components via catalytic hydrocracking of bitumen and the subsequent viscosity reduction of bitumen presence in the oil pool as a result of contact with emitted hot gases.

Chapter 4 In situ Upgrading of Athabasca Bitumen Using Multimetallic Ultra-Dispersed Nanocatalysts in a in an Oil-Sands-Packed Bed Column: Part 1, Produced Liquid Quality Enhancement³

4.1 Abstract

The increase in energy demand of the world resulted in increasing consumption of petroleum-based fuel. However, the conventional crude oil is declining and, therefore, bitumen and heavy oil exploitation has increased recently. However, in the present context, heavy oil and bitumen exploitation process is not just high-energy and water intensive, but also it has significant environmental footprints as it produces significant amount of gaseous emissions, such as CO₂ and generates huge amount (approximately 370 million cubic meters) of produced water. In-situ catalytic conversion or upgrading is a promising cost-effective and environmentally friendly technology for production of high quality oil that meets pipeline and refinery specifications.

In this study, in-situ prepared NiWMo ultra-dispersed (UD) nanocatalysts (within vacuum gas oil matrix) were used for Athabasca bitumen upgrading in a continuous packed bed flow reactor at a high pressure and temperature. Experiments were performed

³ Hashemi, Rohallah, Nashaat N. Nassar, and Pedro Pereira-Almao. Enhanced Heavy Oil Recovery by In-Situ Prepared Ultra-Dispersed Multi-metallic Nanoparticles: A Study of Hot Fluid Flooding for Athabasca Bitumen Recovery. *Energy & Fuel* (In processing).

at a pressure of 3.5 MPa, temperatures from 320 to 340 °C and hydrogen flow rate of 1 cm³/min. The produced liquid was analyzed on the basis of residue conversion, micro carbon residue (MCR) content, sulfur and nitrogen contents, API gravity and viscosity. Results showed that UD nanocatalysts enhanced the upgrading of Athabasca bitumen by significantly increasing the API gravity and decreasing the viscosity, MCR, sulfur and nitrogen contents. This is because nanocatalysts open new pathways in the reaction scheme that effectively favored the hydrogenation reactions and inhibited the massive formation of coke that usually occurs during the classical thermal processing of heavy oils.

4.2 Introduction

With more than 170 billion barrels of estimated oil sands, Canada has the second largest oil reserve in the world. However, 80 percent of these reserves are deep underground and cannot be accessed by surface mining (Bergerson and Keith 2006, Patel 2007, St-Denis 2007). Nonetheless, several innovative technologies have been explored to extract heavy oil and bitumen from deep reservoirs (Paitakhti Oskouei et al. 2010, Sharpe, Richardson, and Lolley 1995, Chu 1977, Weissman et al. 1996, Greaves, Xia, and Ayasse 2005, Liu et al. 2004, Butler and Mokrys 1991, Moore, Mehta, and Ursenbach 2002).

The steam assisted gravity drainage (SAGD) process is the most promising technology for in situ thermal recovery of heavy oil and bitumen (Nasr et al. 2003, Butler 1994, Butler 1991b). However, there are a number of challenges associated with bitumen recovery and upgrading in the present context. It is well known that pure steam-based oil sand exploitation process is not just high-energy intensive, but also it has significant

environmental footprints as it produces significant amount of gaseous emissions such as CO₂ and consumes considerable amount of water as well. Furthermore, under current economic conditions and technologies, considerable percent of vast bitumen resources could not be recovered (e.g., SAGD has a recovery factor in the range 20-50%) (Birn and Khanna).

Due to its high viscosity and low American Petroleum Institute (°API) gravity, transportability of bitumen from remote well sites is challenging. Accordingly, to meet the pipeline specification for transportation, it is crucial to increase the API gravity of produced bitumen and decrease its viscosity (Syncrude_Canada 1996). This is usually accomplished by mixing bitumen with diluents to meet pipeline feedstock specification (Anderson, Chambers, and McMurray 1995). Although using solvent for viscosity reduction was successfully implemented, however, many drawbacks were reported; including availability of the solvents and the possibility of asphaltene deposition (Anhorn and Badakhshan 1994).

In addition, there exists high level of contaminants in bitumen matrix, such as sulfur, nitrogen and metal which has also environmental repercussions and requires special removal techniques (Gosselin 2010). Moreover, bitumen residue percentage is very high (about 51% for Athabasca bitumen) in unconventional bitumen resources which must be converted to high value products (Rahimi et al. 2001). Processing of these resources requires high hydrogen consumption as well as high waste of liquids via gas and solids yield to improve the quality and hydrogen to carbon atomic ratio of the resulting liquid hydrocarbons (Lee 1996, Billon and Bigeard 2001).

Once produced to surface, bitumen is transferred to surface upgrading facilities converting low quality oil to synthetic crude oil. Carbon removal (in the form of coke) and direct addition of hydrogen are two possible methods for heavy oil and bitumen conversion in favor of enhanced oil quality. For hydroprocessing, breaking of heavy hydrocarbons and impurity removal from bitumen occur simultaneously, with hydrocracking (HCK), hydrodesulfurization (HDS), hydrodenitrogenation (HDN), and hydrodemetallisation (HDM) processes occurring altogether (Gary and Handwerk 2001).

HCK is a two-stage process combining cracking and hydrogenation to produce higher value products depending on reaction conditions, such as pressure, temperature and catalytic activity (Craig et al. 1966, Dufresne, Bigeard, and Billon 1987, Scherzer and Gruia 1996). The process is usually performed at high pressure, high temperature and in presence of high partial pressure of hydrogen and a dual functional catalyst (Del Bianco, Panariti, Anelli, et al. 1993, Panariti, Del Bianco, Del Piero, Marchionna, et al. 2000, Ayasse et al. 1997). Bi-functional catalyst is used to break and rearrange heavy molecules as well as adding hydrogen to saturate the unsaturated products of cracking. During HCK processes (i.e., HDS, HDN, and HDM) most of sulfur, nitrogen and metal are removed from the heavy feedstock (Steijns et al. 1981). Products of HCK have lower average molecular mass and higher hydrogen to carbon atomic ratio compared to original feed. In addition, during HCK processes, catalyst activity should be maintained at high level to have better quality products as well as lower coke deposition (Mohanty, Kunzru, and Saraf 1990).

Most commonly used catalysts for HCK processes are Mo, Ni, W, Co and Fe, with Mo and Fe having the highest and lowest catalytic activity for residue hydrocracking,

respectively (Le Perche et al. 1995, Bearden and Aldridge 1981, Liu et al. 1994). However, presence of sulfur, nitrogen and metals in heavy hydrocarbon feedstock causes fast deactivation of supported conventional hydrocracking catalysts (Lee et al. 1995). Nonetheless, catalyst activity is controlled by degree of catalyst dispersion as well as catalyst composition. Over the past 30 years, unsupported dispersed catalysts have been widely studied for conversion of heavy hydrocarbons to distillates (Laine, Vastola, and Walker Jr 1963, Panariti, Del Bianco, Del Piero, Marchionna, et al. 2000, Lee et al. 1995, Panariti, Del Bianco, et al. 2000b, Okamoto et al. 1995, Fixari et al. 1994).

Dispersed catalysts improve the processing economics due to improvement of catalytic performance which is obtained by accessing much larger surface area of small particles (Köseoglu and Phillips 1988). Also, suspended particles increase the contact probability as well as effective reactor volume for the transformations. In addition, probability of preferential channeling is decreased, and longer run time for conversion is offered by dispersed catalysts compared to catalysts implemented in fixed bed reactors (Pereira-Almao 2007a). Nonetheless, hydroprocessing or carbon removal are found to be limited because of the high capital and operating costs and/or the ineffectiveness in meeting environmental regulations (Speight and Ebrary 1999).

Innovative processes are much needed to improve the energy efficiency and reduce the environmental footprints of heavy oils and bitumen extraction activities worldwide with cost-effective and environmentally friendly techniques. In-situ catalytic conversion or upgrading is a promising cost-effective and environmentally friendly potential technology for the production of transportable-via-pipeline oil without subsequent surface treatment or diluent addition (Hashemi, Nassar, and Pereira Almao 2013c).

Bitumen or extra-heavy oil upgrading could be achieved during steam injection as steam could provide sufficiently high temperature inside the reservoir porous medium and hydrogen could be generated locally from water, and subsequently heavy hydrocarbons break down into lighter components (Hashemi, Nassar, and Pereira-Almao 2012).

Produced liquid through conversion process will have similar quality to conventional crude oil if the conversion occurs inside the reservoir (Herron 2000). A possible approach is a combination of catalysts and steam in order to speed up the process and maximize the conversion (Hashemi, Nassar, and Pereira-Almao 2012). In-situ heavy oil upgrading using thermal methods based on combustion via air injection has also been found to enhance the API gravity and viscosity of heavy crude oils (Moore et al. 1999). However, thermal methods generate more and denser asphaltenes and produce olefins, thus the produced crude oil requires immediate hydrotreating on surface before pipelining which ramps up investments and complexity of facilities on surface (Xia and Greaves 2006).. Nonetheless, the incorporation of pre-fabricated catalysts in the perimeter around the production wells have already been proposed and combined with air injection methods to generate heat and produce upgrading reactions (Xia and Greaves 2006). It is claimed that this resulted in increase of the API gravity of the crude oil by 6-8 °API additional to that obtained via combustion through air injection (Xia and Greaves 2006). However, these conventional catalysts would eventually plug the pore size and hence increase the risks of well plugging and loss of stability and quality of the crude oil being produced. Further, the stability of the enhanced crude oil may be jeopardized since hydrogen is not substantially present during this cracking therefore the produced liquid may not be adequate for pipeline transportation.

The use of tri-metallic nanocatalysts coupled with marginal levels of hydrogen injection and/or in-situ/locally generation of hydrogen (e.g., water-gas-shift reaction) for in-situ upgrading represents an option for incorporating chemical processing in the reservoir (Hashemi, Nassar, and Pereira-Almao 2012). It is perceived that this process is less energy intensive and reduces water-related issues (Pereira-Almao and Larter 2008). In this process, dissolved hydrogen and the nanocatalysts suspension could be injected into the reservoir during the steam assisted gravity drainage (SAGD) or any thermal recovery process.

Nanocatalysts for hydroprocessing reactions were successfully developed in heavy oil matrices and subsequently tested in batch reactor using marginal levels of hydrogen and sand for Athabasca bitumen upgrading by our research group at the University of Calgary (Vasquez 2009, Nassar, Hassan, and Pereira-Almao 2011a, Galarraga and Pereira-Almao 2010). Experimental results showed that nanocatalysts enhanced the upgrading of Athabasca bitumen by significantly increasing the hydrogen/carbon atomic ratio and reducing both viscosity and coke formation (Galarraga and Pereira-Almao 2010). In addition, a significant reduction of sulfur and micro carbon residue was observed (Galarraga and Pereira-Almao 2010).

To test the applicability of the nanocatalysts in continuous flow mode, a pilot plant setup was designed and constructed to simulate the major elements of SAGD reservoir, such as injection and production lines, oil pool and reservoir top. The nanocatalysts were injected into the oil pool via hot fluid nanocatalysts carrier. The transport behavior of these multimetallic nanocatalysts in an oil sands-packed bed column at a typical SAGD temperature and pressure was investigated in a previous study with a series of

experiments at various temperatures and pressure conditions (Hashemi, Nassar, and Pereira-Almao 2012). It has been found that propagation of multimetallic nanocatalysts in oil sands media is feasible under typical pressure and temperature of SAGD process, in the absence of steam. Depending on the experimental conditions and surface properties, percentages of injected nanocatalysts were retained inside the medium. Furthermore, neither major permeability reduction nor pore plugging was observed. (Hashemi, Nassar, and Pereira-Almao 2012). In a recent study, we have shown that the presence of trimetallic nanocatalysts in an Athabasca oil sands-packed bed column enhanced the bitumen recovery (Hashemi, Nassar, and Pereira Almao 2013c). This was attributed to the production of lighter components via catalytic hydrocracking of bitumen and the subsequent viscosity reduction of bitumen presence in the oil pool as a result of contact with emitted hot gases (Hashemi, Nassar, and Pereira Almao 2013c).

This work is a continuation on our previous studies (Hashemi, Nassar, and Pereira-Almao 2012, Galarraga March 2011) and it aims at experimentally investigating the effect of nanocatalysts on upgrading of Athabasca bitumen in a one dimensional (1D) continuous flow oil sand packed bed reactor. This part of the study mainly focuses on the quality of upgraded bitumen (i.e., produced liquid) and investigates its suitability as a refinery feedstock. Accordingly, the extent quality of produced liquid was analyzed on the basis of residue conversion, MCR content, sulfur and nitrogen contents, API gravity and viscosity. It is worth noting that the whole study consists of two continuous papers; Part 1 and 2. Part 1 covers the detailed results of produced liquid quality analysis. In the second Part, we investigated the effect of reaction severity (time and temperature) as well as the presence of nanocatalysts on solid and gaseous product. It should be noted that, to

the best of our knowledge, a study on in-situ catalytic upgrading of Athabasca bitumen by using in-house prepared multi-metallic nanocatalysts in a continuous flow mode is conducted for the first time.

4.3 Materials and methods

4.3.1 Chemicals

Silica sand was purchased from AGSCO (99% of SiO₂, AGSCO, Hasbrouck Heights, NJ, USA) and was used as a source of porous media. The sand has a size of 12–20 mesh (U.S. Sieves) and absolute permeability about 250 Darcy. Sand selection and consequently obtained permeability was based on the dimensional analysis for a typical SAGD process (Butler 1991b). Athabasca bitumen (JACOS, AB, Canada) was used as a source of heavy oil. VGO (Nexen, AB, Canada) was used as nanocatalysts carrier into the porous media. Properties of utilized Athabasca bitumen and VGO were reported in our previous study (Hashemi, Nassar, and Pereira Almao 2013c) and are presented in Table 4.1 as a reference.

Tri-metallic nanocatalysts were prepared by using the following precursors: nickel acetate tetrahydrate (99%, Sigma–Aldrich), ammonium metatungstate (99%, Sigma–Aldrich), and ammonium molybdate tetrahydrate (99%, Sigma–Aldrich). Carbon disulphide (99%, Sigma–Aldrich) was used for sample solution preparation of simulated distillation analysis. Utilized gases for experiments including hydrogen, nitrogen, helium, air and argon were provided by Praxair Specialty Gases & Equipment (Calgary, AB, Canada).

Table 4-1: Properties of Athabasca bitumen and Nexen VGO considered in this study

Property	Bitumen	VGO
Viscosity at 40 °C, (cP)	7550	122.314
API gravity, (°API)	9.5	19.1
Microcarbon Residue, (wt %)	12	NA
H/C (atomic ratio)	1.52 ± 0.001	NA
Sulfur, (wt %)	4.25	2.73
<i>Distillation Cuts, (wt %)</i>		<i>Distillation Cuts, (wt %)</i>
Naphtha: IBP- 213 °C	2.76± 0.29	IBP- 235 °C
Distillates: 213 - 343 °C	14.89 ± 0.81	235 - 280 °C
VGO: 343 - 545 °C	34.68 ± 1.81	280 - 343 °C
Residue: >545 ⁺ °C	47.95 ± 1.57	Residue: >343 ⁺ °C
		64.51

4.3.2 Preparation of nanoparticles suspension

Water-in-vacuum gas oil microemulsion method was employed for preparing nanocatalysts suspension (Nassar and Husein 2010, Husein et al. 2010); (Eriksson et al. 2004, Nassar 2010, Husein and Nassar 2008, Nassar and Husein 2007a, b). Details on the preparation procedure of colloidal tri-metallic nanocatalysts in VGO have been described in our previous studies (Hashemi, Nassar, and Pereira-Almao 2012, Hashemi, Nassar, and Pereira Almao 2013c). In brief, preparation of nanocatalysts suspension was started by mixing 99.57 wt% VGO and 0.43 wt% HLB-8 surfactant at 700 rpm and 60 °C, and then the mixture was stirred for about 30 min to reach stability. Aqueous solutions of the corresponding metallic precursors were added to the mixture and then agitated for about 30 min at 60 °C.

The mixture of metallic precursors, surfactant and VGO was kept for 8 h at a temperature of 40 °C and under low stirring (200 rpm) to evaporate the water (down to at least 0.5 wt %) and subsequently initiate nucleation and growth of tri-metallic

nanoparticles, which remained stable in suspension (Zekel' et al. 2007, Thompson et al. 2008, Vasquez 2009). The resultant concentration of VGO-suspended tri-metallic nanocatalysts used in this study were 72, 240 and 408 ppm for Ni, Mo and W, respectively. The atomic metallic ratios (metal/total metal) were as follows: Mo = 0.6267, Ni = 0.1808 and W = 0.1924.

4.3.3 Experimental set-up

A schematic diagram of the experimental setup is presented in Figure 4.1. (Hashemi, Nassar, and Pereira Almaso 2013c) The setup consists mainly of the followings: Bitumen and VGO containing nanocatalysts reserve tanks, stainless steel column reactor; Isco pumps (Teledyne Isco, Lincoln, NE, USA), hydrogen and nitrogen gas cylinders, gas analysis instruments and fraction collectors. The column reactor has 90 cm height and 2.16 cm inside diameter.

Bitumen and VGO containing suspension of nanocatalysts are maintained inside two stainless steel reserve tanks under nitrogen pressure to be utilized during the tests. Hot fluid generator was used for injecting hot fluid (virgin VGO or VGO containing nanocatalysts) inside the porous media. A special designed 10-point thermocouple was placed in the middle of packed bed reactor to record all temperatures along the porous media. Two Isco pumps were used to inject bitumen and VGO or VGO-containing nanocatalysts inside the medium. All produced liquid samples were collected inside a hot separator (500 cm³) and at certain times were transferred to sampling containers for further analysis. Nitrogen was used to purge and pressurize the lines at the start of

experiments. Hydrogen was used during the hot fluid injection to enhance the hydrocracking reaction and to avoid coke production and plugging of the reactor.

All produced gases were passed through the wet test meter to measure rate and cumulative gas production for later analysis.

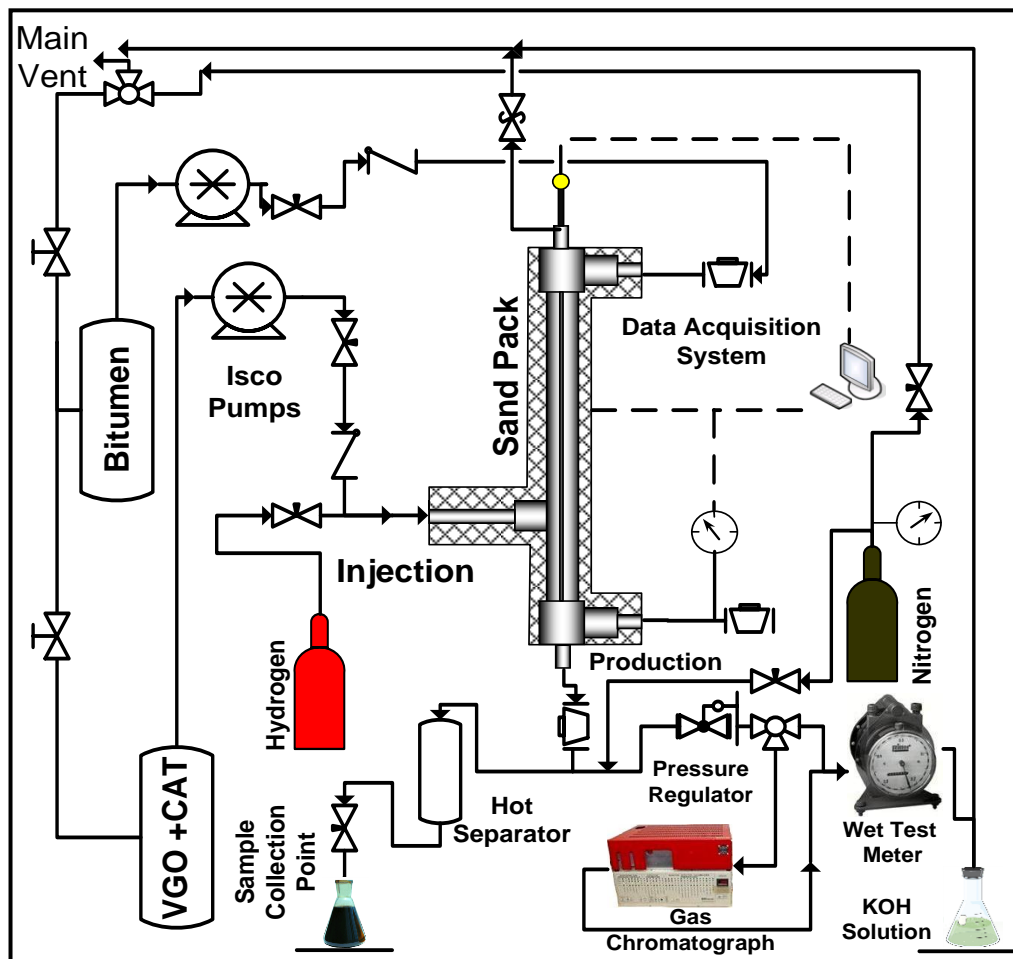


Fig 4.1: Schematic representation of the experimental setup

4.3.4 Experimental procedure

Before any use, silica sand was washed by deionized water to remove dust, tiny particles and any kind of impurities that may exist within the provided silica sand. Washed sands

were placed in a vacuum oven for 24 h at 60 °C to evaporate any remaining water. After that, cleaned and dried sands were used in the reactor column. In a typical experiment, the reactor column was charged with approximately 452 g cleaned silica sand. Sand production was prevented from the reactor column by using three mesh rings in the top, bottom and entrance of the injection point.

To ensure a uniform sand packing and to avoid air entrapment, the column was first filled with water and the sand media was introduced into the column from the top while the column was constantly patted gently with a metal rod until it was fully packed. Heating tapes were installed at the outside body of the reactor column to maintain the test temperature, and the column was insulated by fiber glass casing. Leak test was performed for all tests by pressurizing the packed bed reactor with pure nitrogen up to 5.5 MPa. A 1% change in pressure per hour was considered as the maximum allowable pressure reduction during the leak test. A 3.5 MPa pressure was maintained after the termination of the leak test. Nitrogen was also used for purging the system until oxygen disappeared completely, as confirmed by the gas chromatograph (GC).

Following purging, the packed bed column was heated to the desired temperature. When the reactor column working pressure and temperature were attained, approximately 5 pore volumes of Athabasca bitumen were first injected through the column in the down-flow mode to displace the water and saturate the bed with bitumen to simulate the oil sands conditions. The actual experiment started by switching off the inlet gas from pure nitrogen to pure hydrogen and introducing the injecting fluid (VGO containing nanocatalysts). At this point, the zero reaction time for upgrading experiment was considered. Before introducing of nanocatalysts inside medium, the VGO-containing

nanocatalysts-suspension was heated to the test temperature by covering the hot fluid generator with heating tapes.

Hot fluid was injected from injection point, and then it penetrates inside the reaction zone where it reacts with bitumen and subsequently produces better quality liquid from the production point. The run was conducted until approximately 100 cm³ of VGO-containing nanocatalysts was injected into the porous media. During the tests and at different time intervals, the produced liquid sample was taken for analysis and the produced gas was taken from the bottom of the reactor column to be analyzed by the GC. At the end of the run, the reactor column was vented and cooled to room temperature, and the solid products (packed media) were carefully discharged from the reactor column for analysis. It should be noted here that solid analysis was carried out to determine the amount of produced coke as well as the morphology, size and chemical composition of the nanocatalysts after reaction. These analyses are presented in Part 2 of this study. After discharging the packed media, the column and assembly were washed with toluene, soap and hot water; therefore, the apparatus could be ready for another cycle of experiments. It should be noted here that control runs of the same experimental conditions and feed composition, missing only the nanocatalysts, was conducted for comparison.

4.3.5 Analytical methods

To confirm the extent of upgrading process, different characterization techniques were implemented to analyze the produced liquid, solids and gases. In this part of study, the produced liquid samples were analyzed using standard characterization techniques as follows: (a) water content in produced liquid was measured by the Karl Fischer titration

method using Mettler- Toledo model DL-32 (A. Daigger & Company, Illinois, USA); (b) residue content ($545\text{ }^{\circ}\text{C}^+$) was estimated following ASTM procedure (D7169-2005) by using high-temperature simulated distillation (HTSD) that was carried out in a Agilent GC (Mississauga, ON, Canada) following the method developed by Carbognani et al. (Carbognani et al. 2007); (c) viscosity of produced liquid was measured by Brookfield DV II+ Pro II at $40\text{ }^{\circ}\text{C}$; (d) micro-carbon residues (MCR content) of produced liquid was measured by a method developed by Hassan et al. (Hassan, Carbognani, and Pereira-Almao 2008b) MCR is considered as a measure for potential coke formation; (Lal, Otto, and Mather 1999) and (e) API gravity was measured by a technique developed by Carbognani et al. (Carbognani et al.) Sulfur and nitrogen content were determined in an Antek Instruments (Model 9000SN Analyzer, Houston, TX, USA) which contains photomultiplier tube to detect emitted light as ultraviolet (UV) form which is exposed as excess energy.

Optical Microscopy (National Digital Microscope model DC3-163, TX, USA) combined with Motic Images Plus 2.0 software was used for selected produced liquid samples obtained in the presence and absence of nanocatalysts in packed bed column to observe the quality of produced liquids. In this technique visible light was used to magnify images of very small samples to be analyzed qualitatively. Accordingly, liquid sample homogeneity and presence of solid materials as well as cock formation could be observed by this method.

4.4 Results and discussions

Because the main goal of this study was to investigate the extent of in-situ catalytic upgrading of Athabasca bitumen in an oil sand packed bed column via tri-metallic nanocatalysts, the experiments were performed at different temperatures in the presence and absence of nanocatalysts in porous media. Table 4.2 shows the specifications of the tests considered in this study. It should be noted that reactor pressure, hydrogen flow rate, initial nanocatalysts concentration, injection rates and medium permeability were kept fixed for all tests. First two tests were considered as control tests, without the presence of tri-metallic nanocatalysts, to evaluate the quality of produced fluid in high permeability sand pack. After that, Tests 3 and 4 were performed at different temperatures in the presence of tri-metallic nanocatalysts. The results of these tests were compared to evaluate the extent of upgrading quality during the reaction.

Table 4-2: Specifications of the experimental tests considered in this study

Type	Without nano-catalysts		With nano-catalysts	
	1	2	3	4
Test Number	1	2	3	4
Temperature (°C)	320	340	320	340
Pressure (MPa)	3.5	3.5	3.5	3.5
Porosity (%)	33.1	33.2	32.9	33.2
Absolute Permeability (Darcy)	246	245.3	244	244.7
Nominal Particle Concentration (ppm)	720	720	720	720
Residence Time (h)	36	36	36	36
Suspension Injection Rate (cm³/min)	0.01	0.01	0.01	0.01
Hydrogen flow rate (cm³/min)	1	1	1	1

4.4.1 Recovery enhancement and overall mass balance analysis

Before conducting any analysis on the produced liquid quality, we thought to confirm the recovery enhancement of bitumen by hot fluid injection, in the presence and absence of nanocatalysts. It should be noted here that a complete study on recovery enhancement was performed recently and detailed analysis for each element of produced liquids from porous media was evaluated and consequently recoveries were demonstrated (Hashemi, Nassar, and Pereira Almaso 2013a). For the aforementioned experimental tests (Table 4.2) mass balance calculations were conducted and the results are presented in Figures 4.2a-d. As seen, in all tests, recovery of bitumen increased with time and continues until the end of the experiment. Increasing the temperature favored the bitumen recovery. Further, bitumen recovery was enhanced in the presence of nanocatalysts. It can be interpreted that the presence of nanocatalysts inside the packed bed enhanced the production of gases and lighter components via catalytic hydrocracking which were confirmed with the analysis of produced gases from porous media (Hashemi, Nassar, and Pereira Almaso 2013b). Consequently, produced gases penetrate toward the top section of oil pool and act as a solvent to diffuse and dissolve in bitumen matrix, and subsequently reduce the bitumen viscosity.

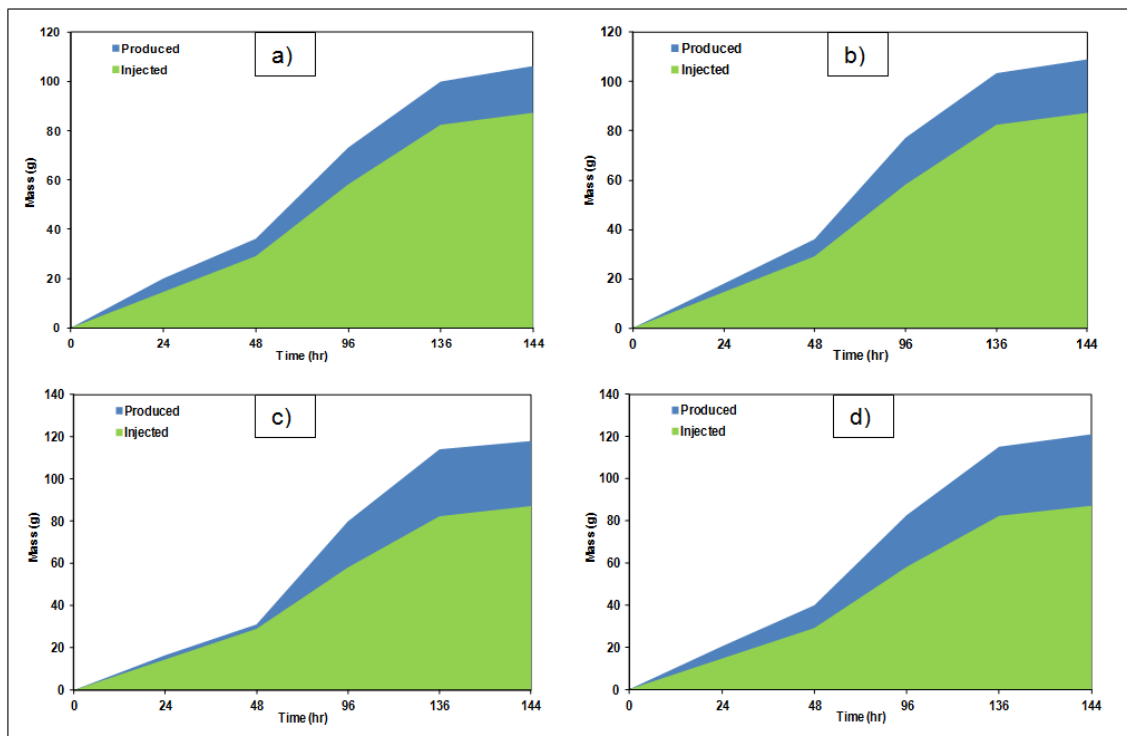


Fig 4.2: Material balance for the hot VGO injection into the an oil sand packed bed at different conditions: (a) in the absence of UD nanocatalysts and temperature of 320 °C, (b) in the absence of UD nanocatalysts and temperature of 340 °C, (c) in the presence of UD nanocatalysts and temperature of 320 °C, (d) in the presence of UD nanocatalysts and temperature of 340 °C. System pressure was 3.5 MPa, hot fluid injection rate of 0.01 cm³/min, and hydrogen flow rate of 1 cm³/min

Figure 4.3 shows the percentages of different cuts (naphtha, distillate, VGO and residue) in the produced samples for the experiments conducted in the presence and absence of nanocatalysts at different temperatures. In all samples, the percentages of naphtha are comparable. However, there exist quite clear difference for the percentages of distillate and VGO. This supports that not only nanocatalysts enhanced the recovery of bitumen, but also it enhanced the upgrading process. Further, temperature also has a significant impact on recovery and upgrading of bitumen. In the following sections, detailed analysis of the produced liquid are presented. It should be noted here that the extent of bitumen upgrading was evaluated on the basis of residue conversion, MCR

content, amount of sulfur and nitrogen, API gravity and viscosity. It is worth noting that the measurements of MCR, sulfur, and nitrogen content were performed in triplicates to confirm the validity of the obtained results.

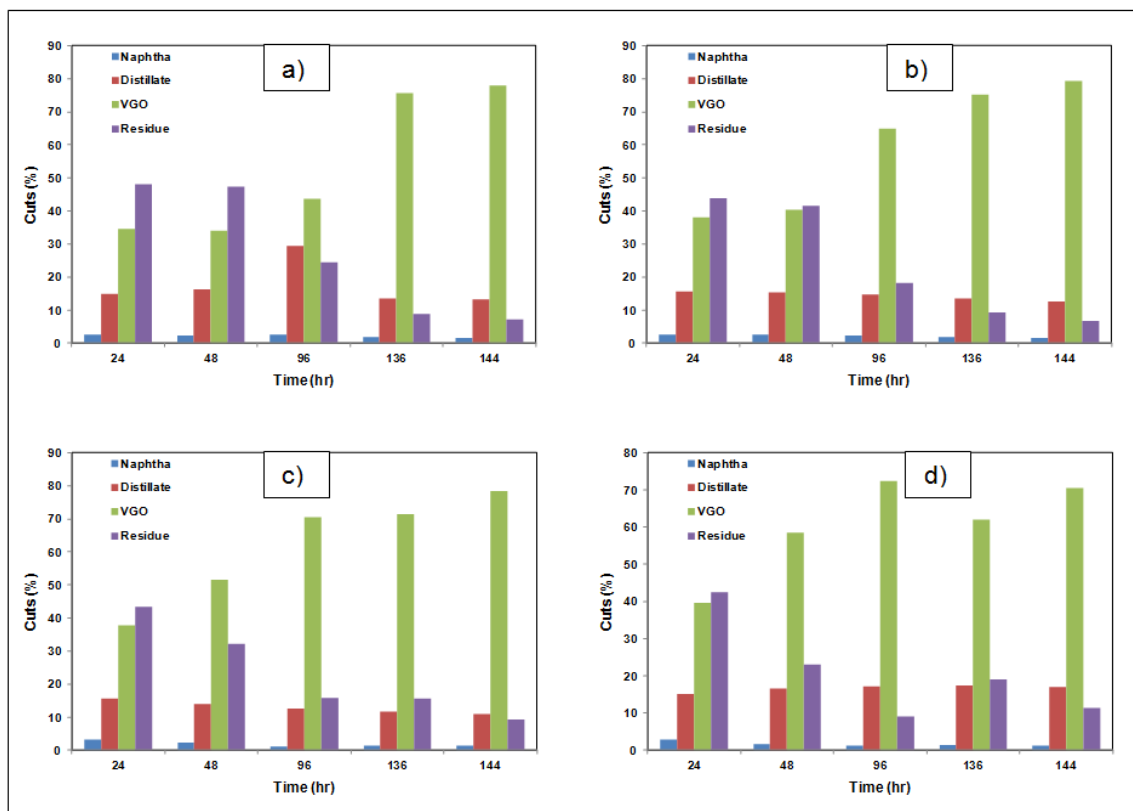


Fig 4.3: Simulated distillation analysis of produced liquid samples obtained from an oil sand packed bed at different conditions: (a) in the absence of UD nanocatalysts and temperature of 320 °C, (b) in the absence of UD nanocatalysts and temperature of 340 °C, (c) in the presence of UD nanocatalysts and temperature of 320 °C, (d) in the presence of UD nanocatalysts and temperature of 340 °C. System pressure was 3.5 MPa, hot fluid injection rate of 0.01 cm³/min, and hydrogen flow rate of 1 cm³/min

4.4.2 Enhancement of API gravity and viscosity

Athabasca bitumen has extremely high viscosity (around 500000 cP at 4°C) and low API gravity (~9.5°) (Galarraga and Pereira-Almao 2010). Therefore, bitumen has poor mobility that causes difficulties in transportation via pipelines. Accordingly, to meet the

pipeline specification for transportation, it is crucial to increase the API gravity of produced bitumen to 19-21°API and decrease the viscosity to approximately 250 cP at 10 °C (Syncrude_Canada 1996).

Figure 4.4 shows the API gravity for produced liquid samples at different temperatures and reaction times in the presence and absence of tri-metallic nanocatalysts. Clearly, API was improved with the increase of reaction time and temperature in the presence and absence of nanocatalysts. Further, API gravity was enhanced in the presence of nanocatalysts. Viscosities of produced liquid samples at 40 °C for all experiments are depicted in Figure 4.5. Again, significant viscosity reduction can be observed with the increase of temperature and reaction time, and the presence of tri-metallic nanocatalysts enhanced the viscosity reduction. The lowest measured viscosity was around 220 cP at 40 °C for experiment conducted at temperature of 340 °C and reaction time of 144 h in the presence of nanocatalysts. This is in excellent agreement with the results reported by Galarraga and Pereira-Alamo for a significant viscosity reduction of Athabasca bitumen via in-situ hydrocracking with the aid of nanocatalysts in a batch reactor process (Galarraga and Pereira-Almao 2010). This shows that the integration of thermal cracking and nanocatalysts could be capable for in-situ upgrading of Athabasca bitumen which results in production of a stable crude oil that can be directly transportable via pipelines, without subsequent diluent addition. Nanocatalysts are easy to be prepared in-situ compared to conventional catalysts commonly used for heavy oil upgrading, overcome the issue of pore plugging experienced in support catalysts and maintain high dispersive properties, adsorption affinity and catalytic activity.

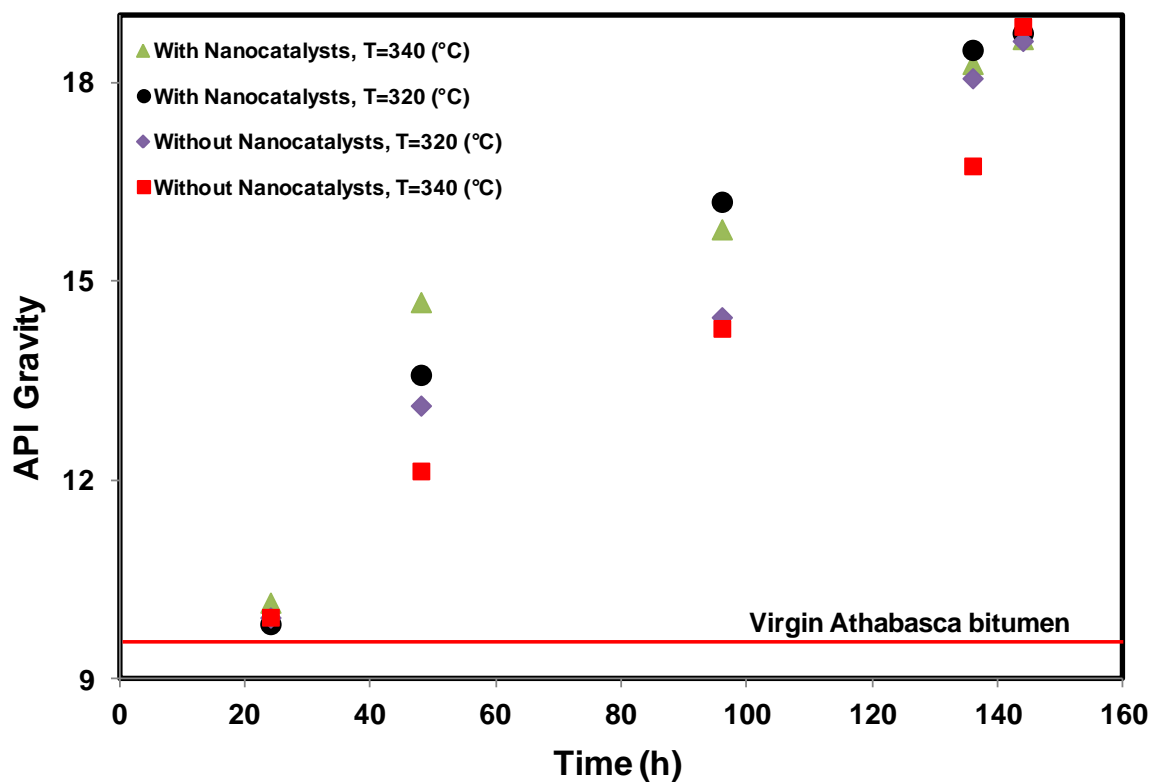


Fig 4.4: API gravity of produced liquid samples from porous media at different times in the absence and presence of tri-metallic UD nanocatalysts at pressure of 3.5 MPa, hydrogen flow rate of 1 cm³/min, and temperatures of 320 and 340 °C

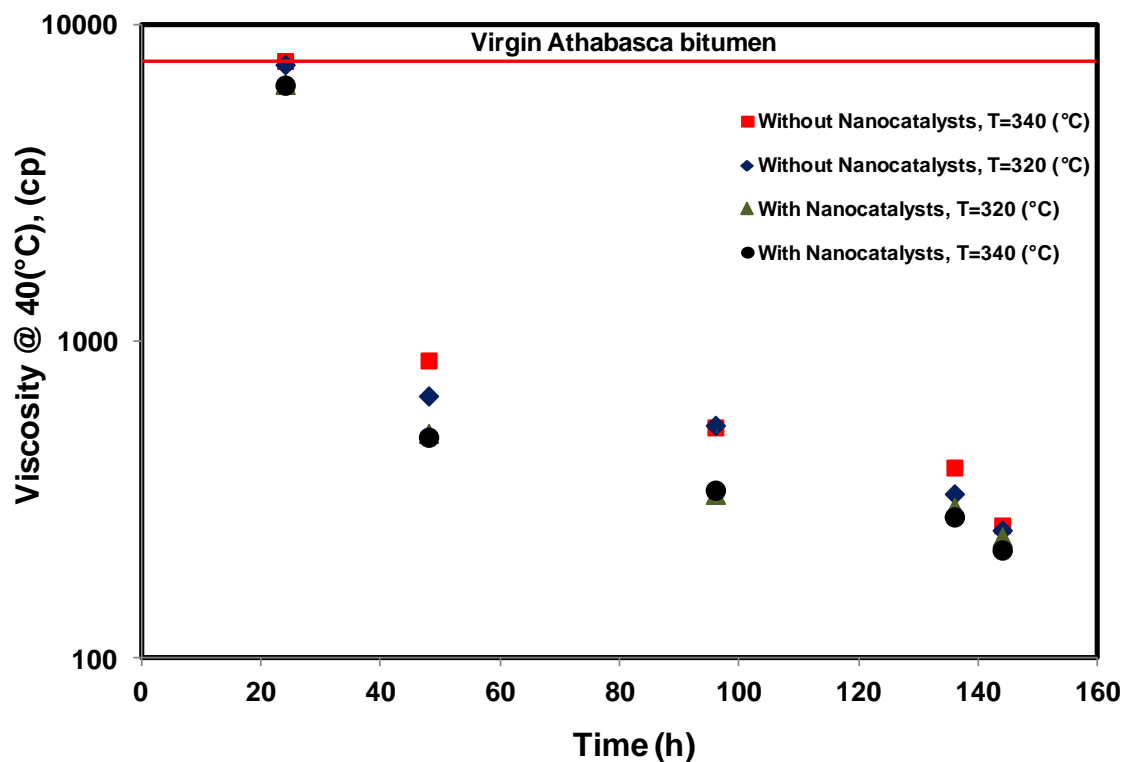


Fig 4.5: Viscosity of produced liquid samples from porous media at 40 °C. Sample was produced at different times in the absence and presence of tri-metallic UD nanocatalysts at pressure of 3.5 MPa, hydrogen flow rate of 1 cm³/min, and temperatures of 320 and 340 °C

4.4.3 Residue conversion

High temperature simulated distillation (HTSD) was employed in this study for qualitative and quantitative characterization of the produced liquid. Figure 4.6 shows the HTSD curves for virgin bitumen and for different liquid samples obtained at different temperatures in the presence and absence of nanocatalysts for a reaction time of 48 h. Clearly, in all cases (except sample obtained at 340 °C without nanocatalysts), the produced liquid was lighter compared to the virgin bitumen. Further increase in the temperature, in absence of nanocatalysts, reduced the quality of produced liquid possibly

due to coke formation. On the other hand, the liquid quality was further enhanced in the presence of nanocatalysts. This is not surprising, as nanocatalysts open new pathways in the reaction scheme that may lead to less coke formation.

A cut point of 545 °C⁺ was considered as the dividing line between distillates and residual components. Accordingly, the residue content of produced liquid samples obtained at different reaction times were estimated and presented in Figure 4.7. As seen, in all cases, the residue content decreased as the reaction time increased. Increasing the temperature in the absence of nanocatalysts favored the formation of residue. On the other hand, the presence of nanocatalysts inside the porous media improved the quality of produced liquids as reduction of residue content is a clear sign for higher conversion inside the medium. Similar observations have been reported by Galarraga and Pereira-Almao for catalytic hydrocracking of Athabasca bitumen performed in a batch reactor experiment (Galarraga and Pereira-Almao 2010). Presence of appropriate nanocatalysts inside the porous media with the help of controlled temperature, pressure and hydrogen could change the reaction mechanism in favor of desired products. To better represent the catalytic effect of nanocatalysts on liquid quality enhancement, the results were presented in terms of residue conversion that was calculated from eq. 4.1 at fixed temperature.

$$\text{Residue 545 }^{\circ}\text{C}^{\text{+}} \text{ Reduction (\%)} = \frac{\text{Residue 545 }^{\circ}\text{C}^{\text{+}} \text{ without Nanocatalyst} - \text{Residue 545 }^{\circ}\text{C}^{\text{+}} \text{ with Nanocatalyst}}{\text{Residue 545 }^{\circ}\text{C}^{\text{+}} \text{ without Nanocatalyst}} \times 100 \quad (4.1)$$

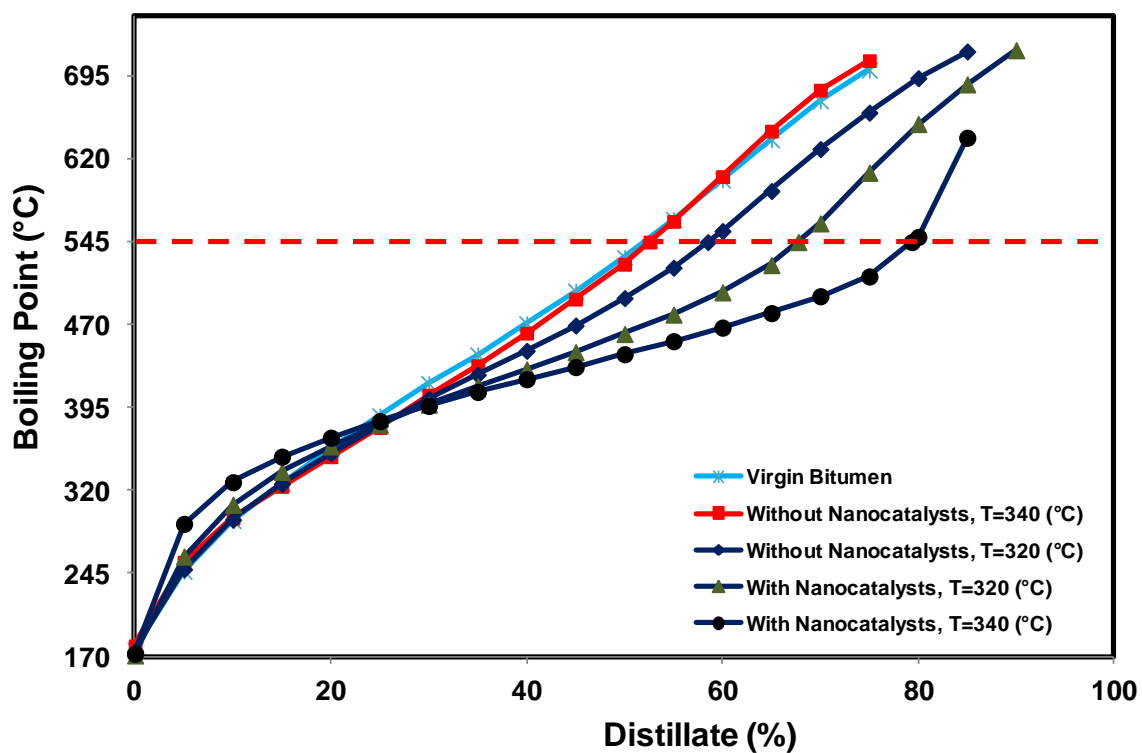


Fig 4.6: Boiling point simulated distillation curves for different produced liquid samples obtained at different temperatures in presence and absence of nanocatalysts for reaction time of 45 h, hydrogen flow rate of 1 cm³/min, and total pressure of 3.5 MPa. The horizontal dashed line is the cut points between distillates and residual components

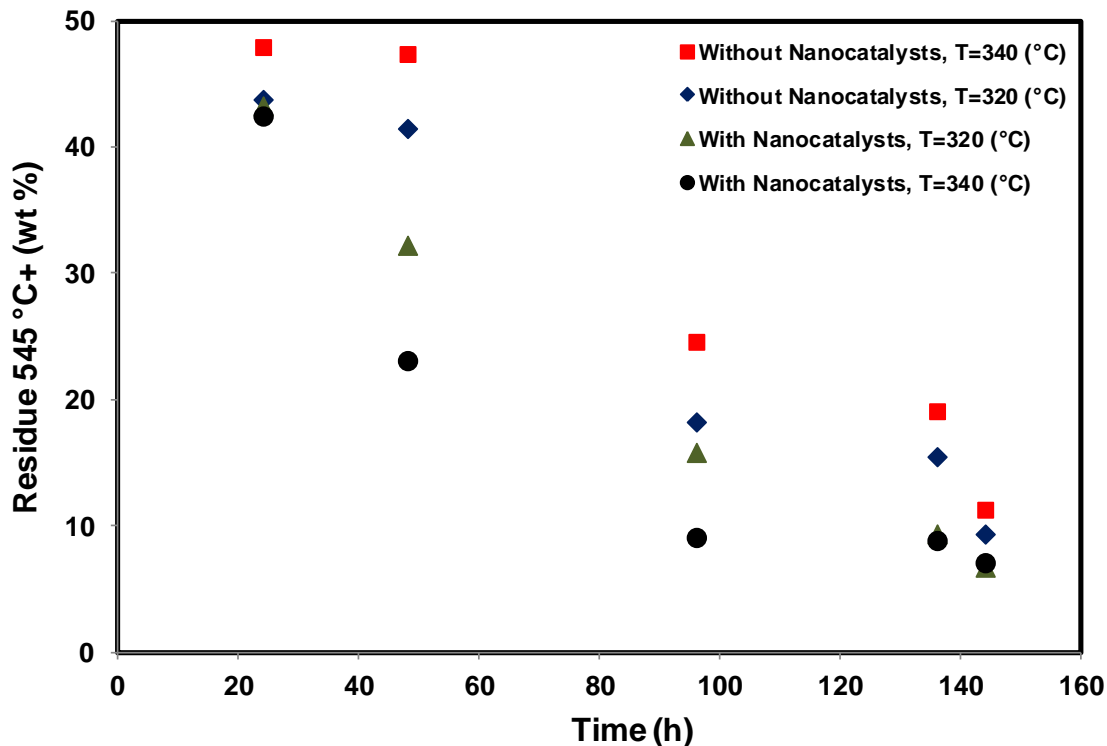


Fig 4.7: Residue contents of produced liquid samples from porous media as a function of time in the presence and absence of tri-metallic nanocatalysts at pressure of 3.5 MPa, hydrogen flow rate of 1 cm³/min, and temperatures of 320 and 340 °C

Figure 4.8 shows the percentage of residue content reduction of produced liquid samples from porous media with respect to the control experiments (without tri-metallic nanocatalysts) as a function of time. As seen, increasing the temperature and reaction time in the presence of nanocatalysts favored the conversion of residue. High conversion was obtained at reaction time of 96 h and temperature of 340 °C. This high conversion indicates that the tri-metallic UD nanocatalysts effectively favored the hydrogenation reactions and inhibited the massive formation of coke by 50% that usually occur during the thermal processing of heavy oils (Del Bianco, Panariti, Di Carlo, et al. 1993). However, further increase in reaction time, at high temperature, caused decrease in

conversion possibly due to that the porous media was highly affected during the thermal processes via coke formation. It should be noted that the increase in residue conversion, in the presence of nanocatalysts, at high temperature is not only due to a thermal effect, but it also due to the increase in concentration of nanocatalysts deposited inside the porous media (Hashemi, Nassar, and Pereira-Almao 2012) that subsequently enhanced the catalytic upgrading.

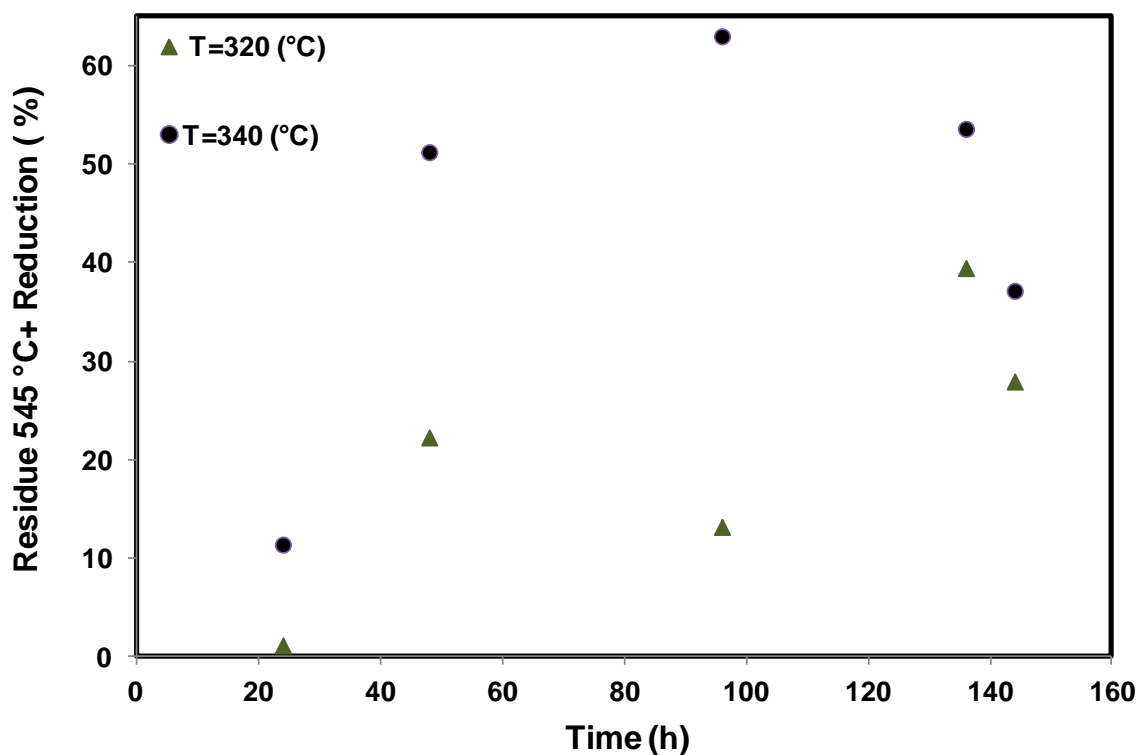


Fig 4.8: Percentage of residue content reduction of produced liquid samples from porous media in the presence of nanocatalysts with respect to control experiments (without nanocatalysts) as a function of time at pressure of 3.5 MPa, hydrogen flow rate of 1 cm³/min, and temperatures of 320 and 340 °C

4.4.4 Micro carbon residue (MCR) content

The content of micro carbon residue (MCR) is a useful technique that considered as a measure for potential coke formation (Lal, Otto, and Mather 1999). Figure 4.9 depicts the MCR content as a function of reaction time for different produced liquid samples from porous media at different temperatures and in presence and absence of UD tri-metallic nanocatalysts. In all cases, the MCR content decreased linearly with the increase in reaction time. The content of MCR also increased as the temperature increased. In the contrary, in the presence of nanocatalysts, increasing the temperature favored the reduction in MCR content, confirming the catalytic effect of the UD tri-metallic nanocatalysts and their role in favoring the hydrogenation reactions.

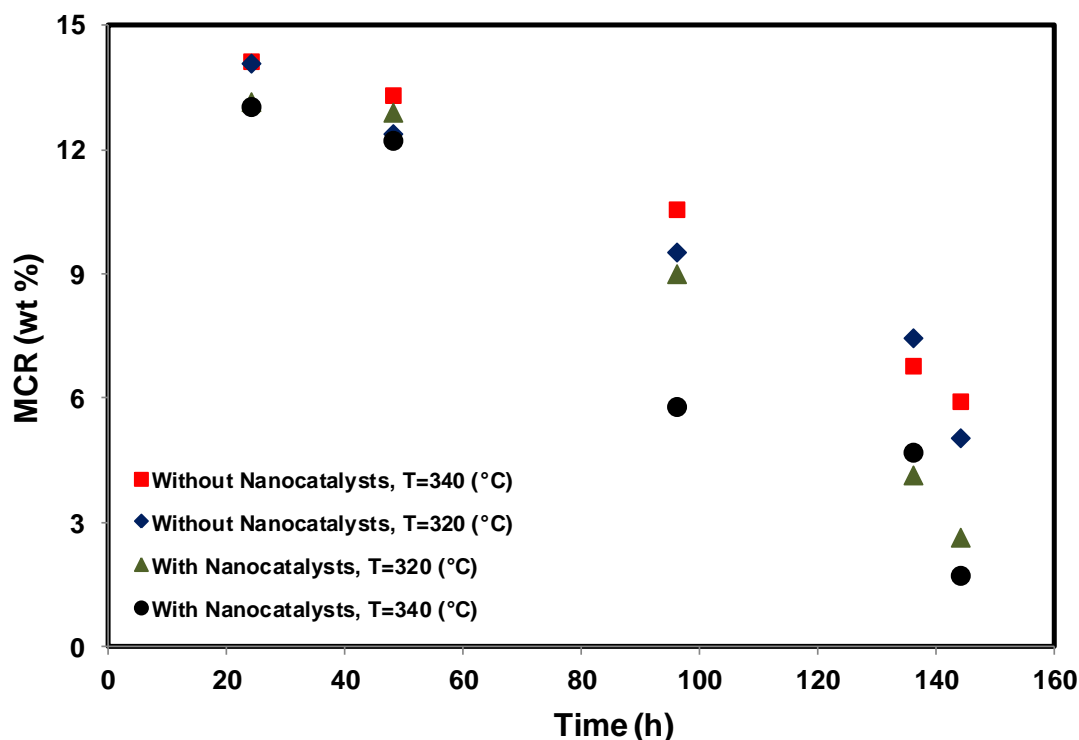


Fig 4.9: MCR content of produced liquid samples from porous media as a function of reaction time in the absence and presence of tri-metallic UD nanocatalysts at pressure of 3.5 MPa, hydrogen flow rate of 1 cm³/min, and temperatures of 320 and 340 °C

Figure 4.10 presents the percentage of MCR reduction calculated on the basis of control experiments (without UD tri-metallic nanocatalysts) from eq. 4.2. As seen, the percentage of MCR reduction increased with both time and temperature. Within experimental error, at both considered temperatures, the increase was exponential with time. This again, confirms that nanocatalysts improved the hydroprocessing reactions and consequently reduced the potential for coke formation.

$$\text{MCR Reduction (\%)} = \frac{\text{MCR without Nanocatalyst} - \text{MCR with Nanocatalyst}}{\text{MCR without Nanocatalyst}} \times 100 \quad (4.2)$$

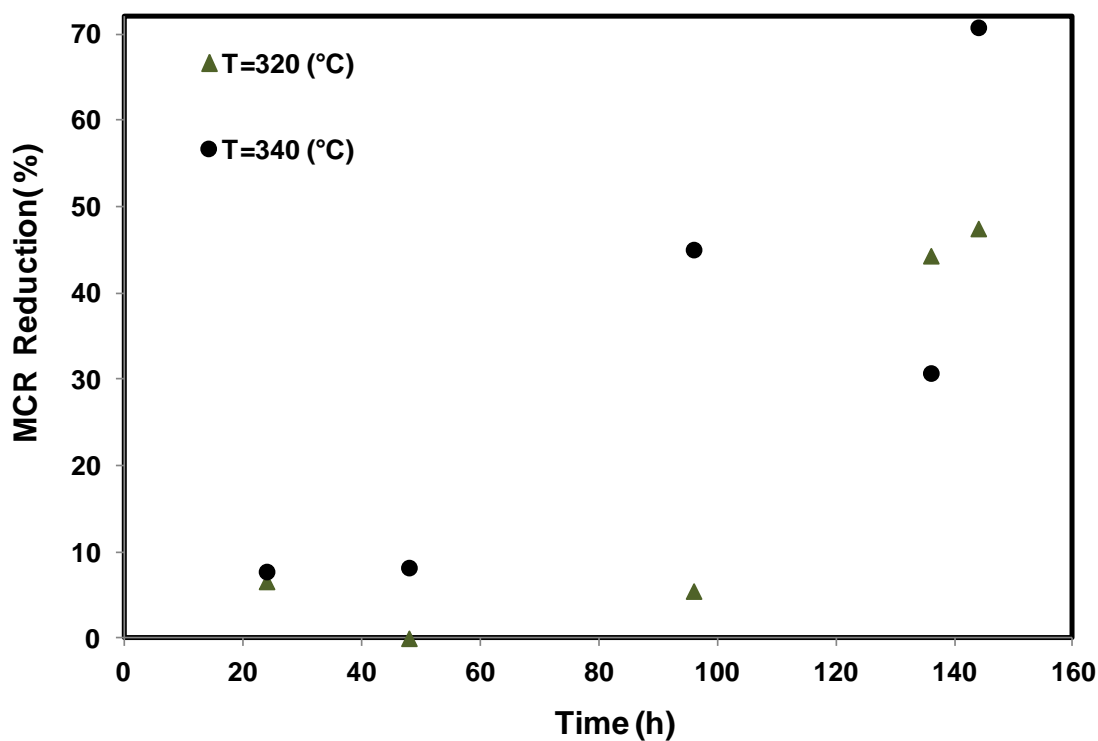


Fig 4.10: Percentage of MCR content reduction of produced liquid samples from porous media at different times in the absence and presence of tri-metallic UD nanocatalysts at pressure of 3.5 MPa, hydrogen flow rate of 1 cm³/min, and temperatures of 320 and 340 °C

4.4.5 The homogeneity of the produced liquid

The homogeneity of the produced liquid was also tested by observing one drop of each liquid samples produced at different conditions using optical microscopy (OM). Figure 4.11 presents the OM micrographs (40×) for selected samples. The figure includes optical images of virgin bitumen (Figure 4.11a), virgin VGO (Figure 4.11b), VGO emulsion containing tri-metallic UD nanocatalysts (Figure 4.11c), images collected of produced liquid samples from catalytic experiment at different time intervals at 320 °C (Figure 4.11d), images collected from catalytic experiment samples at 340 °C for different time intervals (Figure 4.11e) and images collected from experiments that were run without tri-metallic UD nanocatalysts at 340 °C and different reaction times (Figure 4.11f).

As seen, no major solid materials were observed in Figures 4.11a, b, and c. Similar observations can be seen for early reaction of the samples obtained from liquid produced from porous media in presence of nanocatalysts at different temperatures (Figures 4.11d and e). However, coke materials starts to appear with further increase in the temperature and reaction time. On the other hand, coke appeared earlier for reaction occurred without nanocatalysts and increased with reaction time (Figure 4.11f). These observations confirm the previous findings on the effectiveness of the UD nanocatalysts to activate hydrogen and, consequently, decrease the rate of coke formation. However, care must be taken for higher severity reaction conditions (high temperature and reaction time) because the probability of coke formation is increased, which require more control on reaction process to avoid unwanted product formation. These observations are in

excellent agreement with the ones reported by Galarraga and Pereira-Almao for catalytic bitumen upgrading in a batch reactor (Galarraga and Pereira-Almao 2010).

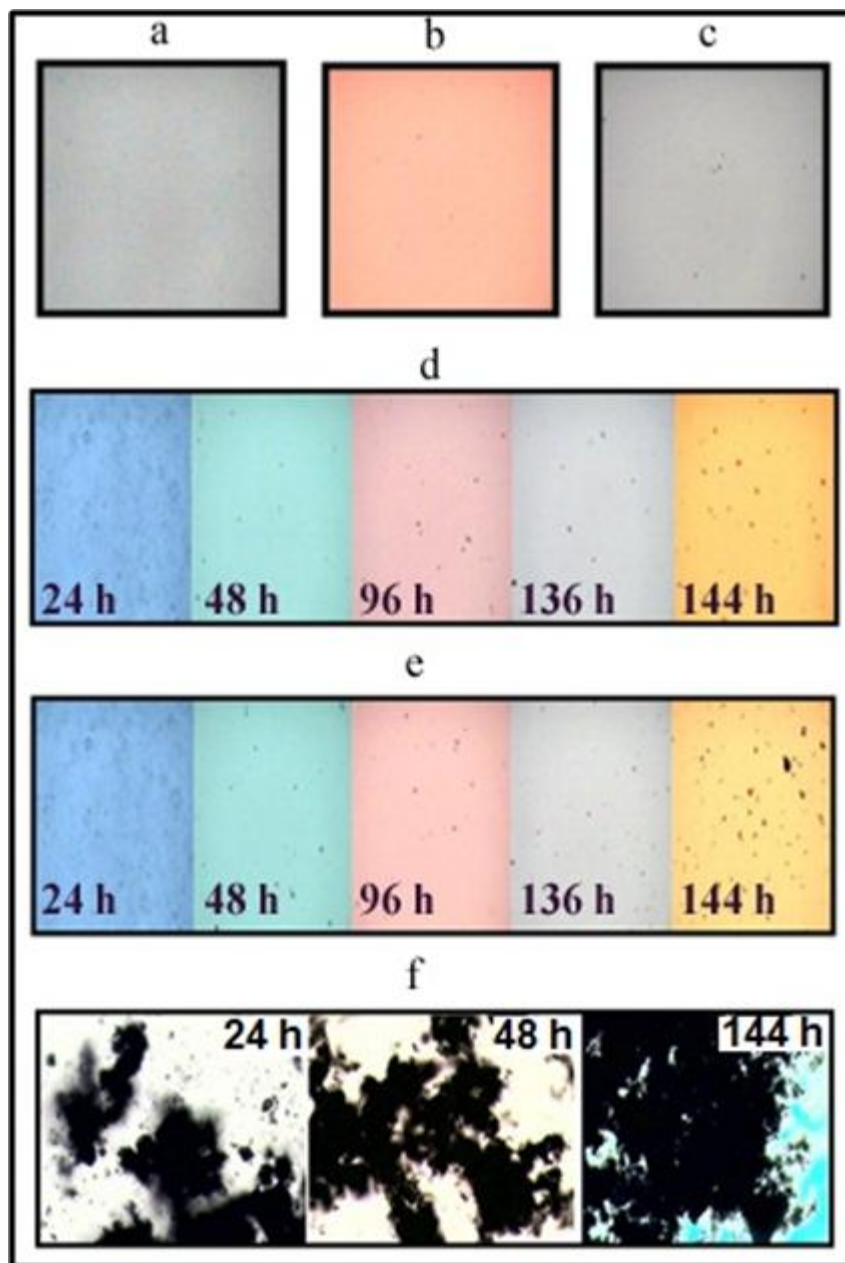


Fig 4.11: Optical micrographs (40 \times) of a liquid drop for samples obtained at different conditions: (a) virgin Athabasca bitumen, (b) virgin Nexen VGO, (c) VGO emulsion containing tri-metallic nanocatalysts, (d) produced from porous media in presence of nanocatalysts at 320 $^{\circ}$ C, (e) produced from porous media in presence of nanocatalysts at 340 $^{\circ}$ C, (f) produced from porous media in the absence of nanocatalysts at 340 $^{\circ}$ C

4.4.6 Sulfur content

Athabasca bitumen contains considerable amount of sulfur (about 4.25 wt %) that can impact the product quality and consequently result in environmental impact. Accordingly, sulfur removal or hydrodesulphurization (HDS) is considered an important parameter not just for examining the bitumen upgrading process (Galarraga and Pereira-Almao 2010) but also to meet the environmental regulations, pipeline and refinery specifications of the allowable concentration in the commercial crude oil in the market. The permissible concentration of sulfur in good quality upgraded oil is around 0.1-0.2 wt% (Syncrude_Canada 1996).

Figure 4.12 shows the sulfur concentration in produced liquid samples against the reaction time for different temperatures, in the presence and absence of UD tri-metallic nanocatalysts. As expected, the sulfur concentration decreased with both time and temperature. Sulfur removal was further enhanced in the presence of nanocatalysts, especially at lower temperature. Under these conditions, coke formation is well controlled and the hydrogenating reactions outperformed the thermal cracking reactions. This resulted in the hydrogenation of unsaturated heteroatoms containing compounds (like porphyrins and quinolines) and the hydrocracking of the cyclic compounds (Panariti, Del Bianco, Del Piero, Marchionna, et al. 2000); and consequently removal of sulfur in the form of hydrogen sulfide.

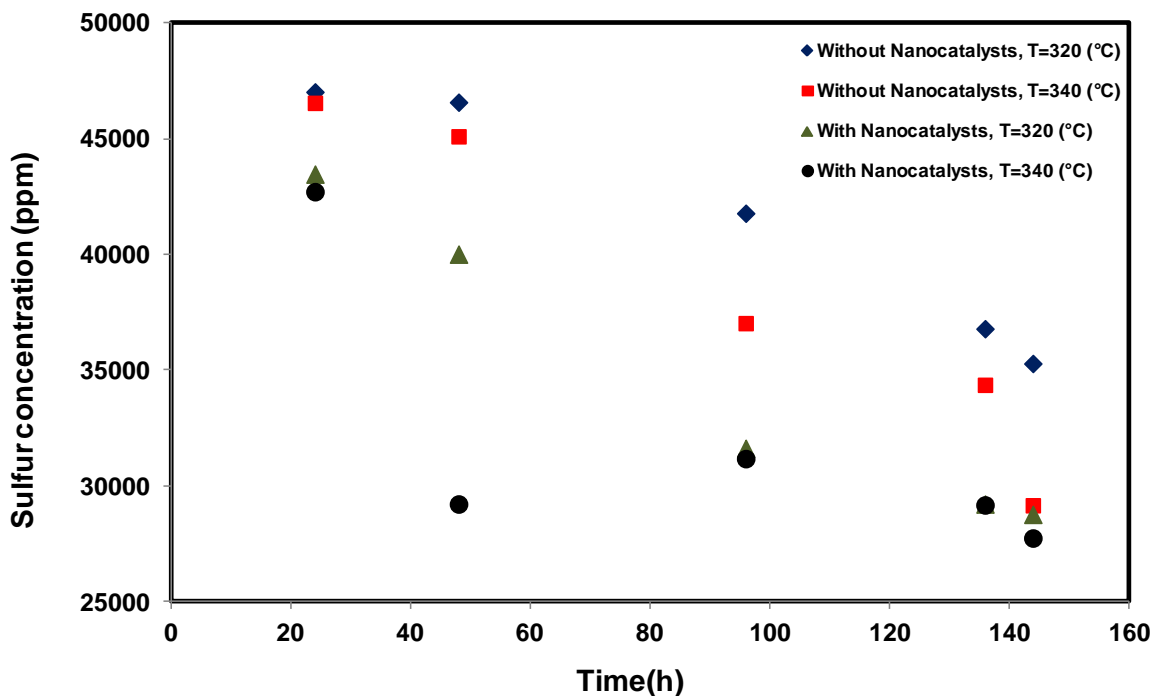


Fig 4.12: Sulfur content of produced liquid samples from porous media at different times in the absence and presence of tri-metallic UD nanocatalysts at pressure of 3.5 MPa, hydrogen flow rate of 1 cm³/min, and temperatures of 320 and 340 °C

4.4.7 Nitrogen content

In addition to sulfur compounds, Athabasca bitumen contains considerable portion of nitrogen (about 0.33-0.68 wt %), which exists in the heteroatom structures. The presence of nitrogen in the structure of produced liquid can cause poisoning of catalysts during refinery processes. In addition, the probability of nitrogen oxides (NO_x) production is increased, if nitrogen remained within the produced liquid structure (Speight and Özüm 2002). Nitrogen removal or hydrodenitrogenation (HDN) is more difficult than sulfur removal and the expected level of nitrogen content of petroleum is approximately less than 0.1 wt% (Speight and Özüm 2002).

Figure 4.13 shows nitrogen concentration in produced liquid samples from porous media obtained at different reaction times and temperatures in the presence and absence of nanocatalysts. Clearly, similar to the observations of sulfur removal, nitrogen removal increased with temperature and reaction time. The removal was further enhanced in the presence of tri-metallic nanocatalysts. This again supports that catalytic upgrading coupled with hydrogen injection would enhance the HDN reaction and favor the removal of nitrogen as NH_3 or N_2 , based on nanocatalysts selectivity.

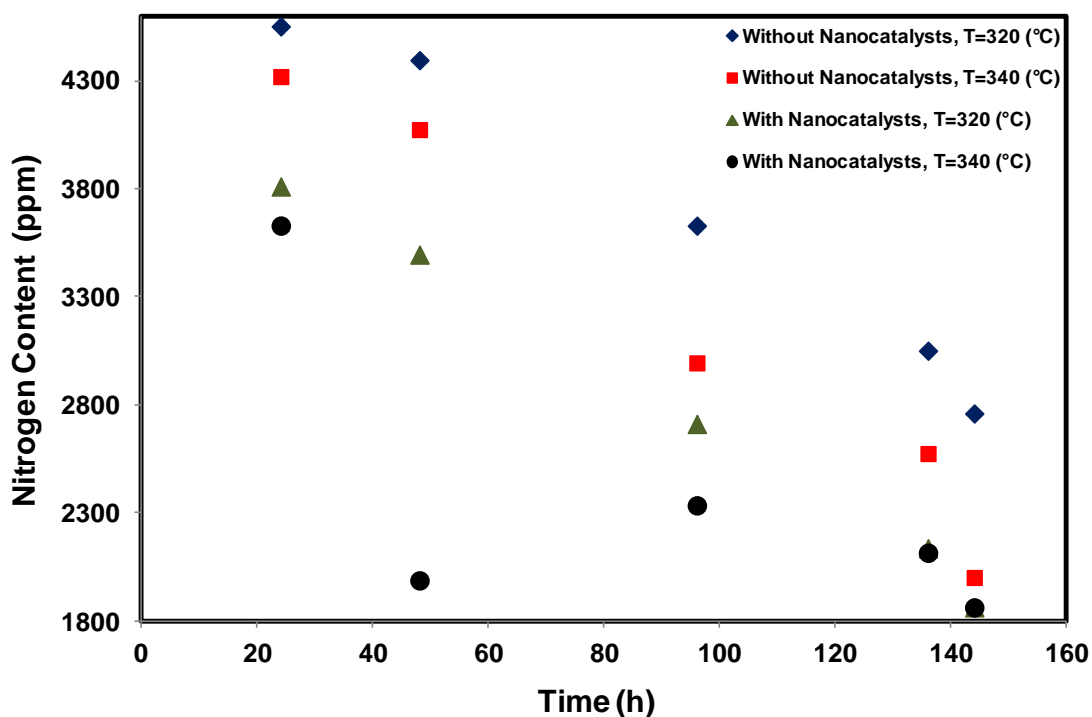


Fig 4.13: Nitrogen content of produced liquid samples from porous media at different times in the absence and presence of tri-metallic UD nanocatalysts at pressure of 3.5 MPa, hydrogen flow rate of $1 \text{ cm}^3/\text{min}$, and temperatures of 320 and 340 °C

4.4.8 Average quality enhancement

Figure 4.14 shows a histogram of the percentage improvement of the average properties of the liquid produced during the whole life of the process (144 h) in the presence of nanocatalysts. These results are generated by comparing the quality improvement for experiments run in the presence of nanocatalysts with the ones without the presence of nanocatalysts. Clearly, the presence of nanocatalysts inside the porous media has highest effect on MCR content and residue reduction. Nanocatalysts could reduce the nitrogen content as well as sulphur content of produced samples, which is environmentally beneficial. Furthermore, viscosity and API gravity of produced materials could be significantly changed by selection appropriate nanocatalysts.

It is worth noting here that for the real field application the injection of hot VGO containing nanocatalysts is not just an environmentally friendly approach that leads to reduction in water consumption during SAGD process, but also cost effective as most of the injected VGO will be produced via the production well. In addition, injected VGO clearly enhances many other properties of the in-situ bitumen such as API, viscosity, etc.

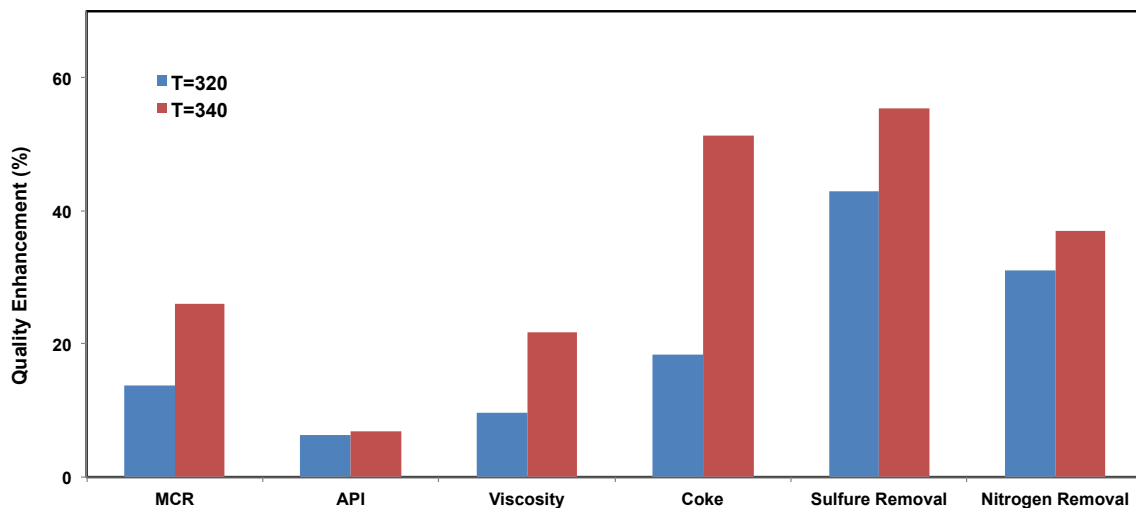


Fig 4.14: Average quality enhancement of produced liquid from porous media during the whole life of process at different temperatures in the presence of tri-metallic UD nanocatalysts at pressure of 3.5 MPa, hydrogen flow rate of 1 cm³/min, and temperatures of 320 and 340 °C

4.5 Conclusions

In this study, in-situ catalytic upgrading of Athabasca bitumen by using in-situ prepared tri-metallic ultra-dispersed nanocatalysts and hydrogen injection inside a continuous packed bed reactor was investigated. The quality of produced liquid was analyzed, at different reaction times and temperatures, on the basis of its viscosity, API gravity and content of sulfur, nitrogen, and MCR.

Tri-metallic nanocatalysts upgraded the Athabasca bitumen in presence of hydrogen, to saturate the free radicals and inhibit coke formation. The presence of tri-metallic nanocatalysts enhanced the reduction of hydrocarbon residue and MCR content. In addition, significant enhancement of liquid viscosity and API gravity was achieved. Furthermore, catalytic upgrading coupled with hydrogen injection enhanced the hydrodesulfurization (HDS) and hydrodenitrogenation (HDN) reactions. Therefore,

catalytic in-situ upgrading in conjunction with hydrogen injection and/or generation not just can result in produced high quality liquid, but also it has the advantages of less environmental impact and cost-effectiveness.

Chapter 5 In situ Upgrading of Athabasca Bitumen Using Multimetallic Ultra-Dispersed Nanocatalysts in an Oil-Sands-Packed Bed Column: Part 2, Solid Analysis and Gaseous Product Distribution⁴

5.1 Abstract

Thermal cracking of Athabasca bitumen was carried out in an oilsand packed bed column, in the presence and absence of in-situ prepared tri-metallic nanocatalysts at a pressure of 3.5 MPa, residence time of 36 h, and temperatures of 320 and 340 °C. The effect of reaction severity (time and temperature) as well as nanocatalysts on solid and gaseous product was investigated. Results showed that the presence of tri-metallic nanocatalysts enhanced the hydrogenation reactions and consequently led to significant coke and CO₂ emission reduction. Further, the analysis of the gaseous product and deposited solid confirmed the previous findings reported in Part 1 of this study. The accumulative volume of coke precursor gases, such as ethylene and propylene, increased with the reaction severity. However, reaction severity has no significant effect on the atomic metallic ratios (metal/total metal) of the employed tri-metallic nanocatalysts which clearly demonstrates the stability of injected UD nanocatalysts in the porous media

⁴ Hashemi, Rohallah, Nashaat N. Nassar, and Pedro Pereira-Almao. Enhanced Heavy Oil Recovery by In-Situ Prepared Ultra-Dispersed Multi-metallic Nanoparticles: A Study of Hot Fluid Flooding for Athabasca Bitumen Recovery. *Energy & Fuel* (In processing)

at high pressure and temperature. Nonetheless, aggregation of nanocatalysts inside the porous media was observed and graphically demonstrated by ESEM images. Overall, the presence of tri-metallic nanocatalysts in porous media not just enhanced bitumen upgrading, but also it improves the produced liquid quality and reduces the produced liquid coke content as well as CO₂ emission by 50%.

5.2 Introduction

World oil reserves are classified as conventional and unconventional reserves. Conventional oils have high API gravity (>15 °API) and relatively low levels of contaminants and residue while unconventional oils contain higher levels of residue cut as well as lower quality and API gravity (Radler 2005, Speight 2000). World unconventional reserves are estimated to be about 5.6 trillion barrels; while rapidly declining conventional oil reserves about 1.02 trillion barrels are estimated (Hein 2006). Conventional oils have so far been the first choice to supply the market demands due to its higher quality and lower processing costs. However, these reserves are limited and their productions are not enough to satisfy the current and future market demands. Therefore, the production of oil from unconventional resources is of paramount importance. However, unconventional oils have much higher viscosity due to abundance of heavy compounds in their structures which impose serious concerns for their production, transportation and recovery. In addition to transportation problem and poor recovery performance, unconventional oils contains considerable fractions of heteroatoms, such as sulphur, nitrogen, and metals, which cause more difficulty in processing as well as marketability (Gosselin 2010). In Alberta, heavy oil and bitumen

production and upgrading from oil sands, with more than 170 billion barrels of estimated oil sands, are more water and energy intensive. As a result, more pollution is created, such as heavier residue, wastewater, solid waste, and air emissions (Bergerson and Keith 2006). For instance, approximately two to four barrels of fresh water are generated for extraction and upgrading one barrel of bitumen (Griffiths, Dyer, and Institute 2008). It is worth noting that these numbers are obtained after subtracting the volumes of recycled water. For example, mining operations use about 12 barrels of fresh water to produce one barrel of bitumen (70% of which is recycled). Nonetheless, almost none of the water resources which are used for oil sands operations returns to its natural cycle. Surface mining operations are subject to a zero-discharge policy because of the toxin in the wastewater and the tailing ponds that store the non-recyclable wastewaters (Griffiths et al. 2006).

In addition to fresh water consumption, extraction and upgrading of bitumen with the current technology produce considerable amounts of greenhouse gas (GHG) emissions (Charpentier, Bergerson, and MacLean 2009). Nonetheless, the province of Alberta was the first in North America to legislate GHG reductions on large industrial facilities in 2008. All facilities including, oil sands facilities that emits more than 100,000 tons of GHGs a year must reduce emissions intensity of GHG by 12 percent. Many processes such as carbon capture and storage, sulfur removal, etc. were developed to meet these regulations. Furthermore, increasingly stringent legislation limits on the level of transportation fuels contaminants has encouraged the markets to develop new methods for processing of heavy feedstocks (Gosselin 2010). However, it would be very beneficial to mitigate the GHG emissions from the source of production. For instance, in-

situ upgrading, underground refinery, aims to decrease the level of Athabasca bitumen contaminants such as sulfur and nitrogen to a good extent (McEachern 2009). Improved recovery and upgrading techniques, which could decrease the fresh water consumption and the GHG emissions, seem necessary to overcome the challenges for the sustainable development of the Alberta oil sands (Isaacs 2005).

Part I of the current work investigated the effect of tri-metallic nanocatalysts on the quality enhancement of produced liquid by in-situ catalytic upgrading of Athabasca bitumen using in-situ prepared tri-metallic ultra-dispersed nanocatalysts in conjunction with hydrogen injection inside a continuous oil sands packed bed reactor. Results from Part I showed that the presence of tri-metallic nanocatalysts enhanced the reduction of hydrocarbon residue and MCR content in the produced liquid. In addition, significant enhancement of liquid viscosity and API gravity was achieved. Furthermore, catalytic upgrading coupled with hydrogen injection enhanced the hydrodesulfurization (HDS) and hydrodenitrogenation (HDN) reactions.

Coke formation and catalysts deactivation is one of the most important technological and economic problems in upgrading processes of petrochemical industry. During the upgrading reactions, activity of the upgrading catalysis (especially cracking catalysis) rapidly decreases (Gielen and Palekar 1989). To reduce coke deposition, it is very beneficial to understand the mechanism of coke formation during the reaction and its effects on the catalysts performance. A major step for coke deposition is the formation of precursors such as olefins and di-olefines (McLaughlin and Anthony 1985, Venuto and Hamilton 1967, Langner et al. 1980, Langner 1980, 1981). Specifically, formation of ethylene and propylene as coke precursors was reported in literature (Langner 1980,

1982, Anderson et al. 1979, Mole, Anderson, and Creer 1985, Vedrine et al. 1980, Zou et al. 1987, Zou et al. 1993). In other words, any significant increase in ethylene/propylene is interpreted as a clear sign of coke production mechanism. Thus, analysis of produced gases during catalytic upgrading reactions could be used to predict and/or evaluate the coke formation quality during the hydrocracking reactions.

Part II of the current investigation explores the effectiveness of the ultradispersed tri-metallic nanocatalysts in reducing coke formation and CO₂ emission during bitumen upgrading. Accordingly, in this part of the study, an experimental system for studying gaseous emissions during in-situ catalytic upgrading of Athabasca bitumen in oil sands packed bed reactor is investigated. Further, characterizations of the nanocatalysts after the reaction, specifically in the liquid filtrate and packed bed solids, are reported. In is worth noting here that economics of the process was not considered as the focus of the current study. To evaluate the whole process economics, it is required to investigate more aspects of nanocatalysts usage as upgrading and recovery enhancement catalysts.

5.3 Materials and methods

5.3.1 Chemicals

Silica sand (99% of SiO₂, AGSCO, Hasbrouck Heights, NJ, USA) from AGSCO was used as the porous media in the packed bed column. The sand particles size is in the range 12-20 mesh (U.S. Sieves). Athabasca bitumen (JACOS, AB, Canada) was used to saturate the porous media and mimic Athabasca oil sands. VGO (Nexen, AB, Canada) was used as a carrier for in-house prepared tri-metallic nanocatalysts to be introduced

inside the porous media. Properties of utilized Athabasca bitumen and VGO have been presented in part I of this study (Hashemi, Nassar, and Pereira Almao 2013a). Nickel acetate tetrahydrate (99%, Sigma-Aldrich), ammonium metatungstate (99%, Sigma-Aldrich), and ammonium molybdate tetrahydrate (99%, Sigma-Aldrich) were used as precursors for tri-metallic nanocatalysts preparation. Chloroform (CHCl_3 , 99%, Sigma Aldrich) was used as a digesting agent to determine percentage of coke in produced samples. Utilized gases for gas chromatography and pilot plant including hydrogen, air, nitrogen, helium and argon (all gases 99.9% Purity) were purchased from Praxair Specialty Gases & Equipment (Calgary, AB, Canada).

5.3.2 Preparation of nanoparticles suspension

Nanocatalysts tri-metallic colloidal suspension in vacuum gas matrix was prepared following our method detailed in Part 1 of this study (Hashemi, Nassar, and Pereira Almao 2013a). The atomic metallic ratios (metal/total metal) of the colloidal suspension were as follows: Mo = 0.6267, Ni = 0.1808 and W = 0.1924.

5.3.3 Experimental procedure

Details of the experimental set-up were presented in our previous study (Hashemi, Nassar, and Pereira Almao 2013a). In this part, we mainly focus on the solid and gaseous emissions produced during bitumen upgrading. Figure 5.1 shows a schematic representation of the set-up of the gas analysis section in more details.

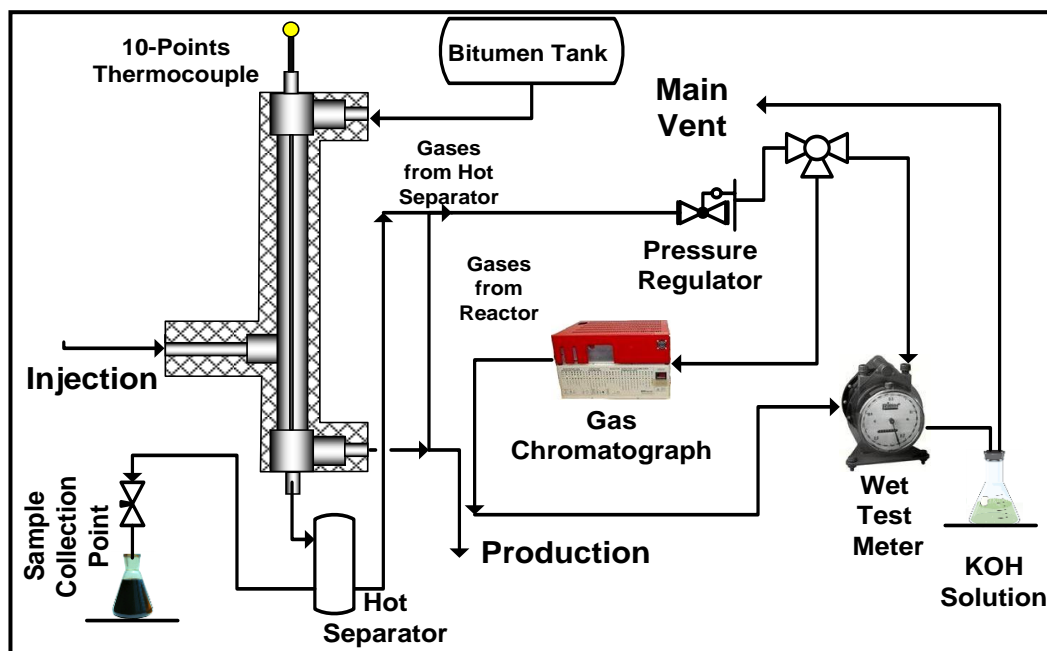


Fig 5.1: Schematic representation of the gaseous emissions experimental set-up

After the installation of the sand packed bed and completion of the leak test, the sand bed was saturated with Athabasca bitumen and set to a pressure of 3.5 MPa. Then, the packed bed column was heated to the desired temperature. Once the reaction temperature and pressure were attained, the actual experiment started by consequently introducing hydrogen gas and the injecting fluid (VGO-containing nanoparticles) into the reactor column. At this point, the zero time for gaseous emission production was considered.

The produced gases at the outlet of the column were analyzed at regular time intervals and their concentrations were measured, at atmospheric pressure and 25 °C, by a gas chromatograph (SRI 8610C, SRI Instruments, Torrance, CA) equipped with two thermal conductivity detectors (TCD), a flame photometric detector (FPD), and a flame ionization detector (FID) to detect the type and measure the concentration of produced gases. Before sending to vent, all gases were passed through a basic solution (KOH).

After the run, the reactor column was cooled to room temperature and carefully disassembled. The packed materials (sand, bitumen, nanoparticles, VOG, etc) were carefully discharged from the reactor column for analysis.

After that, all parts of the set-up were washed with toluene, soap and hot water; therefore, the apparatus could be ready for another cycle of experiments. Light hydrocarbons (C1-C5) were quantified in a Hewlett-Packard GC model 6900 provided with a 50 m length capillary column for PONA characterization. This instrument was also used to detect other produced gases such as ethylene, propylene, carbon dioxide, carbon monoxide, hydrogen sulfide and hydrogen. Coke content was measured as follows: Approximately 2 g of produced sample was dissolved in 100 cm³ of chloroform (ratio 1:50 g/cm³). Accordingly, insoluble species, namely coke and metal were precipitated out. The precipitate was separated from the final solution by filtration using a nylon membrane filter paper (0.45 µm) (Nylaflo™, Pall Corporation, Port Washington, NY, USA) and the amount of total solid formed was estimated by mass balance.

Total mass of solids in the produced liquid includes both the mass of eluted nanocatalysts and the formed coke. The mass of nanocatalysts was determined by inductively coupled plasma–atomic emission spectroscopy (ICP–AES, IRIS Intrepid II XDL, Thermo-Instruments Canada, Inc., Ontario, Canada) as explained in our previous study (Hashemi, Nassar, and Pereira Almao 2013a). Accordingly, the difference between total mass and mass of nanocatalysts was considered as the coke content. In addition, selected samples obtained from porous media (sand oil) and filtration cake were analyzed for its surface morphology, compositions and particles size using Environmental Scanning Electron Microscopy (ESEM, Philips model XL-30, 20kV) with Energy

Dispersive Spectrometry (EDS). This instrument is used for conventional high vacuum imaging, or in the environmental mode, can be used to examine wet, oily, gassy or non-conducting samples. For elemental analysis and quantification of samples EDAX Genesis Spectrum V5.2 software was implemented to see the spectrum of detected metals.

5.4 Results and discussions

In this part of the study, results of two sets of experiments (with and without nanocatalysts) conducted at different temperatures (320 and 340 °C) were demonstrated. Other experimental conditions, namely: residence time, reactor pressure, initial nanocatalysts concentration; injection rates and medium permeability were kept fixed for all tests. The results of these two sets were compared to evaluate the effect of nanocatalysts and temperature on bitumen upgrading in terms of coke formation and gaseous emissions.

5.4.1 Solids characterization and morphology

Solid analysis was carried out to determine the amount of produced coke as well as morphology, size and chemical composition of the nanocatalysts after reaction. To do this, qualitative and quantitative characterization were performed after the experiments. Two types of solid were analyzed: (1) Solids recovered from the produced liquid by standard solubilization/filtration techniques, this solid is expected to contain both coke and eluted nanocatalysts; (2) samples from extracted porous media, which contains sand, nanocatalysts, and coke in addition to other hydrocarbon residues attached to the sand.

5.4.1.1 Coke content

In a typical thermal upgrading process, thermal decomposition of bitumen occurs in the presence of hydrogen to saturate the free radicals, and subsequently produce lighter components as well as huge amount of coke (by 50%) and considerable amount of light gas such as methane, ethane, CO₂, etc (Kennepohl and Sanford 1996, Sanford 1995). It is expected that catalytic thermal decomposition would result in less amount of coke as catalysts can create new pathways in the reaction schemes. In this set of experiments, the amount of coke formed in the produced liquid during the reaction time was measured qualitatively and quantitatively.

Figure 5.2 shows pictures that were taken from two filter papers, after the completion of the filtration processes for produced liquid samples obtained at 340 °C for a reaction time of 96 h in the presence and absence of UD nanocatalysts. Clearly, a significant difference can be observed by naked eyes. In the absence of nanocatalysts, a dark color with some black coke particles is observed; while a lighter color without coke particles is observed for a sample produced in the presence of nanocatalysts. This simply shows the significant effect of nanocatalysts in coke reduction, and confirms the optical micrograph observations for MCR reported in Part 1 of this study (Hashemi, Nassar, and Pereira Almaso 2013a).

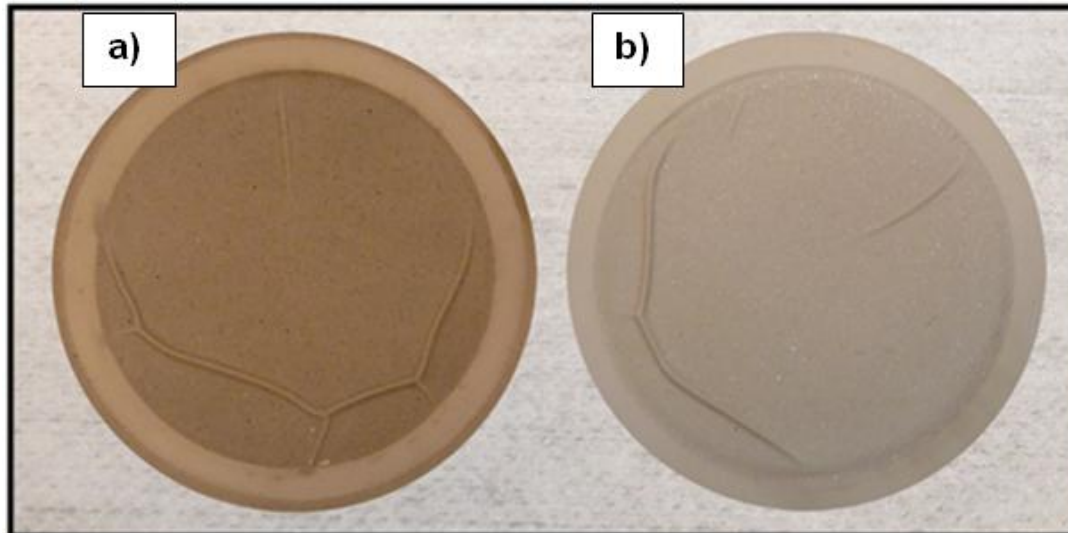


Fig 5.2: Images for different filter papers after filtering different produced liquid samples obtained from porous media at pressure of 3.5 MPa and temperatures of 340 °C. (a) sample produced in absence of nanocatalysts, (b) sample produced in presence of tri-metallic nanocatalysts

Figure 5.3 presents coke contents (wt %) of produced samples against the reaction time at different temperatures in the presence and absence of UD tri-metallic nanocatalysts. Coke content was calculated based on the method that has been explained in the experimental procedure section. It can be seen that the lowest coke content was observed at 320 °C, in the presence of nanocatalysts.

The highest amount of coke (0.47 wt %) was detected at 340 °C in the absence of nanocatalysts. Further, these results are in agreement with the results obtained with optical micrograph images reported in Part 1 of this study (Hashemi, Nassar, and Pereira Almao 2013a), which shows high amount of coke formation at 340 °C. It is worth noting that temperature has a very drastic and sensitive effect on the coke formation during thermal processes (Wang, Guo, and Que 1998). Increasing the temperature speeds up the rate of thermal cracking reactions, which outperform the hydrogenating reactions that are

thermodynamically hindered with temperature. Therefore, a higher proportion of free radicals will form, and subsequently lead to the formation of a higher amount of coke (Demirel and Wiser 1998). Similar observations have been reported by Galarraga and Pereira-Almao for catalytic hydrocracking of Athabasca bitumen performed in a batch reactor experiment (Galarraga and Pereira-Almao 2010).

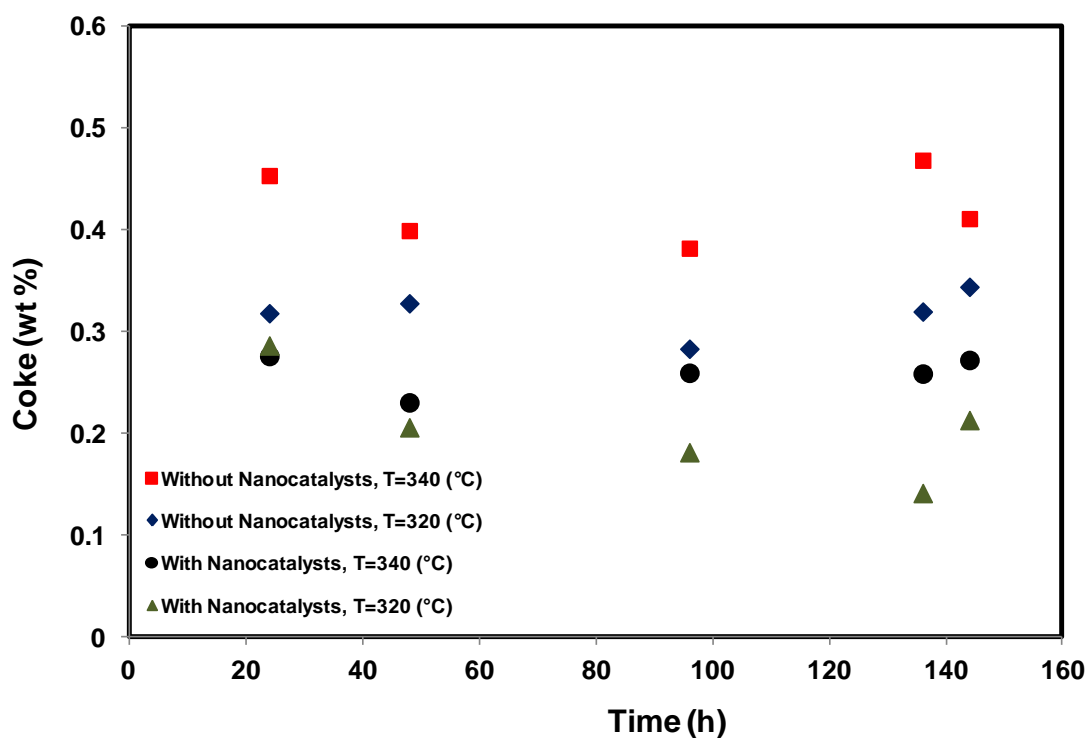


Fig 5.3: Coke content of produced samples from porous media as function of reaction time in the absence and presence of tri-metallic UD nanocatalysts at pressure of 3.5 MPa, hydrogen flow rate of 1 cm³/min, and temperatures of 320 and 340 °C

Figure 5.4 shows ESEM micrograph of a selected filter paper containing the filtered cake (coke + eluted nanocatalysts). The quantity of the existed elements in this cake was analyzed by EDAX (zone a). EDAX confirms that this sample is composed mainly of C,

O, Mo, Ni, and W as seen Table 5.2. As expected, C is the most abundant element in the sample, and then followed by O (comes from SiO_2), Mo, W, and Ni. The EDAX analysis shows that approximately 81 wt % of the sample is C, which accounts for the unconverted hydrocarbons in the sample. The atomic metallic ratios (metal/total metal) of the detected tri-metallic nanocatalysts in the analyzed zone are about 0.67, 0.11 and 0.22 for Mo, Ni, and W, respectively. These values are very close to the desired value of Mo = 0.6267, Ni = 0.1808 and W = 0.1924. This suggests that the composition of the tri-metallic nanocatalysts is stable at the reaction temperature and pressure.

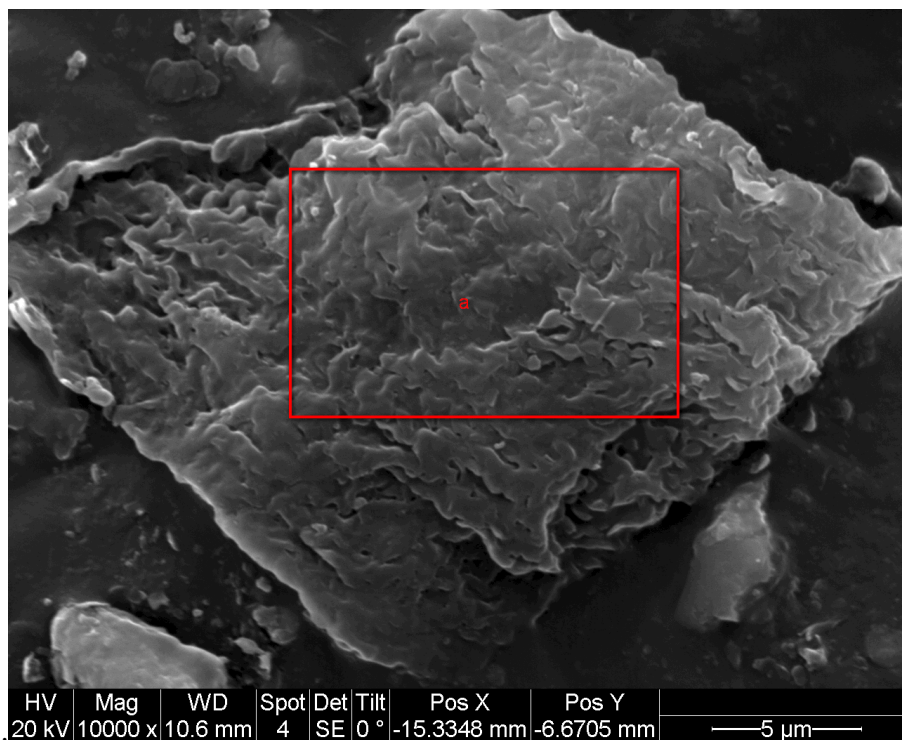


Fig 5.4: ESEM micrographs of filter paper after the filtration process for selected produced liquid sample obtained at 340 °C in the presence of nanocatalysts. Red area shown indicates the zone where EDAX analysis was performed

Table 5-1: Compositional analysis (wt %, atomic %) of zone indicated in Figure 5.4

Element	Wt %	At %
C	80.85	87.55
O	14.58	11.91
Mo	2.62	0.36
Ni	0.27	0.06
W	1.69	0.12

5.4.1.2 Characterization and morphology of packed bed solids after reaction

Using ESEM micrographs and with the help of EDAX spectra analysis, composition, morphology, size and quality of solid samples taken from porous media could be explored.

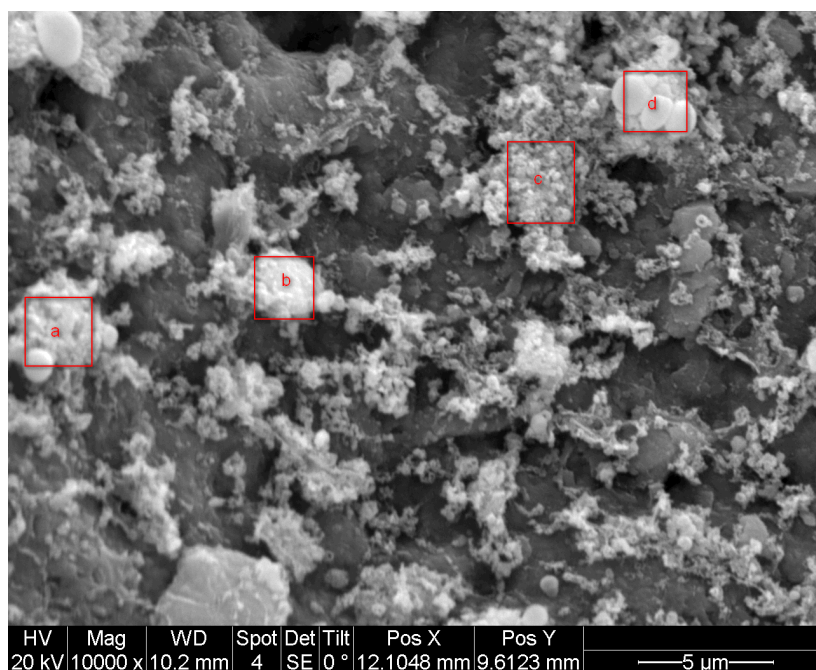


Fig 5.5: ESEM microphotographs of an oil sand sample containing tri-metallic nanocatalysts obtained from the top of the reactor column. Experimental conditions include; residence time: 36 h, porosity: 32.9%, pressure: 3.5 MPa, and temperature: 320 °C

Figure 5.5 shows a general view of ESEM microphotographs of a selected sample obtained from the top of the reaction zone of the packed bed column at 320 °C in the presence of nanocatalysts. Several types of morphologies in a variety of sizes are observed. A closer view into different selected zones (Figure 5.5 a-d) clearly shows that the main structure of the nanocatalysts are individual particles, aggregates and agglomerates ranging from 50 to 600 nm diameters. Quantity of the existed elements in this selected sample was analyzed by EDAX. The scanning was performed on the whole frame and by zones (indicated in the image as a square covering the analyzed area). It should be noted that the compositional analysis was demonstrated both in atomic and weight percent for detected elements.

EDAX confirms that this sample is composed mainly of C, O, Si, Mo, Ni, and W. The quantification results of the elemental analysis on the images on Figures 5.5 and 5.6 are summarized in Table 5.2. As expected, Si and O are the most abundant elements in the sample, which represents the porous media. Noteworthy, the detected C percentage in the whole sample was less than 7 wt%, which accounts for the unconverted hydrocarbons as well as the trapped bitumen in the sample. For the tri-metallic nanocatalysts elements, all the three elements (Mo, W and Ni) were detected and their quantity depends on the selected zone. Moreover, in all the selected zones, V percentage was insignificant.

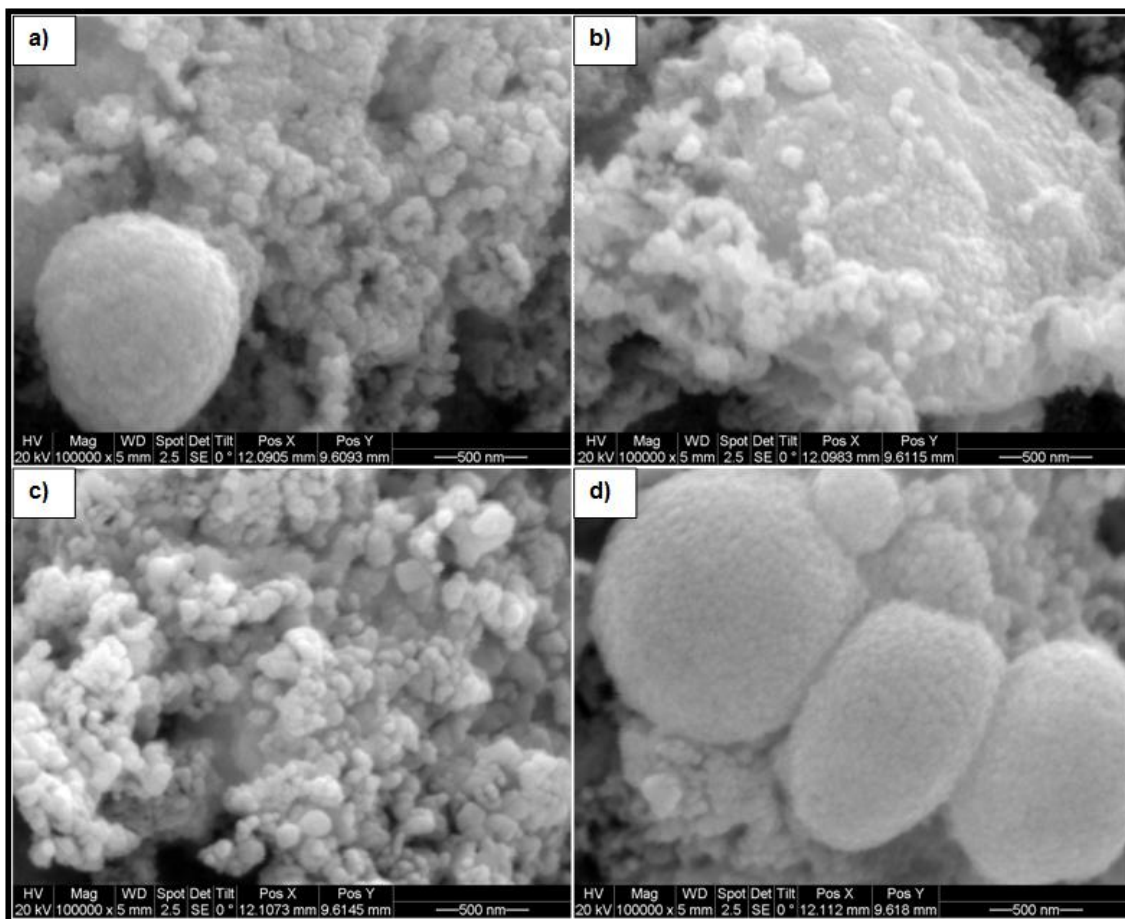


Fig 5.6: ESEM microphotographs of an oil sand sample containing tri-metallic nanocatalysts obtained from the top of the reactor column for selected zones a, b, c and d in Figure 5.5. Experimental conditions include; residence time: 36 h, porosity: 32.9%, pressure: 3.5 MPa, and temperature: 320 °C

Further, clearly and in agreement with the previous findings, high population of deposited nanocatalysts in the top of the reaction zone is observed. Within the whole area, W has the highest percentage among the other elements of the tri-metallic nanocatalysts followed by Mo and then Ni. This order is in agreement with the ICP-AES analysis reported in our previous study (Hashemi, Nassar, and Pereira-Almao 2012). It is worth mentioning that the estimated atomic ratio of the whole area was 0.44, 0.3 and 0.27 for Mo, Ni, and W, respectively. This is slightly different than the desired value of Mo =

0.6267, Ni = 0.1808 and W = 0.1924. This difference can be explained as follows: In the previous study (Hashemi, Nassar, and Pereira-Almao 2012), W had the highest amounts of deposited nanocatalysts inside the medium while Ni had the lowest one. This explains the increase of W atomic ratio as well as Mo atomic ratio reduction. Furthermore, Ni atomic ratio enhancement could be because of presence of Ni in the original matrix of bitumen (Hashemi, Nassar, and Pereira-Almao 2012, Ovalles et al. 1996). It can be seen that the same trend has been observed in the other selected zones as well. Nonetheless, the atomic ratios do not vary significantly, and this supports the stability of UD nanocatalysts in the porous media, even after the reaction.

Table 5-2: Compositional analysis (wt %, atomic %) of zones indicated in Figure 5.5

Element	Whole area		Zone a		Zone b		Zone c		Zone d	
	Wt %	At %	Wt %	At %	Wt %	At %	Wt %	At %	Wt %	At %
C	6.90	13.47	6.67	15.03	11.13	20.93	6.12	14.07	6.3	15.43
O	31.20	45.73	28.03	47.44	34.56	48.79	24.81	42.81	25.88	47.55
Si	44.31	37.00	28.4	27.38	31.36	25.22	35.49	34.89	21.88	22.89
V	0.00	0.00	00.0	0.00	0.00	0.00	0.00	0.00	0.32	0.19
Mo	6.81	1.67	14.48	4.09	11.29	2.66	11.96	3.44	17.70	5.42
Ni	2.80	1.12	8.79	4.05	3.69	1.42	4.83	2.27	11.92	5.97
W	7.97	1.02	13.63	2.01	7.98	0.98	16.79	2.52	15.99	2.56

Figure 5.7 shows ESEM micrographs of a selected sample obtained from the bottom of the reaction zone at 320 °C, in the presence of UD nanocatalysts. EDAX analysis was performed to see the elemental compositions in the whole sampling area as well as selected zones shown in Figure 5.7 by red squares (a-e). Results of the analysis are summarized in Table 5.3. Similar to the sample obtained from the top of the reactor, Si and O have the highest percentages because of sand presence inside the sampling area. It

can be seen that different percentages of tri-metallic nanocatalysts were detected based on the selected regions. However, compared to the sample obtained from the top of the reactor, compositions of nanocatalysts is different from zone to zone. These differences are attributed to the different transport behavior of the metal in the oil sand porous media (Hashemi, Nassar, and Pereira-Almao 2012). Furthermore, as expected, W has the highest amount of deposition, which is in agreement with the breakthrough curves obtained in our previous study. Noteworthy, there exists a small percentage of V amongst the detected metals, which could be coming from bitumen or sand matrix.

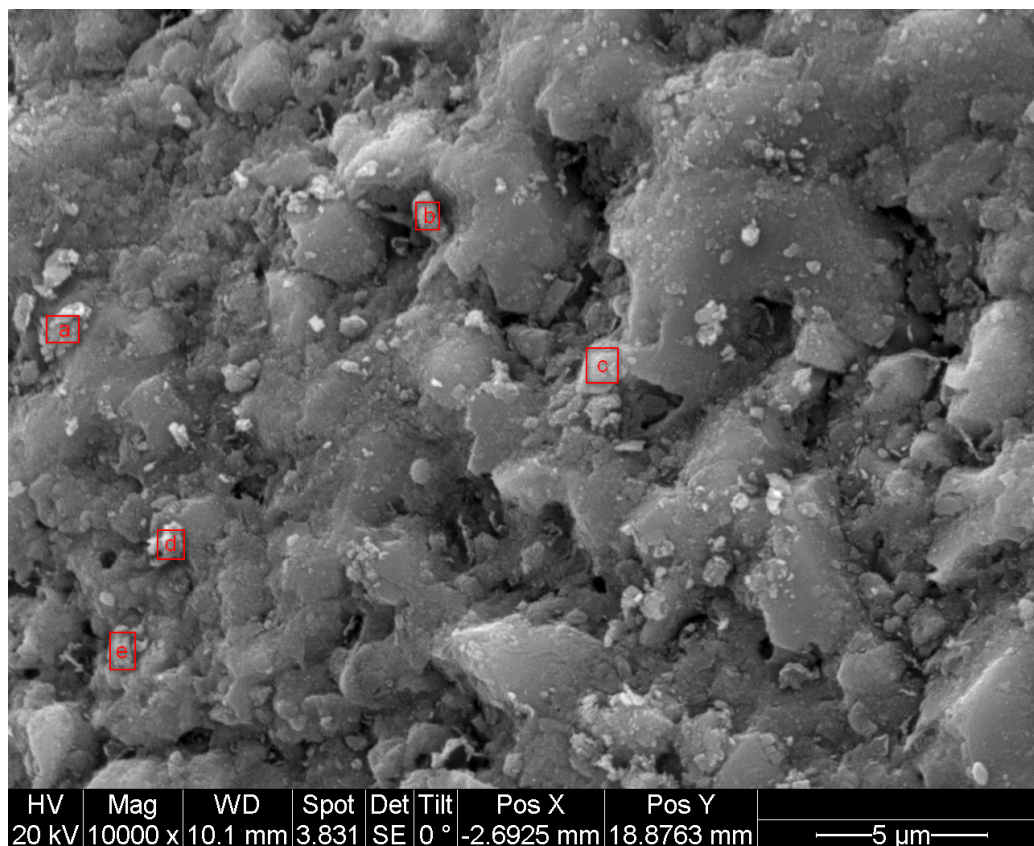


Fig 5.7: ESEM microphotographs of an oil sand sample containing tri-metallic nanocatalysts obtained from the bottom of the reactor column. Experimental conditions include; residence time: 36 h, porosity: 32.9%, pressure: 3.5 MPa, and temperature: 320 °C

Table 5-3: Compositional analysis (wt %, atomic %) of zone indicated in Figure 5.7

Element	Whole area		Zone a		Zone b		Zone c		Zone d		Zone e	
	Wt %	At %	Wt %	At %	Wt %	At %	Wt %	At %	Wt %	At %	Wt %	At %
C	8.01	14.77	6.15	11.98	10.13	19.35	8.42	15.42	13.22	23.56	13.68	24.14
O	25.34	35.06	26.81	39.22	23.51	33.71	27.41	37.67	24.51	32.77	24.31	32.19
Si	62.58	49.33	55.33	46.11	54.17	44.24	58.49	45.79	55.62	42.37	56.23	42.43
V	0.24	0.11	0.49	0.22	0.34	0.15	0.37	0.16	0.34	0.14	0.41	0.17
Mo	0.79	0.18	7.73	1.88	8.04	1.92	1.04	0.24	3.49	0.78	1.70	0.38
Ni	0.70	0.26	0.52	0.21	0.57	0.22	0.82	0.31	0.22	0.08	1.11	0.40
W	2.34	0.28	2.97	0.38	3.24	0.40	3.45	0.41	2.60	0.30	2.56	0.29

By looking at the atomic ratios (metal/total metal), it can be seen the same trend of atomic ratio has been observed at the bottom of the reactor. This again supports the stability of UD nanocatalysts inside the porous media after injection and in presence of high pressure and temperature.

5.4.2 Characterization of produced gases during bitumen upgrading

During the catalytic upgrading reaction tests, a mixture of various gases containing light hydrocarbons, such as methane, ethane, propane, butane and pentane was produced. In addition, other gases were also detected; including hydrogen (feed in excess), hydrogen sulfide, carbon monoxide, carbon dioxide, ethylene and propylene. It should be noted that in the blank experiments, tests conducted in the absence of nanocatalysts, only carbon dioxide was detected as a continuous produced gas. Other gases had a very small percentage as well as discrete order. This again supports that nanocatalysts has a significant effect on the upgrading reaction and could create new pathways in the reaction schemes.

Detailed analysis of the produced gaseous emissions during the upgrading reaction in the presence and absence of tri-metallic nanocatalysts are presented below. However,

before presenting the results of analysis for the gas section, it is beneficial to show the gas mass balance of the aforementioned experimental tests. Figure 5.8 shows the total produced gas mass against the time of the experiment for different reaction conditions. As seen, in all tests, mass of produced gas was increased with time and continues until the end of the experiment.

It can be clearly observed that the amount of produced gas in the experiments performed in the presence of nanocatalysts is much higher than the blank experiments, conducted in the absence of nanocatalysts. In addition, increasing the temperature favored the total mass of produced gases from the reaction. It is worth noting that analysis of the produced gases showed that the production of gaseous hydrocarbon inside the medium increased significantly in presence of nanocatalysts.

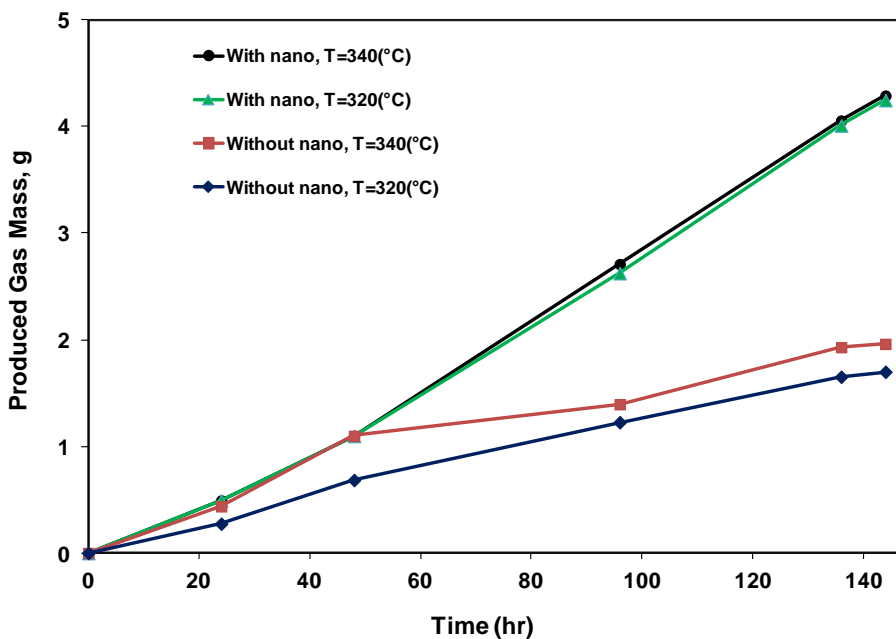


Fig 5.8: Produced gas mass balance of hot VGO injection into the high permeability sand packed bed at different times in the presence of tri-metallic UD nanocatalysts at pressure of 3.5 MPa, hot fluid injection rate of 0.01 cm³/min, hydrogen flow rate of 1 cm³/min, and temperatures of 320 and 340 °C

5.4.2.1 Blank experiments, without tri-metallic nanocatalysts

The objective of these blank experiments was to evaluate the effect of temperature in the presence of hydrogen on product yields and quality as well as to be used as control experiments for comparison. The experiments were carried out by varying the temperature at a fixed pressure of 3.5 MPa and hydrogen flow rate of 1 cm³/min. The analysis of produced gases showed that most of these gases are mainly carbon dioxide and small percentages of methane, ethane and hydrogen sulfide. However, except for carbon dioxide the other gases had discrete curves. Figure 5.9 shows the trends of cumulative volume of carbon dioxide produced during the experiment as a function of time. Clearly, production of carbon dioxide increased with time. Increasing the reaction temperature favored the production of carbon dioxide. These findings agree well with the ones reported in Part 1 of this study, which shows that catalytic reactions are thermally controlled at high temperature (Panariti, Del Bianco, et al. 2000a, Galarraga and Pereira-Almao 2010). These reactions involved C-C bond cleavage (Panariti, Del Bianco, Del Piero, Marchionna, et al. 2000, Panariti, Del Bianco, et al. 2000b) which subsequently form higher proportion of free radicals that lead to significant coke deposition and CO₂ emissions.

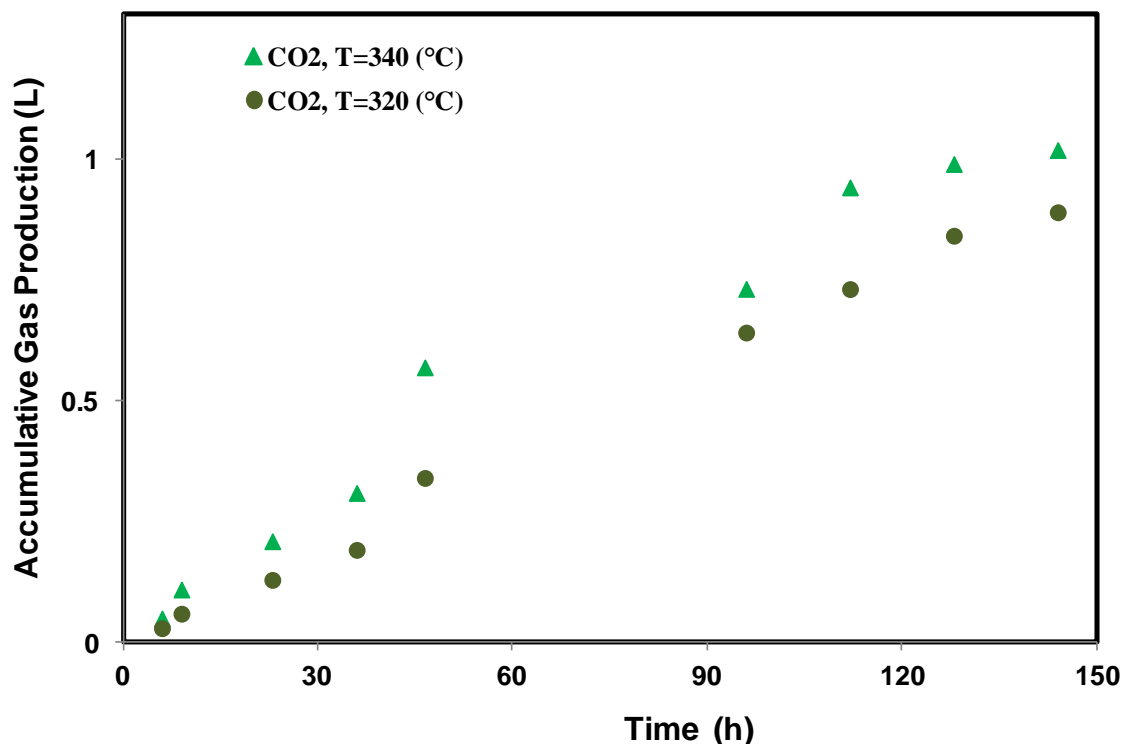


Fig 5.9: Accumulative volume of carbon dioxide produced from oil sand porous media at different times, in the absence of tri-metallic nanocatalysts and test pressure of pressure of 3.5 MPa and temperatures of 320 and 340 °C

Due to the discrete production behavior of the all gases, except carbon dioxide, it is hard to obtain a final conclusion on the reaction scheme due to the lack of specific trend on the production of gases from blank experiments. However, produced volumes of these gases were demonstrated to show the presence of different types of gases produced in the blank experiments. Details are provided in next sections.

5.4.2.2 Effect of tri-metallic nanocatalysts

It has been found in the Part 1 of this study that the presence of nanocatalysts inside the porous media enhanced the hydrogenating reactions and consequently inhibited coke formation (Hashemi, Nassar, and Pereira Almaso 2013a). This resulted not just in better

liquid quality, but also in significant reduction of CO₂ emissions. Detailed analysis of various gaseous products released during bitumen upgrading in the presence of tri-metallic nanocatalysts are presented below.

5.4.2.2.1 Carbon dioxide and monoxide

Figure 5.10 shows the produced cumulative volumes of carbon dioxide and carbon monoxide gases during the catalytic upgrading of bitumen as a function of time and temperatures of 320 and 340 °C. Compared to the blank experiments, about 50% reduction of total carbon dioxide production is observed which again proves that the presence of tri-metallic nanocatalysts has a significant effect on CO₂ production. These findings confirm the previous statement regarding the effectiveness of the UD tri-metallic nanocatalysts on the hydrogenation reactions, which consequently, decrease the rate of coke production and CO₂ emissions and enhance the production CO, a valuable product for synthetic gas.

Evidently, CO production was at the cost of CO₂ elimination; as the figure shows that at the time of CO₂ volume is plateauing the production of CO increased significantly. Moreover, the temperature shows insignificant effect on CO₂ production during catalytic reactions for this specific experiment, which support that the reaction is not thermally limited in the presence of nanocatalysts.

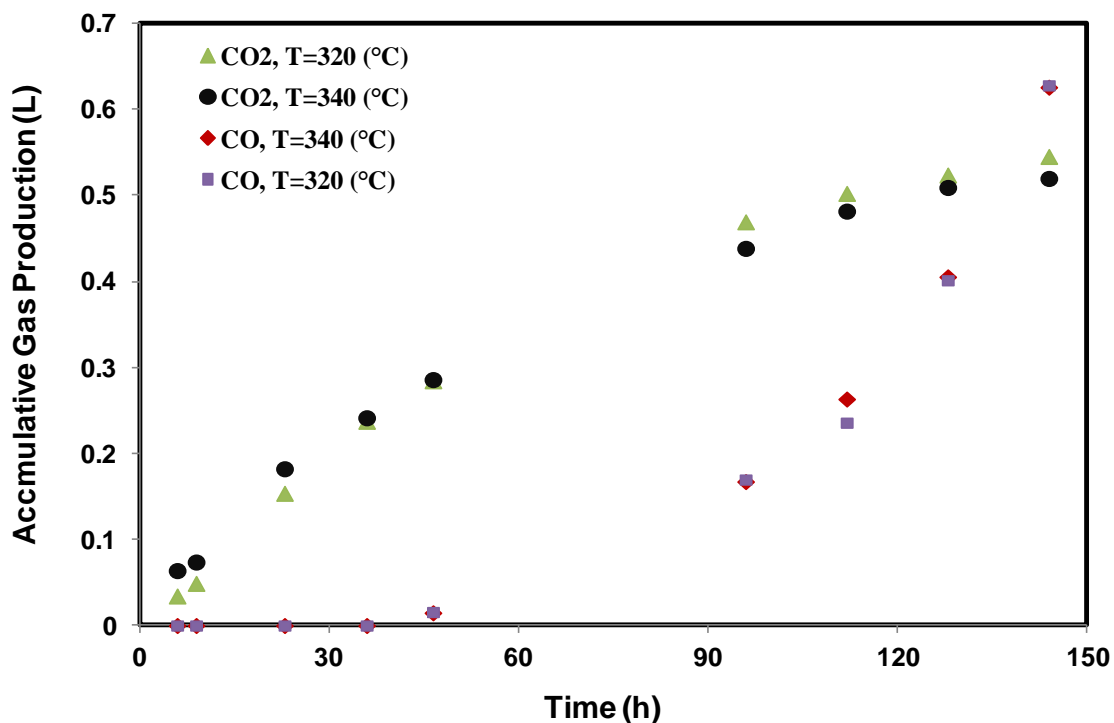


Fig 5.10: Accumulative volume of carbon dioxide and monoxide production from porous media in presence of tri-metallic nanocatalysts as function of time at pressure of 3.5 MPa and temperatures of 320 and 340 °C

5.4.2.2.2 Hydrocarbon gases

Presence of nanocatalysts in the porous media with the help of sufficient temperature, hydrogen and pressure caused production of alkane gases, such as methane, ethane, propane, butane and pentane. Cumulative productions of hydrocarbon gases were depicted in Figure 5.11-a, 5.11-b and 5.12. Clearly, in comparison to the blank experiments, the presence of tri-metallic UD nanocatalysts in the porous media significantly enhanced the production of hydrocarbon gases at both reaction temperatures. For all gases, except pentane, the trend was pseudo-exponential.

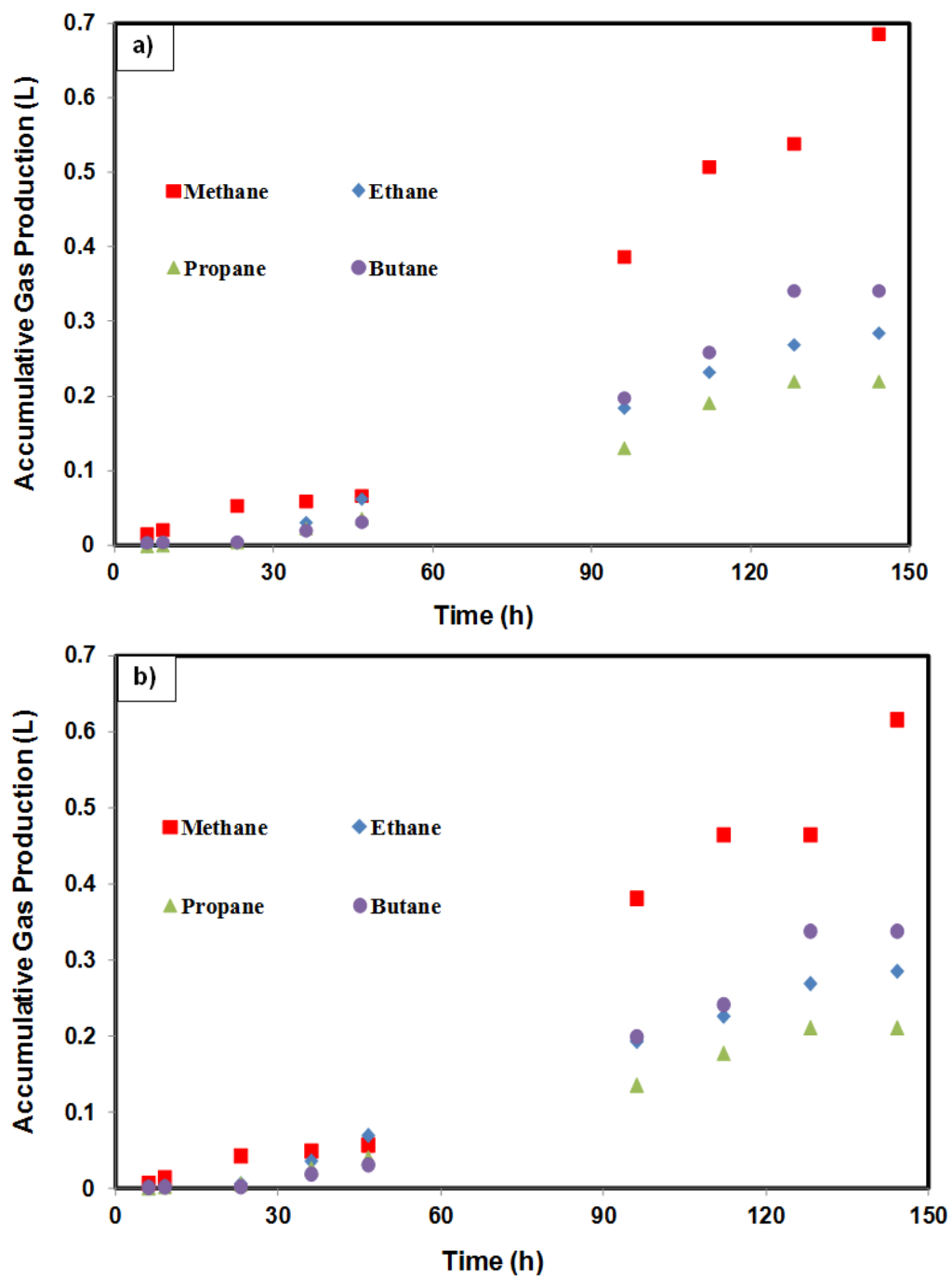


Fig 5.11: Accumulative volume of methane, ethane propane and butane production from porous media in the presence of tri-metallic nanocatalysts as function of time at a pressure of 3.5 MPa. (a) temperatures of 340 °C, (b) temperatures of 320 °C

As seen, methane has the highest produced volume while pentane was the lowest. It seems higher temperature favors the production of light hydrocarbon components, to some extent. It is worthy to mention that the production of light hydrocarbon gases inside the porous media is a potential mechanism for enhanced oil recovery (Butler and Mokrys 1991). Vaporized light hydrocarbon gases could diffuse in the areas saturated with heavy hydrocarbons and help the production of heavier cuts by solubilization mechanism, and consequently viscosity reduction.

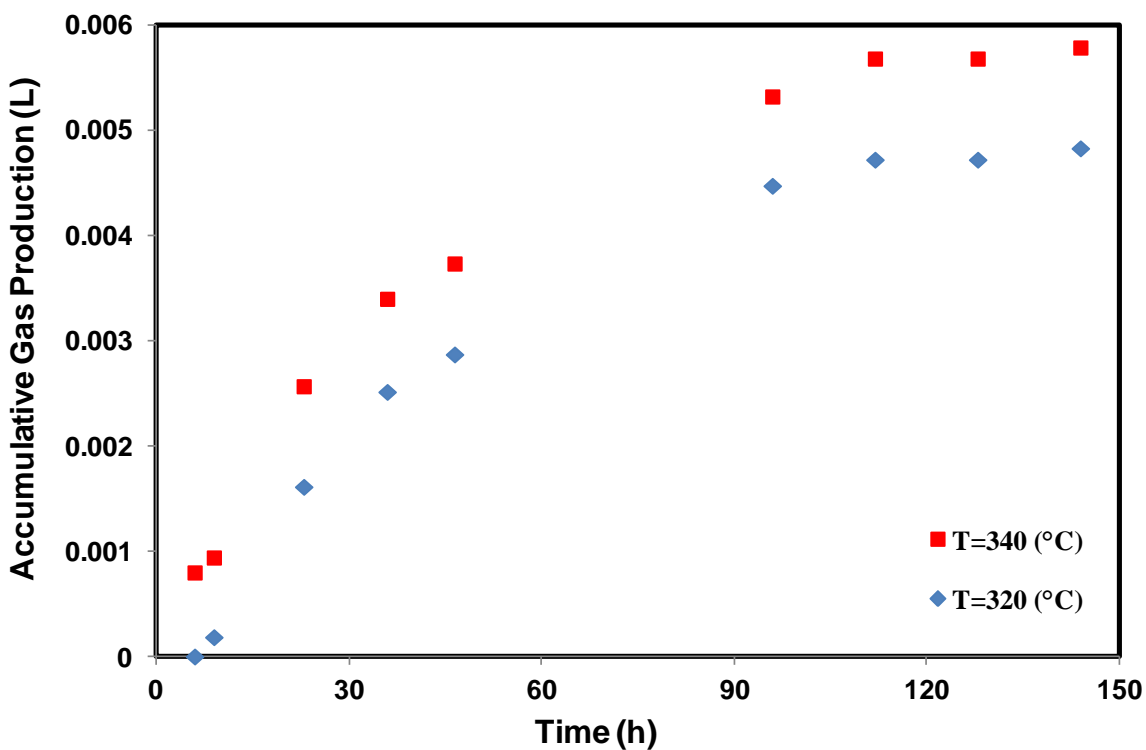


Fig 5.12: Accumulative volume of pentane production from porous media in presence of tri-metallic nanocatalysts as function of time at pressure of 3.5 MPa and temperatures of 320 and 340 °C

5.4.2.2.3 Hydrogen sulfide (H₂S)

As described in Part 1 of this study (Hashemi, Nassar, and Pereira Almao 2013a), the presence of tri-metallic nanocatalysts inside the porous media enhances the hydrodesulphurization reaction that involves the removal of sulfur from heavy oil compounds to produce H₂S and desulfurized products. In this Part of the study, the produced H₂S gas was detected by the GC.

Figure 5.13 shows the accumulative volume of H₂S produced as function of time at temperatures 320 and 340 °C. Clearly, the production of H₂S increased linearly with time. This supports that the hydrodesulphurization reaction was enhanced with time and shows that the integration of thermal cracking and nanocatalysts could be capable in production of a stable crude oil that can be directly transportable via pipelines and in enhancing its quality as well. It should be noted here that the increase in reaction temperature did not show any significant impact on H₂S production. This again supports that, apparently, in this experiment the hydrogenating reactions outperformed the thermal cracking reactions (Galarraga and Pereira-Almao 2010). It is noteworthy mentioning that the production of H₂S is considered unfavorable, because of its negative environmental impact. However, this issue has been tackled by our research group with use of nanoparticles as well (Nassar and Pereira-Almao 2010, Nassar, Husein, and Pereira-Almao 2010).

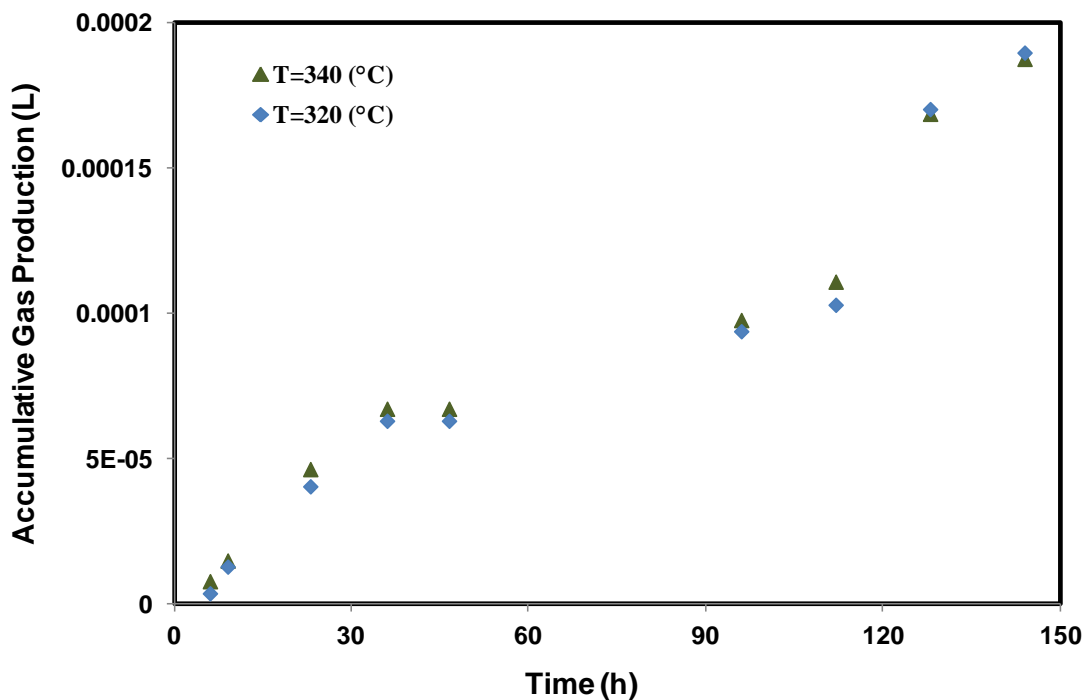


Fig 5.13: Accumulative volume of H₂S production from porous media in the presence of tri-metallic nanocatalysts as a function of time at pressure of 3.5 MPa and temperatures of 320 and 340 °C

5.4.2.2.4 Ethylene and propylene

During the upgrading reactions the activity of the upgrading catalysis (especially cracking catalysis) rapidly decreases (Gielen and Palekar 1989). To reduce coke deposition, it is very beneficial to understand the mechanism of coke formation during the reaction and its effects on the catalysts performance. A major step for coke deposition is the formation of coke precursors, such as olefins and di-olefines (McLaughlin and Anthony 1985, Venuto and Hamilton 1967, Langner et al. 1980, Langner 1980, 1981). Specifically, formation of ethylene and propylene as coke precursors was reported in the literatures (Langner 1980, 1982, Anderson et al. 1979, Mole, Anderson, and Creer 1985, Vadrine et al. 1980, Zou et al. 1987, Zou et al. 1993). In other words, any significant

increase in ethylene/propylene is interpreted as a clear sign of coke formation mechanism. Therefore, analysis of produced gases during catalytic upgrading reactions could be used to predict and/or evaluate the coke formation quality during the hydrocracking reactions.

In this set of experiments, ethylene and propylene, as coke precursors, were detected by the GC during the catalytic upgrading reaction. Figure 5.14 shows the accumulative volume of ethylene and propylene produced as function of time at temperatures 320 and 340 °C during the catalytic upgrading reaction. Clearly, the produced volume of both ethylene and propylene increased with reaction time, with high volume of gas obtained at higher severity. Consequently, the probability of coke formation is increased. This is in excellent agreement with the previous results pertaining to the coke formation at high severity reported in part 1 of this study (Hashemi, Nassar, and Pereira Almao 2013a) as well as those reported by Galarraga and Pereira-Almao for catalytic bitumen upgrading in a batch reactor (Galarraga and Pereira-Almao 2010). Accordingly, during the catalytic thermal cracking process, to avoid coke formation and subsequent catalyst poisoning a delicate balance between reaction time and temperature is of paramount importance. It is worth noting here that no trace of ethylene/propylene was observed in the blank experiments, without tri-metallic nanocatalysts. It can be interpreted that the intermediate step of ethylene/propylene production, before coking process, was very fast that makes it undetectable by the GC.

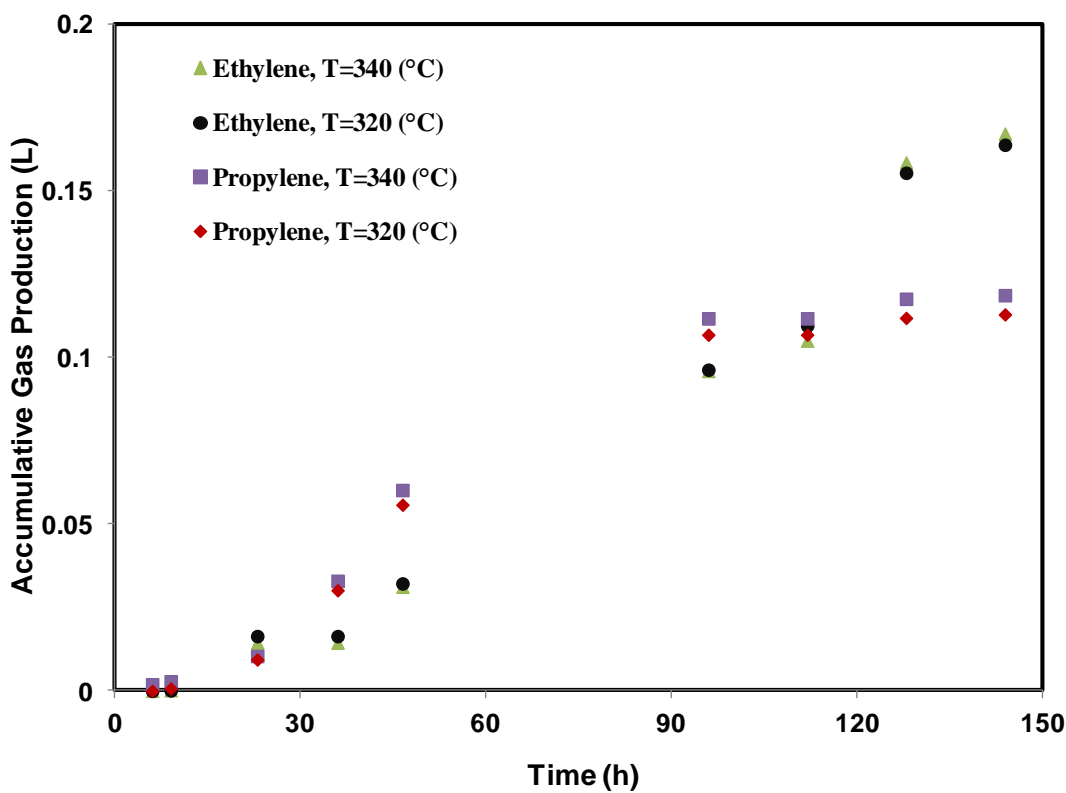


Fig 5.14: Accumulative volumes of ethylene and propylene production (measured at standard condition) from porous media in the presence of tri-metallic nanocatalysts for pressure of 3.5 MPa and temperatures of 320 and 340 °C

5.5 Overall product distributions

Figure 15 shows the big picture of the of the coke and gases distributions obtained for the whole experiments conducted at temperatures 320 - 340 °C, and pressure of 3.5 MPa, in the presence and absence of tri-metallic nanocatalysts . Evidently, the presence of tri-metallic nanocatalysts favors the reduction of coke formation and increase the production of gases but significantly decrease the CO₂ emission. This again supports that the tri-metallic nanocatalysts enhances the hydrogenation reactions that resulted in the increase of the amount of hydrogenating species available to cap the free radicals produced during the thermal cracking of bitumen(Galarraga and Pereira-Almao 2010). These

results hold great promise for in-situ heavy oil upgrading process. However, before any field test, scaling up process aiming at evaluating the behavior of these tri-metallic nanocatalysts at reservoir operation conditions is of paramount importance.

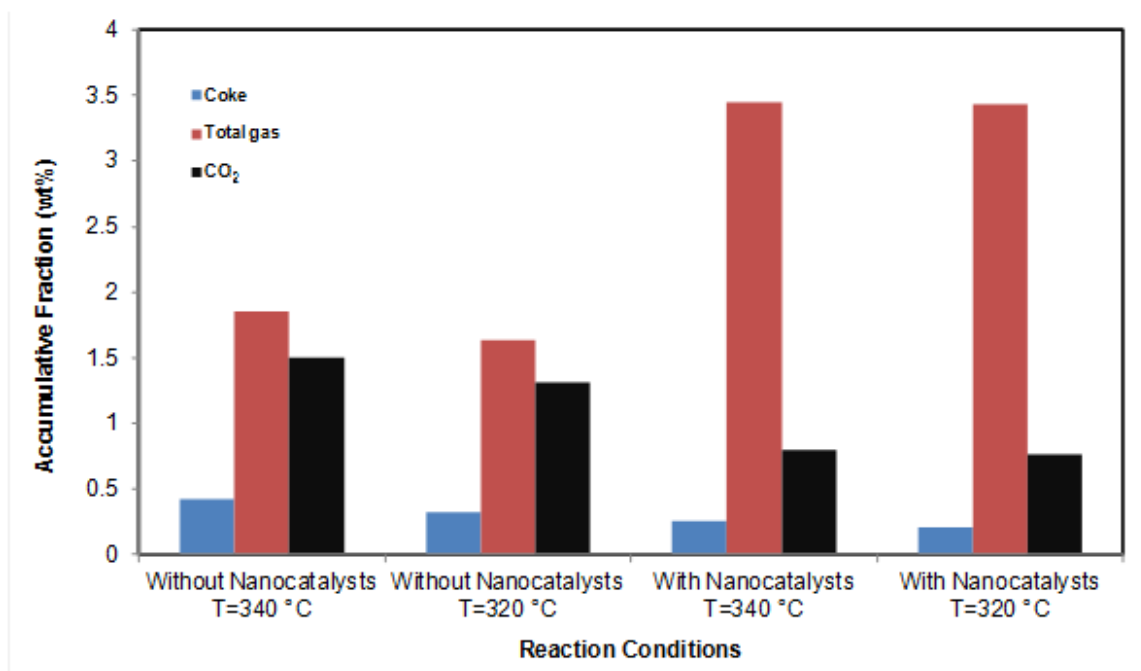


Fig 5.15: Overall gas and solid distribution from HCK of Athabasca bitumen in the presence and absence of UD tri-metallic at oil sand packed bed column at a pressure of 3.5 MPa, residence time of 36 h, and hydrogen flow rate of 1 cm³/min

5.6 Conclusions

In the current context, bitumen production and upgrading has been proven to be energy and water intensive as well as environmentally unfriendly. Therefore, development of new process and/or improvement of current processes for bitumen recovery and upgrading are of paramount importance. In-situ upgrading of bitumen is a new approach,

which involves utilizing the reservoir as a reactor, and aims at enhancing production and reducing the cost and the environmental impact of on-surface upgrading.

This research work assists in understanding the behavior of tri-metallic nanocatalysts for the hydrocracking of Athabasca bitumen in a continuous mode in oil sand packed bed column. The in-situ prepared tri-metallic nanocatalysts not just enhanced the HCK reactivity of Athabasca bitumen by effectively activating hydrogen and subsequently inhibit coke formation, but it also contributed to a significant reduction in CO₂ emission and improved the produced liquid quality. Online gas analysis of the catalytic upgrading process showed the production of hydrocarbonic gases, carbon dioxide, carbon monoxide and hydrogen sulfide as well as ethylene/propylene as coke precursors. Further, the characterizations of the nanocatalysts after the reaction, specifically in the liquid filtrate and packed bed solids, showed that these nanocatalysts are mainly spherical in shape with a diameter from 50 to 150 nm and can associate together to form micro-size aggregates, especially at the entrance of the packed bed reactor. Nonetheless, EDAX analysis indicated that, despite the high reaction severity these catalysts (Ni-Mo-W) maintained their designed atomic ratio (metal/total metal).

Chapter 6 Nanotechnology for heavy oil upgrading and recovery: Opportunities and challenges⁵

6.1 Abstract

With more than 170 billion barrels of estimated oil sands reserves, Canada has the second largest oil reserve of this kind in the world. However, more than 80 percent of oil sand reserves are located deep underground and could not be accessed by surface mining. Nonetheless, a number of in-situ recovery methods have been developed to extract heavy oil and bitumen from deep reservoirs. Once brought to surface, bitumen is transferred to upgraders converting that low quality oil into synthetic crude oil. However, in the present context, heavy oil and bitumen exploitation process is not just high-energy and water intensive, but also it has significant environmental footprint as it produces significant amount of gaseous emissions and wastewater. In addition, the level of contaminants in bitumen requires special equipment, and has also environmental repercussions.

Recently, nanotechnology has emerged as an alternative technology for in-situ heavy oil upgrading and recovery. Nanocatalysts are one of the important examples on nanotechnology applications. Nanocatalysts portray unique catalytic and sorption

⁵ Hashemi, Rohallah, Nashaat N. Nassar, and Pedro Pereira-Almao. Enhanced Heavy Oil Recovery by In-Situ Prepared Ultra-Dispersed Multi-metallic Nanoparticles: A Study of Hot Fluid Flooding for Athabasca Bitumen Recovery. *Fuel Processing Technology* (Submitted)

properties due to their exceptionally high surface area-to-volume ratio and active surface sites. In-situ catalytic conversion or upgrading of heavy oil with the aid of multi-metallic nanocatalysts is a promising cost effective and environmentally friendly technology for production of high quality oil that meets pipeline and refinery specifications. Nevertheless, as with any new technologies, there are a number of challenges facing the employment of nanoparticles for in-situ catalytic upgrading and recovery enhancement. The main goal of this article is to provide an overview of the use of nanoparticles technology in enhancing the in-situ catalytic upgrading and recovery process of heavy crude. Furthermore, the article sheds light on the advantages of employment of nanoparticles in heavy oil industry and addresses some of the limitations and challenges facing this new technology.

6.2 Introduction

There is no doubt that the world is facing formidable challenges in meeting energy demands as the available conventional energy supplies are decreasing due to several factors (Gill et al. 2011), such as enormous growth of world population, competing demands from a variety of users, increasing industrialization and motorization of the world, increasing technical development and living standard, etc. Therefore, it is necessary to look for alternative energy supplies that can be produced from natural resources.

Various natural energy resources have been explored; including biomass, vegetable oils, biodiesel, etc. (Perman 2003). These resources are believed to be environment-friendly fuel (Agarwal 2007), but they are costly and insufficient in meeting the energy

demands, which have led to an increased demand on the upgrading and recovery of unconventional oil. This way Alberta oilsands have now become an important source of alternative energy resources (Berkowitz and Speight 1975). Actually, the International Energy Agency (IEA) has predicted that, by the year 2030, about 60% of the total worldwide energy growth will be met by fossil fuel sources such as heavy oil, coal, and natural gas (Kobayashi 2005). Nonetheless, due to its high viscosity, low hydrogen to carbon ratio and high sulphur and nitrogen content, there are a number of challenges associated with bitumen recovery and upgrading in the present context. These challenges need to be surmounted to make it a sustainable and economically feasible alternative (Charpentier, Bergerson, and MacLean 2009, Lacombe and Parsons 2007, Birn and Khanna, Golden 2008, Nassar, Husein, and Pereira-Almao 2011b, Taylor 2009, Board 2006, Hall and Vredenburg 2012).

Among the challenges to be solved are the reduction in costs associated with the production and transportation of oil sands and the improvement of synthetic crude quality to meet stringent market specifications with less environmental footprints (Pereira-Almao 2012). Nanotechnology is a rapidly growing technology with considerable potential applications and benefits (Foster 2005). It provides unprecedented opportunities to develop more cost effective and environmentally friendly heavy oil upgrading and recovery processes. Interest in using nanotechnology in heavy oil processing is driven from the unique physical and chemical properties of the nano-scale particles (Xiangling and Ohadi 2010).

In the world of nanotechnology, a nanoparticle acts as a whole unit in terms of its transport behavior and properties, and its diameter is sized between 1 and 100

nanometers. In other words, as the size of a particle reduces to nanoscale (i.e., 1-100 nm) the properties begin to change dramatically as the percentage of atoms at the surface of a material becomes significant, a phenomena which is attributed to the large surface area to volume ratio (Bell 2003). Quantum confinement, surface Plasmon resonance, high adsorption affinity, enhanced catalytic activity, good dispersion ability and intrinsic reactivity are just some of the unique properties associated with nanoparticles (Perez 2007).

Nowadays, because of these properties nanoparticles are used in vast areas of engineering applications, such as heavy oil upgrading (Hashemi, Nassar, and Pereira-Almao 2012, Hashemi and Pereira-Almao 2011, Zarkesh et al. 2008, Langdon and Ware 2010), polymer nanocomposites (Winey and Vaia 2007, Roy et al. 2005, Tanaka et al. 2005), catalysis(Thomas et al. 2003, Joo et al. 2008, Jaramillo et al. 2007) , and wastewater treatment(Han et al. 2009, Hildebrand, Mackenzie, and Kopinke 2009, Kaegi et al. 2011), to name only a few. However, there are uncertainties associated with nanoparticles applications, which should be deeply explored.

Among the potential applications enumerated for nanoparticles are in oil and gas industry, specially upgrading and recovery of heavy feedstocks by nanocatalysts (Krishnamoorti 2006). In addition to its high surface area, this catalyst should maintain ultra-dispersion ability and high catalytic activity. The ability to engineer desired surface functionalities of nanoparticles by tuning its characteristics as well as the possibility of its in-situ preparation makes nanotechnology an attractive unique option for heavy oil upgrading and recovery. In addition, owing to their small size and transport behavior,

nanoparticles can be employed in-situ within the reservoir environment where upgrading and recovery are needed (Almao 2012).

Extensive research has been pioneered at the University of Calgary for in-reservoir upgrading, ranging from synthesis of nanocatalysts to their real case application (Galarraga and Pereira-Almao 2010, Zamani, Maini, and Pereira-Almao 2011, Thompson et al. 2008, Nassar, Husein, and Pereira-Almao 2011b, Hashemi, Nassar, and Pereira-Almao 2012). However, there is still long way to investigate all aspects of these nanocatalysts properties and performances. Here, we briefly review what is known about nanoparticles and their behavior as adsorbent/catalysts for heavy oil upgrading and recovery as well as possible challenges for future implementations. We also discuss state-of-the-art knowledge and instrumentations related to nanocatalysts implementation for upgrading and recovery of Athabasca bitumen. It should be noted here that a comprehensive discussion of the applications of nanotechnology to heavy oil upgrading and recovery is beyond the scope of this article. The main objective here is to discuss the opportunities and challenges of using nanoparticles as adsorbent/catalysts in the simultaneous upgrading and recovery of heavy oil.

6.3 In-situ prepared ultradispersed nanoparticles

Placement of catalysts inside the porous media is one of the important steps to apply the idea of “underground upgrading” for bitumen upgrading and recovery (Weissman and Kessler 1996). Supported catalysts could be placed inside or at the surroundings of the production well to perform in-situ upgrading. However, due to coke deposition and metal poisoning supported catalysts will deactivate (Bartholomew 2001). The deactivation of

catalysts will be caused by metal deposition and blocking active catalysts sites, coke deposition on the fresh catalyst network and rapid deactivation of catalyst also caused by metal deposition or by the metals impregnated in the conventional catalysts when hydrogen deficiency exists, all these mechanisms result in constriction of pore mouth (Thompson et al. 2008). Therefore, upgrading of heavy feeds with desired efficiency requires a large pores network as well as tolerance to the feedstock constituents and a coke preventing environment, the most convenient of which is hydrogen gas.

Good catalytic properties, such as high porosity and resistance to pore plugging are favorable properties for processing of heavy feedstocks (Newson 1975). In order to overcome mainly the pore plugging problem ultra-dispersed nanocatalysts were developed for industrial applications (Thompson et al. 2008). In addition, dispersion is a very important concept in catalyst industry (Lemaitre, Menon, and Delannay 1984). Experts in commercial catalysis research are looking to find the higher dispersed catalysts to achieve higher conversion at the applied pressure and temperature conditions (Okamoto et al. 1995, Velu and Gangwal 2006). This is the reason for using dispersed catalysts for hydrocracking of heavy feedstocks.

There exist several advantages with the usage of nanocatalysts; including: a) small size of nanocatalysts offers large surface area to volume ratio which results in improved catalytic performance for processing purposes, b) the probability of contact between reactants is increased because of nanocatalysts mobilization inside the reactor which ultimately increases the economics of the upgrading process, c) absence of any fixed bed catalysts because of nanocatalysts implementation inside the medium make possible longer run times for conversion as there is no need of catalyst replacement, d) in absence

of any pores in UD nanocatalysts, loss of activity will not be presented compared to supported catalysts (Yoosuk et al. 2008), e) propagation of nanocatalysts inside the porous media and reacting in-situ cause bitumen dissolution as well as viscosity reduction of produced liquid, and f) successful in situ processing reduces the operating costs as well as environmental concerns associated with bitumen production such as greenhouse gas (GHG) emissions, SO_x and NO_x production, solid waste by-products and even fresh water consumption (Almao 2012). It is generally accepted that two types of processes can be used to convert heavy feedstock into valuable products; namely: carbon rejection and hydrogen addition (Speight and Özüim 2002).

Nanocatalysts were introduced into the porous media to perform upgrading inside the reservoir to convert bitumen to lighter products. A cartoon representation shown in Figure 6.1 shows the potential mechanism of nanocatalysts application for bitumen upgrading and recovery during the steam assisted gravity drainage (SAGD) process (Nassar, Husein, and Pereira-Almao 2011a). Since SAGD is the dominant mechanism for bitumen production, then the final goal for the nanocatalysts usage is to couple both the benefits of nanocatalysts presence inside the porous media as well as thermal drive mechanism simultaneously. However, there is a long way and extensive work to commercialize and test the proposed method for in situ processes inside the porous media.

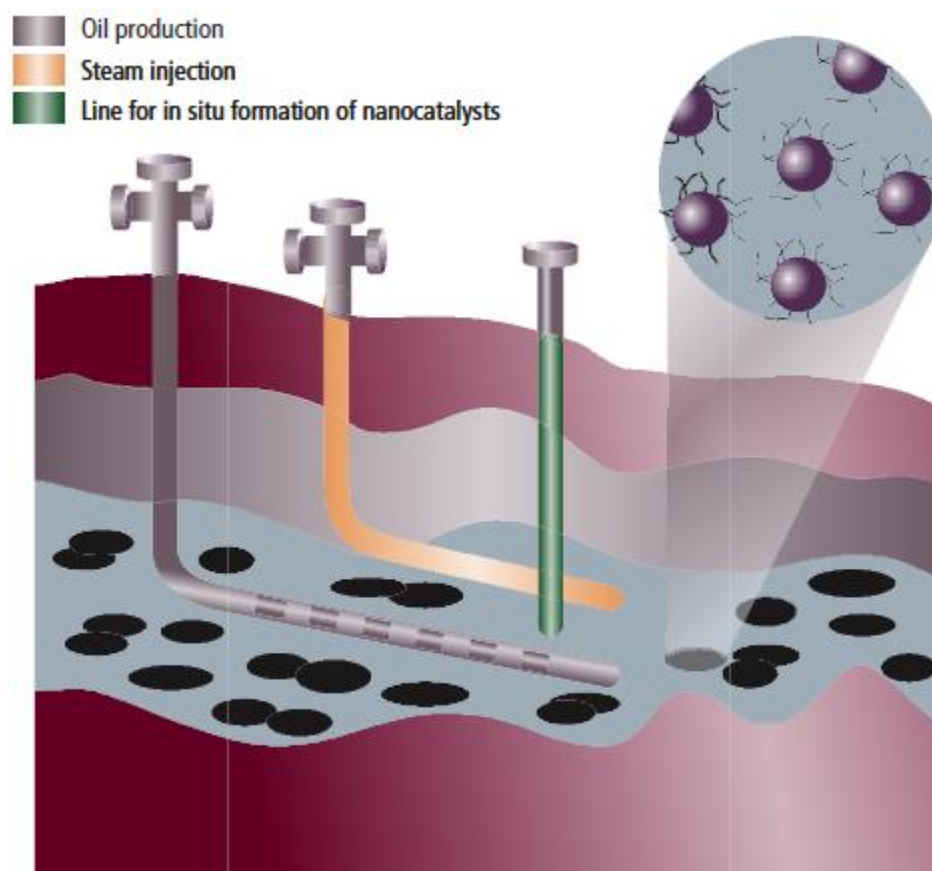


Fig 6.1: Cartoon representation of in-situ heavy oil upgrading and recovery coupling ultradispersed nanocatalysts and the SAGD process, whereupon light oil is produced at the surface and heavy molecules, solids and minerals stay sub-surface. Obtained from (Nassar, Husein et al. 2011) with permission.

6.4 Synthesis of nanocatalysts

A number of preparation techniques have been reported for manufacturing nanoparticles (Nassar 2012, Husein and Nassar 2008). These methods can be grouped into top-down and bottom-up methods as seen in Figure 6.2 (Nassar 2012). Top-down methods are defined as those by which nanoparticles are directly prepared from bulk materials via the generation of isolated atoms by using various distribution techniques that involve

physical methods such as milling or grinding, laser beam processing, repeated quenching and photolithography (Niemeyer 2001). Bottom-up approaches involve molecular components as starting materials linked with chemical reactions, nucleation and growth processes to promote the formation of nanoparticles (Husein and Nassar 2009, Husein and Nassar 2008, Nassar and Husein 2007b). This method is commonly used for *in-situ* formation of nanoparticles (Husein and Nassar 2009; 2008; Nassar and Husein 2007).

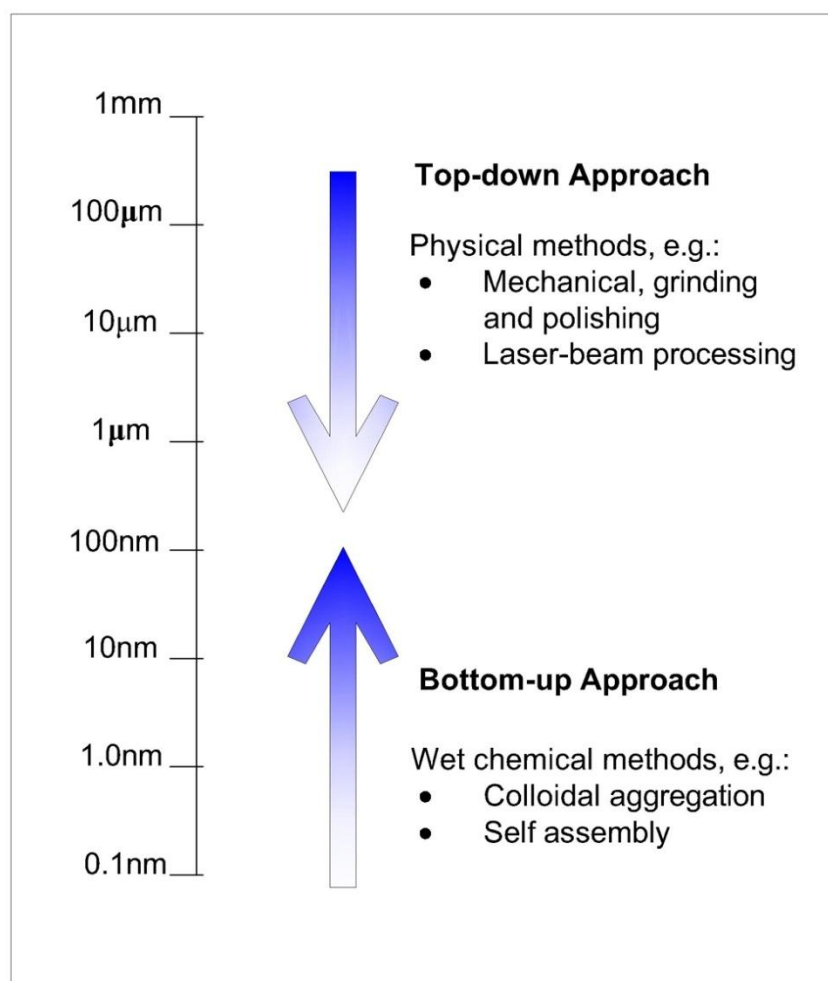


Fig 6.2: Schematic representation illustrating the top-down and bottom-up approaches for nanocatalysts preparation. Obtained from (Nassar 2012) with permission.

There are various bottom-up methods for preparation of nanocatalysts, such as microemulsion or reversed micelles (Jung, Price, and McQuade 2003, Gobe et al. 1983), chemical reduction (Bock et al. 2004), hot-soap (Murray, Norris, and Bawendi 1993, Alivisatos et al. 1996), sol-gel (Shen et al. 2004), pyrolysis (Yao et al. 2006), and spray pyrolysis (Pluym et al. 1993). Emulsion preparation is obtained by mixing oil, water and a stabilizing agent such as surfactant (Hellweg 2002). Preparation procedure and conditions is selected in such a way to have microemulsion in the media. Microemulsion hold specific properties such as very low interfacial tension, small microstructure, thermodynamic stability and translucence that can be used in variety of applications (Galarraga March 2011). Water-in-oil (w/o) microemulsion preparation technique was described in the literatures (Nassar and Husein 2007b, a, Nassar and Husein). In brief, aqueous solution of corresponding metals were added to a w/o emulsion and then mixed for a certain time. After that, a base aqueous solution is added to initiate nucleation and growth of the nanoparticles, which remain stable in suspension. Figure 6.3 shows a simple cartoon representation illustrating the structure of reverse-micelle “nano-reactor” used for in-situ formation of nanoparticles (Nassar, Husein, and Pereira-Almao 2011b).

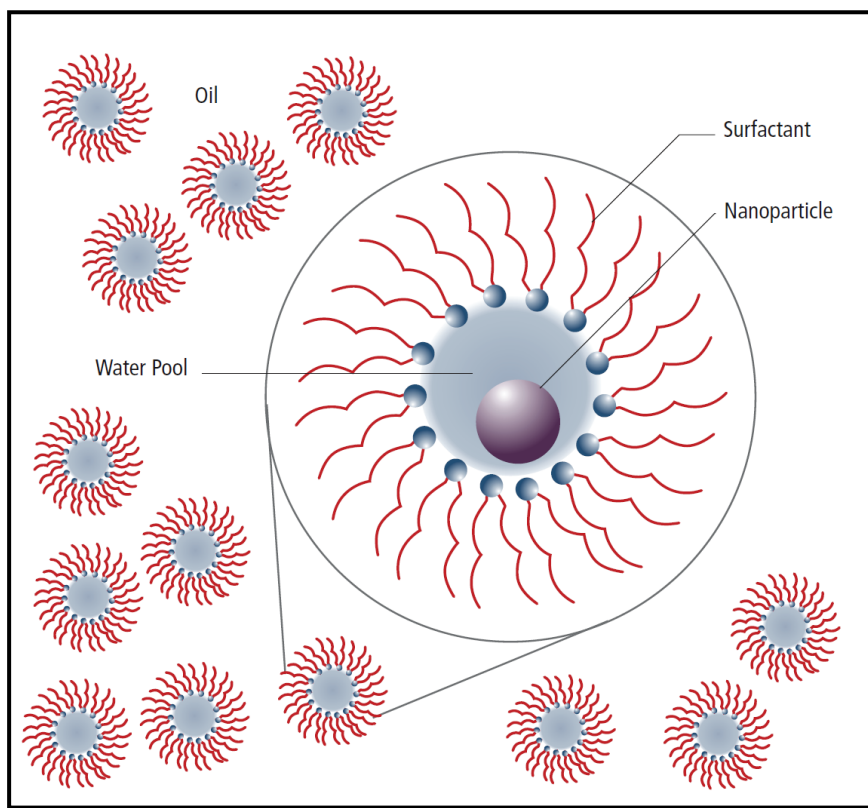


Fig 6.3: Schematic representation of water-in-oil microemulsions. The water pools solubilise the precursors and accommodate the resultant nanoparticles. The size of the water pool can be manipulated by controlling the ratio of mole water/mole surfactant. Obtained from (Nassar, Husein, and Pereira-Almao 2011b) with permission.

Preparation of nanocatalysts could be obtained by mixing two reacting systems (one containing the precursor salt and the other a reducing agent) in the form of a microemulsion (Capek 2004). Capek, 2004, has reported a comprehensive study on the preparation of nanoparticles in w/o microemulsion with formulations for Fe, Pt, Ni, Au, Cd, Pd, Ag and Cu. Thus, microemulsion is considered as a breakthrough for nanocatalysts preparation, especially for in-situ application such as upgrading and recovery of bitumen. For heavy oil conversion, an emulsion was developed in presence of water claiming steam cracking of vacuum gas oil (VGO) catalyzed by catalytic emulsion (Pereira et al. 1999). Furthermore, a catalytic nanoparticles solution prepared by

decomposition of w/o emulsion was successfully implemented to catalyze hydroprocessing reaction (Vasquez 2009). Thompson et al, 2008, performed work on Mo nanoparticles reaction performance for Athabasca bitumen upgrading (Thompson et al. 2008). A lab scale reactor packed with sand particles were used to explore the formation of mixed oxy-carbides composed by MoO_2 , MoO_3 and MoC as well as agglomeration of nanocatalysts promoted by surfactant-media interactions. Using the microemulsion method, Ni, Mo and Ni-Mo nanoparticles (approximately 10 nm) were prepared for hydrodesulfurization with the potential of using for in situ upgrading as well as on surface (Lapeira 2009). It can be concluded that synthesis and preparation of nanocatalysts were performed successfully based on literature. However, stability of nanoparticles inside the prepared/reaction media and control over particle size as well as particle recovery and regeneration are still an important issue for nanoparticles implementation.

Mechanical separation and deposition of UD nanocatalysts based on their motion inside the viscous fluid media has been investigated in a cylindrical geometry (Molina 2009). 2D and 3D convective-dispersive models were developed and validated based on experimental tests (Molina 2009). In addition, concentration profiles for particles (ranging from micro to the nano scale) movement through fluid media as a function of their position and time were successfully predicted. Published results by the author showed that dispersion coefficient is a function of fluid medium properties (density, viscosity and volumetric flux) and a large number for dispersion coefficient in the medium shows particles tendency for sedimentation. In addition, deposition tendency of particles were related to a factor namely “critical particle diameter” (Molina 2009). For

different scenarios (i.e., initial particle concentration, velocity change and medium viscosity change), change in medium properties caused sedimentation of UD particles to occur in lower or higher critical particle diameter. It is worth mentioning that agglomeration of UD nanoparticles inside the medium plays an important role in sedimentation of nanoparticles as well as efficiency of produced nanoparticles from desired metal precursors.

As a part of commercial application for the nanocatalysts in heavy oil upgrading and recovery industries, it should be noted that there exists another challenge, which is the mass production of nanocatalysts in the field scale applications. Syntheses of the nanocatalysts for the batch reactor experiments as well as pilot plant tests have been conducted successfully (Hashemi, Nassar, and Pereira Almao 2013c, Galarraga and Pereira-Almao 2010). However, for the field scale applications, there should be availability of surface facilities or suppliers that can provide large quantities of required nanoparticles with the economically viable prices.

6.5 Required facilities for nanocatalysts application in heavy oil upgrading and recovery

Implementation of new advanced technologies is directly associated with the usage of hi-tech systems for industrial developments (Cassiolato and Schmitz 2002). Due to the nature of UD nanocatalysts upgrading difficulties, it is essential to acquire control systems to avoid or mitigate any associated risks. Presence of hydrogen as well as high pressure and temperature conditions will introduce risk of plugging and even explosion which enforce need for high level of control systems.

Figure 6.4 shows a schematic representation of the experimental set-up which were used to mimic nanocatalysts injection inside the porous media at a high pressure and temperature (Hashemi, Nassar, and Pereira Almaso 2013c). As seen, it is required to use many analysis tools as well as sophisticated control systems to ensure the process is meeting the required desired product while taking safety into consideration. Further, to the best of our knowledge, the cost of nanocatalysts for in-situ upgrading and recovery of bitumen is never mentioned in the literature. The cost of nanocatalysts depends primarily on the local availability of their precursors, types, preparation techniques and method of application. Because the nanocatalysts could be prepared in-situ, within the reservoir environment, the materials costs could be reduced. Nevertheless, more investigations on the cost effectiveness of the nanocatalysts as an alternate technology for bitumen upgrading and recovery are needed and significantly important.

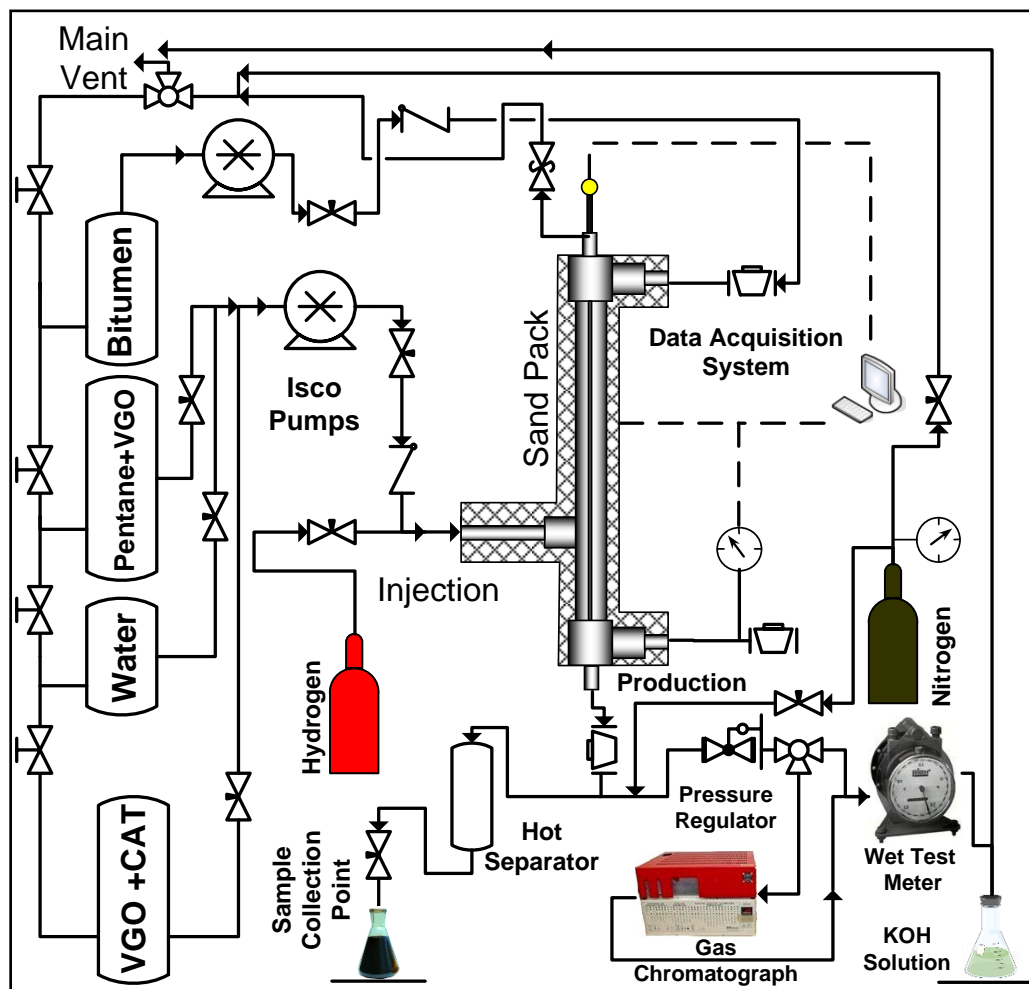


Fig 6.4: Schematic representation of the experimental setup for in- situ upgrading and recovery enhancement of Athabasca bitumen. Obtained from (Hashemi et al. 2013) with permission.

6.6 Nanocatalysts transport behavior inside the porous media

After preparation and synthesis of nanocatalysts in a microemulsion system, an important issue regarding the usage of nanocatalysts for bitumen upgrading is the feasibility of nanocatalysts transport inside the porous media. To conduct successful upgrading process underground, placement of nanocatalysts in the appropriate zone inside the oil sand medium is necessary. It should be noted that there exists a huge area of research for the transport behavior of nanoparticles in porous media (Zamani, Maini, and Pereira-Almao

2010). However, most of the studies are focused on the transport behavior of the nanoparticles in deep bed filtration for wastewater treatment, and the obtained results could not be applied for reaction conditions in the oil sand based matrix. Accordingly, very little information is available on the flow behavior of UD nanocatalysts in oil sand packed bed.

Recently, our research group reported on the transport behavior of metallic and multimetallic UD nanocatalysts, suspended in vacuum gas oil, inside an oil sand porous media at different experimental and operational conditions (Hashemi, Nassar, and Pereira-Almao 2012, Zamani, Maini, and Pereira-Almao 2011, 2010). Results demonstrated that the propagation of UD nanocatalysts in an oil sands packed bed column at typical SAGD configuration is feasible, as neither major permeability reduction nor pore plugging were observed.

It should be noted that the experiments conducted by Zamani et al., 2010, were performed at low temperatures and in the absence of cracking reaction which showed that nanocatalysts were able to propagate through the sand medium, but larger agglomerated particles were filtered out and remained inside the porous media (Zamani, Maini, and Pereira-Almao 2010). However, the authors reported that the retention of nanocatalysts had a negligible effect on the pressure drop and caused no permeability damage inside the experimental medium. Further, retention mechanism on the surface was mainly attributed to chemisorption, and analysis showed that adsorption is not reversible. In addition, specific deposit profile along the sand pack showed that nanocatalysts continued to be filtered out deep inside the porous medium, but higher retention occurred in the entrance of the sand pack. Moreover, Zamani et al, 2010, reported that the sand media retained

14–18% of injected UD nanocatalysts, mainly at the bed entrance (Zamani, Maini, and Pereira-Almao 2010).

Hashemi et al., 2012, (Hashemi, Nassar, and Pereira-Almao 2012) investigated the transport behavior of nanocatalysts in an oil sands porous media at high pressure and temperature of typical SAGD conditions (i.e., presence of reaction). In their study, the authors reported on the effects of temperatures and permeability reduction on the transport behavior of ultradispersed multimetallic (Ni-Mo-W) nanocatalysts inside an Athabasca oil sands packed bed column. Experiment results showed that aggregation of nanocatalysts was observed in all cases (i.e., low and high temperatures and different sand permeability). The authors showed that the deposition tendency for nanocatalysts is strongly affected by the type of metal, temperature, and sand permeability. Increasing the temperature favored the aggregation, this was attributed to the increase in frequency of particle collision because of heavy oil viscosity reduction and subsequently, higher aggregation rate. Further, a high-permeability-oil-sands-packed bed has a lower amount of deposited nanocatalysts compared to the low-permeability medium. Again, deposition of nanocatalysts mainly occurred at the entrance of the injection zone and rapidly decreased across the reaction zone. However, the same for the low temperature experiments, deposition of nanocatalysts inside the porous media has a meager influence on medium permeability. Again, pressure drop analysis showed no major permeability damage across the reaction zone (Hashemi, Nassar, and Pereira-Almao 2012).

One of the most important aspects of nanocatalysts transport inside the porous media is the control over the particle size during the injection and reaction times. In addition to pressure drop via permeability reduction, particle size would impact on dispersion ability,

adsorption affinity and catalytic activity of nanoparticles inside the medium (Hashemi, Nassar, and Pereira-Almao 2012). Our group performed a series of experimental studies on this important aspect with successful results (Nassar, Hassan, and Pereira-Almao 2011a, Nassar, Hassan, and Pereira-Almao 2011d, Hassan et al. 2012). It should be noted that most of these studies are at the initial steps for fulfilling the idea of in-situ upgrading with the promising results to future enhancement in the area of heavy oil technologies.

In addition to numerous experimental studies, robust mathematical modeling of nanocatalysts transport behavior inside the porous media would provide valuable information on the concept of particle mass transfer. Modeling of mass transfer and deposition behavior of fine particles in cylindrical channels were studied by several researchers (Adamczyk and Van de Ven 1981, Brady 1994, Sarimeseli and Kelbaliyev 2004, Yoshioka, Karaoka, and Emi 1972, Thompson et al. 2008, Molina 2009). It should be noted that mathematical modeling of such processes are very complex and sometimes require incorporating empirical correlation as well. Furthermore, presence of viscous fluid in the medium enforces even more complexity to the equations; nonetheless, importance of UD nanocatalysts in the heavy oil and bitumen industries justifies the necessity of conducting scrutinizing study in this area.

In one of the novel studies (Molina 2009), our research group has developed a mathematical model for nanocatalysts transport and deposition that takes into account the geometry of the channel, fluid medium properties and characteristics, particle diameter and concentration, and the effects of the temperature on the particle agglomeration and deposition of nanocatalysts. 2-D and 3-D convective-dispersive model, which delivers the concentration profile of particles immersed in fluid media enclosed in a circular cross

section, were validated by experiments performed in an injection rig (Molina 2009). Despite the very large effort, by changing the physical properties of media and geometry, it is required to conduct new experiments to estimate the coefficient existed in the mathematical model equations (Molina 2009).

In conclusion, propagation of nanocatalysts inside the porous media is feasible and ultradispersed multimetallic nanocatalysts could be controllably delivered through oil sands porous media into a targeted heavy oil reservoir, where they could work as catalysts for heavy oil upgrading. However, some portion of injected particles could be retained inside the porous media. Nonetheless, the deposited particles inside the medium can potentially increase the activity of the medium (R.Hashemi Dec 2011) and could be predicted by mathematical modeling (Molina 2009).

6.7 Modeling of reaction kinetics

Hydrocracking kinetics of heavy oil was investigated in many aspects considering various kinetics models based on the proposed cracking reaction schemes (Alhumaizi et al. 2001, Krishna and Saxena 1989, Scherzer and Gruia 1996, Ancheyta, Sánchez, and Rodríguez 2005, Sánchez, Rodríguez, and Ancheyta 2005, Ayasse et al. 1997, Aoyagi, McCaffrey, and Gray 2003). Presence of many parallel reactions in hydrocracking at the same time would suggest proposing network of reactions for kinetics modeling (Alhumaizi et al. 2001, Krishna and Saxena 1989). Figure 6.5 shows a schematic representation of a generic family of hydrocracking reactions and approximate velocity constants for a conventional oil (Scherzer and Gruia 1996). As can be observed, some reactions are faster than others depending on the nature of the reaction process.

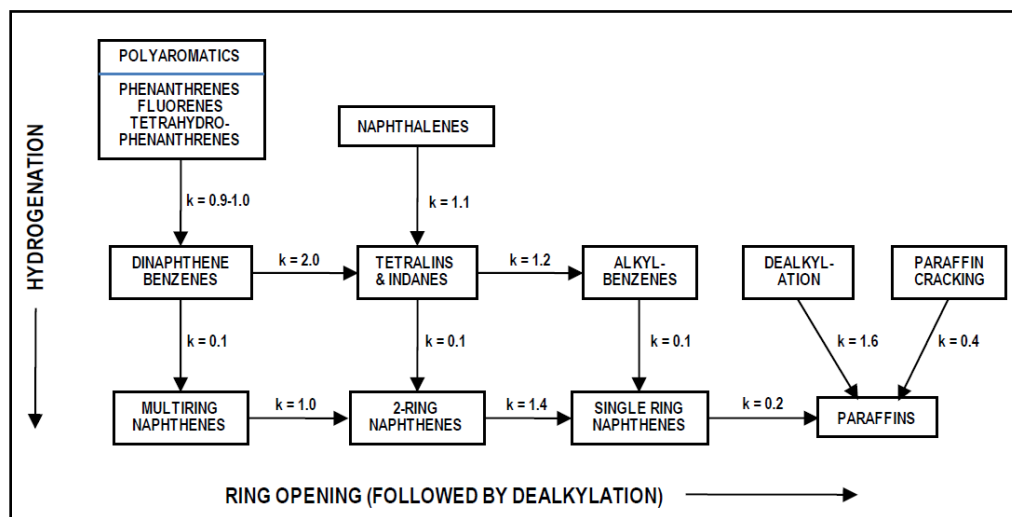


Fig 6.5: Proposed scheme for lumped-kinetic modeling of HCK reactions. Obtained from (Scherzer and Gruia 1996, Sánchez, Rodríguez, and Ancheyta 2005) with permission.

For the case of unconventional oil, the presence of large molecules such as resins and asphaltenes in the heavy oil and bitumen matrixes makes the kinetics process very complex. However, using the traditional grouped lumping concept along with pseudo components definition representing the heavy feedstock are common methods for bitumen kinetic study (Singh et al. 2005, Gray 1990, Martens and Marin 2001). It should be noted that group selection is a very crucial step in this approach and consequently determines the amount of required experimental study to estimate the kinetics parameters. Generally, first order rate equation with respect to bitumen is considered for the kinetic study of bitumen (Köseoğlu and Phillips 1987, 1988a, Sánchez, Rodríguez, and Ancheyta 2005). In addition, incorporating higher number of lumped groups was considered in literature, which resulted in more complex equations as well as higher precision in kinetic modeling (Köseoğlu and Phillips 1987, Köseoglu and Phillips 1988, Köseoğlu and

Phillips 1988b). Figure 6.6 shows a schematic representation of a proposed lumped kinetic model which contains series of reactions with certain velocity constants (Sánchez, Rodríguez, and Ancheyta 2005).

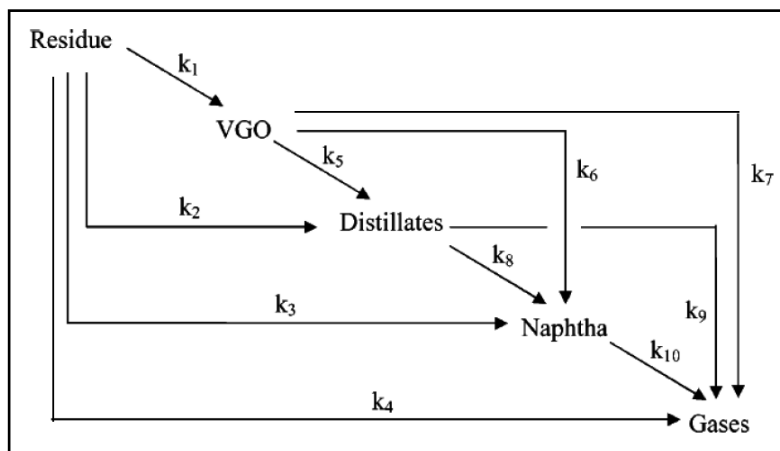


Fig 6.6: Proposed scheme for lumped-kinetic modeling of HCK reactions. Obtained from Sanchez, Rodriguez et al. 2005 with permission.

Kinetics modeling of Athabasca bitumen reaction at various conditions has been reported in literature (Phillips and Hsieh 1985, Phillips, Haidar, and Poon 1985, Gray et al. 1995, Owusu-Boakye et al. 2005). In particular, performance of catalytic and non-catalytic hydrocracking of Athabasca bitumen was evaluated using the lump kinetic method which includes combination of separated functions (Köseoglu and Phillips 1988, Köseoğlu and Phillips 1988b).

It is believed that the introduction of the nanocatalysts into bitumen or heavy oil matrix causes a considerable change in the reaction mechanisms as nanocatalysts open new pathways for the reaction. Galaragga et al. (Galarraga et al. 2011) performed a preliminary hydroprocessing reaction's kinetic in the presence of UD nanocatalysts for Athabasca bitumen proposing two different kinetics models to fit their lab test data. The

first model was based on a simple power law of first order reactions and the second one was similar to the kinetics model which was proposed by Sanchez et al. (Sánchez, Rodríguez, and Ancheyta 2005). This model was used a lumping method with series of reactions connected as a network scheme. Loria et al., 2011, (Loria et al. 2011) proposed a modified kinetics model using the same reaction scheme for the UD nanocatalysts. Figure 6.7-a and 6.7-b shows both models. As can be observed, there exists quite a difference between the kinetic rate constants corresponding to the reactions.

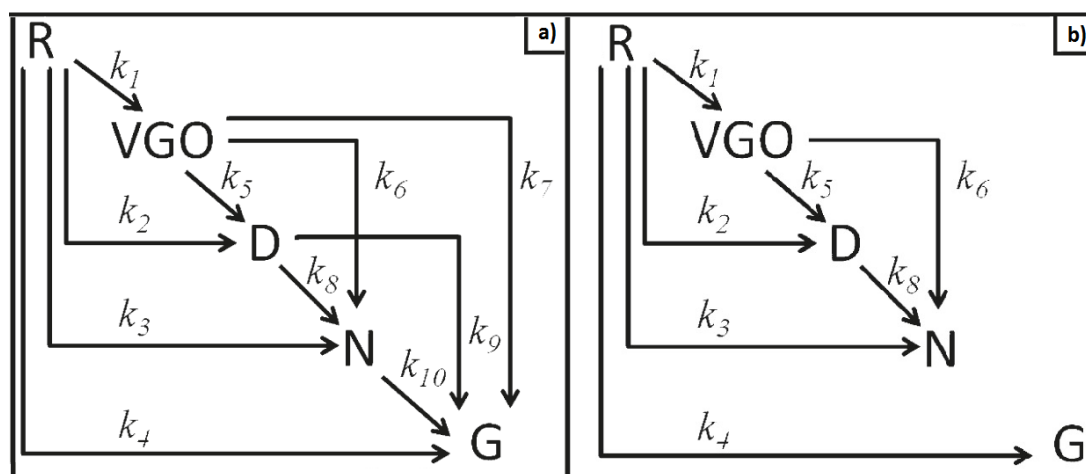


Fig 6.7: Proposed kinetic models (a) hydroprocessing of bitumen in presence of UD catalysts (Sánchez, Rodríguez, and Ancheyta 2005) with permission; (b) Modified model for the UD catalyst (Loria et al. 2011) with permission.

Results of predicted product's compositions were in good agreement with the lab data with the absolute error value of less than 7% (Loria et al. 2011). In addition, predicted viscosity of produced liquids shows great reduction depending on temperature and residence time (Loria et al. 2011). More importantly, it reveals that correct modeling scheme as well as accurate solution conditions would provide successful product prediction. Along with other studies, our group published a series of articles on the

kinetics decomposition of Athabasca bitumen and asphaltenes in the presence of nanocatalysts as well (Almao 2012, Nassar et al. 2013a, Nassar, Hassan, and Pereira-Almao 2011a, Galarraga and Pereira-Almao 2010, Nassar et al. 2013b, Nassar et al. 2013c, Nassar, Hassan, and Pereira-Almao 2012). Despite all of the studies that have been performed in this field, there exists many area of research to fully understand the kinetics decomposition of heavy oil and bitumen.

6.8 Bitumen recovery enhancement

Presence of nanocatalysts inside the porous media led to the production of lighter components via catalytic hydrocracking of heavy oil and bitumen and the subsequent viscosity reduction of bitumen in the oil pool as a result of bitumen contact with emitted hydrocarbon gases (Hashemi, Nassar, and Pereira Almao 2013c). Hashemi et al, 2013, showed that there exists a recovery enhancement via injection of nanocatalysts inside the medium. However, recovery process would be more efficient by coupling another thermal method with the injection of nanocatalysts since the individual nanocatalysts recovery enhancement is not that high. It should be mentioned that by selecting higher quality catalyst carrier into the porous media, higher recovery enhancement is expected.

One of the key challenges for the nanocatalysts usage in upgrading and recovery enhancement is the method of incorporating the nanocatalysts for hydrocracking processes. In heavy oil in-situ upgrading and SAGD process, there exist numerous factors that still are not fully explored. Clearly, adding another recovery mechanism coupled with the existing methods will add much higher complexity to the process of thermal

recoveries. In the subsequent Sections we highlight some of the potential opportunities and challenges on bitumen recovery enhancement.

6.9 Quality Enhancement

Evaluation of product's quality is very important in any upgrading process to determine the extent of increased value of heavy feedstocks. In addition to process cost-effectiveness, transportation pipe designs as well as processing facility specifications depend upon the quality of products (Martínez-Palou et al. 2011b). Therefore, the produced streams were characterized in order to determine hydrogen to carbon ratio (HCR), API gravity, viscosity, micro carbon residue (MCR) content, sulphur and nitrogen content.

One of the characteristic properties of heavy oil and bitumen is low value for H/C ratio. Figure 6.8 shows H/C ratio for the various petroleum cuts (Billon and Bigeard 2001). Any enhancement to H/C ratio can be used as an indication for extent of heavy feedstock upgrading. Any thermal upgrading process involves simultaneous cracking and hydrogenation of heavy molecules to produce lighter components with smaller molecules as well as higher H/C ratios (Gates, Katzer, and Schuit 1979). Galarraga and Pereira-Almao, 2010, (Galarraga and Pereira-Almao 2010) successfully tested the catalytic hydroprocessing reactions of Athabasca bitumen in a batch mode. The authors employed nanocatalysts suspension in-situ by using heavy oil emulsion and subsequently tested in batch reactor using marginal levels of hydrogen and sand for bitumen upgrading. Experimental results showed that nanocatalysts enhanced the upgrading of Athabasca bitumen by significantly increasing the H/C atomic ratio and reducing both viscosity and

coke formation (Galarraga and Pereira-Almao 2010). In addition, a significant reduction of sulfur and micro carbon residue was observed. Figure 6.9 illustrates the H/C ratio enhancement for products obtained at 380 °C and 3.45 MPa as a function of residue conversion. It can be seen that there exists a polynomial trend for H/C ratio enhancement, which clearly provides enough evidence for effectiveness of nanocatalysts presence inside the porous media and effective incorporation of hydrogen within the liquid products. Based on produced results, nanocatalysts can enhance the H/C ratio via hydrocracking followed by hydrogenation process. In addition, higher H/C ratio occurs in higher conversion values.

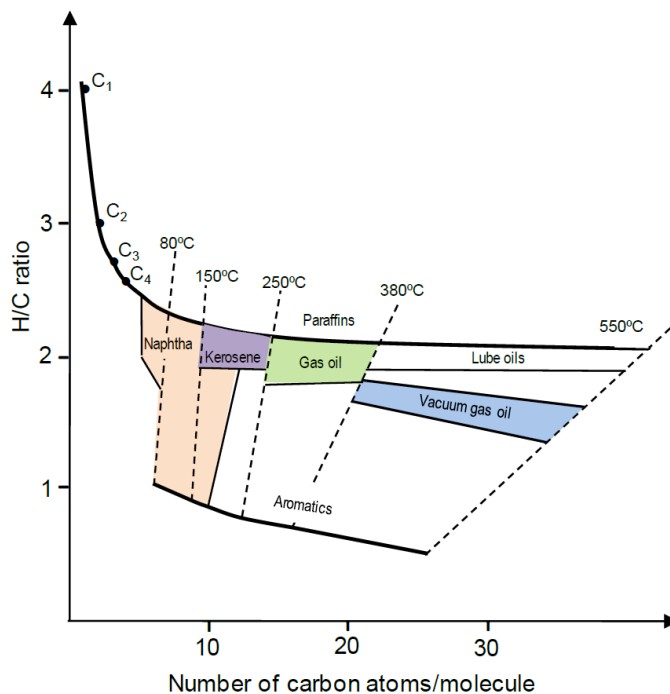


Fig 6.8: Hydrogen to carbon ratio for the various petroleum cuts (Billon and Bigeard 2001) with permission.

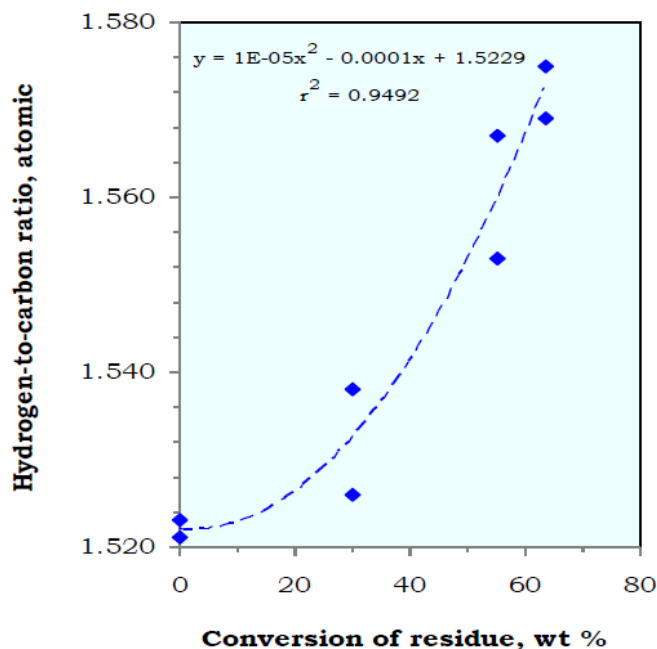


Fig 6.9: Hydrogen-to-carbon ratio (H/C) of Athabasca bitumen at different conversion of residue for reaction performed at 380 °C (Galarraga and Pereira-Almao 2010) with permission.

Produced results of nanocatalysts effectiveness for viscosity reduction showed successful records in batch and pilot tests (Hashemi, Nassar, and Pereira Almao 2013c, Galarraga and Pereira-Almao 2010). Viscosity is considered as one of the most important factors for bitumen transportation via pipelines. For commercial transportation, bitumen API gravity is increased to a number of 19-21°API and viscosity of bitumen is decreased to approximately (250 cP at 10 °C) (Syncrude_Canada 1996). In the current context, most of mobility enhancement is performed on surface using surface upgrading facilities or appropriate diluent is used to meet refinery feedstock specifications (Anderson, Chambers, and McMurray 1995). UD nanocatalysts experiments using hydrogen performed in batch and packed bed reactors showed that in-situ upgrading and recovery processes can be implemented to enhance the quality of Athabasca bitumen that can meet

pipeline transportation criteria without any diluent addition. Figures 6.10 (Galarraga and Pereira-Almao 2010) and 6.11 (Hashemi, Nassar, and Pereira Almao 2013a) are examples of produced liquid viscosities from a batch reactor and packed bed reactor, respectively. As seen, presence of nanocatalysts inside the medium has dramatic effect on viscosity reduction of Athabasca bitumen.

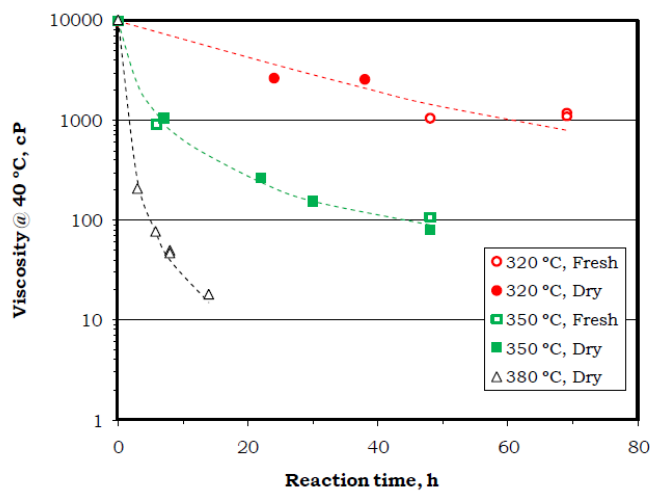


Fig 6.10: Viscosity of liquid products from reaction at constant pressure of 3.45 MPa, temperatures of 320, 350 and 380 °C at reaction times from 3 up to 70 hours (Galarraga March 2011) with permission.

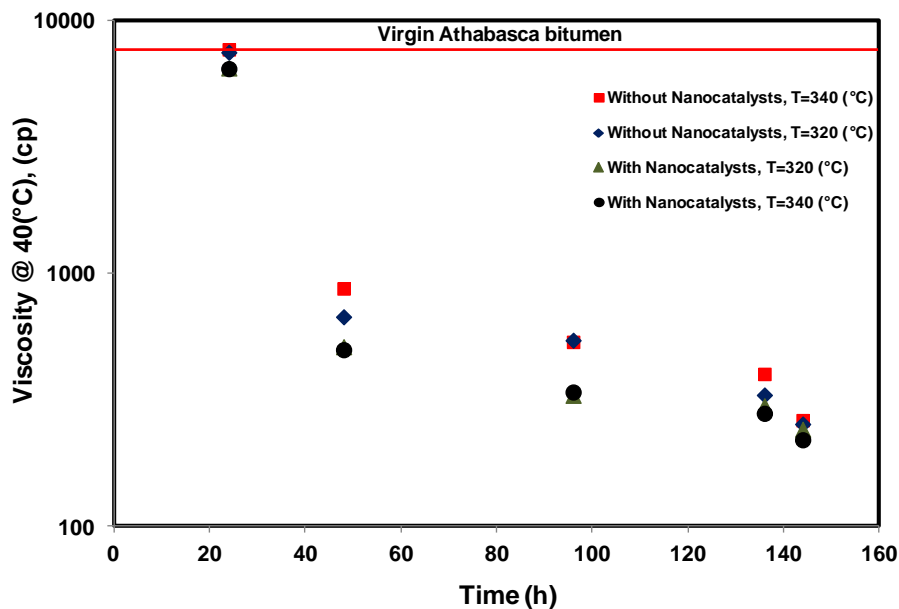


Fig 6.11: Viscosity of produced liquid samples from oil sand porous media measured at 40 °C. Sample was produced at different times in the absence and presence of tri-metallic UD nanocatalysts at pressure of 3.5 MPa, hydrogen flow rate of 1 cm³/min, and temperatures of 320 and 340 °C. Obtained from reference (Hashemi et al., 2013) with permission.

Clearly, in both processes (i.e., batch and pilot tests), viscosity of products reduced against the time of the reaction. In addition, higher viscosity reduction occurred at higher temperatures. In both of the experimental series VGO was used as nanocatalysts carrier into the medium, and certainly by using lighter carrier, higher viscosity reduction can be observed since dilution was coupled with the thermal catalytic process during upgrading experiments. In addition to viscosity reduction, API gravity of products can be employed as a sign of quality enhancement.

As a result of heavy feedstocks upgrading, products density decreases and API gravity increases. Both experiments, batch and pilot plant, for Athabasca bitumen upgrading using UD nanocatalysts showed higher API gravity of the produced liquid. Figure 6.12 shows the API gravity against conversion percentages in batch reactor

(Galarraga March 2011). It can be observed that API of 16 was achieved for higher conversion percentages. Furthermore, in pilot plant tests for different reaction times, API enhancement was measured in presence and absence of UD nanocatalysts and considerable improvement was detected for the experiment conducted in the presence of UD nanocatalysts (Hashemi, Nassar, and Pereira Almao 2013a). Figure 6.13 presents the API gravity measurements at different conditions. Clearly, nanocatalysts improved the API gravity significantly in both series of the tests, which again supports the potentials application of UD nanocatalysts for enhancing upgrading of heavy feedstocks.

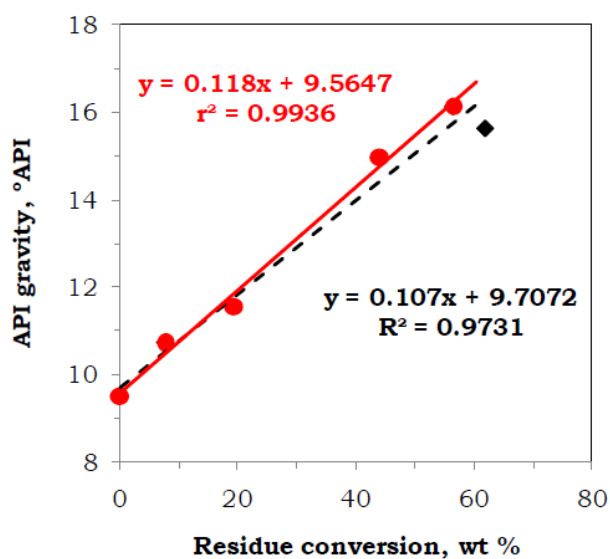


Fig 6.12: API gravity of liquid products as a function of conversion for dry emulsion of UD nanocatalysts in batch reactor. Obtained from (Galarraga et al., 2011) with permission.

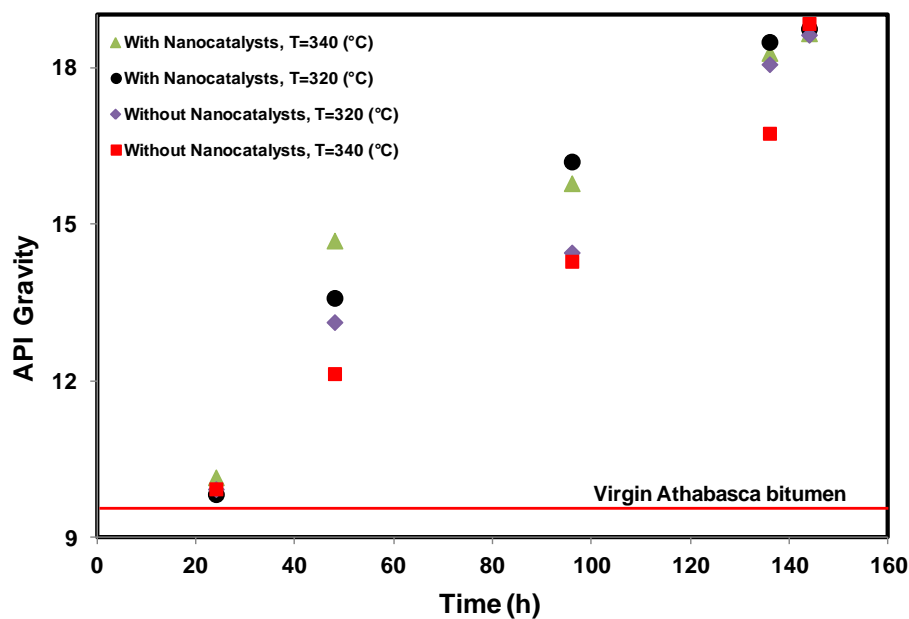


Fig 6.13: API gravity of produced liquid samples from porous media at different times in the absence and presence of tri-metallic UD nanocatalysts at pressure of 3.5 MPa, hydrogen flow rate of 1 cm³/min, and temperatures of 320 and 340 °C. Obtained from (Hashemi et al., 2013) with permission.

Furthermore, micro carbon residue (MCR) contents of produced liquid samples were measured as another indication for quality enhancement by using a standard method (Hassan, Carboynani, and Pereira-Almao 2008a). MCR content measurement refers to amount of carbon residue which is left behind after the thermal treatment of the heavy feedstocks. High value of MCR content for a sample was interpreted as low quality product. Again, published results showed potential of UD nanocatalysts application for reducing the MCR content of heavy feedstocks. In batch reactor test for Athabasca bitumen catalytic hydrocracking, MCR content was improved by including the UD nanocatalysts particles. Implementing the UD nanocatalysts changed the MCR from 16 wt% in the blank experiment up to about 11 wt% for selected experimental conditions (Galarraga March 2011). For the continuous mode experiments, same observations were

published regarding MCR reduction in produced samples (Hashemi, Nassar, and Pereira Almao 2013a). Figure 6.14 shows MCR reduction for the produced samples in presence and absence of UD nanocatalysts. It can be seen that, at higher temperature and in presence of nanocatalysts, lowest amount of MCR was measured which proves the effectiveness of nanocatalysts for hydrocracking reaction as well as quality enhancement confirming that UD nanocatalysts are improving the hydrogenation reactions and consequently reducing the potential for coke formation.

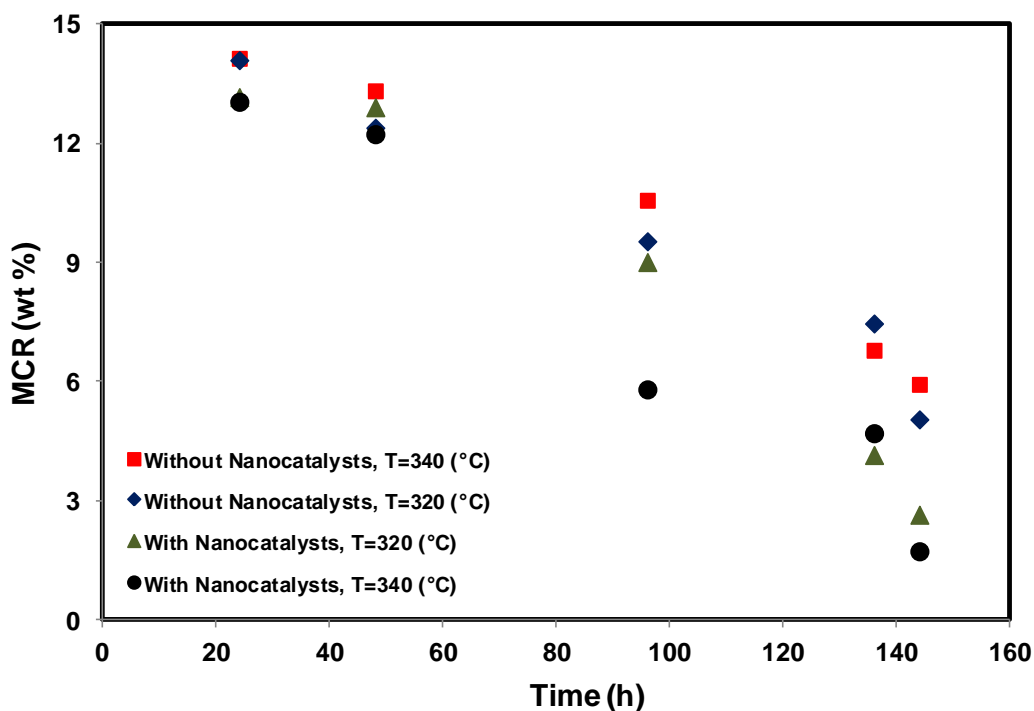


Fig 6.14: MCR content of produced liquid samples from porous media as a function of reaction time in the absence and presence of tri-metallic UD nanocatalysts at pressure of 3.5 MPa, hydrogen flow rate of 1 cm³/min, and temperatures of 320 and 340 °C. Obtained from (Hashemi et al., 2013) with permission.

6.10 Sulfur removal

Environmental considerations enforce very stringent regulations on the sulfur content of fossil combustibles (Breysse et al. 2003). In hydrotreating processes, hydrodesulfurization is considered as one of the most important reactions which involves removing the sulfur from petroleum compounds to produce hydrogen sulfide as well as desulfurized compounds (Gates, Katzer, and Schuit 1979). Generally, dispersed catalysts shows higher percentages of sulfur removal compared with supported catalysts; owing to their effective accessibility (de Agudelo and Galarraga 1989, Ramirez de Agudelo and Galarraga 1991, Chen et al. 2007, Kennepohl and Sanford 1996) . Figures 6.15 and 6.16 show the extent of sulfur removal for Athabasca bitumen in batch reactor and pilot plant tests at different temperature, respectively. For batch reactor, at 380 °C up to 50% of sulfur content was removed at low reaction time (about 14 h).

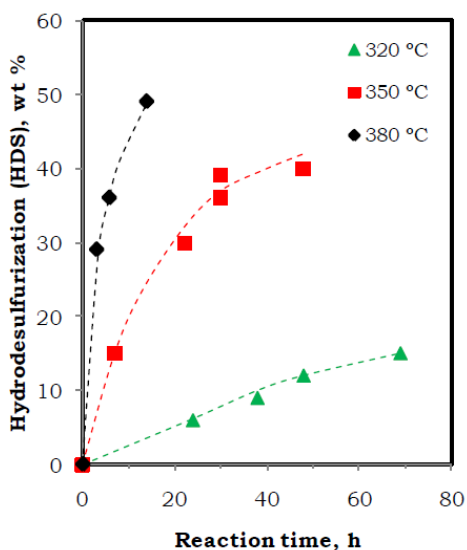


Fig 6.15: Hydrodesulfurization of Athabasca bitumen as a function of reaction time evaluated at 3.45 MPa of hydrogen pressure and at temperatures of 320, 350, 380 °C using UD NiWMo catalysts. Obtained from (Galarraga et al., 2011) with permission.

In continuous mode experiments, the sulfur concentration decreased with both time and temperature. It can be observed that presence of UD nanocatalysts enhanced the sulfur removal quite significantly, especially at lower temperature. This again confirms the effectiveness of UD nanocatalysts for enhancing the hydrodesulfurization reaction. However, sulfur removal is associated with hydrogen sulfide production which can cause some negative aspects for the nanocatalysts implementation inside the porous media.

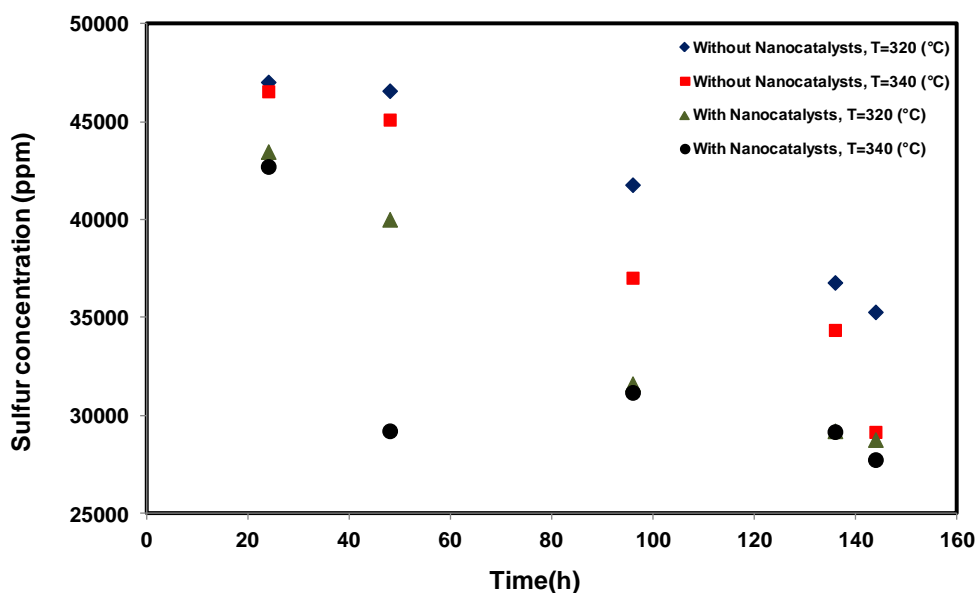


Fig 6.16: Sulfur content of produced liquid samples from porous media at different times in the absence and presence of tri-metallic UD nanocatalysts at pressure of 3.5 MPa, hydrogen flow rate of 1 cm³/min, and temperatures of 320 and 340 °C (Hashemi et al., 2013) with permission.

6.11 Coke formation mitigation

During a typical thermal upgrading process, decomposition of heavy feedstocks occurs in the presence of hydrogen to saturate the free radicals, and subsequently produce lighter

components as well as huge amount of coke and considerable amount of light gas such as methane, ethane, CO₂, etc (Kennepohl and Sanford 1996, Sanford 1995). It is expected that presence of catalysts inside the reaction medium would result in less amount of coke as catalysts can create new pathways in the reaction schemes (Hashemi, Nassar, and Pereira Almao 2013a) .

Heavy oil and bitumen usually contain about 50 wt% of residue fraction with the normal boiling point higher than 545 °C (Altgelt and Boduszynski 1994). For the purpose of heavy feedstocks upgrading, hydroprocessing catalysts should be resistant to deactivation caused by metal deposition and coke formation (Ancheyta, Rana, and Furimsky 2005). In this sense, there exists extensive research work to improve the catalysts activity by introducing UD nanocatalysts which navigate along with the heavy feedstocks as well as catalyzing the upgrading processes (Pereira-Almao 2007b). Furthermore, deactivation of UD nanocatalysts is less strong than conventional supported catalysts (Lee et al. 1995).

Published results on the nanocatalysts usage for Athabasca bitumen upgrading show successful outcome which again confirms the potential application of UD nanocatalysts for upgrading purposes. In batch reactor tests for Athabasca bitumen upgrading, coke formation was significantly reduced by using tri-metallic nanocatalysts emulsion with no detriment in residue conversion (Galarraga March 2011). However, by increasing the severity of conditions coke formation increased dramatically.

For the continuous mode experiments, Figure 6.17 depicts the coke contents (wt %) of produced samples against the reaction time at different temperatures in the presence and absence of UD tri-metallic nanocatalysts. Clearly, presence of nanocatalysts inside

the porous medium significantly improved the quality of produced samples regarding coke content. It is worth noting that temperature has a very drastic and sensitive effect on the coke formation during thermal processes (Wang, Guo, and Que 1998). Increasing the temperature speeds up the rate of thermal cracking reactions, which outperform the hydrogenating reactions that are thermodynamically hindered with temperature. Therefore, a higher proportion of free radicals will form and subsequently lead to the formation of a higher amount of coke (Demirel and Wisler 1998).

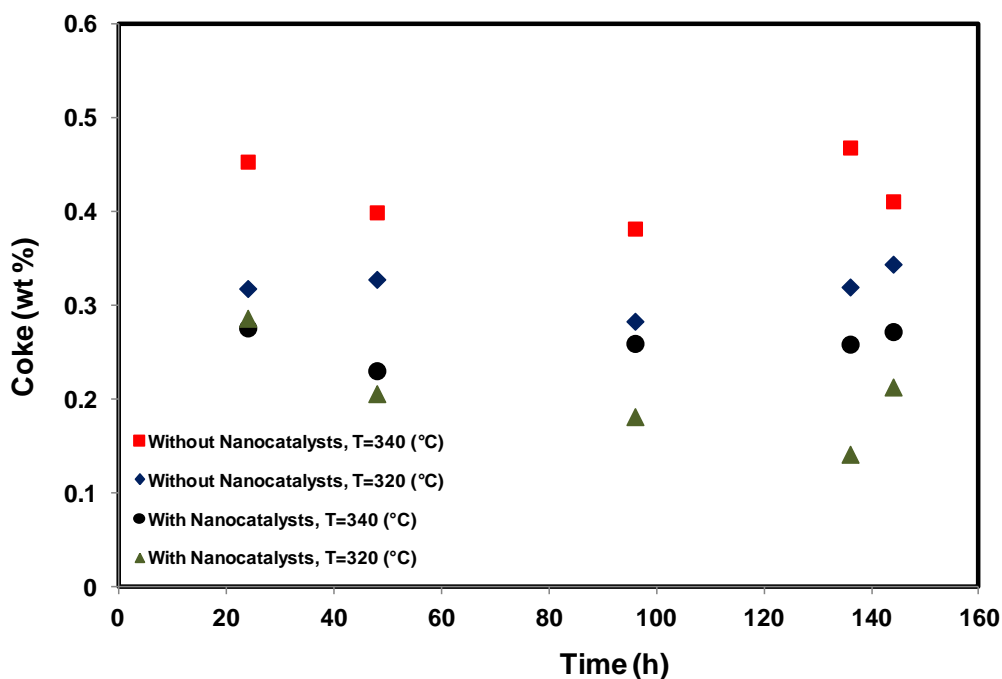


Fig 6.17: Coke content of produced samples from porous media as a function of reaction time in the absence and presence of tri-metallic UD nanocatalysts at pressure of 3.5 MPa, hydrogen flow rate of 1 cm³/min, and temperatures of 320 and 340 °C (Hashemi et al., 2013) with permission.

It is beneficial to mention that Kennepohl and Sanford, 1996, showed that the dispersed catalyst helped to reduce the coke formation much better than the supported

catalyst during the upgrading of Athabasca bitumen at typical upgrading conditions. However, as dispersed concentration increases this benefit was reversed because the catalytic particles acted as coke seeds (Kennepohl and Sanford 1996).

6.12 Gas emission reduction

There is no doubt that upgrading of heavy oil and bitumen with the current technologies produces considerable amounts of greenhouse gas (GHG) emissions. As an example, the province of Alberta was the first in North America to legislate the GHG emission reduction for large industrial facilities (Alberta 2008). Furthermore, increasingly stringent legislation limits on the level of fuels contaminants has enforced the industry to invest in the exploration of cost-effective and environmentally acceptable new technologies, integration with or enhancing the currently available technologies for heavy feedstocks processing (Gosselin 2010).

One possible promising new technology is the in-situ upgrading, sometimes known as underground refinery, aims to improve the quality of crude oil and decrease the level of its contaminants, such as sulfur and nitrogen to a good extent (McEachern 2009) as well as the GHG emissions. However, not much is known about the produced gases emitted during the in-situ upgrading process by using nanocatalysts.

In a recent study, Hashemi et al. investigated the effectiveness of nanocatalysts on gaseous emission reductions (Hashemi, Nassar, and Pereira Almao 2013b). Results showed that the presence of tri-metallic nanocatalysts enhanced the hydrogenation reactions and consequently led to significant reduction in CO₂ emission. In the best case, at a high pressure and temperature conditions, CO₂ emission was reduced up to 50%

compared with the case without the presence of nanocatalysts in the medium. It is worth noting that gas emissions would remain as one of the most important challenges of the nanocatalysts upgrading process. Therefore, more laboratory investigations and pilot scale testing will be needed to investigate this issue with more details. Furthermore, UD nanocatalysts particles produce hydrocarbon gases as results of hydrocracking that works as diffusing solvent for enhancing heavy oil production.

6.13 Nanocatalysts recycling

Presence of nanocatalysts inside the medium along with hydrogen incorporation aims to improve the quality of produced liquid via catalytic hydrocracking. As previously mentioned, fast deactivation of conventional supported catalysts is one of the major disadvantages compared to UD nanocatalysts. Presence of large molecules in the heavy feedstock has limited accessibility into the porous network of the conventional catalysts. This is the reason that hydroprocessing catalysts should be resistant to deactivation caused by metal deposition and coke formation (Ancheyta, Rana, and Furimsky 2005).

UD nanocatalysts could provide desirable level of reaction activity as well as option to perform in the well level between injector and producer (Nares et al. 2007). A key bottleneck to the in-situ applications will be the recyclability of the spent nanocatalysts that can provide cost-effectiveness for the process as well as reduction in the environmental footprints. Our research group developed a promising alternative for downhole upgrading process. Figure 6.15 shows a schematic representation of this process .As can be observed, nanocatalysts are injected through injector well inside the

porous media and upgraded oil is produced via recovery well. Produced liquid from the reservoir contains some active nanocatalysts inside the non-distillable residue which can be recycled and re-injected to the porous reservoir (Peluso 2011).

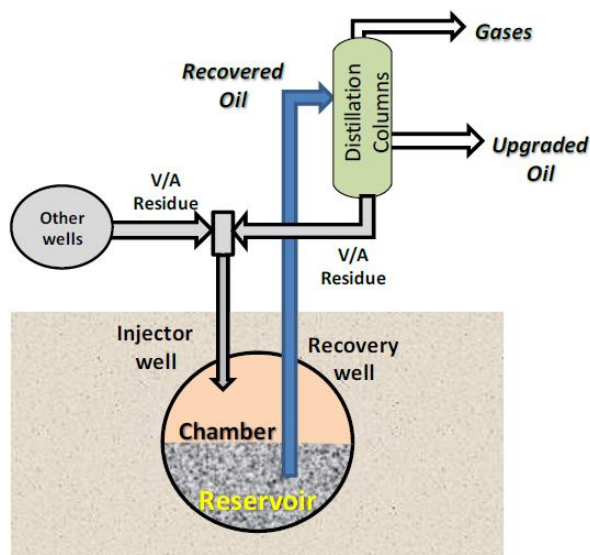


Fig 6.18: Schematic representation of in-situ upgrading (ISU) process for non-conventional oil in the presence of UD catalysts. Obtained from (Peluso 2011) with permission.

It is absolutely crucial to understand the nanocatalysts behavior in many aspects such as the stability and the potential recycling methods of these particles. It will be in favor of the process economics if the UD catalysts could be used several times before losing stability and catalytic activity. Reviewing of literature shows that a lack of extensive study in this area is quite tangible. As one important piece of work, Enzo Peluso showed that it is feasible to recycle the UD nanocatalysts particles. However, there is the possibility of particle agglomeration which is a slow and reversible process. To have a clear understanding of recycling potential and challenges, more laboratory investigations

and pilot scale testing will be needed to implement this economically beneficent technique in the existing heavy oil industry.

6.14 Hydrogen consumption

In a typical hydroconversion process, heavy molecules of petroleum feedstocks with high boiling points are split and saturated with hydrogen, forming lighter components with lower boiling points as well as less impurities (Rana et al. 2007). High investment is required to conduct these types of processes since hydrogen consumption is an important issue. Presence of hydrogen promotes bond cleavage reactions which results in mitigating the coke formation as well as removing heteroatoms by controlling the polymerization process (Rana et al. 2007, Del Bianco, Panariti, Di Carlo, et al. 1993).

For on surface upgrading process at severe conditions (350-430 °C and 8.5- 20 MPa), the required hydrogen is typically in the range of 200 and 590 nm^3/m^3 which is related to the H_2 to oil ratio of 505 and 1685 nm^3/m^3 (Scherzer and Gruia 1996). In the same sense for UD nanocatalysts application subsurface, hydrogen is required to interact with the heavy feedstocks in presence of nanocatalysts to improve the quality of reactions. As an initial guess, the required amount of hydrogen could be estimated on the basis of its solubility in crude oil. However, to perform the upgrading process, much higher amounts of hydrogen are needed. Further, as the reaction severity increased the hydrogen consumption would increase. Finally, we would point out that working with hydrogen at high pressure and temperature conditions also exhibit a high risk, of safety issues. Therefore, a key challenge will be to maintain and enforce a high level of safety consideration upon the conduction of in-situ hydrocracking process.

It is very important to mention that processes involving hydrogen usage are very sensitive in the industry due to hazards related to this gas. In addition, to conduct a field scale application, it is crucial to provide required sources of hydrogen for the subsurface upgrading processes. Furthermore, there are some challenges in the operational side such as method of introducing hydrogen to the porous media. For in-situ upgrading in the SAGD operations, one possible approach is to inject hydrogen from the injectors. Finally, in the presence of high temperature and pressure as well as the catalyst, risk of coking and plugging of porous media and consequently reduction of permeability should be considered as one of the possible risk of in-situ upgrading reactions.

6.15 Environmental effect of nanocatalysts

Nanotechnology is the science and technology of controlling matters at nanoscale (Bergeson and Auerbach 2004), promising to enhance the economics in areas ranging from transportation to agriculture to health (Morris, Willis, and Gallagher 2007). Over the last decade many nanomaterials have moved into the marketplace (Kahan and Rejeski 2009) with the direct and indirect applications in the society. However, there are only minimal data on the nanomaterials exposure effect on the human health and environment. Moreover, results of the primitive studies show some concerns about the effect of these nanomaterials (Nel et al. 2006).

From the environmental perspective, associated benefits of nanoparticles are combined with the potential challenges that may be difficult to predict. In addition, there exists little information about the manufacturing, usage and disposal of the nanomaterials. Furthermore, detection methods, measurement, analyzing and tracing the

nanomaterials are in the process of development (Breggin and Carothers 2006). This issue become more important when the nanomaterials show different behavior compared with the chemical properties in the bulk. As an example aluminum is inert in the form of a Coke can while it is highly explosive in the nanostructure which shows that properties change at the scale (Jurvetson and Jurvetson 2007).

The process of heavy oil upgrading using nanocatalysts is quite new and challenging chemical process, and it is likewise the other areas of nanotechnologies with the opportunities and challenges. To the best of our knowledge, some of the challenges have been presented in this study. However, there exist many challenges that should be scrutinized to cover all the aspects of the nanocatalysts. As an example, percentages of injected nanocatalysts into the formation are deposited inside the medium (Hashemi, Nassar, and Pereira-Almao 2012) and will remain in-situ for many years no study was performed on the long term environmental effect of these nanocatalysts. On the other side, some portion of the injected nanoparticles is produced by the upgraded oil which is used in the car engines after some refinery processes. Furthermore, in the operational side, the possibility of groundwater contamination by the synthesized nanoparticles should be considered as an operational failure risk.

Green chemistry is a concept, which is designed to eliminate chemicals and processes that may have negative impact on the environment (Kalidindi and Jagirdar 2012). Produced sustainable nanocatalysts aim to show higher activity, higher selectivity, efficient recovery as well as durability and recyclability in a cost-effective process. In recent years, our group is working on naturally occurring nanocatalysts which could have much less environmental risk compared to the synthesized nanocatalysts.

6.16 Conclusions

To the best of our knowledge, advantages of nanocatalysts employment for in-situ catalytic upgrading were scrutinized. For further applications and studies, limitations and challenges facing this new technology were discussed and current situation of this process was presented. This paper intends to be the current reference for the level of enhancement of in-situ upgrading processes using UD nanocatalysts. As the highlights of this study, it can be mentioned that in-situ catalytic upgrading process requires considerable hydrogen consumption and produces considerable amounts of gases. However, qualities of produced liquid samples are improved and sulfur contents are reduced. Furthermore, nanoparticles analysis showed that considerable amount of injected nanoparticles retained inside the porous media, but retention of nanoparticles has no significant impact on permeability formation damage. In addition, recycling of nanocatalysts is feasible and agglomeration occurred during the injection process, which is slow and reversible mechanism. Future improvement of the nanocatalysts could be associated with the new generation of naturally occurring nanocatalysts, fulfilling the green chemistry concept.

Chapter 7 Conclusions and Recommendations

Since each chapter contains a separate detailed conclusion, only key conclusions and major contributions of this thesis are presented below followed by a few recommendations for the future studies.

7.1 Conclusions

Tri-metallic (Ni-Mo-W) nanocatalysts upgrading performance and its transport behavior inside an oil sand packed bed column at a high temperature and pressure has been investigated. Results showed that it is feasible to propagate these nanoparticles inside the porous media without major formation damage. However, certain amounts of the injected particles get retained inside the porous media which possibly helps the quality enhancement of the produced liquids. It should be noted that the deposition inside the medium has an exponential trend from entrance of injection towards the production point. Based on the investigated parameters, it is concluded that deposition of the nanoparticles is a function of temperature, type of metal and porous media permeability.

Successful results were obtained on controlled delivery of nanoparticles inside the porous media, proposed to compare the recovery results of different hot fluid injection scenarios in presence and absence of the UD nanocatalysts to see the effectiveness of these nanoparticles. For the different injection tests, the amount of produced bitumen was depicted by recovery curves, at different times and temperatures and compared with the base case. Results showed that, increasing the percentages of light oil components in the

injecting fluid enhanced the recovery of bitumen from the oil pool due to expansion of solvent and consequent viscosity reduction of Athabasca bitumen. In addition, presence of tri-metallic nanocatalysts in the injected hot fluid enhanced the Athabasca bitumen recovery via catalytic hydrocracking of bitumen and production of lighter components, which led to viscosity reduction of the produced stream.

In the experiments with nanocatalysts at different temperatures, quality of produced liquid sample was analyzed to observe the enhancement on different properties such as viscosity, API gravity and content of sulfur, nitrogen, and MCR. In all experiments with nanocatalysts, reduction of hydrocarbon residue and MCR content were observed. In addition, using the nanocatalysts enhanced the API gravities as well as produced liquid viscosities along with reduction on the nitrogen and sulphur content of the samples which is environmentally beneficial for the bitumen production and upgrading processes.

In addition to liquid quality enhancement, presence of nanocatalysts inside the porous media inhibits the production of coke by enhancement in the hydrocracking reaction via effectively hydrogen incorporation during the process. Furthermore, production of carbon dioxide decreased during the reaction with the nanocatalysts which is environmentally favorable in the in-situ processes. It should be noted that quality of produced gases from porous media enhanced by producing higher percentages of hydrocarbon gases as well as ethylene/propylene as coke precursors. Also, the results of EDAX analysis showed that stability of injected nanocatalysts was maintained even at the high reaction severity.

As a result of performing this study for some years, some of the advantages and limitations of UD nanocatalysts implementation inside the porous media has been reported in Chapter 6 of the thesis. High hydrogen consumption, considerable amount of

emitted gas production, enhancement in the produced liquid and gas qualities and reduction in coke formation are some of the observed results. Based on the reported observations, any future study on nanocatalysts area should be conducted with consideration of the reported challenges.

7.2 Recommendations for Future Work

- Preparation of UD nanocatalysts using a lighter carrier could be beneficial in many ways. Higher viscosity reduction could be achieved by implementing a lighter carrier in the process of UD nanocatalysts preparation. In addition, lighter carrier would result in lighter suspension.
- Running the experiments in a 3D physical model could provide more valuable results and better understanding of the upgrading and recovery enhancement. The reactor considered in this study was a small tube and observed results should be implemented with higher consideration compared with the results of a 3D physical model which mimics real SAGD reservoir criteria.
- Coupling the presented catalytic EOR method with the steam injection would be very useful to have a better evaluation of the operational problems. Since most of the Athabasca bitumen reservoirs are under steam injection, coupling this process with the catalytic EOR method seems quite reasonable.
- There exist some solid metallic content in the injecting feedstock, which are going to incorporate in the same way as UD nanocatalysts acts inside the porous media. Designing a methodological experimental study to investigate the effect of these

particle activities would determine the effect of metallic content in the quality and recovery enhancement.

- Optimizing the catalytic formulation to evaluate the effect of different metallic ratio on Athabasca bitumen upgrading would help to use optimum catalytic emulsion in the process. This optimization is not only on the performance of the nanocatalysts but it would benefit economically as well.

References

- Adamczyk, Z, TGM Van de Ven. 1981. Deposition of particles under external forces in laminar flow through parallel-plate and cylindrical channels, *Journal of Colloid and Interface Science* **80** (2): 340-356.
- Afanasiev, P., I. Bezverkhy. 2002. Synthesis of MoS_x (5 > x > 6) Amorphous Sulfides and Their Use for Preparation of MoS₂ Monodispersed Microspheres, *Chemistry of materials* **14** (6): 2826-2830.
- Afanasiev, P., G.F. Xia, G. Berhault et al. 1999. Surfactant-assisted synthesis of highly dispersed molybdenum sulfide, *Chemistry of materials* **11** (11): 3216-3219.
- Agarwal, Avinash Kumar. 2007. Biofuels (alcohols and biodiesel) applications as fuels for internal combustion engines, *Progress in Energy and Combustion Science* **33** (3): 233-271.
- Akin, Serhat, Suat Bagci. 2001. A laboratory study of single-well steam-assisted gravity drainage process, *Journal of Petroleum Science and Engineering* **32** (1): 23-33.
- Al-Honi, M., M. Greaves, AY Zekri. 2002. Enhanced recovery of medium crude oil in heterogeneous reservoirs using air injection/in situ combustion—horizontal well technology, *Petroleum science and technology* **20** (5-6): 655-669.
- Government of Alberta. 2008. Alberta's oil sands; resourceful, responsible; Available at: http://www.oilsands.alberta.ca/documents/AB_Environment_OilSands_FINAL.pdf. (accessed November 16, 2008).
- Alberta_Energy. What is Oil Sands?, <http://www.energy.gov.ab.ca/OilSands/793.asp>.
- Alhumaizi, KI, VM Akhmedov, SM Al-Zahrani et al. 2001. Low temperature hydrocracking of n-heptane over Ni-supported catalysts: study of global kinetics, *Applied Catalysis A: General* **219** (1): 131-140.
- Alivisatos, A Paul, Kai P Johnsson, Xiaogang Peng et al. 1996. Organization of nanocrystal molecules' using DNA.
- Almao, P. Pereira. 2012. In situ upgrading of bitumen and heavy oils via nanocatalysis, *The Canadian Journal of Chemical Engineering* **90** (2): 320-329. <http://dx.doi.org/10.1002/cjce.21646>.
- Altgelt, K.H., M.M. Boduszynski. 1994. *Composition and analysis of heavy petroleum fractions*, M. Dekker (New York) (Reprint).
- Ananth Govind, P., S. Das, S. Srinivasan et al. Expanding Solvent SAGD in Heavy Oil Reservoirs.

- Ancheyta, J., M.S. Rana, E. Furimsky. 2005. Hydroprocessing of heavy petroleum feeds: Tutorial , *Catalysis Today* **109** (1-4): 3-15.
- Ancheyta, Jorge, Sergio Sánchez, Miguel A. Rodríguez. 2005. Kinetic modeling of hydrocracking of heavy oil fractions: A review , *Catalysis Today* **109** (1-4): 76-92. <http://www.sciencedirect.com/science/article/pii/S0920586105005973>.
- Anderson, BS, JI Chambers, DR McMurray. Market Outlook For Athabasca Bitumen-- The Economics of Location.
- Anderson, JR, K. Fogar, T. Mole et al. 1979. Reactions on ZSM-5-type zeolite catalysts , *Journal of Catalysis* **58** (1): 114-130.
- Anhorn, JL, A. Badakhshan. 1994. Athabasca Bitumen: Oxygenate Blends and Viscosity Models , *Scientia Iranica* **1** (3).
- Aoyagi, Ko, William C McCaffrey, Murray R Gray. 2003. Kinetics of hydrocracking and hydrotreating of coker and oilsands gas oils, *Petroleum science and technology* **21** (5-6): 997-1015.
- Assessment, Energy Market. June 2006. Canada's Oil Sands: Opportunities and Challenges to 2015: An Update.
- Ayasse, Alan R, Hiroshi Nagaishi, Edward W Chan et al. 1997. Lumped kinetics of hydrocracking of bitumen , *Fuel* **76** (11): 1025-1033.
- Bartholomew, Calvin H. 2001. Mechanisms of catalyst deactivation , *Applied Catalysis A: General* **212** (1): 17-60.
- Bearden, R., CL Aldridge. 1981. Novel catalyst and process to upgrade heavy oils , *Energy Prog.:(United States)*.
- Belgrave, J., B. Nzekwu, H. Chhina. SAGD optimization with air injection.
- Bell, Alexis T. 2003. The impact of nanoscience on heterogeneous catalysis , *Science* **299** (5613): 1688-1691.
- Bergerson, J., D. Keith. 2006. Life cycle assessment of oil sands technologies.
- Bergeson, Lynnl, Bethami Auerbach. Reading the small print. Vol. 21, 30-32: The environmental law institute.
- Berkowitz, Norbert, James G Speight. 1975. The oil sands of Alberta , *Fuel* **54** (3): 138-149.
- Billon, A., PH Bigeard. 2001. Chapter 10. Hydrocracking, *Petroleum Refining, Conversion Processes* **3**: 331-364.
- Birn, K., P. Khanna. A discussion paper on the oil sands: challenges and opportunities.
- Board, National Energy. 2006. *Canada's Oil Sands. Opportunities and Challenges to 2015: An Update*, National Energy Board Calgary, Alberta, Canada (Reprint).

- Bock, Christina, Chantal Paquet, Martin Couillard et al. 2004. Size-selected synthesis of PtRu nano-catalysts: reaction and size control mechanism, *Journal of the American Chemical Society* **126** (25): 8028-8037.
- Bohn, J.R. 1988. Process for recovering petroleum from formations containing viscous crude or tar, Google Patents (Reprint).
- Brady, John F. 1994. The long-time self-diffusivity in concentrated colloidal dispersions, *Journal of Fluid Mechanics* **272** (1): 109-134.
- Breggin, Linda K, Leslie Carothers. 2006. Governing uncertainty: the nanotechnology environmental, health, and safety challenge, *Colum. J. Envtl. L.* **31**: 285.
- Breysse, Michele, Gérald Djega-Mariadassou, Stéphanie Pessayre et al. 2003. Deep desulfurization: reactions, catalysts and technological challenges, *Catalysis Today* **84** (3): 129-138.
- Butler, R. 1994. Steam-assisted gravity drainage: concept, development, performance and future, *Journal of Canadian Petroleum Technology* **33** (2).
- Butler, R., IJ Mokrys. 1991. A new process (VAPEX) for recovering heavy oils using hot water and hydrocarbon vapour, *Journal of Canadian Petroleum Technology* **30** (1).
- Butler, R.M. 1991a. *Thermal recovery of oil and bitumen*, 285–359. Englewood, Prentice-Hall (Reprint).
- Camacho-Bragado, GA, JL Elechiguerra, A. Olivas et al. 2005. Structure and catalytic properties of nanostructured molybdenum sulfides, *Journal of Catalysis* **234** (1): 182-190.
- Capek, I. 2004. Preparation of metal nanoparticles in water-in-oil (w/o) microemulsions, *Advances in colloid and interface science* **110** (1): 49-74.
- Carbognani, L., J. Lubkowitz, M.F. Gonzalez et al. 2007. High temperature simulated distillation of Athabasca vacuum residue fractions. Bimodal distributions and evidence for secondary “on-column” cracking of heavy hydrocarbons, *Energy & Fuels* **21** (5): 2831-2839.
- Carbognani, L.A., L. Carbognani-Arambarri, F.A. Lopez-Linares et al. Suitable Density Determination for Heavy Hydrocarbons by Solution Pycnometry: Virgin and Thermal Cracked Athabasca Vacuum Residue Fractions, *Energy & Fuels*.
- Cassiolato, Jose E, Hubert Schmitz. 2002. *Hi-tech for industrial development: lessons from the Brazilian experience in electronics and automation*, Psychology Press (Reprint).
- Charpentier, Alex D, Joule A Bergerson, Heather L MacLean. 2009. Understanding the Canadian oil sands industry's greenhouse gas emissions, *Environmental Research Letters* **4** (1): 014005.

- Chen, K., P.C. Leung, B.E. Reynolds et al. 2007. *Process for upgrading heavy oil using a highly active slurry catalyst composition*, Google Patents (Reprint).
- Chu, C. 1977. A Study of Fireflood Field Projects (includes associated paper 6504), *Journal of Petroleum Technology* **29** (2): 111-120.
- Craig, RG, EA White, AM Henke et al. 1966. HG hydrocracking today, *Hydrocarbon Process Pet Refiner* **45**: 159-64.
- de Agudelo, M.M.R., CE Galarraga. 1989. *Catalyst for the simultaneous hydrodemetallization and hydroconversion of heavy hydrocarbon feedstocks*, Google Patents (Reprint).
- Dean, EW, DD Stark. 1920. A Convenient Method for the Determination of Water in Petroleum and Other Organic Emulsions, *Industrial & Engineering Chemistry* **12** (5): 486-490.
- Del Bianco, A., N. Panariti, M. Anelli et al. 1993. Thermal cracking of petroleum residues: 1. Kinetic analysis of the reaction, *Fuel* **72** (1): 75-80.
- Del Bianco, A., N. Panariti, S. Di Carlo et al. 1993. Thermocatalytic hydroconversion of heavy petroleum cuts with dispersed catalyst, *Applied Catalysis A: General* **94** (1): 1-16.
- Demirel, B., W.H. Wiser. 1998. Thermodynamic probability of the conversion of multiring aromatics to isoparaffins and cycloparaffins, *Fuel processing technology* **55** (1): 83-91.
- Dew, JN, WL Martin. 1965. Recovery of hydrocarbons by in-situ hydrogenation.
- Duerkson, CH, A. Eloyan. Evaluation of solvent-based in-situ processes for upgrading and recovery of heavy oil and bitumen. 353-361.
- Dufresne, P., PH Bigeard, A. Billon. 1987. New developments in hydrocracking: low pressure high-conversion hydrocracking, *Catalysis Today* **1** (4): 367-384.
- Erdoğan, Asaf. 2013. Governing Policies for the 21 st Century, School of International and Public Affairs (SIPA), Columbia University.
- Eriksson, S., U. Nylén, S. Rojas et al. 2004. Preparation of catalysts from microemulsions and their applications in heterogeneous catalysis, *Applied Catalysis A: General* **265** (2): 207-219.
- Fixari, B., S. Peureux, J. Elmouchnino et al. 1994. New developments in deep hydroconversion of heavy oil residues with dispersed catalysts. 1. Effect of metals and experimental conditions, *Energy & Fuels* **8** (3): 588-592.
- Foster, Lynn E. 2005. *Nanotechnology: science, innovation, and opportunity*, Prentice Hall PTR (Reprint).
- Frauwallner, Maria Laura. 2009. Catalyst Development for Hydrogenation at Low Temperature, Pressure, and Hydrocarbon Space Velocity. Master of Science, University of Calgary, Calgary.

- Galarraga, Carmen E, Pedro Pereira-Almao. 2010. Hydrocracking of Athabasca bitumen using submicronic multimetallic catalysts at near in-reservoir conditions, *Energy & Fuels* **24** (4): 2383-2389.
- Galarraga, Carmen E, Carlos Scott, Herbert Loria et al. 2011. Kinetic models for upgrading athabasca bitumen using unsupported NiWMo catalysts at low severity conditions, *Industrial & engineering chemistry research* **51** (1): 140-146.
- Galarraga, Carmen Elena. March 2011. Upgrading Athabasca Bitumen using Submicronic NiWMo Catalysts at conditions near to In-reservoir operation. Ph.D, University of Calgary, Calgary.
- Gary, J.H., G.E. Handwerk. 2001. *Petroleum refining: Technology and economics*, CRC Press (Reprint).
- Gates, B.C., J.R. Katzer, G.C.A. Schuit. 1979. *Chemistry of catalytic processes*, Vol. 311, McGraw-Hill New York (Reprint).
- Gielen, B., MG Palekar. 1989. Some observations on coke precursor on ZSM-5 during n-hexane cracking, *Zeolites* **9** (3): 208-216.
- Gill, S. S., A. Tsolakis, K. D. Dearn et al. 2011. Combustion characteristics and emissions of Fischer-Tropsch diesel fuels in IC engines, *Progress in Energy and Combustion Science* **37** (4): 503-523.
- Gobe, Masao, Kijiro Kon-No, Kazuhiko Kandori et al. 1983. Preparation and characterization of monodisperse magnetite sols in WO microemulsion, *Journal of Colloid and Interface Science* **93** (1): 293-295.
- Golden, Scott. 2008. Canadian crude processing challenges, *Petroleum technology quarterly* **13** (1): 53.
- Gosselin, P. Environmental and Health Impacts of Canada's Oil Sands Industry. Royal Society of Canada Ottawa, ON.
- Gray, Murray R. 1990. Lumped kinetics of structural groups: hydrotreating of heavy distillate, *Industrial & engineering chemistry research* **29** (4): 505-512.
- Gray, Murray R, Alan R Ayasse, Edward W Chan et al. 1995. Kinetics of hydrodesulfurization of thiophenic and sulfide sulfur in Athabasca bitumen, *Energy & Fuels* **9** (3): 500-506.
- Greaves, M., T. Xia, C. Ayasse. Underground Upgrading of Heavy Oil Using THAI- 'Toe-to-Heel Air Injection'.
- Griffiths, M., S. Dyer, Pembina Institute. 2008. *Upgrader Alley: Oil Sands Fever Strikes Edmonton*, Pembina Institute (Reprint).
- Griffiths, M., A. Taylor, D. Woynillowicz et al. 2006. *Troubled waters, troubling trends: Technology and policy options to reduce water use in oil and oil sands development in Alberta*, Pembina Institute (Reprint).

- Hall, Jeremy, Harrie Vredenburg. 2012. The challenges of innovating for sustainable development.
- Hamedi Shokrlu, Y., T. Babadagli. Effects of Nano-Sized Metals on Viscosity Reduction of Heavy Oil/Bitumen During Thermal Applications.
- Hamrick, J.T., L.C. Rose. 1976. *In situ hydrogenation of hydrocarbons in underground formations*, Google Patents (Reprint).
- Han, Fang, Venkata Subba Rao Kambala, Madapusi Srinivasan et al. 2009. Tailored titanium dioxide photocatalysts for the degradation of organic dyes in wastewater treatment: a review, *Applied Catalysis A: General* **359** (1): 25-40.
- Hashemi, R., N.N. Nassar, P. Pereira-Almao. 2012. Transport Behavior of Multimetallic Ultradispersed Nanoparticles in an Oil-Sands-Packed Bed Column at a High Temperature and Pressure, *Energy & Fuels* **26** (3): 1645-1655.
- Hashemi, R., P. Pereira-Almao. 2011. Experimental Study of Simultaneous Athabasca Bitumen Recovery and Upgrading Using Ultradispersed Catalysts Injection, *Society of Petroleum Engineers SPE-144558-PP*.
- Hashemi, Rohallah, Nashaat N Nassar, Pedro Pereira Almao. 2013a. In situ Upgrading of Athabasca Bitumen Using Multimetallic Ultra-Dispersed Nanocatalysts in a in an Oil-Sands-Packed Bed Column: Part 1, Produced Liquid Quality Enhancement, *Energy & Fuels*.
- Hashemi, Rohallah, Nashaat N Nassar, Pedro Pereira Almao. 2013b. In situ Upgrading of Athabasca Bitumen Using Multimetallic Ultra-Dispersed Nanocatalysts in an Oil-Sands-Packed Bed Column: Part 2, Solid Analysis and Gaseous Product Distribution .
- Hashemi, Rohallah, Nashaat N. Nassar, Pedro Pereira Almao. 2013c. Enhanced Heavy Oil Recovery by in Situ Prepared Ultradispersed Multimetallic Nanoparticles: A Study of Hot Fluid Flooding for Athabasca Bitumen Recovery, *Energy & Fuels* **27** (4): 2194-2201. <http://dx.doi.org/10.1021/ef3020537>.
- Hassan, A., L. Carbognani, P. Pereira-Almao. 2008a. Development of an alternative setup for the estimation of microcarbon residue for heavy oil and fractions: Effects derived from air presence, *Fuel* **87** (17): 3631-3639.
- Hassan, A., L. Carbognani, P. Pereira-Almao. 2008b. Effect of O₂ on Microcarbon Residue Standards Analysis, *Energy & Fuels* **22** (6): 4062-4069.
- Hassan, Azfar, Francisco Lopez-Linares, Nashaat N Nassar et al. 2012. Development of a support for a NiO catalyst for selective adsorption and post-adsorption catalytic steam gasification of thermally converted asphaltenes, *Catalysis Today*.
- Hein, F.J. 2006. Heavy oil and oil (Tar) sands in North America: an overview & summary of contributions, *Natural Resources Research* **15** (2): 67-84.
- Hellweg, T. 2002. Phase structures of microemulsions, *Current opinion in colloid & interface science* **7** (1-2): 50-56.

- Herron, E. H. 2000. *Heavy Oil: A Solution to Dwindling Domestic Oil Supplies*, <http://www.petroleumequities.com/HeavyOilReport.htm>.
- Herzig, JP, DM Leclerc, P.L. Goff. 1970. Flow of suspensions through porous media— Application to deep filtration, *Industrial & Engineering Chemistry* **62** (5): 8-35.
- Hildebrand, Heike, Katrin Mackenzie, Frank-Dieter Kopinke. 2009. Pd/Fe₃O₄ nanocatalysts for selective dehalogenation in wastewater treatment processes— Influence of water constituents, *Applied Catalysis B: Environmental* **91** (1): 389-396.
- Husein, M. M., N. N. Nassar. 2008. Nanoparticle preparation using the single microemulsions scheme, *Current Nanoscience* **4** (4): 370-380.
- Husein, M. M., L. Patruyo, P. Pereira-Almao et al. 2010. Scavenging H₂S(g) from oil phases by means of ultradispersed sorbents, *Journal of Colloid and Interface Science* **342** (2): 253-260.
- Husein, Maen M., Nashaat N. Nassar. 2009. Nanoparticle uptake by (w/o) microemulsions. In *Microemulsions: Properties and Applications*, ed. Munzer Fanun, 465-479. Boca Raton, FL, USA., CRC Press, Taylor & Francis Group LLC.
- Isaacs, E. 2005. Canadian Oil Sands: development and future outlook , *Alberta Energy Research Institute, Calgary*.
- Jaramillo, Thomas F, Kristina P Jørgensen, Jacob Bonde et al. 2007. Identification of active edge sites for electrochemical H₂ evolution from MoS₂ nanocatalysts, *science* **317** (5834): 100-102.
- Jiang, S., X. Liu, Y. Liu et al. In situ upgrading heavy oil by aquathermolytic treatment under steam injection conditions.
- Joo, Sang Hoon, Jeong Young Park, Chia-Kuang Tsung et al. 2008. Thermally stable Pt/mesoporous silica core-shell nanocatalysts for high-temperature reactions, *Nature materials* **8** (2): 126-131.
- Jung, Hyun M, Kristin E Price, D Tyler McQuade. 2003. Synthesis and characterization of cross-linked reverse micelles, *Journal of the American Chemical Society* **125** (18): 5351-5355.
- Jurvetson, Steve, Draper Fisher Jurvetson. 2007. Transcending Moore's law with molecular electronics and nanotechnology, *Nanotechnology: Societal Implications—Individual Perspectives*: 43.
- Kaegi, Ralf, Andreas Voegelin, Brian Sinnet et al. 2011. Behavior of metallic silver nanoparticles in a pilot wastewater treatment plant, *Environmental science & technology* **45** (9): 3902-3908.
- Kahan, Dan M, David Rejeski. 2009. PProject on emeRging nanotechnologies.

- Kalidindi, Suresh Babu, Balaji R Jagirdar. 2012. Nanocatalysis and Prospects of Green Chemistry, *ChemSusChem* **5** (1): 65-75.
- Kasraie, M. Role of Foam, Non-Newtonian Flow, and Thermal Upgrading in Steam Injection.
- Kennepohl, D., E. Sanford. 1996. Conversion of Athabasca bitumen with dispersed and supported Mo-based catalysts as a function of dispersed catalyst concentration, *Energy & Fuels* **10** (1): 229-234.
- Kobayashi, Kenji. Forecasting Supply and Demand up to 2030. the International Energy Agency, http://www.iea.org/speech/2005/kk_melbourne.pdf, November 2, 2010.
- Kok, Mustafa Versan, Ender Okandan. 1995. Kinetic analysis of in situ combustion processes with thermogravimetric and differential thermogravimetric analysis and reaction tube experiments, *Journal of Analytical and Applied Pyrolysis* **31** (0): 63-73. <http://www.sciencedirect.com/science/article/pii/016523709400812F>.
- Köseoglu, Refa Ö, Colin R Phillips. 1988. Effect of reaction variables on the catalytic hydrocracking of Athabasca bitumen, *Fuel* **67** (9): 1201-1204.
- Köseoglu, Refa Ö, Colin R Phillips. 1987. Kinetics of non-catalytic hydrocracking of Athabasca bitumen, *Fuel* **66** (6): 741-748.
- Köseoglu, Refa Ö, Colin R Phillips. 1988a. Kinetic models for the non-catalytic hydrocracking of Athabasca bitumen, *Fuel* **67** (7): 906-915.
- Köseoglu, Refa Ö, Colin R Phillips. 1988b. Kinetics and product yield distributions in the CoO-MoO₃/Al₂O₃ catalysed hydrocracking of Athabasca bitumen, *Fuel* **67** (10): 1411-1416.
- Krishna, Rajamani, Alok K Saxena. 1989. Use of an axial-dispersion model for kinetic description of hydrocracking, *Chemical engineering science* **44** (3): 703-712.
- Krishnamoorti, Ramanan. 2006. Extracting the benefits of nanotechnology for the oil industry, *Journal of petroleum technology* **58** (11).
- Lacombe, Romain H, John E Parsons. 2007. Technologies, markets and challenges for development of the Canadian Oil Sands industry.
- Laine, NR, FJ Vastola, PL Walker Jr. 1963. THE IMPORTANCE OF ACTIVE SURFACE AREA IN THE CARBON-OXYGEN REACTION1, *The Journal of Physical Chemistry* **67** (10): 2030-2034.
- Lal, D., FD Otto, AE Mather. 1999. Solubility of hydrogen in Athabasca bitumen, *Fuel* **78** (12): 1437-1441.
- Langdon, John E, Charles H Ware. 2010. *Process for dispersing nanocatalysts into petroleum-bearing formations*, Google Patents (Reprint).
- Langner, B.E. 1980. Reactions of olefins on zeolites: The change of the product distribution with time on stream in the reaction of butene-1 on calcined NaNH₄-Y, *Journal of Catalysis* **65** (2): 416-427.

- Langner, B.E. 1981. Coke formation and deactivation of the catalyst in the reaction of propylene on calcined NaNH₄-Y, *Industrial & Engineering Chemistry Process Design and Development* **20** (2): 326-331.
- Langner, B.E. 1982. Reactions of methanol on zeolites with different pore structures , *Applied catalysis* **2** (4): 289-302.
- Langner, BE, S. Meyer, B. Delmon et al. 1980. Catalyst Deactivation , *Studies on Surface Science Catalysis*: 91.
- Lapeira, Carola Contreras. 2009. Development of a New Methodology for Preparing Nanometric Ni, Mo and NiMo. Catalytic Particles Using Transient Emulsions. M.Sc, University of Calgary, Calgary.
- Le Perchec, P., B. Fixari, M. VRINTA et al. 1995. Hydroconversion of heavy oil residues with sulfided additives or catalysts, *Preprints-American Chemical Society. Division of Petroleum Chemistry* **40** (4): 747-751.
- Lee, D.K., P.S. Koon, W.L. Yoon et al. 1995. Residual oil hydrodesulfurization using dispersed catalysts in a carbon-packed trickle bed flow reactor, *Energy & Fuels* **9** (1): 2-9.
- Lee, S. 1996. *Alternative fuels*, CRC (Reprint).
- Lemaitre, JL, P Govind Menon, F Delannay. 1984. The measurement of catalyst dispersion, *Characterization of Heterogeneous Catalysts*, Marcel Dekker, New York: 325-327.
- Liu, C., J. Zhou, G. Que et al. 1994. Hydrocracking of Gudao residue with dispersed-phase Mo catalyst, *Fuel* **73** (9): 1544-1550.
- Liu, Y., L. Zhong, S. Jiang et al. 2004. Research Progress of Recovering Heavy Oil by Aquathermolysis, *Journal of Fuel Chemistry and Technology* **32** (1): 117-122.
- Loria, Herbert, Gustavo Trujillo-Ferrer, Clementina Sosa-Stull et al. 2011. Kinetic modeling of bitumen hydroprocessing at in-reservoir conditions employing ultradispersed catalysts, *Energy & Fuels* **25** (4): 1364-1372.
- Martens, GG, GB Marin. 2001. Kinetics for hydrocracking based on structural classes: Model development and application, *AIChE journal* **47** (7): 1607-1622.
- Martínez-Palou, R., M.L. Mosqueira, B. Zapata-Rendón et al. 2011a. Transportation of heavy and extra-heavy crude oil by pipeline: A review, *Journal of Petroleum Science and Engineering* **75** (3): 274-282.
- Martínez-Palou, Rafael, María de Lourdes Mosqueira, Beatriz Zapata-Rendón et al. 2011b. Transportation of heavy and extra-heavy crude oil by pipeline: A review, *Journal of Petroleum Science and Engineering* **75** (3): 274-282.
- McEachern, P. 2009. Environmental management of Alberta's oil sands.
- McLaughlin, KW, RG Anthony. 1985. The role of zeolite pore structure during deactivation by coking, *AIChE journal* **31** (6): 927-934.

- Mohanty, S., D. Kunzru, DN Saraf. 1990. Hydrocracking: A review, *Fuel* **69** (12): 1467-1473.
- Mokrys, IJ, RM Butler. In-situ upgrading of heavy oils and bitumen by propane deasphalting: the VAPEX process.
- Mole, T., JR Anderson, G. Creer. 1985. The reaction of propane over ZSM-5-H and ZSM-5-Zn zeolite catalysts, *Applied catalysis* **17** (1): 141-154.
- Molina, Herbert Javier Loria. 2009. Transport of Catalytic Particles Immersed in Fluid Media through Cylindrical Geometries under Heavy Oil Upgrading Conditions. Ph.D, University of Calgary, Calgary.
- Monin, JC, A. Audibert. 1988. Thermal cracking of heavy-oil/mineral matrix systems, *SPE Reservoir Engineering* **3** (4): 1243-1250.
- Moore, RG, CJ Loureshen, SA Mehta et al. 1999. TECHNICAL PAPERS-ABSTRACTS-IV) Heavy Oil (HO)-A Downhole Catalytic Upgrading Process for Heavy Oil Using In Situ Combustion (96-72), *Journal of Canadian Petroleum Technology* **38** (13): 54.
- Moore, RG, SA Mehta, MG Ursenbach. A guide to high pressure air injection (HPAI) based oil recovery.
- Morris, J, J Willis, K Gallagher. 2007. Nanotechnology White Paper , *US Environmental Protection Agency, Washington, DC, www. epa. gov/osa/pdfs/nanotech/epa-nanotechnology-whitepaper-0207. pdf (Feb. 2007).*
- Murray, CBea, DJ Norris, Mounji G Bawendi. 1993. Synthesis and characterization of nearly monodisperse CdE (E= sulfur, selenium, tellurium) semiconductor nanocrystallites, *Journal of the American Chemical Society* **115** (19): 8706-8715.
- Nares, H.R., P. Schachat, M. Ramirez-Garnica et al. Heavy-Crude-Oil Upgrading With Transition Metals.
- Nasr, T, G Beaulieu, H Golbeck et al. 2003. Novel Expanding Solvent-SAGD Process" ES-SAGD", *Journal of Canadian Petroleum Technology* **42** (1).
- Nassar, N. N., M. M. Husein. 2010. Ultradispersed particles in heavy oil: Part I, preparation and stabilization of iron oxide/hydroxide, *Fuel Processing Technology* **91** (2): 164-168.
- Nassar, N. N., M. M. Husein, P. Pereira-Almao. 2010. Ultradispersed particles in heavy oil: Part II, sorption of H₂S(g), *Fuel Processing Technology* **91** (2): 169-174.
- Nassar, N.N., M.M. Husein. Preparation of ultradispersed iron oxide colloidal particles in heavy oil matrix and its application as sorbents for H₂S (g).
- Nassar, N.N., M.M. Husein. 2007a. Effect of microemulsion variables on copper oxide nanoparticle uptake by AOT microemulsions, *Journal of colloid and interface science* **316** (2): 442-450.

- Nassar, N.N., M.M. Husein. 2007b. Study and modeling of iron hydroxide nanoparticle uptake by AOT (w/o) microemulsions, *Langmuir* **23** (26): 13093-13103.
- Nassar, Nashaat N, Azfar Hassan, German Luna et al. 2013a. Kinetics of the catalytic thermo-oxidation of asphaltenes at isothermal conditions on different metal oxide nanoparticle surfaces, *Catalysis today* **207**: 127-132.
- Nassar, Nashaat N, Azfar Hassan, Pedro Pereira-Almao. 2011a. Application of nanotechnology for heavy oil upgrading: Catalytic steam gasification/cracking of asphaltenes, *Energy & Fuels* **25** (4): 1566-1570.
- Nassar, Nashaat N, Maen M Husein, Pedro Pereira-Almao. 2011a. In Situ Prepared Nanoparticles in Support of the Oilsands Industry Meeting Future Environmental Challenges, *Exploration&Production* **2**: 46-48.
- Nassar, Nashaat N. 2010. Study and Modeling of Metal Oxide Solubilization in (w/o) Microemulsions, *Journal of Dispersion Science and Technology* **31** (12): 1714-1720
- Nassar, Nashaat N. 2012. *Iron Oxide Nanoadsorbents for Removal of Various Pollutants from Wastewater: An Overview: Application of Adsorbents for Water Pollution Control* (Reprint).
- Nassar, Nashaat N., Azfar Hassan, Lante Carbognani et al. 2012. Iron oxide nanoparticles for rapid adsorption and enhanced catalytic oxidation of thermally cracked asphaltenes, *Fuel* **95**: 257-262.
- Nassar, Nashaat N., Azfar Hassan, German Luna et al. 2013b. Kinetics of the catalytic thermo-oxidation of asphaltenes at isothermal conditions on different metal oxide nanoparticle surfaces, *Catalysis Today* **207** (0): 127-132.
- Nassar, Nashaat N., Azfar Hassan, Pedro Pereira-Almao. 2011b. Comparative oxidation of adsorbed asphaltenes onto transition metal oxide nanoparticles, *Colloids and Surfaces A: Physicochemical and Engineering Aspects* **384** (1-3): 145-149.
- Nassar, Nashaat N., Azfar Hassan, Pedro Pereira-Almao. 2011c. Effect of surface acidity and basicity of aluminas on asphaltene adsorption and oxidation, *Journal of Colloid and Interface Science* **360** 233-238.
- Nassar, Nashaat N., Azfar Hassan, Pedro Pereira-Almao. 2011d. Metal Oxide Nanoparticles for Asphaltene Adsorption and Oxidation, *Energy & Fuels* **25** (3): 1017-1023. <http://pubs.acs.org/doi/abs/10.1021/ef101230g>.
- Nassar, Nashaat N., Maen M. Husein, Pedro Pereira-Almao. 2011b. In-Situ prepared nanoparticles in support of oilsands industry meeting future environmental challenges, *Exploration and Production: Oil and Gas Review* **9** (1): 46-48.
- Nassar, Nashaat N., Pedro Pereira-Almao. 2010. Capturing H₂S(g) by In Situ-Prepared Ultradispersed Metal Oxide Particles in an Oilsand-Packed Bed Column, *Energy & Fuels* **24** (11): 5903-5906.

- Nassar, NashaatN, Azfar Hassan, German Luna et al. 2013c. Comparative study on thermal cracking of Athabasca bitumen (in English). *Journal of Thermal Analysis and Calorimetry*: 1-8. <http://dx.doi.org/10.1007/s10973-013-3024-4>.
- Nassar, NashaatN, Azfar Hassan, Pedro Pereira-Almao. 2012. Thermogravimetric studies on catalytic effect of metal oxide nanoparticles on asphaltene pyrolysis under inert conditions (in English). *Journal of Thermal Analysis and Calorimetry* **110** (3): 1327-1332. <http://dx.doi.org/10.1007/s10973-011-2045-0>.
- Nel, Andre, Tian Xia, Lutz Mädler et al. 2006. Toxic potential of materials at the nanolevel, *Science* **311** (5761): 622-627.
- Newson, Esmond. 1975. Catalyst deactivation due to pore-plugging by reaction products, *Industrial & Engineering Chemistry Process Design and Development* **14** (1): 27-33.
- Niemeyer, Christof M. 2001. Nanoparticles, Proteins, and Nucleic Acids: Biotechnology Meets Materials Science, *Angewandte Chemie International Edition* **40** (22): 4128-4158.
- Okamoto, Y., M. Odawara, H. Onimatsu et al. 1995. Preparation and catalytic properties of highly dispersed molybdenum and cobalt-molybdenum sulfide catalysts supported on alumina, *Industrial & engineering chemistry research* **34** (11): 3703-3712.
- Ovalles, C., I. Rojas, S. Acevedo et al. 1996. Upgrading of Orinoco Belt crude oil and its fractions by an electrochemical system in the presence of protonating agents, *Fuel processing technology* **48** (2): 159-172.
- Owusu-Boakye, Abena, Ajay K Dalai, Deena Ferdous et al. 2005. Experimental and kinetic studies of aromatic hydrogenation, hydrodesulfurization, and hydrodenitrogenation of light gas oils derived from athabasca bitumen, *Industrial & engineering chemistry research* **44** (21): 7935-7944.
- Paitakhti Oskouei, S., B. Maini, R. Moore et al. Experimental Evaluation of SAGD-ISC Hybrid Recovery Method.
- Panariti, N., A. Del Bianco, G. Del Piero et al. 2000a. Petroleum residue upgrading with dispersed catalysts: Part 1. Catalysts activity and selectivity, *Applied Catalysis A: General* **204** (2): 203-213.
- Panariti, N., A. Del Bianco, G. Del Piero et al. 2000b. Petroleum residue upgrading with dispersed catalysts:: Part 1. Catalysts activity and selectivity, *Applied Catalysis A: General* **204** (2): 203-213.
- Panariti, N., A. Del Bianco, G. Del Piero et al. 2000. Petroleum residue upgrading with dispersed catalysts:: Part 2. Effect of operating conditions, *Applied Catalysis A: General* **204** (2): 215-222.

- Patel, S. 2007. SPECIAL REPORT-CLEAN FUELS-Canadian oil sands: Opportunities, technologies and challenges-Energy resources found at the Arctic Circle have potential to be refined into transportation fuels, *Hydrocarbon Processing*: 65-76.
- Peluso, Enzo. 2011. Hydroprocessing full-range of heavy oils and bitumen using ultradispersed catalysts at low severity. Ph.D, University of Calgary, Calgary.
- Pereira-Almao, P. Fine tuning conventional hydrocarbon characterization to highlight catalytic upgrading pathways. 1-4.
- Pereira-Almao, P. Fine tuning conventional hydrocarbon characterization to highlight catalytic upgrading pathways.
- Pereira-Almao, P. 2012. In situ upgrading of bitumen and heavy oils via nanocatalysis, *The Canadian Journal of Chemical Engineering* **90** (2): 320-329. <http://dx.doi.org/10.1002/cjce.21646>.
- Pereira-Almao, P., S. Larter. An Integrated Approach to On Sitelin Situ Upgrading.
- Pereira, P., R. Marzin, L. Zacarias et al. 1999. *Steam conversion process and catalyst*, Google Patents (Reprint).
- Perez, J. Manuel. 2007. Iron oxide nanoparticles: Hidden talent, *Nature Nanotechnology* **2** (9): 535-536.
- Perman, Roger. 2003. *Natural resources and environmental economics*, Pearson Education (Reprint).
- Phillips, Colin R, Nagib I Haidar, Yiu C Poon. 1985. Kinetic models for the thermal cracking of athabasca bitumen: the effect of the sand matrix, *Fuel* **64** (5): 678-691.
- Phillips, Colin R, It-Chin Hsieh. 1985. Oxidation reaction kinetics of Athabasca bitumen, *Fuel* **64** (7): 985-989.
- Pluym, TC, QH Powell, AS Gurav et al. 1993. Solid silver particle production by spray pyrolysis, *Journal of aerosol science* **24** (3): 383-392.
- R.Hashemi, Nashaat N. Nassar, P. Pereira Almao. Dec 2011. Transport Behavior of Multimetallic Ultra-Dispersed Nanoparticles in an Oil Sands-Packed Bed Column at High Temperature and Pressure, *Energy & Fuels*.
- Radler, M. 2005. Global reserves, oil production show small increases for 2005, *Oil & gas journal* **103** (47): 20-22.
- Rahimi, P., T. Gentzis, E. Taylor et al. 2001. The impact of cut point on the processability of Athabasca bitumen, *Fuel* **80** (8): 1147-1154.
- Ramirez de Agudelo, MM, C. Galarraga. 1991. A stable catalyst for heavy oil processing: III. Activity and selectivity, *The Chemical Engineering Journal* **46** (2): 61-68.
- Rana, M.S., V. Sámano, J. Ancheyta et al. 2007. A review of recent advances on process technologies for upgrading of heavy oils and residua, *Fuel* **86** (9): 1216-1231.

- Rege, SD, H.S. Fogler. 1988. A network model for deep bed filtration of solid particles and emulsion drops, *AIChE journal* **34** (11): 1761-1772.
- Rendon, Vanessa Samantha. 2011. Catalytic Heavy Oil Upgrading with Injection of Ultra-Dispersed Particles and Hydrogen in Porous Media. Master of Science, University of Calgary, Calgary.
- Roy, M, JK Nelson, RK MacCrone et al. 2005. Polymer nanocomposite dielectrics-the role of the interface, *Dielectrics and Electrical Insulation, IEEE Transactions on* **12** (4): 629-643.
- Sánchez, Sergio, Miguel A Rodríguez, Jorge Ancheyta. 2005. Kinetic model for moderate hydrocracking of heavy oils, *Industrial & engineering chemistry research* **44** (25): 9409-9413.
- Sanford, E.C. 1995. Conradson carbon residue conversion during hydrocracking of Athabasca bitumen: Catalyst mechanism and deactivation, *Energy & Fuels* **9** (3): 549-559.
- Sarimeseli, A, G Kelbaliyev. 2004. Modeling of the break-up of deformable particles in developed turbulent flow, *Chemical engineering science* **59** (6): 1233-1240.
- Saskoil, S. Sugianto, R. M. Butler. 1990. The Production Of Conventional Heavy Oil Reservoirs With Bottom Water Using Steam-Assisted Gravity Drainage, *Journal of Canadian Petroleum Technology* **29**: 78-86.
- Scherzer, Julius, Adrian J Gruia. 1996. *Hydrocracking science and technology*, Vol. 66, CRC Press (Reprint).
- Shah, A., R. Fishwick, G. Leeke et al. 2011. Experimental Optimization of Catalytic Process In Situ for Heavy-Oil and Bitumen Upgrading, *Journal of Canadian Petroleum Technology* **50** (11): 33-47.
- Sharpe, HN, WC Richardson, CS Lolley. Representation of steam distillation and in-situ upgrading processes in a heavy oil simulation.
- Shen, SC, Kus Hidajat, Liya E Yu et al. 2004. Simple hydrothermal synthesis of nanostructured and nanorod Zn-Al complex oxides as novel nanocatalysts, *Advanced Materials* **16** (6): 541-545.
- Shu, WR, KJ Hartman. 1986. Thermal visbreaking of heavy oil during steam recovery processes, *SPE Reservoir Engineering* **1** (5): 474-482.
- Singh, Jasvinder, MM Kumar, Alok K Saxena et al. 2005. Reaction pathways and product yields in mild thermal cracking of vacuum residues: A multi-lump kinetic model, *Chemical Engineering Journal* **108** (3): 239-248.
- Speight, J.G. 2000. *The desulfurization of heavy oils and residua*, Vol. 78, CRC (Reprint).
- Speight, J.G., Inc Ebrary. 1999. The chemistry and technology of petroleum.
- Speight, J.G., B. Özüm. 2002. *Petroleum refining processes*, Vol. 85, CRC (Reprint).

- St-Denis, Natalie. 2007. Alberta Ingenuity Centre for In Situ Energy Pamphlet: Unlocking Alberta's Oil Sands Potential.
- Steijns, M., G. Froment, P. Jacobs et al. 1981. Hydroisomerization and hydrocracking. 2. Product distributions from n-decane and n-dodecane, *Industrial & Engineering Chemistry Product Research and Development* **20** (4): 654-660.
- Stine, L.O. 1984. *Method for in situ conversion of hydrocarbonaceous oil*, Google Patents (Reprint).
- Syncrude_Canada. FAQs, <http://www.syncrude.ca/users/folder.asp?FolderID=5745>.
- Tanaka, Toshikatsu, Masahiro Kozako, Norikazu Fuse et al. 2005. Proposal of a multi-core model for polymer nanocomposite dielectrics, *Dielectrics and Electrical Insulation, IEEE Transactions on* **12** (4): 669-681.
- Taylor, Lorne. 2009. Water challenges in oil sands country: Alberta's water for life strategy, *Policy Options*: 44-47.
- Thomas, John Meurig, Brian FG Johnson, Robert Raja et al. 2003. High-performance nanocatalysts for single-step hydrogenations, *Accounts of chemical research* **36** (1): 20-30.
- Thompson, J., A. Vasquez, J.M. Hill et al. 2008. The Synthesis and Evaluation of Up-scalable Molybdenum Based Ultra Dispersed Catalysts: Effect of Temperature on Particle Size, *Catalysis Letters* **123** (1): 16-23.
- Tien, C., A.C. Payatakes. 1979. Advances in deep bed filtration, *AIChE journal* **25** (5): 737-759.
- U.S. National Commission on Energy Policy, Ending the Energy Stalemate, A Bipartisan Strategy to. 2004. Ending the Energy Stalemate, A Bipartisan Strategy to Meet America's Energy Challenge, www.energycommission.org.
- Vasquez, A. 2009. Synthesis, characterization and model reactivity of ultra dispersed catalysts for hydroprocessing, university of calgary.
- Vedrine, JC, P. Dejaifve, ED Garbowski et al. 1980. Aromatics Formation from Methanol and Light Olefins Conversions on H-ZSM-5 Zeolite: Mechanism and Intermediate Species, *Studies in Surface Science and Catalysis* **5**: 29-37.
- Velu, S., S.K. Gangwal. 2006. Synthesis of alumina supported nickel nanoparticle catalysts and evaluation of nickel metal dispersions by temperature programmed desorption, *Solid state ionics* **177** (7): 803-811.
- Venuto, PB, LA Hamilton. 1967. Reverse Molecular-Size Selectivity and Aging in Zeolite-Catalyzed Alkylation, *Industrial & Engineering Chemistry Product Research and Development* **6** (3): 190-192.
- Wang, Z., A. Guo, G. Que. 1998. Coke formation and characterization during thermal treatment and hydrocracking of Liaohe vacuum residuum, *Preprints Division of Petroleum Chemistry* **43** (3): 530-533.

- Weissman, J. G., R. V. Kessler, R. A. Sawicki et al. 1996. Down-Hole Catalytic Upgrading of Heavy Crude Oil, *Energy & Fuels* **10** (4): 883-889.
- Weissman, Jeffrey G. 1997. Review of processes for downhole catalytic upgrading of heavy crude oil, *Fuel Processing Technology* **50** (2-3): 199-213.
- Weissman, Jeffrey G., Richard V. Kessler. 1996. Downhole heavy crude oil hydroprocessing, *Applied Catalysis A: General* **140** (1): 1-16.
- Winey, Karen I, Richard A Vaia. 2007. Polymer nanocomposites, *MRS bulletin* **32** (04): 314-322.
- Xia, TX, M. Greaves. 2006. In Situ Upgrading of Athabasca Tar Sand Bitumen Using Thai, *Chemical Engineering Research and Design* **84** (9): 856-864.
- Xiangling, Kong, Michael Ohadi. Applications of Micro and Nano Technologies in the Oil and Gas Industry-Overview of the Recent Progress.
- Xu, Hai-Ying Helen. 2001. In Situ Upgrading of Heavy Oil. Ph.D, University of calgary, Calgary.
- Yao, Yan-li, Ya Ding, Le-Sheng Ye et al. 2006. Two-step pyrolysis process to synthesize highly dispersed Pt–Ru/carbon nanotube catalysts for methanol electrooxidation, *Carbon* **44** (1): 61-66.
- Yoosuk, B., J.H. Kim, C. Song et al. 2008. Highly active MoS₂, CoMoS₂ and NiMoS₂ unsupported catalysts prepared by hydrothermal synthesis for hydrodesulfurization of 4, 6-dimethyldibenzothiophene, *Catalysis Today* **130** (1): 14-23.
- Yoshioka, N, C Karaoka, H Emi. 1972. On the deposition of aerosol particles to the horizontal pipe wall from turbulent stream, *Kagaku Kogaku* **36** (9): 1010-1016.
- Zamani, A., B. Maini. 2009. Flow of dispersed particles through porous media--Deep bed filtration, *Journal of Petroleum Science and Engineering* **69** (1-2): 71-88.
- Zamani, Amir, Brij Maini, Pedro Pereira-Almao. 2010. Experimental Study on Transport of Ultra-Dispersed Catalyst Particles in Porous Media, *Energy & Fuels* **24** (9): 4980-4988.
- Zamani, Amir, Brij Maini, Pedro Pereira-Almao. 2011. Flow of nanodispersed catalyst particles through porous media: Effect of permeability and temperature, *The Canadian Journal of Chemical Engineering*.
- Zarkesh, Jamshid, Reza Hashemi, Maryam Ghaedian et al. HRH: Nano Catalytic Process to Upgrade Extra Heavy Crude/residual Oils.
- Zekel', LA, AS Maloletnev, AA Ozerenko et al. 2007. Basics of synthesis and application of pseudohomogeneous coal and petroleum feedstock hydrogenation catalysts, *Solid Fuel Chemistry* **41** (1): 31-37.

- Zou, R., Q. Lou, H. Liu et al. 1987. Investigation of coke deposition during the pyrolysis of hydrocarbon, *Industrial & Engineering Chemistry Research* **26** (12): 2528-2532.
- Zou, R., Q. Lou, S. Mo et al. 1993. Study on a kinetic model of atmospheric gas oil pyrolysis and coke deposition, *Industrial & Engineering Chemistry Research* **32** (5): 843-847.